P-08-102

Äspö Hard Rock Laboratory

A comparative study of tunnel mapping results from the Äspö TBM and drill and blast tunnels

Peter Hultgren, Svensk Kärnbränslehantering AB

December 2008

Svensk Kärnbränslehantering AB
Swedish Nuclear Fuel
and Waste Management Co

Box 250, SE-101 24 Stockholm
Phone +46 8 459 84 00

ISSN 1651-4416
SKB P-08-102

Äspö Hard Rock Laboratory

A comparative study of tunnel mapping results from the Äspö TBM and drill and blast tunnels

Peter Hultgren, Svensk Kärnbränslehantering AB

December 2008

Keywords: Äspö Hard Rock Laboratory, Tunnel mapping, Rock types, Fractures, Fracture minerals, P_{21}.

Abstract

A comparative study has been performed to evaluate the tunnel mapping results obtainable from tunnel sections excavated by drill and blast methods compared to excavation by Tunnel Boring Machine (TBM) at the Äspö Hard Rock Laboratory.

This report covers the comparative tunnel mapping data from TASF, TASG and TASZ (drill and blast tunnels) and TASA sections 3,206.8–3,250.6, 3,448.1–3,492.9 and 3,522.6–3,552.7 (excavated by a TBM).

In general, the present study has not identified any significant differences in the mapping results that can be related to the method of tunnel excavation. It should be noted that the available data set is too limited to perform a wide ranging robust statistical analysis, however, none of the results of the present study have identified any significant differences in the mapping parameters that are of sufficient dignity that they need to be taken into account when selecting a tunnel excavation method, e.g. drill and blast or TBM.

Sammanfattning

En jämförelsestudie har genomförts för att utvärdera tunnelkarteringsresultat från olika tunnelsektioner som har borrats och sprängts samt tunnelsektioner som har drivits av en tunnel borrningsmaskin (TBM). Studien är gjord på Äspö laboratoriet.

Tunnel sektioner där karaktäriseringsdata har jämförts är TASF, TASG och TASZ (borrad och sprängd tunnel) och TASA sektioner 3 206,8–3 250,6; 3 448,1–3 492,9 och 3 522,6–3 552,7 (TBM).

Generellt har denna jämförelse studie inte identifierat några större signifikanta skillnader i karteringsresultat för de olika uttagningsmetoderna. Att beakta är den data mängd som använts i denna studie är för liten för att göra några säkra statistiska analyser. Studien visar på att det inte finns några större skillnader på det karteringsunderlag från respektive uttagsmetod som skulle kunna vara av den dignitet att det torde vara avgörande för val av uttagningsmetod.

Contents

1 Introduction

The planning for the construction of the final repository for spent nuclear fuel includes the evaluation of characterisation methods. Important input to the characterisation of the rock mass includes the mapping of the excavated tunnel roof and walls. The aim of the current report is to assess to what extent the results obtainable from the tunnel mapping are dependent on the tunnel excavation technique, whether it was excavated by drill and blast or by TBM.

SKB is currently assessing which reference method will be used for tunnel excavation. As one input for the choice between conventional and TBM excavation methods the current study was initiated (SKB internal document) aiming to see whether there are any significant differences in the mapping results obtainable from the two excavation methods and how they affect the characterisation of the rock mass.

To facilitate the comparison, the main criteria for the selections of tunnel sections for the study were to find two tunnel sections with the same orientation and excavated close to each other, but with different excavation methods. Such an arrangement is not commonly found, however, it does occur at the Äspö Hard Rock Laboratory (Figure 1-1). Ideally it would have been preferably best if remapping of the tunnels had been possible to perform. However, parts of the Äspö tunnels have been covered by shotcrete after excavation and therefore the study is based on available mapping data obtained from the time of the initial excavation.

This report describes how the comparative assessment was made and presents the results of the study.

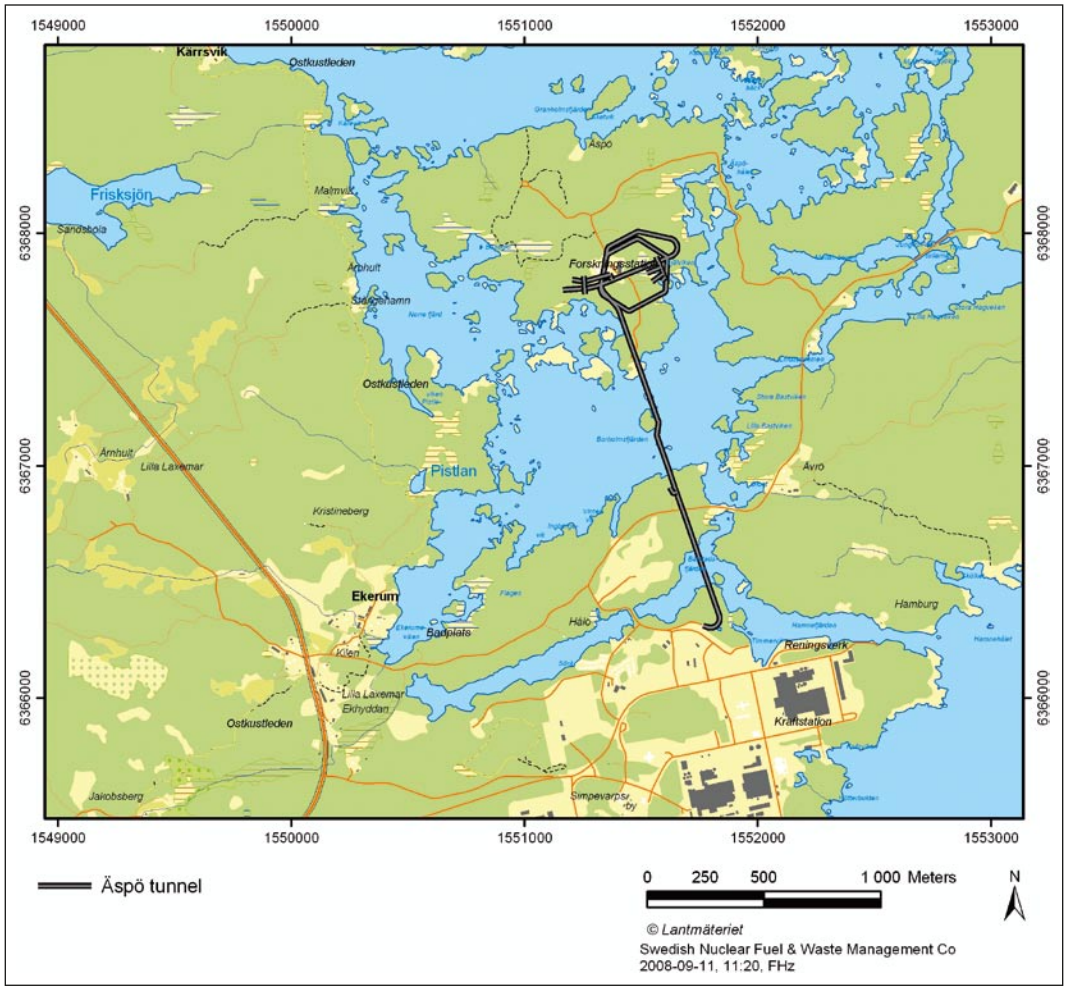

Figure 1-1. *The tunnel at the Äspö Hard Rock Laboratory.*

2 Objective and scope

This report covers a comparative study of tunnel mapping results obtained from tunnels excavated by drill and blast and TBM methods.

The objective of the comparative study was to assess whether there are any significant differences between the resulting geological characterisation of a tunnel that are dependent on the tunnel excavation method. Characterisation parameters considered included rock type distribution, existence of fractures, fracture minerals, water inflow from fractures, deformation zones and Full Perimeter Intersection (FPI- between a fracture and the tunnel circumference) /Munier 2006/.

The results from this study will provide input to the choice of excavation method, drill and blast or TBM that will be used for the final deposition tunnels.

The comparative study uses existing mapping data from earlier excavated tunnel sections in the Äspö Hard Rock Laboratory /Markström and Erlström 1996/ and /Markström 1997/. Tunnel sections of each type, more or less parallel with each other were selected for the study. The drill and blast tunnel sections were TASF, TASG and TASZ, while the TBM tunnel sections were TASA 3,206.8–3,250.6 m (TASA upper section), TASA 3,448.1–3,492.9 m (TASA mid section) and TASA 3,522.6–3,552.7 m (TASA lower section). All tunnels are situated at approximately –450 metres under sea level.

3 Equipment

3.1 Description of softwares

Software that has been used for the study includes:

- ESRI®ArcMap™ 9.1, display of fractures and rock types, creation of new GIS files and metadata to aid data analysis.
- TMS, (tunnel mapping system and database).
- © 2008 Rocscience Inc. Dips Version 5.1, to display fracture orientations.
- Copyright © 2007 Bentley System, Microstaion XM, general data preparation for other programs.
- Microsoft ® Excel 2002, general data preparation for other programs.
- Microsoft ® Access 2002, general data preparation for other programs.
- Statistica, Copyright © StatSoft. Inc 1984–2004, creation of box whisker diagram.

3.2 Terminology

Terminology and abbreviations that have been used in this report are:

- P_{21} – A measure of aerial fracture intensity, expressed in this report as the fracture trace length per unit of mapped area (m/m^2).
- FPI – Full Perimeter Intersection.
- TBM – Tunnel boring machine.
- TMS – Tunnel Mapping System, SKB's in house tunnel mapping system.

3.3 Data

Data that have been used in the production of this report were downloaded from the TMS-database. The database includes all mapping results obtained at the time of and subsequent to the original tunnel excavation. TMS data takes the form of CAD files with geometry representing the rock type boundaries and fracture positions with each drawn object described by an entry in a linked database.

3.4 Source of error

There are some sources of error related to the performance of the original tunnel mapping work and inherent in the TMS system that need to be borne in mind when reading this report.

- Due to practical limitations and in accordance with the original TMS mapping methodology, where a number of closely spaced parallel fractures occur in the tunnel wall or roof they have been represented by a single fracture geometry, with a single ID, in the mapping system. Although the number of fractures and their spacing has been input into a linked database any P_{21} values that are calculated using the drawn fracture geometries alone will be potentially incorrect.

- Intrusions and veins with thicknesses of less than 10 cm have been mapped as fractures and the associated rock types have been input in the database as fracture fillings. This means that any estimate made of the total mapped area for a particular rock type, based solely on the mapped geometries, will be incorrect.
- Often there was a limited time available for undertaking the original mapping work in the tunnel and in some cases this will have lead to a simplified characterisation of fractures and fracture zones.
- In the CAD representations of the fracture traces the fracture trace lengths will be foreshortened in the shoulder of the drill and blast tunnels due to the oversimplification of the real roof geometry. Accordingly fracture trace length estimates based on these recorded geometries will be incorrect for the drill and blast sections of the tunnel.

4 Execution

4.1 General

This comparative study was performed to assess whether there is any difference between a geological characterisation of a drill and blast tunnel compared to a TBM tunnel that is dependent on the excavation method. Characterisation parameters involved in the comparison included rock type distribution, existence of fractures, fracture minerals, water inflow from fractures, FPI (Full Perimeter Intersection) and deformation zones.

The comparative study was based on geological data from the drill and blast tunnels TASF, TASG, and TASZ compared with geological data from sections of the TBM drilled tunnel, see Figure 4-1. The parallel tunnels have approximately the same area, see Table 4-1, with a total area of 2,638 m^2 being included from each of the different excavation methods.

The comparative study of the data from the TMS-database has been performed using ESRI®ArcMap™ 9.1 The CAD files from the TMS-database have been converted to shape-files so they could be used in ArcMap. The coordinate system is RT90 2.5 gonV.

A statistical analysis has been performed on the fracture data. The fracture intensity P_{21} /Dershowitz and Herda 1992/ was determined for: all fractures (including fractures and water-bearing fractures), waterbearing fractures on each tunnel section. The density type was Kernel with a search radius of 0.5, 1, 2 and 4 metres. The output cell size was one square metres. The same was done on fracture minerals, and the minerals that have been compared were chlorite, calcite, epidote, quartz and fractures with associated oxidized walls. No aspect have been taken if the mineral was mapped as first, second, third, fourth or fifth mineral during the mapping.

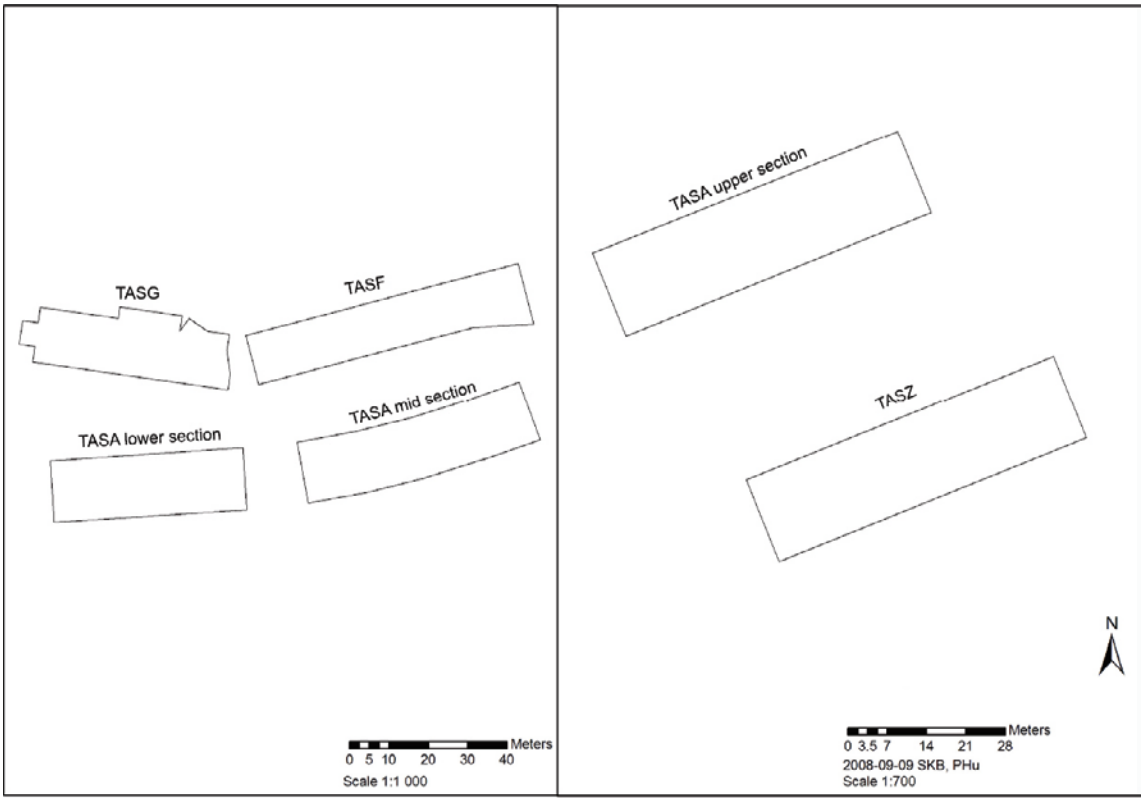

Figure 4-1. *Tunnel sections at Äspö Hard Rock Laboratory that were used for comparison of characterisation of drill and blast tunnels and TBM excavated tunnel sections.*

Table 4-1. Tunnel area in square metres.

TBM tunnels		Drill and blast tunnels	
Tunnel section	Tunnel area m²	Tunnel section	Tunnel area m²
TASA upper section	926	TASZ	926
TASA mid section	941	TASF	941
TASA lower section	771	TASG	771

4.2 Execution of field work

According to the work plan control selections from the TMS data were made and compared with relevant tunnel wall sections. The field observations were limited to inspection of rock types, deformation zones, fractures and FPI in the TASA upper and mid tunnel sections (TBM-tunnel) Figure 4-1. The remaining tunnel sections are covered by shotcrete or were not accessible due to ongoing experiments or other installed equipment.

4.3 Data handling/post processing

The CAD-files were taken from the TMS-database and converted from Äspö 96 coordinate system to RT90 2.5 gonVest. In addition the CAD files were converted to shape-files to aid data analysis in GIS.

4.4 Analyses and interpretations

Geological data from TMS was used to compare the lithologies identified from each of the excavated tunnel sections, both from TBM and the drill and blast tunnels. Within GIS, a Geodatabase was built up allowing an estimation to be made of the surface areas of the various mapped lithologies recorded in the respective tunnel sections. In addition each tunnel section was subdivided into smaller sections of approximately 100 m² in order to identify any variations within individual tunnel sections Appendix A and D. The parallel tunnel sections were compared with each other and finally all the tunnel sections from TBM were compared with all drilled and blast tunnel sections. All the areas have been normalized against the respective tunnel section area.

TMS-data was used to make a statistical analysis of fractures within GIS. For each tunnel section the fracture intensity (P_{21}) was determined for all fractures (fractures and waterbearing fractures) and for waterbearing fractures alone. The density type was Kernel with a search radius of 0.5, 1, 2 and 4 m. This involves a density calculation based on the fracture geometries falling within a specified area, set by the search radius, that area then summed and divided by the overall search area to give density values for each cell. The Kernel density calculation gives a smoother distribution of values due to the lines lying near the centre of a raster cell's search area being weighted more heavily than those lying nearer the edge. The output cell size was one square metre. The same analysis was performed for the fracture minerals chlorite, calcite, epidote, quartz and fractures with associated oxidized walls. Other fracture parameters that have been compared are water leakage, fracture orientation and FPI.

4.5 Nonconformities

No nonconformities have been registered during the comparative study.

5 Results

In this chapter the results and comments of the comparative analyses of mapping data from drill and blast tunnel sections and TBM-drilled tunnel sections are presented parameter by parameter (sections 5.1–5.9). The analyses are visualised in tables and figures. In some cases the tunnel sections are subdivided into smaller parts. Detailed results from these analyses are presented in Appendices A to E.

5.1 Rock type

5.1.1 Results

The tunnel sections in this study are dominated by Äspö diorite. Subordinate rock types comprise Fine-grained granite, Småland Ävrö granite and Greenstone, see Figure 5-1 and Table 5-1. The Äspö diorite mapped in the TBM-drilled sections is characterised as follows: colour = grey, grain size = medium, texture = porphyritic, alteration = weak. The same characterisation was carried out for the drill and blast sections.

There is no statistically significant difference between the various tunnel sections concerning the amount of Fine-grained granite mapped. The variability within an individual tunnel section is of the same order as that occurring between the various sections. The results are given in Appendix A. In summary the differences are small and are considered negligible.

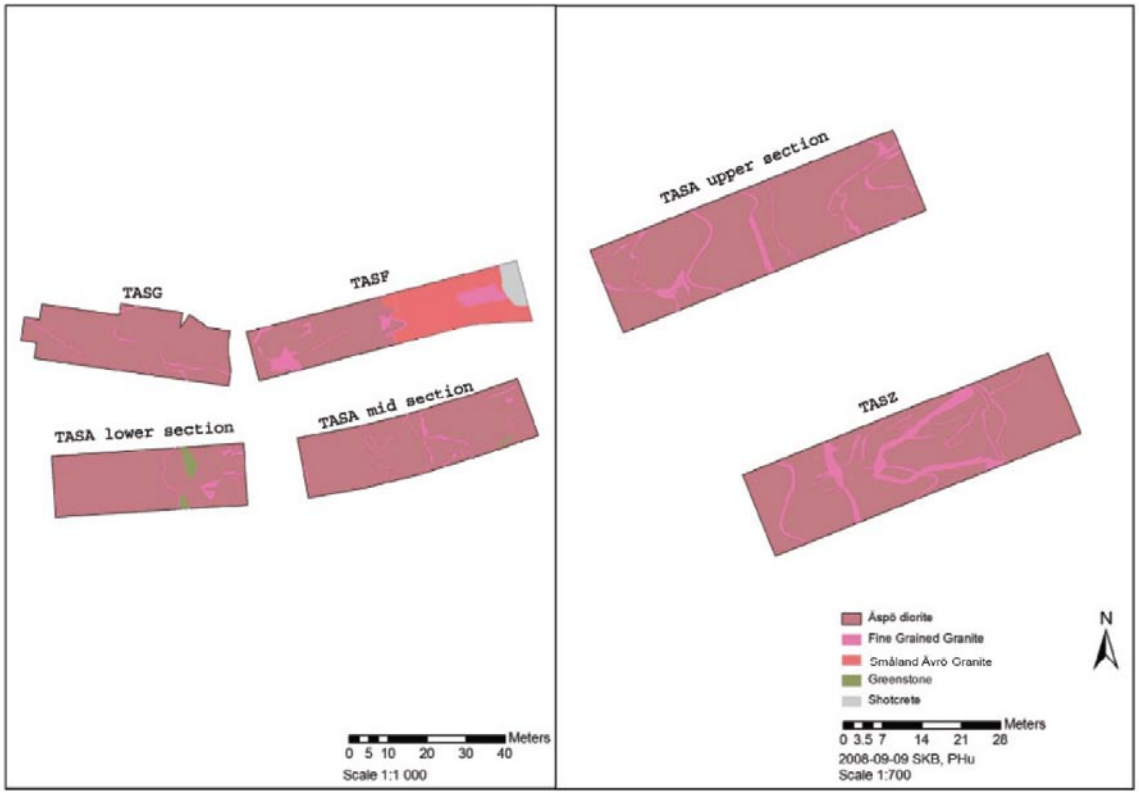

Figure 5-1. *Mapped rock types in the selected tunnels.*

Table 5-1. Percentages of rock types in the respective tunnel sections.

Tunnel section	Äspö diorite	Fine-grained granite	Greenstone	Småland Ävrö granite	Shotcrete
TASA upper section	92.4	7.6	0.0	0.0	0.0
TASZ	87.1	12.9	0.0	0.0	0.0
TASA mid section	95.7	3.9	0.3	0.0	0.0
TASF	44.2	11.5	0.0	38.8	5.5
TASA lower section	93.3	3.5	3.2	0.0	0.0
TASG	97.0	3.0	0.0	0.0	0.0

With the exception of the TASA lower section and TASG the comparison between the parallel tunnel sections shows that the drill and blast tunnels have more recorded Fine-grained granite than the TBM tunnel sections.

For Äspö diorite it is only the TASF section that is markedly different with a notably lower mapped quantity of this rock type. About 38.8% in the TASF tunnel is mapped as Småland Ävrö granite. The results are given in Appendix A. In total there is more mapped Fine-grained granite in the drill and blast tunnel sections. Greenstone is only mapped in two TBM-drilled tunnel sections while Småland Ävrö granite is only mapped in the TASF tunnel.

5.1.2 Comments

The major difference is between TASA mid section and TASF. Småland Ävrö granite is mapped in TASF but not in the TASA mid section nor in any of the other tunnel sections. This may be the fact that Småland Ävrö granite occurs as irregular bodies in the Äspö. The transition forms between the two rock types are very often impossibly to identify macroscopally /Stanfors et al. 1997/. It is also known that the Fine-grained granite occurs as irregular dykes and veins.

Due to the mapping methodology both Pegmatite and Fine-grained granite are classed as a single rock type, Fine-grained granite. The reason being that Fine-grained granite becomes coarser with depth as seen in the Äspö-tunnel. In addition the Fine-grained granite bodies also often have a boarder of Pegmatite. In these cases drill core samples from the tunnel walls were analysed regarding silicate density and checked by means of microscopical analyses /Wikman and Kornfält 1995/. This was mainly performed in 50 m blocks defined in the prediction /Stanfors et al. 1997/ along the tunnel.

The reported differences are not judged to be significant. It is considered that the recording rock type is not sensitive to the type of tunnel excavation method. Consequently there should be no significant differences in recording colour, grain size, texture and alteration that are due to the excavation method. However, it was noted that due to the cylindrical shape of the TBM tunnel, the geometry of the rock contacts was somewhat easier to observe.

5.2 Fractures

5.2.1 Results

In accordance with the TMS methodology the minimum cut of length for a fracture to be included in the mapping is generally 1m. However, in the case of waterbearing fractures there is no lower limit of cut of length. The total number of mapped fractures in the tunnel sections is 593, of which 87 are mapped as waterbearing fractures. There are 338 mapped fractures in the drill and blast tunnels and 255 mapped fractures in TBM-drilled sections, see Table 5-2 and Table 5-3. The distribution of fracture lengths is shown in Figure 5-2 and 5-3.

Table 5-2. Total number of mapped fractures and waterbearing fractures in the differently excavated tunnels.

Excavation method	All fractures	Waterbearing fractures
TBM	255	51
Drill and Blast	338	36
Total	593	87

Table 5-3. Mapped fractures and waterbearing fractures in respective tunnel section.

Tunnel section	All fractures	Waterbearing fractures	Total length of fractures (m)
TASA upper section	76	15	473
TASZ	124	14	514
TASA mid section	115	26	740
TASF	118	15	556
TASA lower section	64	10	495
TASG	96	7	514
Total	593	87	3,292

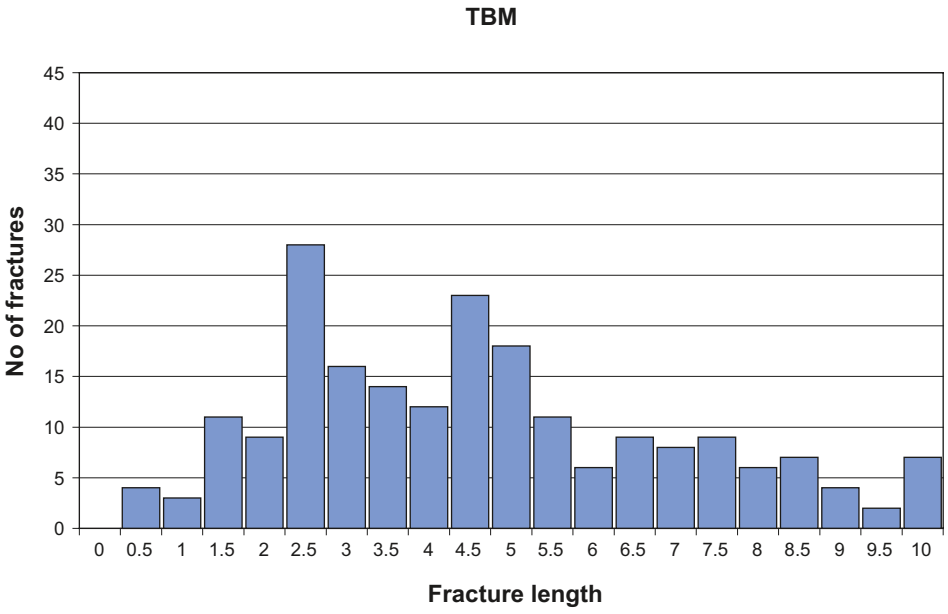

Figure 5-2. *Number of mapped fractures in different fracture length intervals in TBM excavated tunnel sections.*

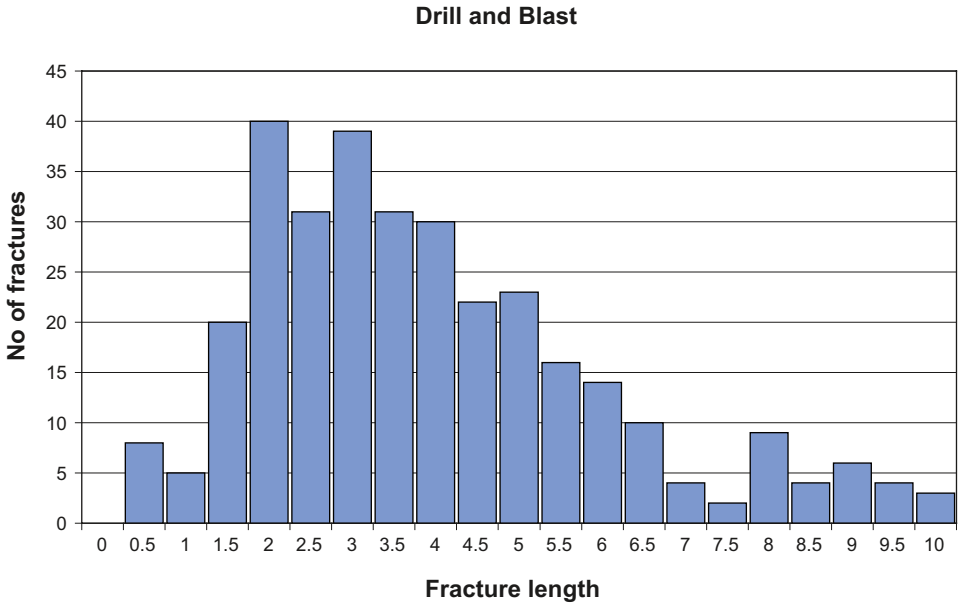

Figure 5-3. *Number of mapped fractures in different fracture length intervals in drill and blast excavated tunnel sections.*

5.2.2 Comments

The drill and blast tunnels have more mapped fractures than the TBM tunnel sections, while waterbearing fractures are more common in the TBM tunnel. The higher number of mapped fractures in the drill and blast tunnels could be due to the better exposure of fracture surfaces in a drill and blast tunnel. Another reason for the increased fracturing could be the opening of existing sealed fractures in the drill and blast tunnels. The better exposure of the actual fracture surfaces in a drill and blast tunnel will make the recording of fracture parameters as orientation, surface character and fracture minerals more straightforward compared, to in a TBM tunnel.

There are more mapped fractures in the drill and blast tunnels although the mean is higher in the TBM-drilled sections, especially in TASA mid section, see appendix B, D, and Figure 5-3 and 5-4. The increased mean fracture length is probably due to the fact that it is easier to follow fracture traces in the TBM tunnel. Another reason could be that it is more difficult to make a judgment as to how a fracture terminates in a drill and blast tunnel due to the irregular nature of the tunnel wall surface in a drill and blast tunnel. Another possible contributing factor is that thin fractures are more difficult to observe in the TBM tunnel.

It is worth noting that it is highly likely that blasting will open up sealed fractures which will influence the ratio between open and sealed fractures. It is possible that in a drill and blast tunnel this opening of fractures may redirect the water flow in the excavation damaged zone and make the flow trace diffuse on the tunnel wall or even impossible to observe. See also section 5.3.

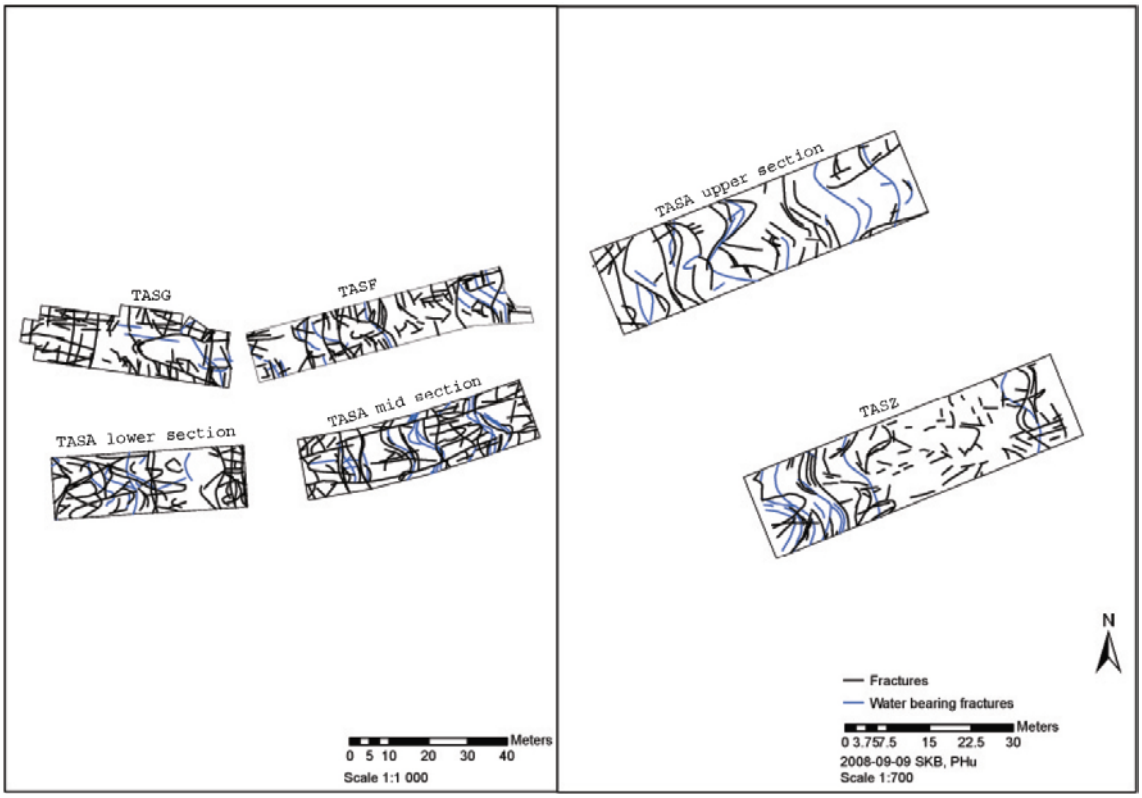

Figure 5-4. *Mapped fractures including waterbearing fractures in respective tunnel sections in drill and blast and TBM excavated tunnels respectively.*

5.3 Water inflow from fractures

5.3.1 Results

Points of water leakage to the tunnel and the amount of water leakage at each point are characterised with a three-point scale, where:

v patch of moisture, sporadic drops
vv drops
vvv flow

There are 60 spots of recorded water leakage in the TBM-drilled and 43 spots in the drill and blast tunnel, Table 5-4.

Table 5-4. Water leakage in respective tunnel sections.

Tunnel section	No of Fractures	v	vv	vvv	No of leakage spots
TASA upper section	15	6	8	3	17
TASZ	14	3	9	1	13
TASA mid section	26	2	6	20	28
TASF	15	2	17	0	19
TASA lower section	10	1	7	7	15
TASG	7	0	10	1	11

5.3.2 Comments

There is a difference in the mapped inflows between the differentl excavated tunnels. The difference could be due to the creation of an excavated damage zone during blasting. Blasting will open new, artificial, ways for the water to reach the tunnel surface and may result in a more diffuse leakage pattern. If the inflow is diffuse it could be difficult to estimate from which fracture(s) the leakage originates. It is considered that a TBM will not generate new fractures or open up existing fractures to the same extent as excavation by blasting and hence the leakage pattern seen in a TBM tunnel is likely to be more representative of the true in situ conditions and is also probably more distinct. Hence more mapped waterbearing fractures are to be expected in the TBM-sections, as can be observed in table 5-4 especially in TASA mid section.

5.4 Fracture orientation

5.4.1 Results

All the fractures that have been mapped in the respective tunnel sections have a recorded strike and dip. The strike and dips vary very little between the excavation methods, see Figures 5-5 and 5-6. However, there is a small increase in observed WNW orientated as well as sub horizontal fractures in the TBM sections.

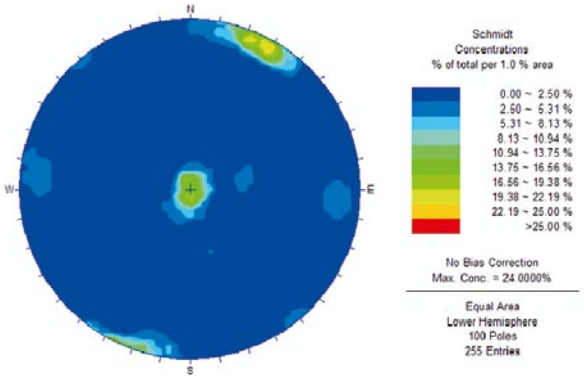

Figure 5-5. *Poles of all mapped fractures in the TBM sections. Lower hemisphere plot.*

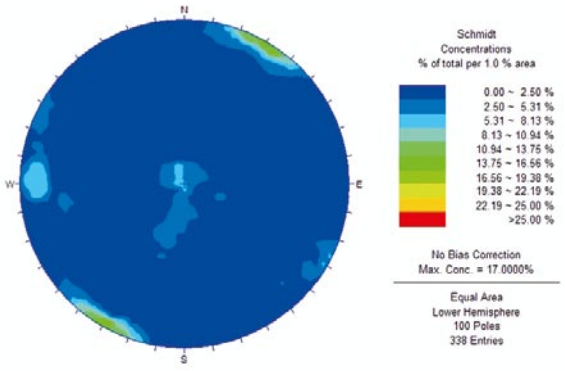

Figure 5-6. *Poles of all mapped fractures in drill and blast sections. Lower hemisphere plot.*

5.4.2 Comments

Theoretically there should be no difference in the pattern of strikes and dips of the recorded fractures since the tunnels are essentially parallel. This assumption is borne out by the recorded results seen in Figures 5-5 and 5-6 and suggests that fracture orientation is not a parameter that is particularly sensitive to tunnel excavation method. It may be easier to record the geometry of longer fractures in a TBM tunnel due to the shape and smooth surface of the tunnel wall. However, it is likely that it is easier to map thin fractures in a drill and blast tunnel due to the increased exposure of the fracture surfaces.

5.5 Intensity of fractures, P_{21}

5.5.1 Results

The P_{21} values for all fractures (including waterbearing fractures) are given in Appendices B and D. An example of an output raster file from GIS is given in Figure 5-7, where the darker blue indicates a higher intensity of fractures for a search radius of 1.0 m.

The variability within an individual tunnel section is of the same order as that occurring between the various sections, except for TASZ and TASA lower section. The results are given in Appendix D. In summary the differences are small and are considered negligible.

P_{21} values for all fractures (including waterbearing fractures) are generally very similar and do not show differences between the different excavated tunnel sections although the P_{21} is somewhat higher for the TASA mid section. An increase in the search radius for P_{21} e.g. 2 and 4 m leads to poorer correlation between the different sections and lower resolution of P_{21}. A lower search radius of P_{21} e.g. 0.5 m gives a higher resolution of P_{21} but the number of observation decreases.

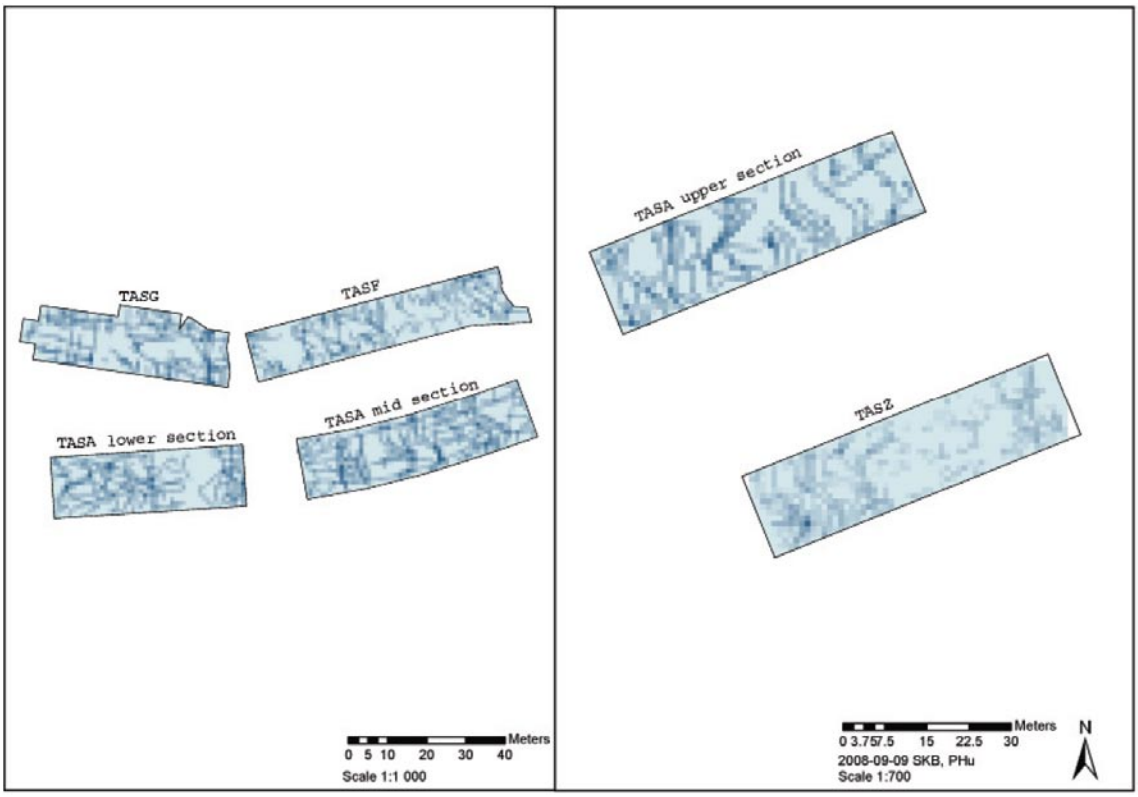

Figure 5-7. *P_{21} for all fractures in respective tunnel section. Search radius 1 m output cell 1 m². Darker blue indicates an increased intensity of fractures.*

5.5.2 Comments

The minor differences in P_{21} values for fractures (including waterbearing fractures) shows that the fracture intensity is not a mapping parameter that is critical to tunnel excavation method.

The minor differences in P_{21} for waterbearing fractures may be due to the excavated damage zone, with blasting opening new artificial paths for the water to reach the tunnel surface and give a more diffuse leakage pattern. If the inflow is diffuse it may be difficult to determine from which fracture(s) the leakage originates.

The peak with P_{21} of 0.2 is due to the fact that even short fractures were mapped if a water leakage was connected to the fracture. Another peak was observed with P_{21} around 2. This might indicate length of waterbearing fractures observed correlates to the dimension of the tunnel.

5.6 Fracture minerals

5.6.1 Results

The dominated fracture mineral in the tunnel sections is chlorite followed by calcite, epidote, fractures associated with oxidized walls and quartz. Chlorite was found in 217 fractures in drill and blast tunnels and 130 fractures in TBM-drilled tunnel sections, Table 5-5. Figure 5-8 show all mapped fractures filled with epidote in the drill and blast and TBM excavated tunnels respectively.

Table 5-5. Mapped fractures in the respective tunnel section where Qz=quartz, Cl=Chlorite, Ca=Calcite, Ep=epidote and Ox= fractures associated with oxidized walls.

Tunnel section	Cl	Ca	Ep	Ox	Qz
TASA upper section	24	31	23	13	7
TASZ	74	46	25	23	4
TASA mid section	74	79	53	42	19
TASF	80	70	21	11	7
TASA lower section	32	38	24	19	11
TASG	63	19	18	31	12
Total	347	283	164	139	60

5.7 Intensity of fracture minerals P_{21}

5.7.1 Results

The P_{21} values for all fracture minerals are given in Appendices C and E. An example of an output raster file from GIS is given in Figure 5-9, where the darker blue indicates a higher intensity of fractures filled with epidote.

There exists small differences in the P_{21} for the various fracture minerals. It is most commonly in the TASA mid section correlate. Chlorite and calcite show an increased P_{21} value. In the TASA upper section and TASZ the P_{21} values for calcite and chlorite is lower. The P_{21} values fore epidote, quartz and fractures associated with oxidized walls the P_{21} values correlates well between the different sections.

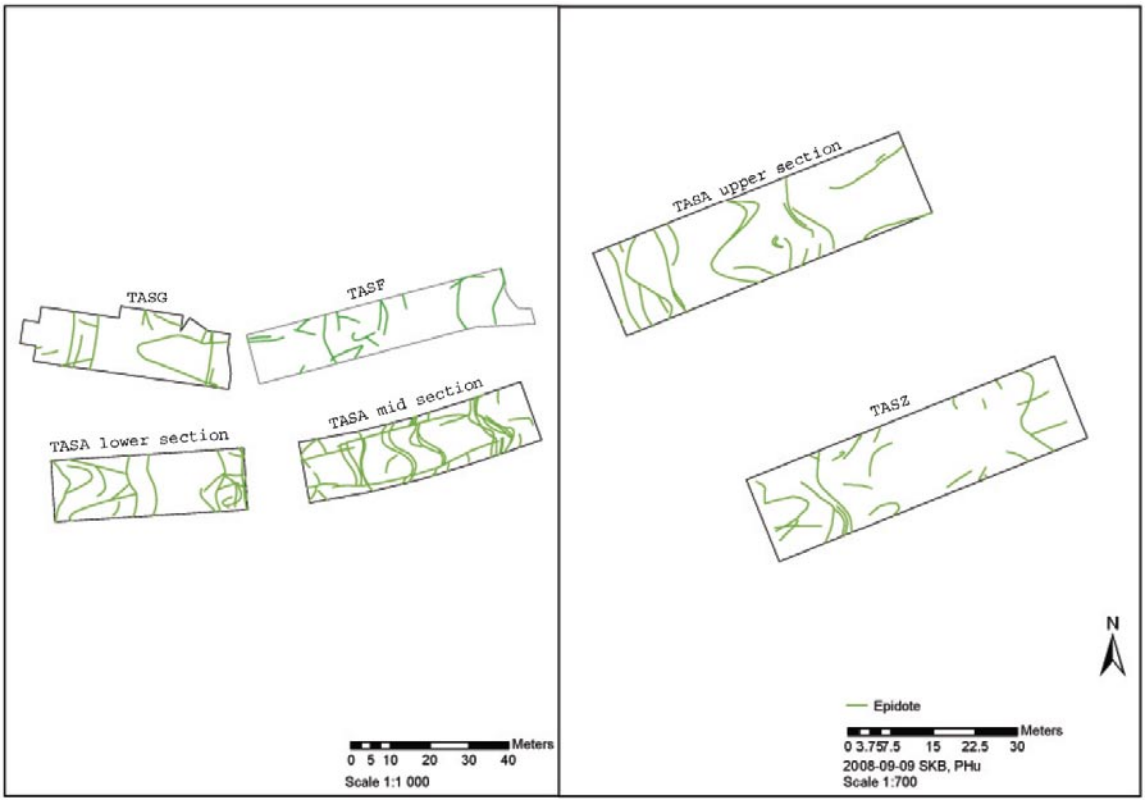

Figure 5-8. *All mapped fractures with epidote in the respective tunnel sections.*

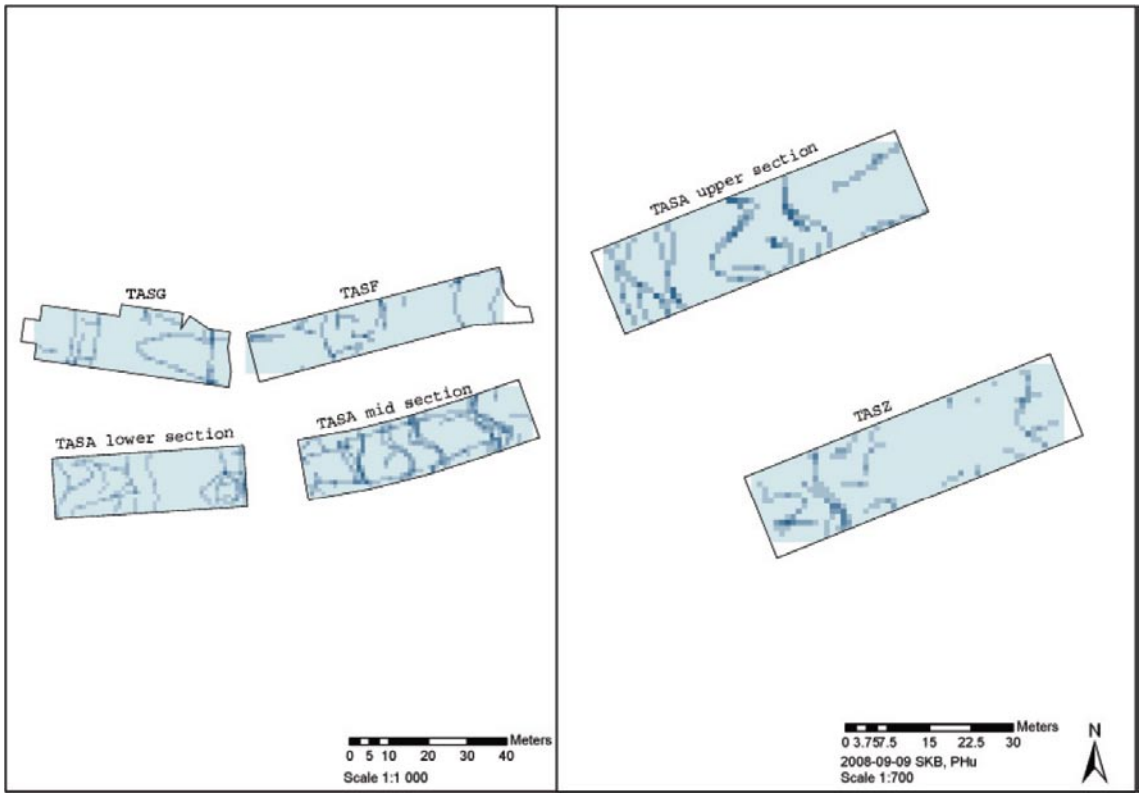

Figure 5-9. *P_{21} for all mapped fractures with epidote in respective tunnel section. Search radius 1 m output cell 1 m^2. Darker blue indicates an increased intensity of fractures filled with epidote.*

5.7.2 Comments

There are onely minor differences in P_{21} for each fracture mineral in the respective tunnel section. This result was unexpected since, based on interviews with geologists from the mapping team, it was generally assumed that it was more difficult to characterise fracture minerals in the TBM-drill tunnel due to the very limited exposure of the fracture surfaces. However, the classification *oxidised walls* describe a penetrative alteration seen as red staining in association with a fracture /Eliasson 1993/. For such a penetrative feature there should be little if any difference between the recorded values in the different tunnels related to excavation method. The results of the current study, in contrast to the general opinion, suggest that fracture minerals in general are not a parameter that is critical to observe depending on the tunnel excavation method.

5.8 Full Perimeter Intersection (FPI)

5.8.1 Results

There are a total of 21 FPIs in the TBM-drilled sections and 16 in the drill and blast tunnel sections, see Table 5-6 and Figure 5-10. These numbers also include possible FPIs (for example, a fracture trace that is interpreted as having been originally a FPI but has at some time had its fracture trace disrupted and offset by shearing).

5.8.2 Comments

There are a few more mapped FPI:s in the TBM-drilled tunnel. This could be due to the shape of the different excavated tunnel profiles. The TBM tunnel is cylindrical and the walls are smoother, while in a drill and blast tunnel the tunnel walls are more irregular, which could make it more difficult to detect and follow an FPI. The difference in FPI:s observed in TASG and TASA lower section can however not be explained.

Table 5-6. FPIs in each tunnel section.

Tunnel section	FPI no.	Possible FPI no.	Total FPI no.	FPI/100 m	Total FPI/100 m	Section length (m)
TASA upper section	7	0	7	11.95	11.95	58.60
TASZ	4	2	6	6.78	10.17	59.00
TASA mid section	4	4	8	6.67	13.33	60.00
TASF	7	0	7	10.43	10.43	67.13
TASA lower section	6	0	6	12.24	12.24	49.00
TASG	3	0	3	5.96	5.96	50.30

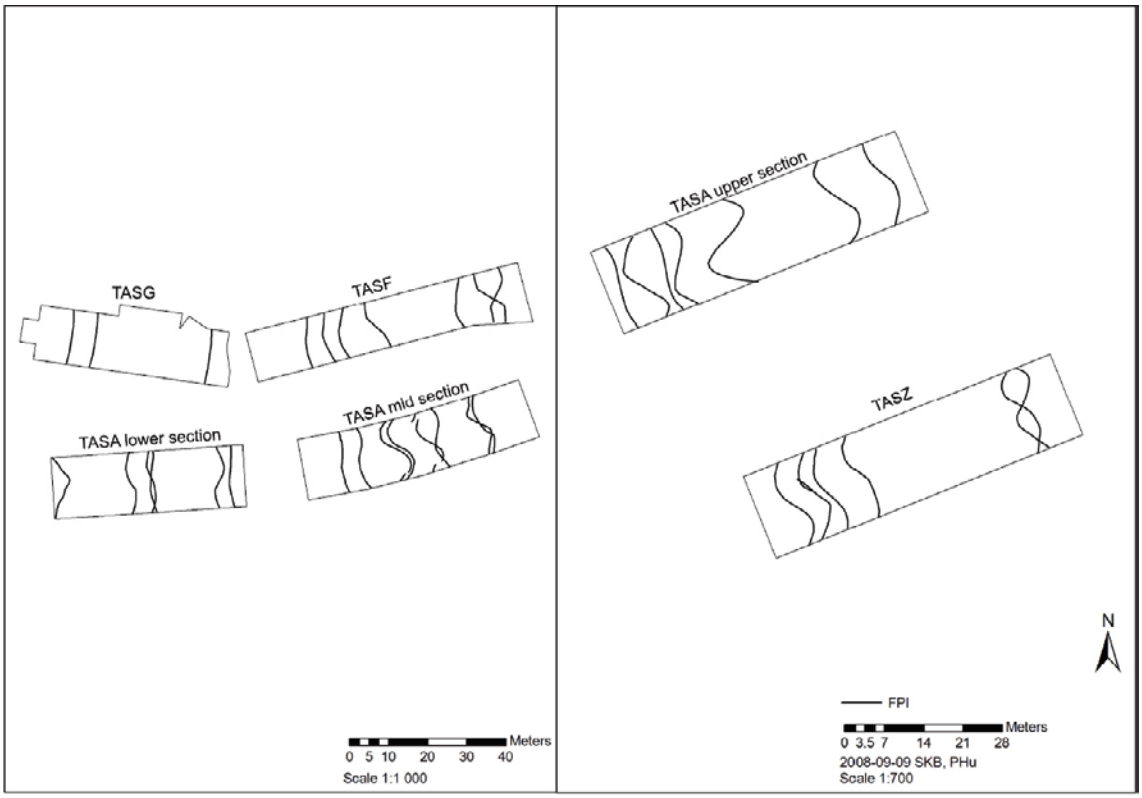

Figure 5-10. *FPI in respective tunnel section including possible FPI:s.*

5.9 Deformation zone

5.9.1 Results

There are two mapped deformation zones in the TBM tunnel sections and one in the drill and blast sections, see Table 5-7 and Figure 5-11.

The deformation zone in the TASA upper section is characterised as a deformation zone: type = unspecified, structure = lamellar, number of fractures 1, fracture spacing = 0 m, strike = 30 and dip = 72. The other deformation zone in TASA lower section is characterised as: type = unspecified, structure = lamellar, fracture spacing = 0.3, strike = 218 and dip = 88. The deformation zone in the drill and blast section, TASF is characterised as: type = unspecified, structure = lamellar, number of fractures = 6, fracture spacing = 0.2 m, strike = 216 and dip = 90.

Table 5-7. Mapped deformation zones in respective tunnel section.

Tunnel section	Stirke	Dip	No Fractures	Spacing (m)	Width (m)	Length (m)	Alteration	Water	Mineral
TASF	216	90	6	0.2	1.2	11.5	3	N	cl, ca
TASA upper section	30	72	1	0	0.5	7.7	2	Y	My
TASA lower section	218	88	8	0.3	3	5.5	3	N	cl, ca

Where cl = chlorite, ca = calcite, My = mylonite.

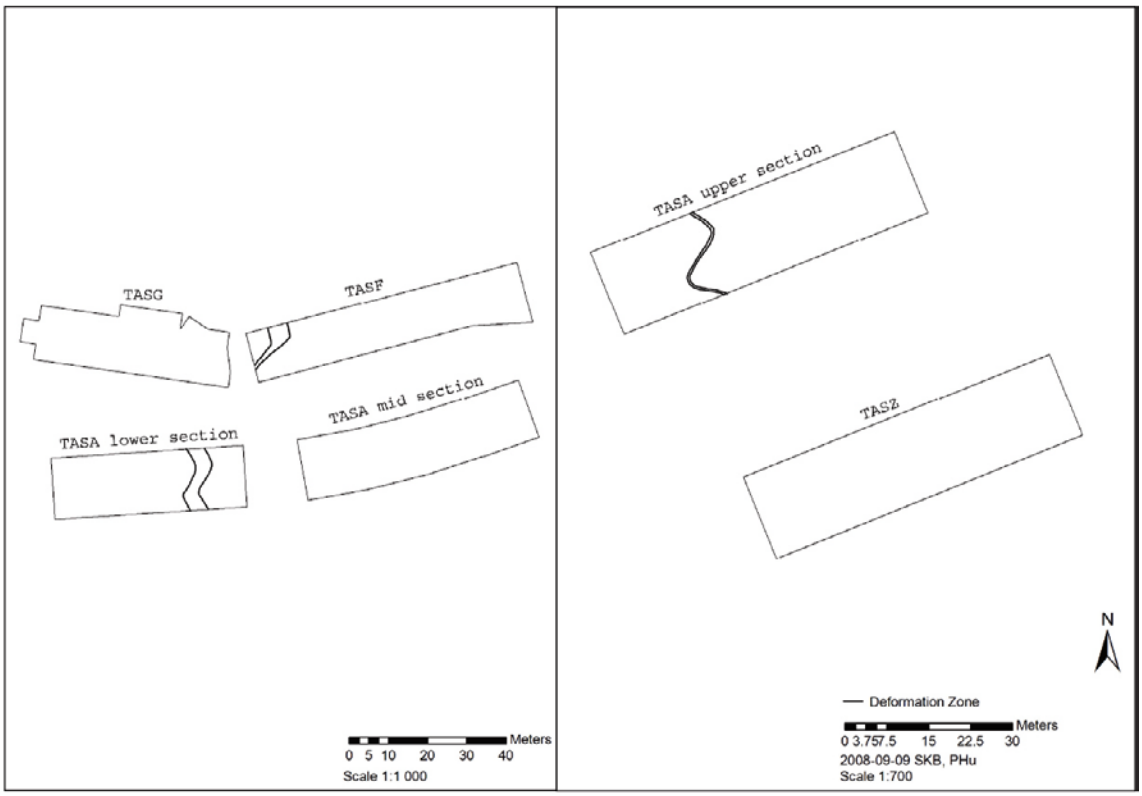

Figure 5-11. *Mapped deformation zones in the respective tunnel sections.*

5.9.2 Comments

There are too few mapped deformation zones in the selected tunnel sections to draw any conclusions regarding the difference to caracterize them depending on the tunnel excavation method. Based on interviews with tunnel mapping geologist it is not anticipated that the mapping and characterisation of deformation zones is sensitive to the difference in tunnel excavation method.

6 Summary and discussions

Even though the present study is very limited it is still considered possible to draw some general conclusions concerning how the choice of tunnel excavation method can affect the performance of the mapping work and subsequent characterisation results. However, when considering these conclusions the following limitations and aspects should be borne in mind:

- Based on the defined criteria for TBM and drill and blast tunnel selection (similar orientation, close proximity to each other, approximate planned repository depth) the only existing tunnels that were identified for assessment were limited to the Äspö Hard Rock Laboratory.
- Total area of tunnels was 5,276 m^2 of which the area of were 2,638 m^2 and 2,638 m^2 in drill and blast and TBM tunnels respectively. Again although the input data is considered good it is at the same time a samll sample population regarding statistical evaluations.
- The evaluations were mainly performed by a limited statistical analysis of characterisation data from the TMS data base. Only very limited control could be performed on the data and the mapping was not performed and tailor made for the purposes of the current study.
- A field inspection could only be performed on two TBM sections since parts of the tunnels were unavailable due to other experiments or their surfaces partly covered by shotcrete. Whilst TMS is considered to provide a reasonable data set for the current study it should be noted that tunnel excavation technology and especially SKB:s tunnel mapping technology are continually being developed and those available at the time of the actual repository excavation may be considerably more advanced than those applied during the Äspö excavations and assessed here. These developments may well lead to changes in the ability to identify fracture geometries and improve fracture characterisation particularly in the processing of complex drill and blast wall geometries.
- The main strategy of the study was to compare results from the earlier performed TMS mapping, parameter by parameter. By evaluation the results of these comparisons, eventual difference in the possibility of geological characterisation of tunnels excavated by the two different tunnelling methods were identified.
- Even if the tunnel sections where data were compared had the same orientations and were close to each other every rock wall are unique, in special for some parameters, in special for larger characterisation objects where individuals rather than statistics are compared.

Based on the results and comments on each specific parameter discussed in Chapter 5, the main results and conclusions of the study are discussed and summarised as follows:

- The mapping and characterisation of rock types, more specifically the parameters colour, grain size, texture and alteration do not appear to be sensitive to the tunnel excavation method applied. Generally speaking it is assumed due to the regular cylindrical form of a TBM tunnel that it is easier to more accurately map rock type boundary geometries compared to the irregular tunnel wall geometry of a drill and blast tunnel.
- Regarding fracture intensity, minor differences in the P_{21} values were noted but differences are small and are not considered significant. The same is true of the differences in fracture orientation data between the two excavation methods. However, it is considered likely the greater accessibility to exposed fracture surfaces that is provided by a drill and blast tunnel wall would make it easier to give a more complete description of the character of the natural fracture surfaces, their detailed geometry as well as their mineralogy and continuity of infillings and any associated alteration.

- For fracture mineral intensity, minor differences in P_{21} values were noted but differences are small and are not considered relevant for the choice of excavation method. However, it should be noted that the mapping geologists have consistently reported that it is easier to map and describe fracture fillings in a drill and blast tunnel.
- It is considered that a TBM tunnel makes it much easier to obtain a more representative picture of the pattern of water flow in the fractures intercepting the tunnel roof and wall. It appears likely that the existence of a damage zone associated with the excavation of a conventional drill and blast tunnel, even employing careful blasting techniques, inevitably leads to a disturbance of the in situ pattern of water flow around the tunnel. This is considered not primarily due to the generation of new fractures associated with blasting but rather to the local modification in the degree of openness, connectivity, resulting channelling and two phase flow through fractures surrounding the tunnel.
- The number of mapped FPI fractures in the TBM tunnels was slightly more than in the drill and blast tunnels. However, the total number of objects were too limited to draw any conclusion whether the cylindrical and smother tunnel wall geometry of the TBM is significant more favourable for detecting FPI fractures.
- There were too few mapped deformation zones in the selected tunnel sections to draw any conclusions as regards how the excavation method may affect the performance or reliability of the characterisation process. However, general mapping experience by the geologists in the mapping team the suggests that the identification of these type of structures is particularly not sensitive to the excavation method.

In general, the present study has not identified any significant differences in the mapping results that can be related to the method of tunnel excavation. It should be noted that the available data set is too limited to perform a wide ranging robust statistical analysis, however, none of the results of the present study have identified any significant differences in the mapping parameters that are of sufficient dignity that they need to be taken into account when selecting a tunnel excavation method, e.g. drill and blast or TBM.

References

Dershowitz W, Herda H H, 1992. Interpretation of fracture spacing and intensity. Proc. U.S. Symp. Rock Mech. 33:757-766.

Eliasson T, 1993. Mineralogy, geochemistry and petrophysics of red coloured granite adjacent to fractures. SKB TR 93-06, Svensk Kärnbränslehantering AB.

Markström I, Erlström M, 1996. Overview of documentation of tunnel, niches and core boreholes. SKB PR HRL-96-19, Svensk Kärnbränslehantering AB.

Markström I, 1997. Uppdated overviwe of documentation of side tunnels and niches. Documentation updated after Supplementary excavations performed during 1996 and 1997. SKB PR HRL-97-20, Svensk Kärnbränslehantering AB.

Munier R, 2006. Using observations in deposition tunnels to avoid intersections with critical fractures in deposition holes. SKB R-06-54, Svensk Kärnbränslehantering AB.

Stanfors R, Olsson P, Stille H, 1997. Äspö HRL-Geosientific evaluation 1997/3. Results from pre-investigations and detailed site characterization. Comparsion of predictions and observations. Geology and Mechanical stability. SKB TR-97-04, Svensk Kärnbränslehantering AB.

Wikman H, Kornfält K A, 1995. Äspö HRL, Updating of a lithological model of the bedrock of the Äspö area. SKB PR 25-95-04, Svensk Kärnbränslehantering AB.

Appendix A

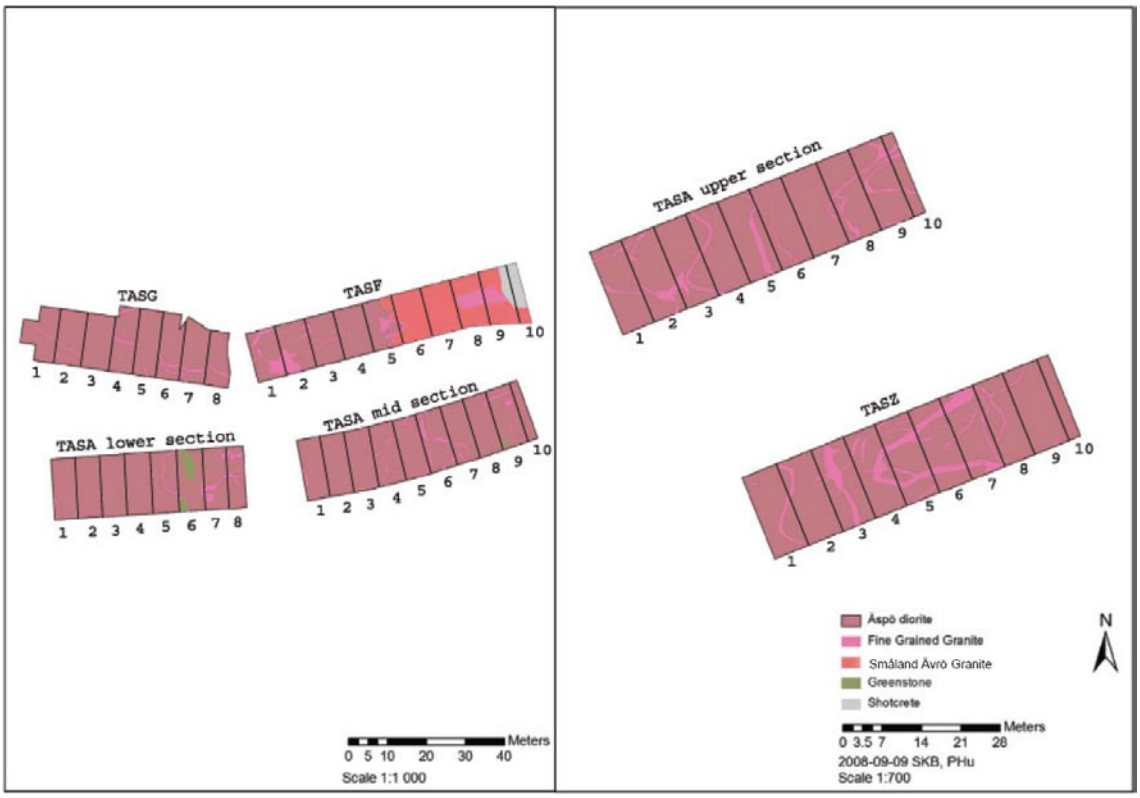

Figure A-1. *Tunnel sections, divided into smaller areas approximately 100 m².*

Table A-1. TASA upper section, rock types in percentage.

TASA upper section	Section area	Äspö diorit	Fine grained granite	Greenstone	Småland Ävrö granite	Shotcrete
Section 1	99.941	96.0	4.0	0.0	0.0	0.0
Section 2	99.768	87.7	12.3	0.0	0.0	0.0
Section 3	98.632	90.8	9.2	0.0	0.0	0.0
Section 4	99.419	94.9	5.1	0.0	0.0	0.0
Section 5	99.977	88.0	12.0	0.0	0.0	0.0
Section 6	100.015	96.3	3.7	0.0	0.0	0.0
Section 7	99.837	99.0	1.0	0.0	0.0	0.0
Section 8	99.895	92.0	8.0	0.0	0.0	0.0
Section 9	99.905	93.9	6.1	0.0	0.0	0.0
Section 10	35.857	89.5	10.5	0.0	0.0	0.0

Table A-2. TASZ, rock types in percentage.

TASZ	Section area	Äspö diorit	Fine grained granite	Greenstone	Småland Ävrö granite	Shotcrete
Section 1	100.006	94.8	5.2	0.0	0.0	0.0
Section 2	100.006	94.9	5.1	0.0	0.0	0.0
Section 3	100.006	76.9	23.1	0.0	0.0	0.0
Section 4	100.006	83.4	16.6	0.0	0.0	0.0
Section 5	100.006	95.1	4.9	0.0	0.0	0.0
Section 6	100.006	83.0	17.0	0.0	0.0	0.0
Section 7	100.006	86.0	14.0	0.0	0.0	0.0
Section 8	100.006	93.8	6.2	0.0	0.0	0.0
Section 9	100.006	98.6	1.4	0.0	0.0	0.0
Section 10	25.811	100.0	0.0	0.0	0.0	0.0

Table A-3. TASA mid section, rock types in percentage.

TASA mid section	Section area	Äspö diorit	Fine grained granite	Greenstone	Småland Ävrö granite	Shotcrete
Section 1	100.37	98.9	1.1	0.0	0.0	0.0
Section 2	100.379	100.0	0.0	0.0	0.0	0.0
Section 3	99.913	96.9	3.1	0.0	0.0	0.0
Section 4	99.95	95.7	4.3	0.0	0.0	0.0
Section 5	99.986	96.5	3.5	0.0	0.0	0.0
Section 6	99.824	86.9	13.1	0.0	0.0	0.0
Section 7	99.938	96.1	3.9	0.0	0.0	0.0
Section 8	100.405	98.8	0.7	0.5	0.0	0.0
Section 9	100.298	91.5	6.3	2.2	0.0	0.0
Section 10	39.975	98.5	1.5	0.0	0.0	0.0

Table A-4. TASF, rock types in percentage.

TASF	Section area	Äspö diorit	Fine grained granite	Greenstone	Småland Ävrö granite	Shotcrete
Section 1	99.963	77.7	22.3	0.0	0.0	0.0
Section 2	99.871	78.7	21.3	0.0	0.0	0.0
Section 3	99.778	95.9	4.1	0.0	0.0	0.0
Section 4	99.688	99.3	0.7	0.0	0.0	0.0
Section 5	99.594	77.2	12.5	0.0	10.3	0.0
Section 6	99.501	0.0	1.8	0.0	98.2	0.0
Section 7	99.409	0.0	0.0	0.0	100.0	0.0
Section 8	99.11	0.0	0.0	0.0	100.0	0.0
Section 9	100.86	0.0	0.0	0.0	81.7	18.3
Section 10	45.46	0.0	0.0	0.0	26.4	73.6

Table A-5. TASA lower section, rock types in percentage.

TASA lower section	Section area	Äspö diorit	Fine grained granite	Greenstone	Småland Ävrö granite	Shotcrete
Section 1	100.041	99.3	0.7	0.0	0.0	0.0
Section 2	100.106	100.0	0.0	0.0	0.0	0.0
Section 3	100.275	100.0	0.0	0.0	0.0	0.0
Section 4	100.391	100.0	0.0	0.0	0.0	0.0
Section 5	100.508	95.2	4.8	0.0	0.0	0.0
Section 6	100.625	74.2	1.3	24.6	0.0	0.0
Section 7	100.111	87.1	12.9	0.0	0.0	0.0
Section 8	68.768	92.4	7.6	0.0	0.0	0.0

Table A-6. TASG, rock types in percentage.

TASG	Section area	Äspö diorit	Fine grained granite	Greenstone	Småland Ävrö granite	Shotcrete
Section 1	99.74	97.3	2.7	0.0	0.0	0.0
Section 2	99.964	98.0	2.0	0.0	0.0	0.0
Section 3	99.965	99.3	0.7	0.0	0.0	0.0
Section 4	100.023	95.4	4.6	0.0	0.0	0.0
Section 5	98.6	99.1	0.9	0.0	0.0	0.0
Section 6	99.915	95.4	4.6	0.0	0.0	0.0
Section 7	99.962	95.1	4.9	0.0	0.0	0.0
Section 8	73.248	97.0	3.0	0.0	0.0	0.0

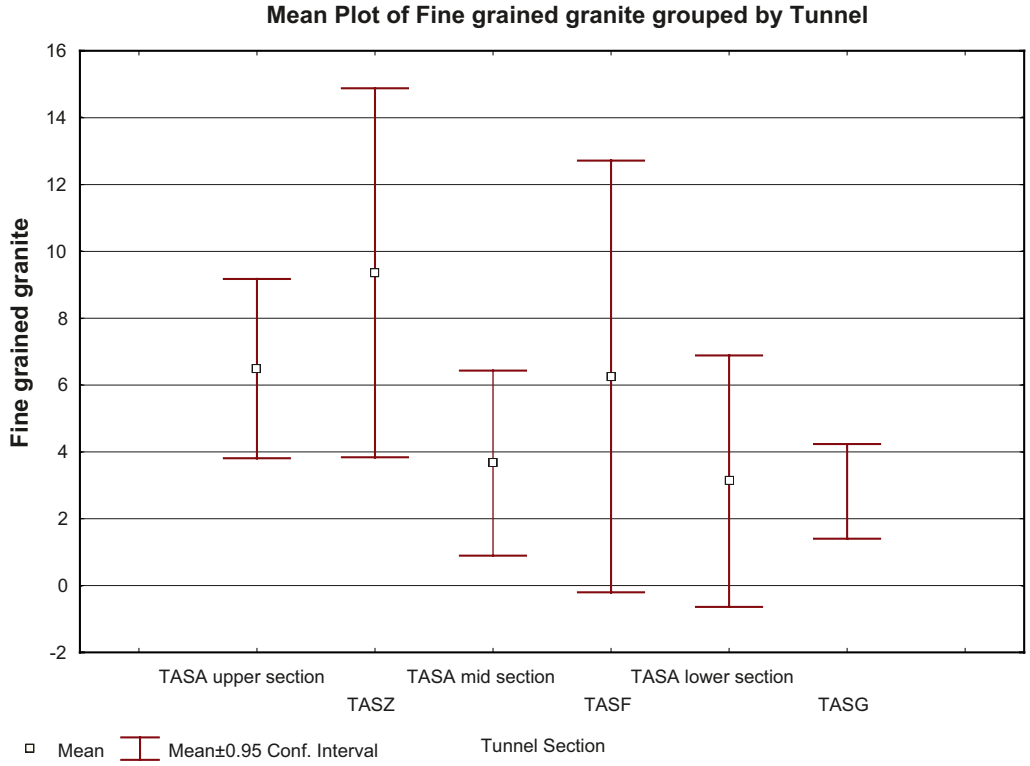

Figure A-2. *Mean Plot of Fine grained granite.*

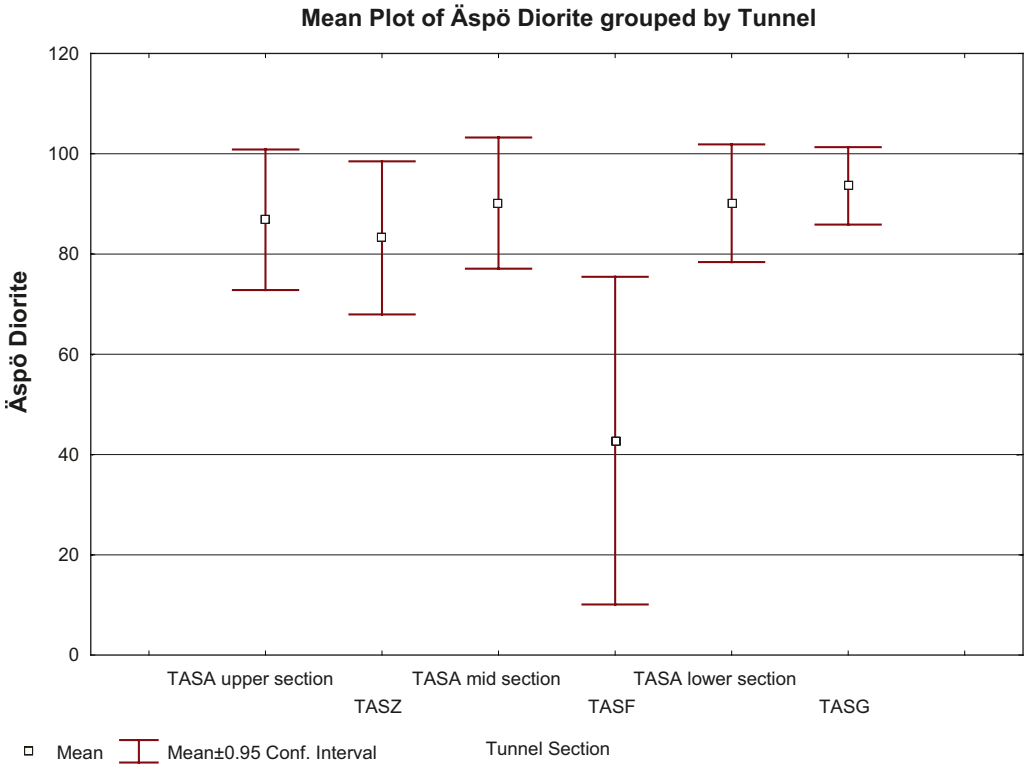

Figure A-3. *Mean Plot of Äspö Diorite.*

Appendix B

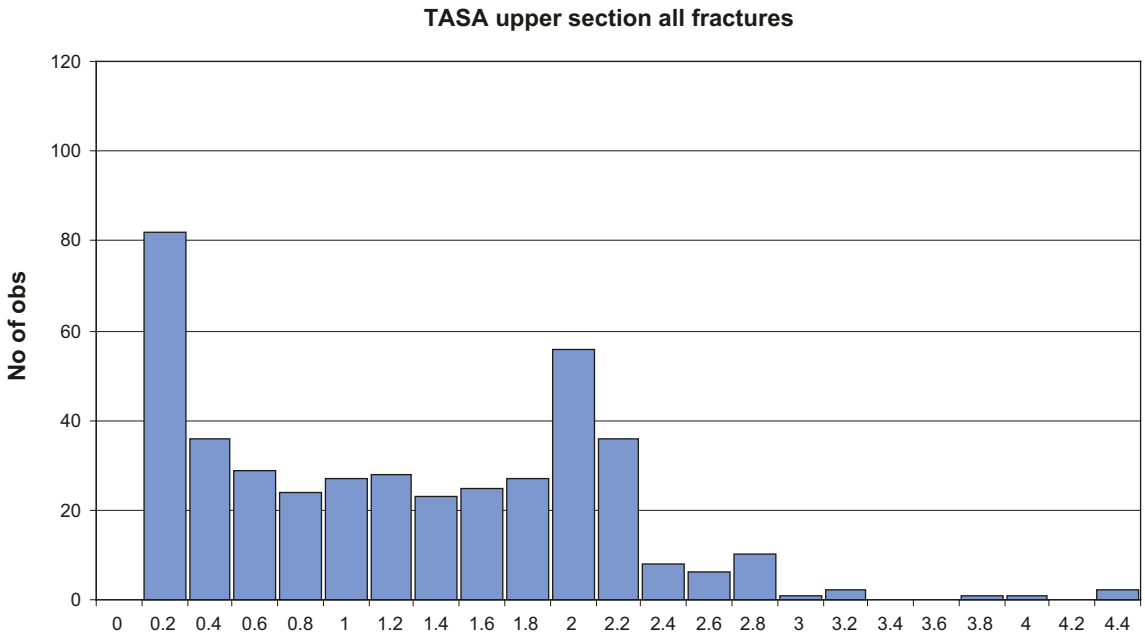

Figure B-1. *Histogram, TASA upper section all fractures search radius 0.5 meters.*

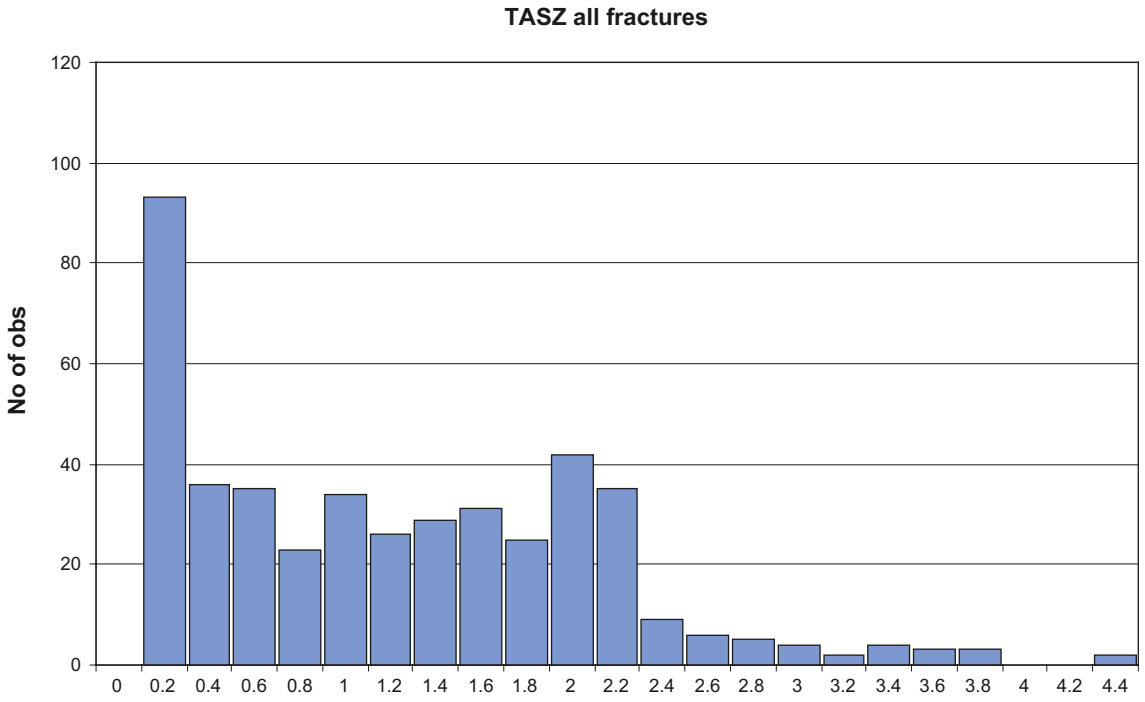

Figure B-2. *Histogram, TASZ all fractures search radius 0.5 meters.*

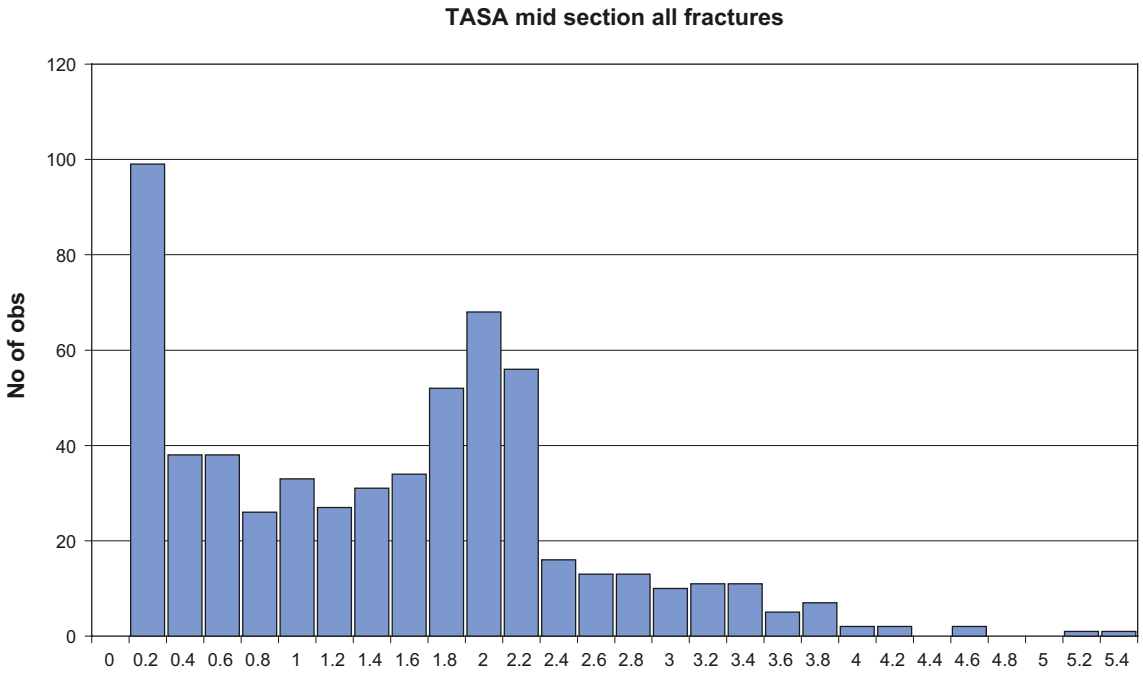

Figure B-3. *Histogram, TASA mid section all fractures search radius 0.5 meters.*

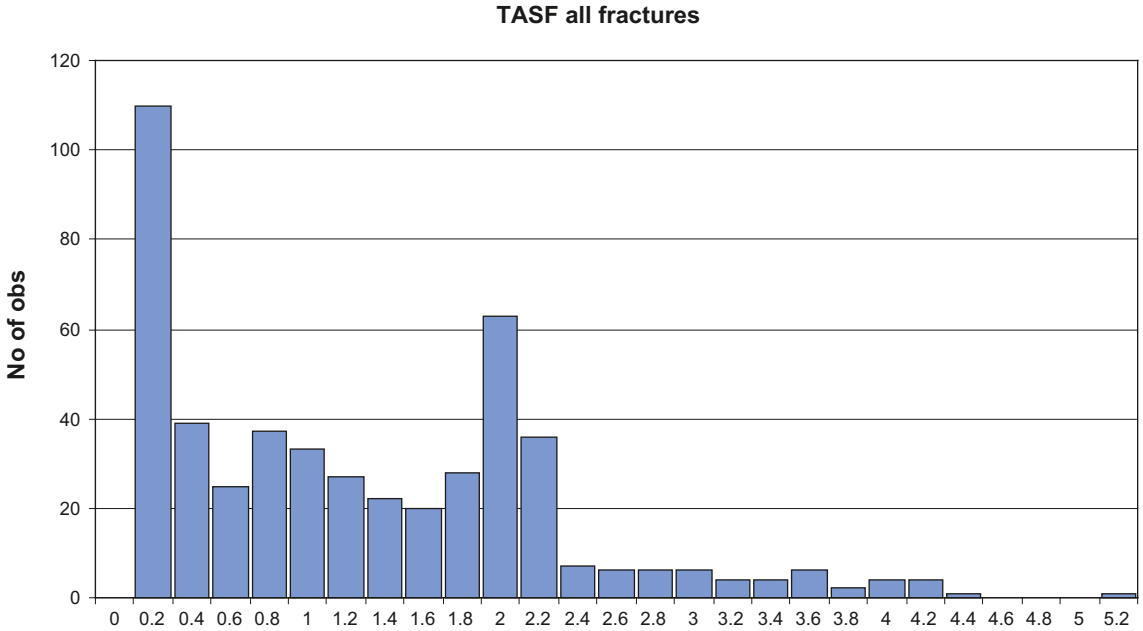

Figure B-4. *Histogram, TASF all fractures search radius 0.5 meters.*

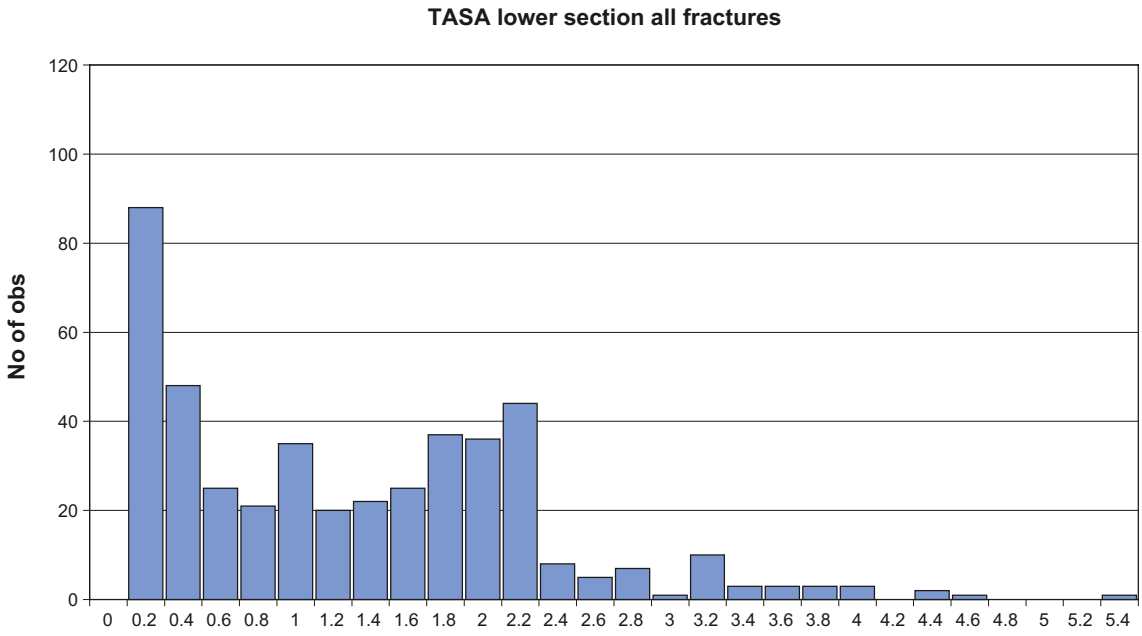

Figure B-5. *Histogram, TASA lower section all fractures search radius 0.5 meters.*

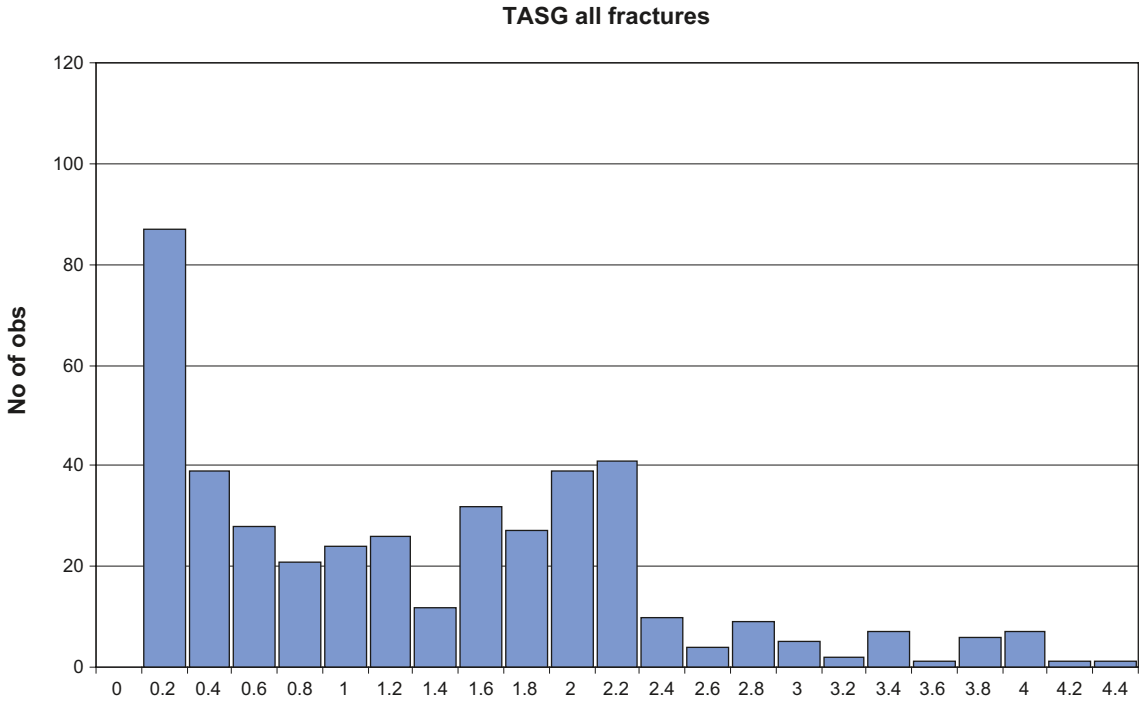

Figure B-6. *Histogram, TASG all fractures search radius 0.5 meters.*

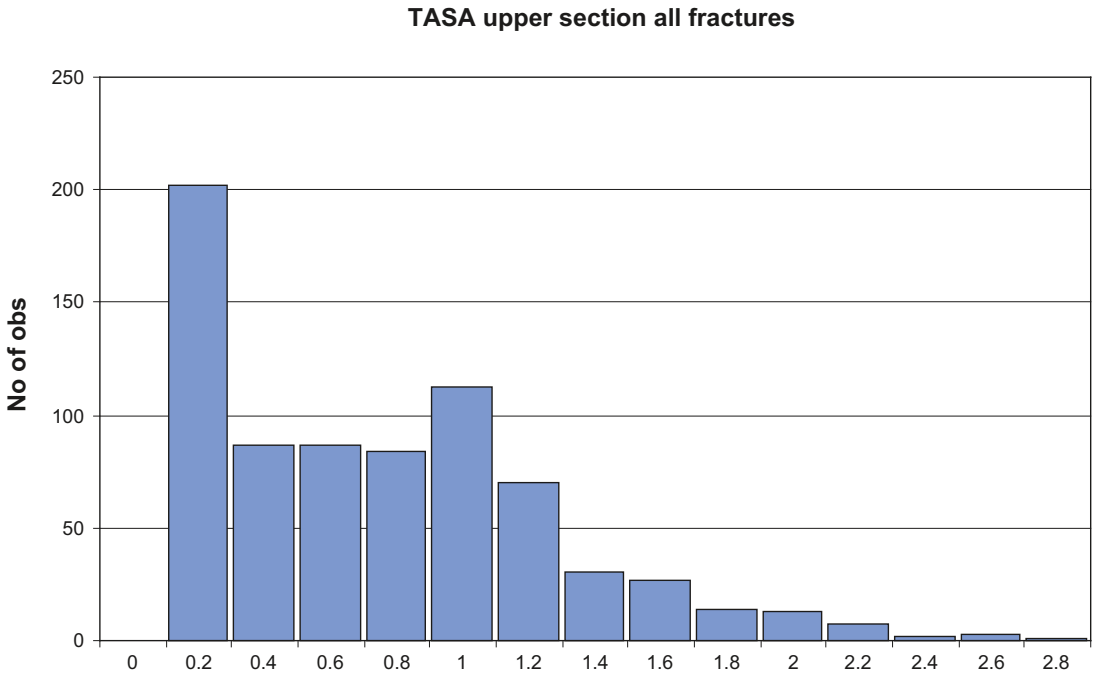

Figure B-7. *Histogram, TASA upper section all fractures search radius 1 meter.*

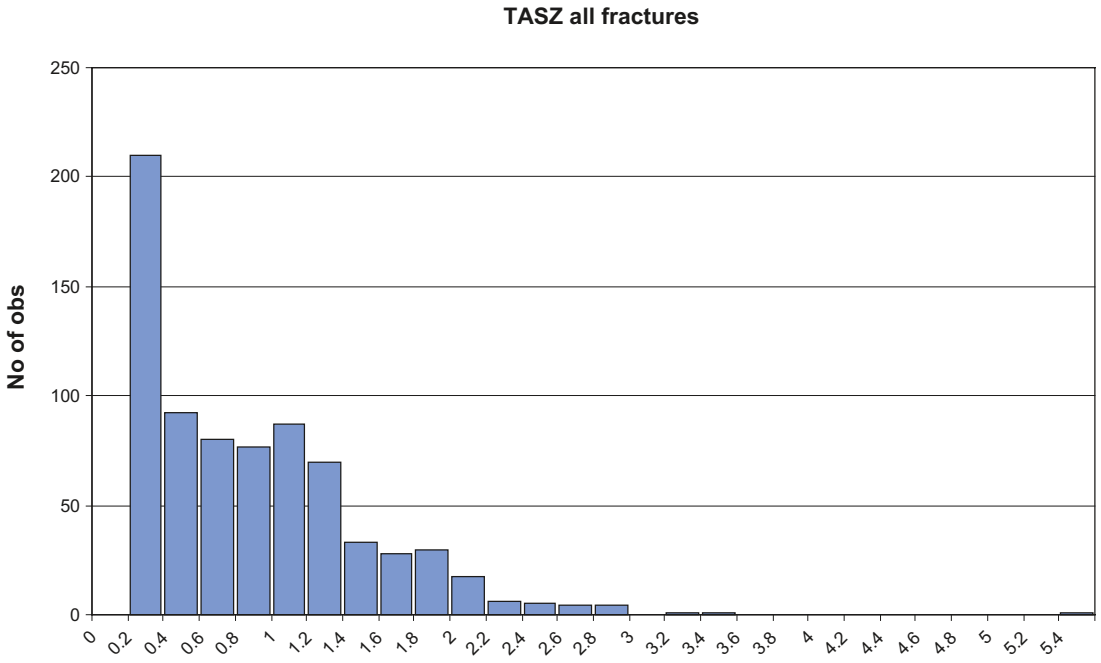

Figure B-8. *Histogram, TASZ all fractures search radius 1 meter.*

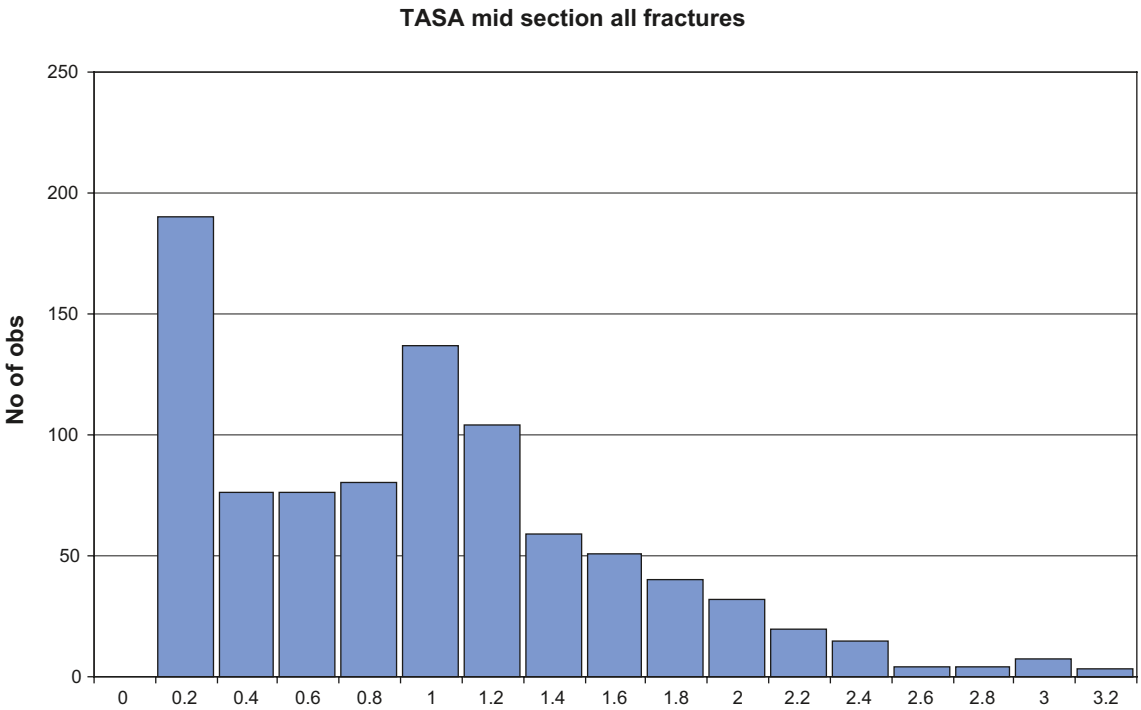

Figure B-9. *Histogram, TASA mid section all fractures search radius 1 meter.*

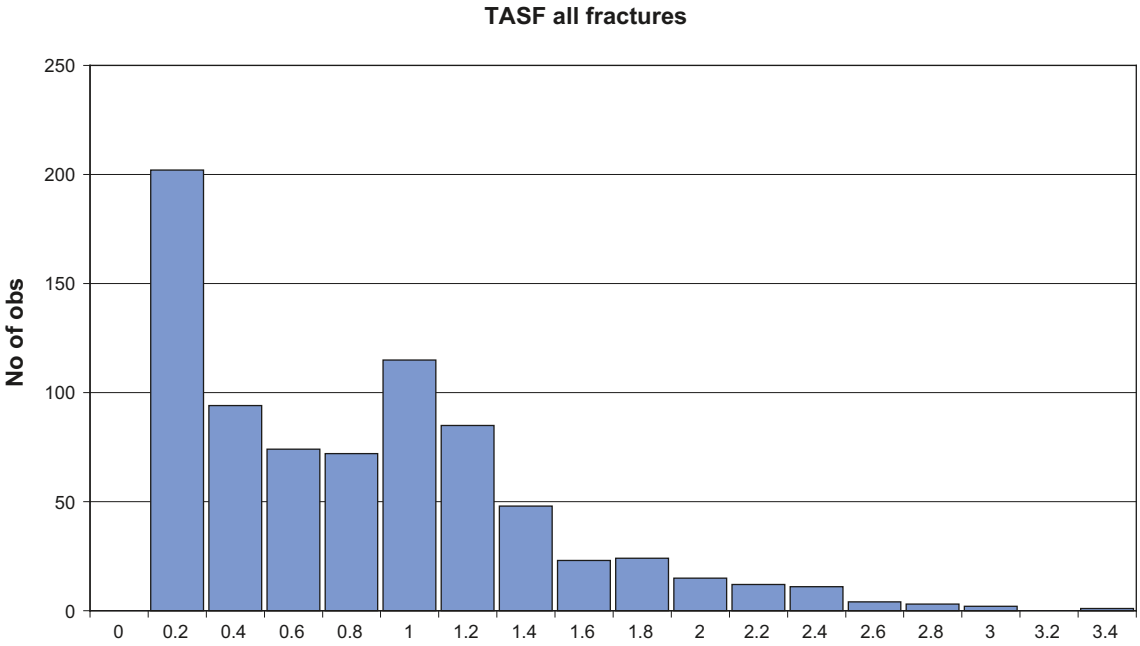

Figure B-10. *Histogram, TASF all fractures search radius 1 meter.*

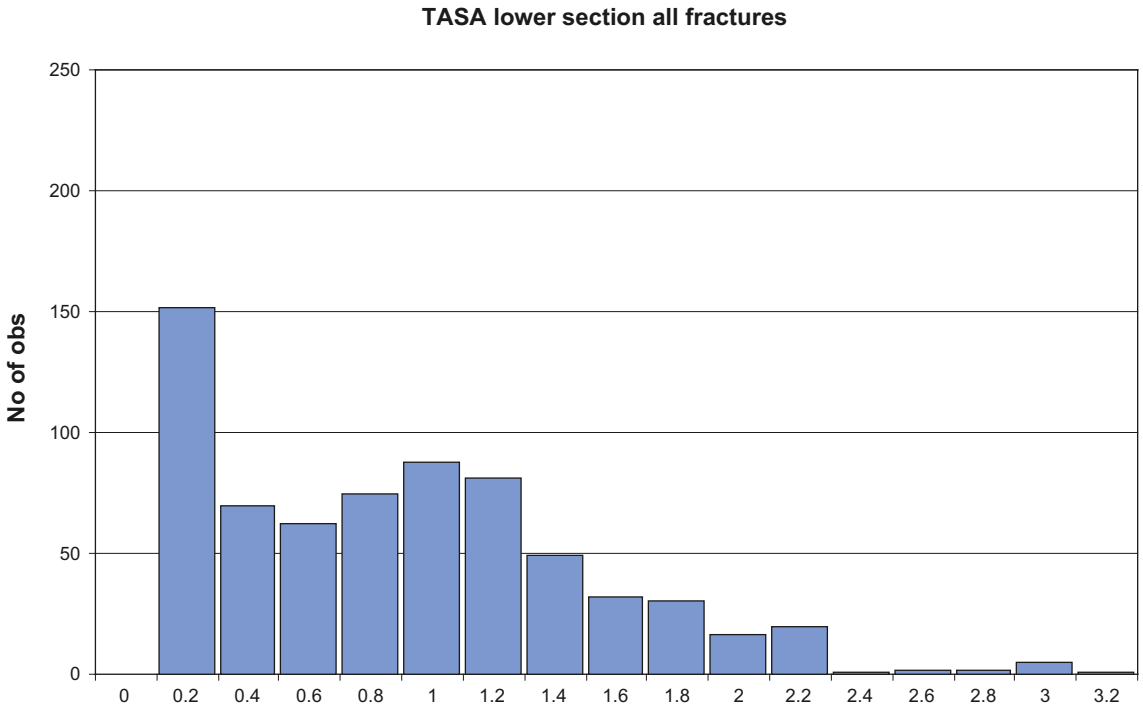

Figure B-11. *Histogram, TASA lower section all fractures search radius 1 meter.*

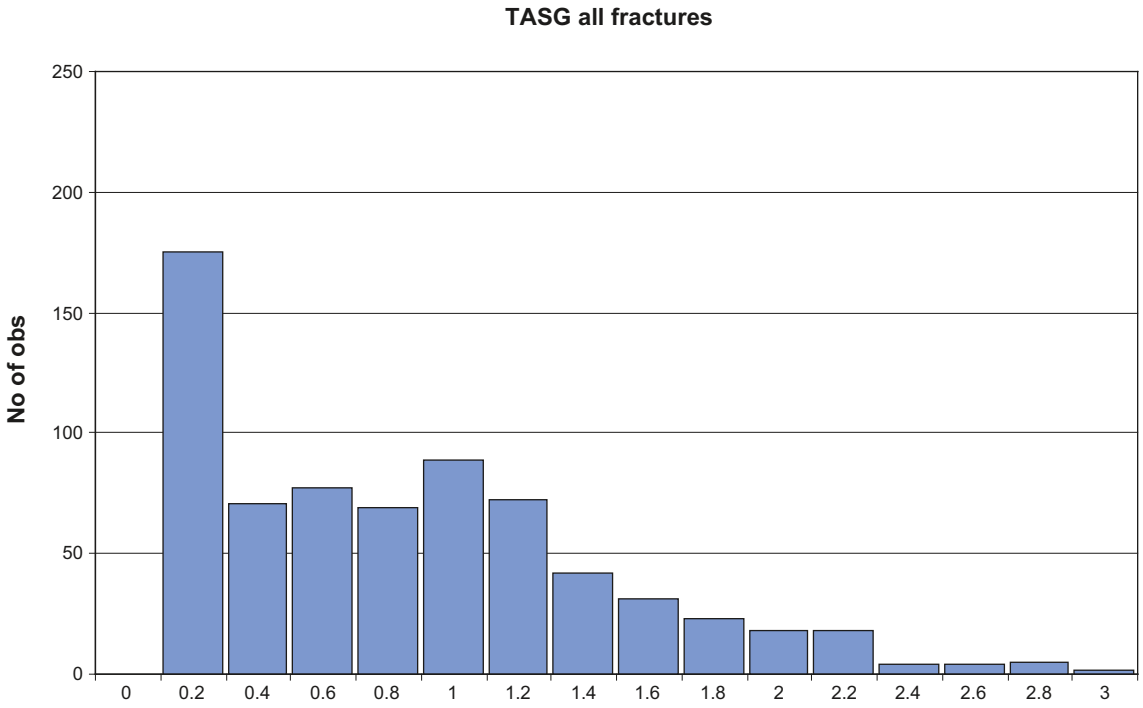

Figure B-12. *Histogram, TASF all fractures search radius 1 meter.*

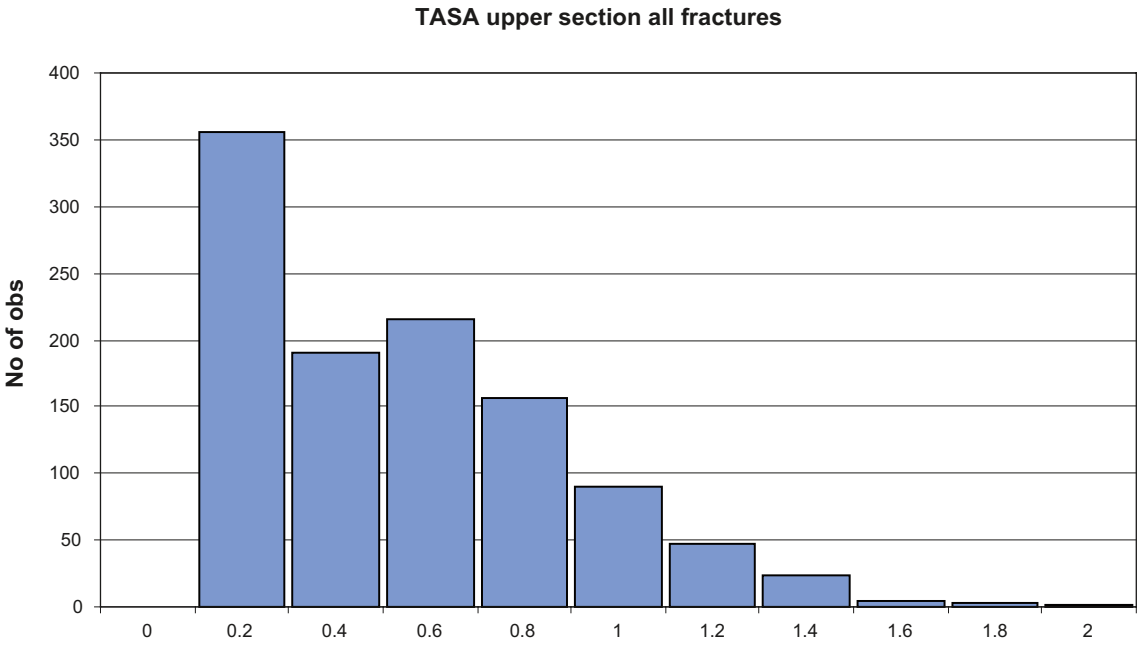

Figure B-13. *Histogram, TASA upper section all fractures search radius 2 meters.*

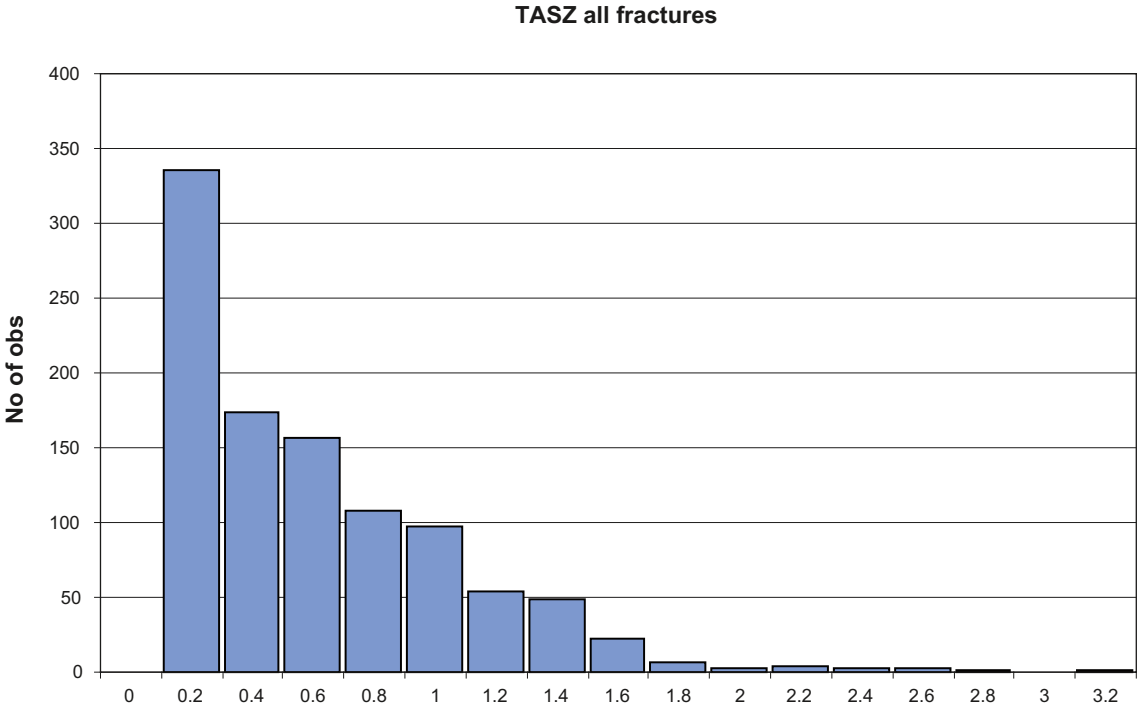

Figure B-14. *Histogram, TASZ all fractures search radius 2 meters.*

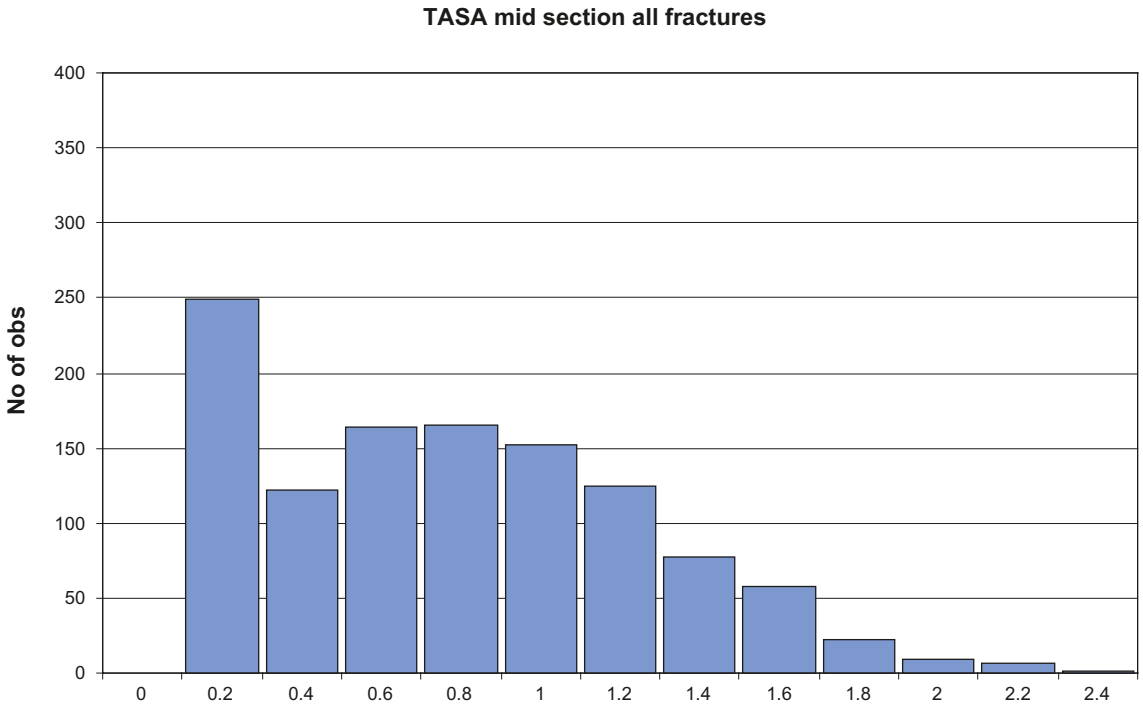

Figure B-15. *Histogram, TASA mid section all fractures search radius 2 meters.*

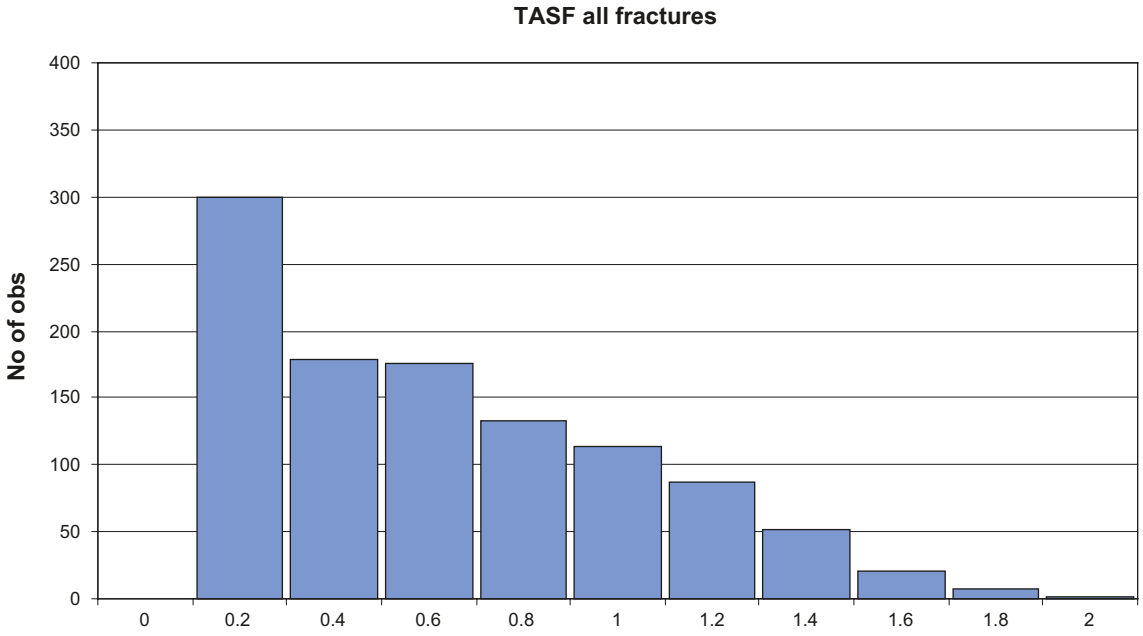

Figure B-16. *Histogram, TASF all fractures search radius 2 meters.*

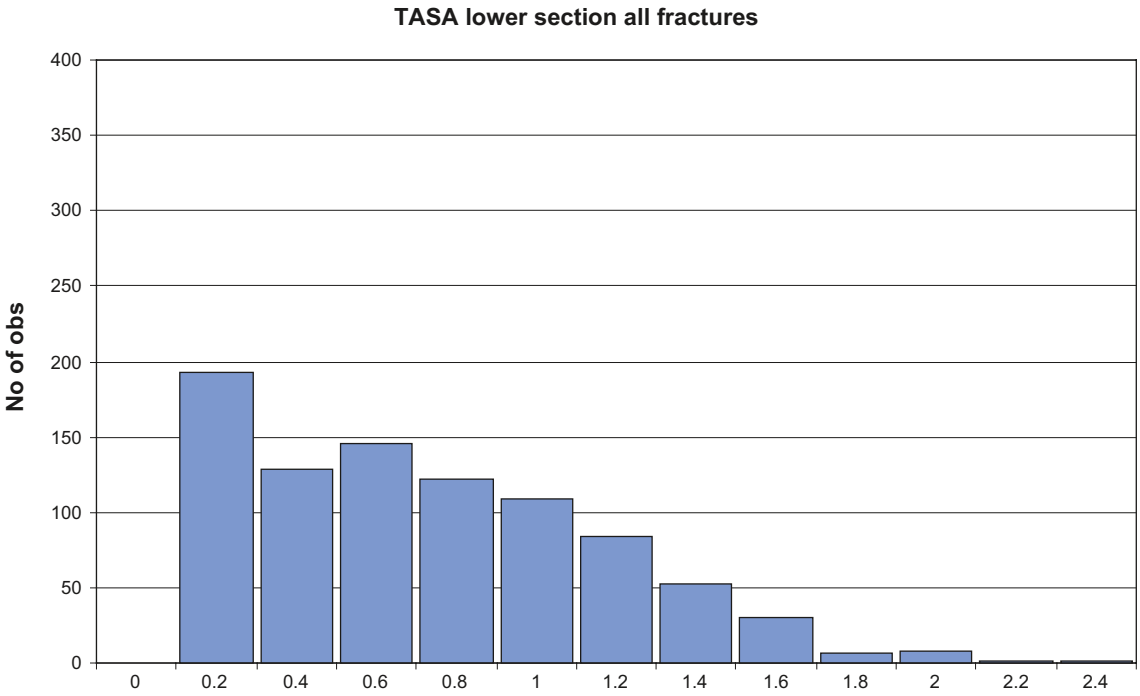

Figure B-17. *Histogram, TASA lower section all fractures search radius 2 meters.*

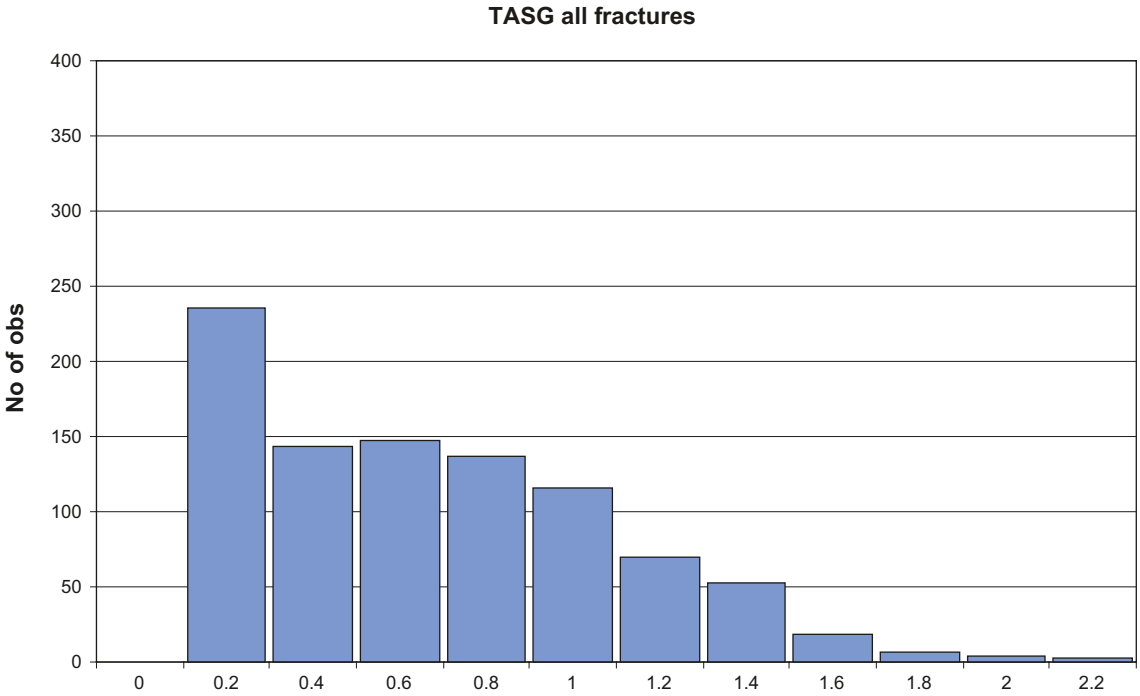

Figure B-18. *Histogram, TASG all fractures search radius 2 meters.*

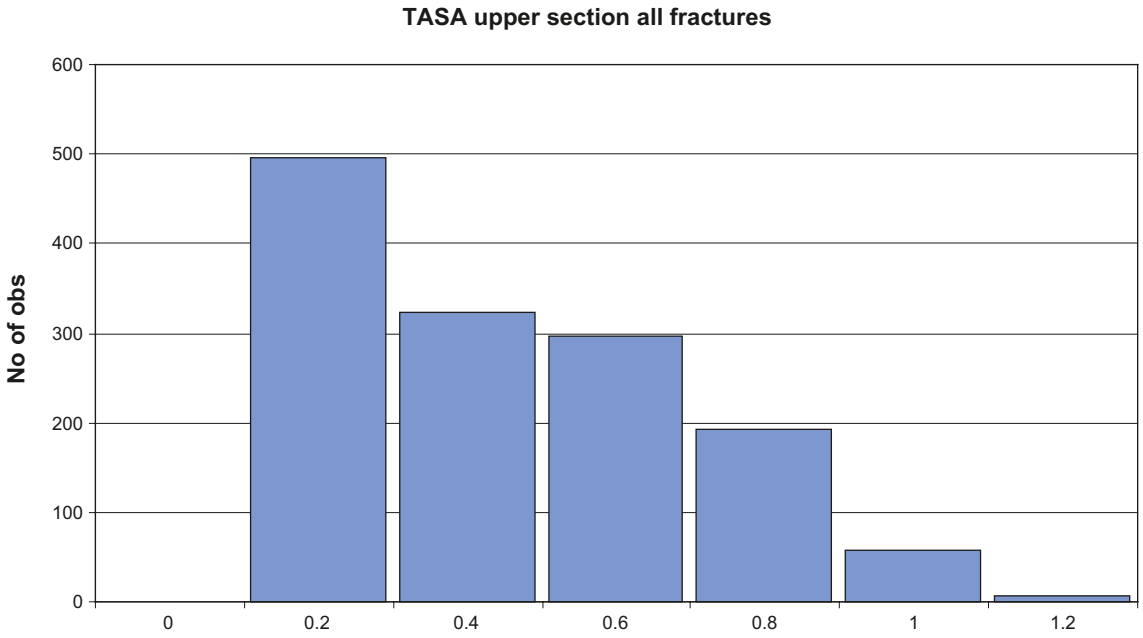

Figure B-19. *Histogram, TASA upper section all fractures search radius 4 meters.*

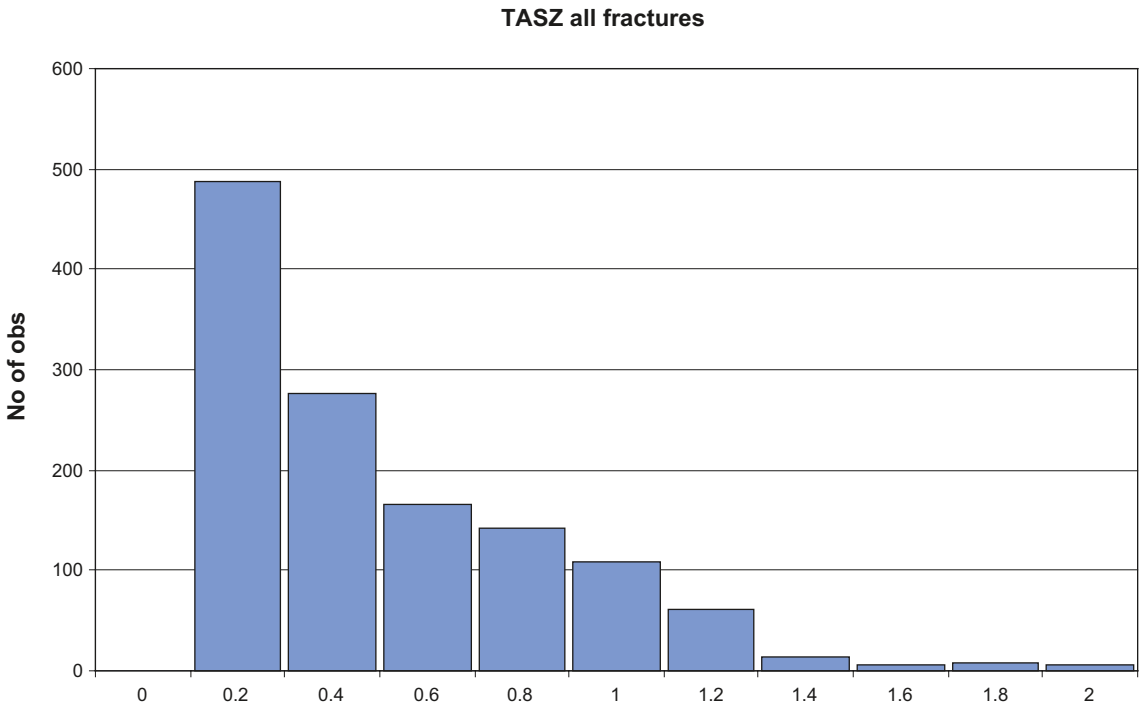

Figure B-20. *Histogram, TASZ all fractures search radius 4 meters.*

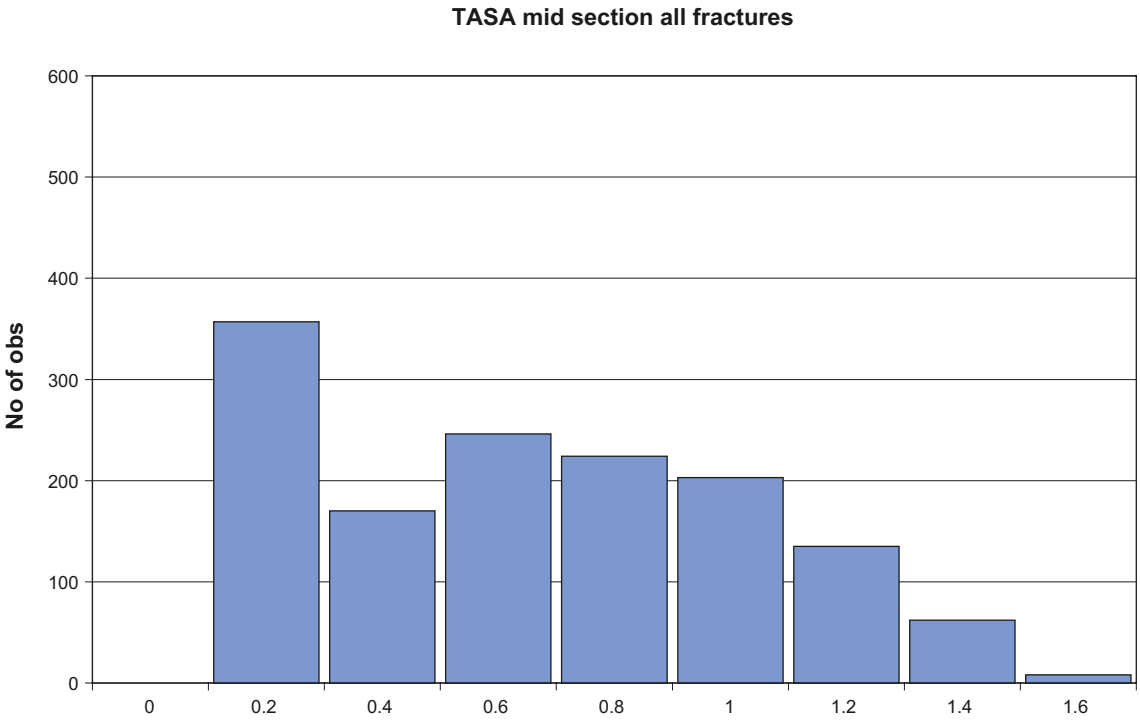

Figure B-21. *Histogram, TASA mid section all fractures search radius 4 meters.*

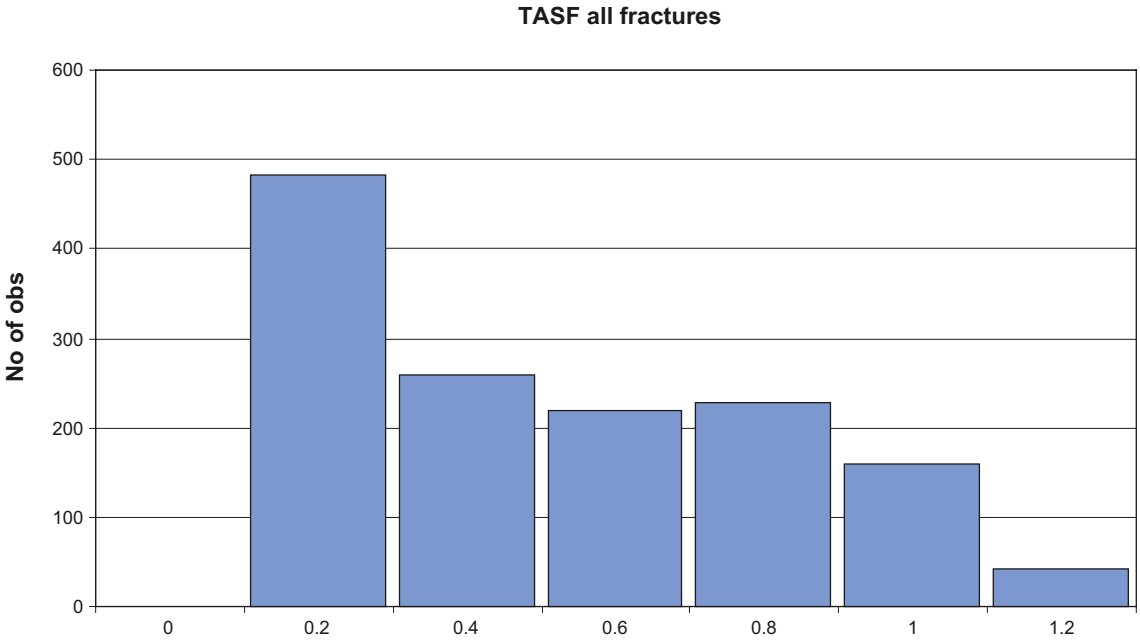

Figure B-22. *Histogram, TASF all fractures search radius 4 meters.*

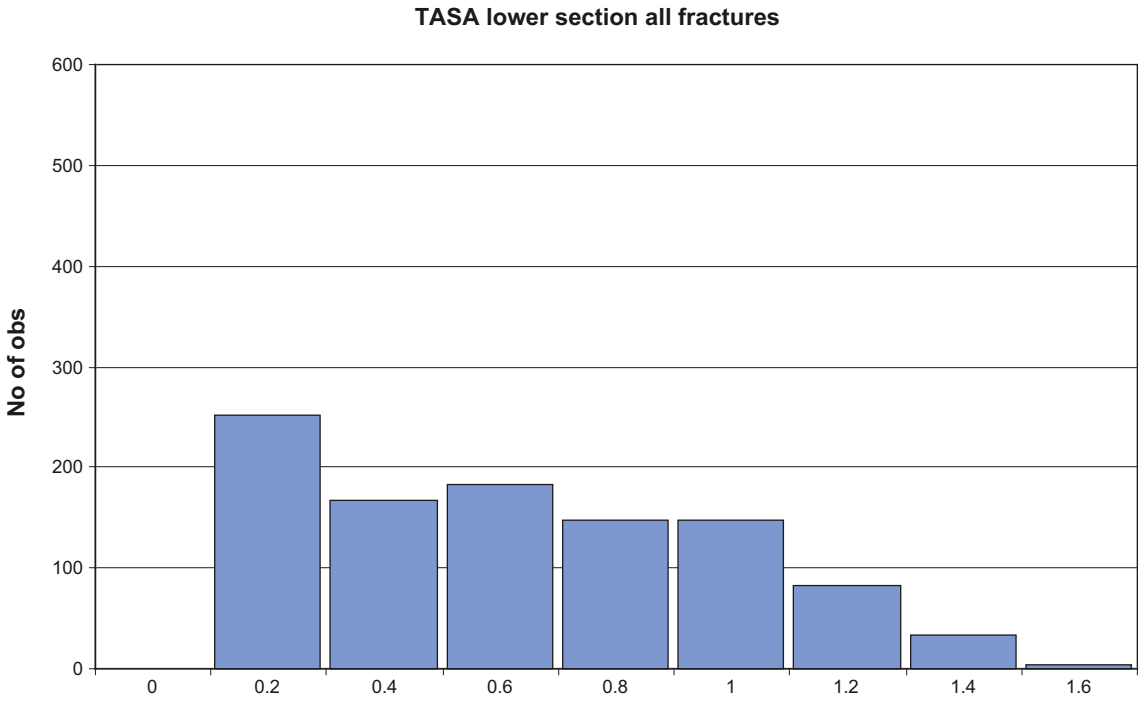

Figure B-23. *Histogram, TASA lower section all fractures search radius 4 meters.*

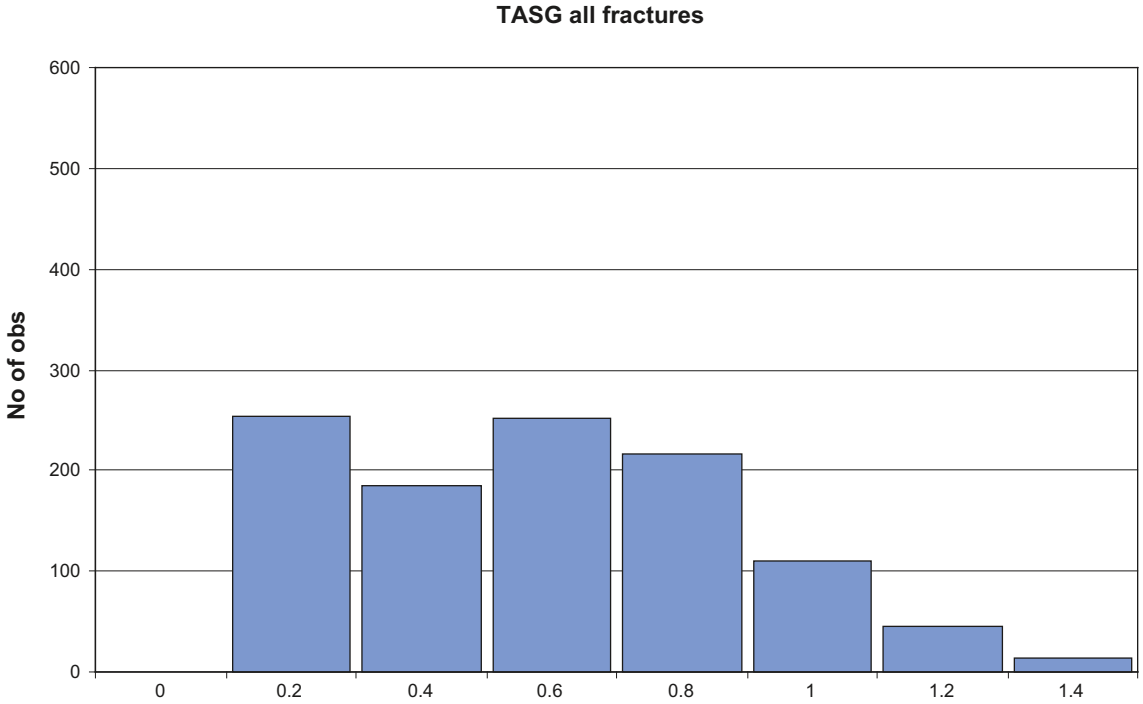

Figure B-24. *Histogram, TASG all fractures search radius 4 meters.*

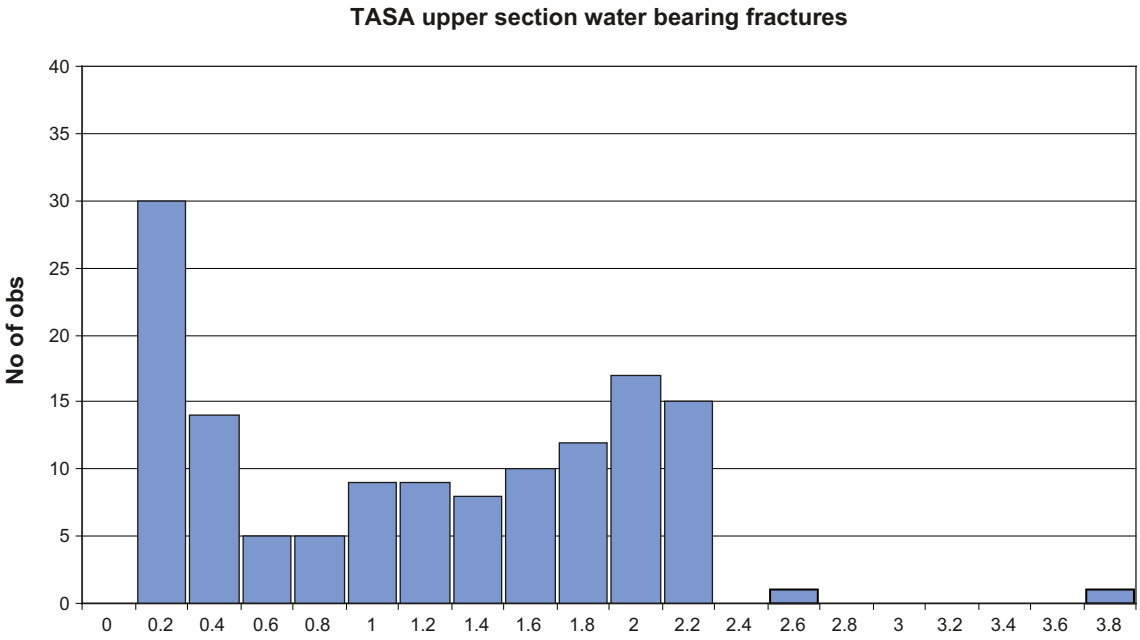

Figure B-25. *Histogram, TASA upper section water bearing fractures search radius 0.5 meters.*

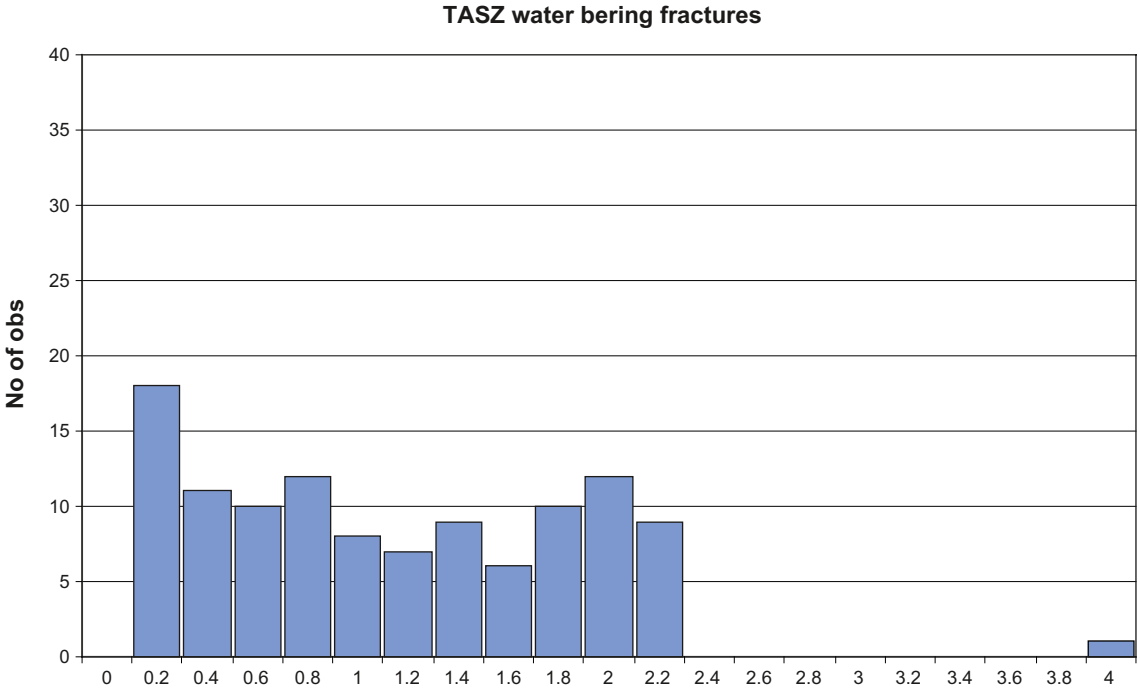

Figure B-26. *Histogram, TASZ water bearing fractures search radius 0.5 meters.*

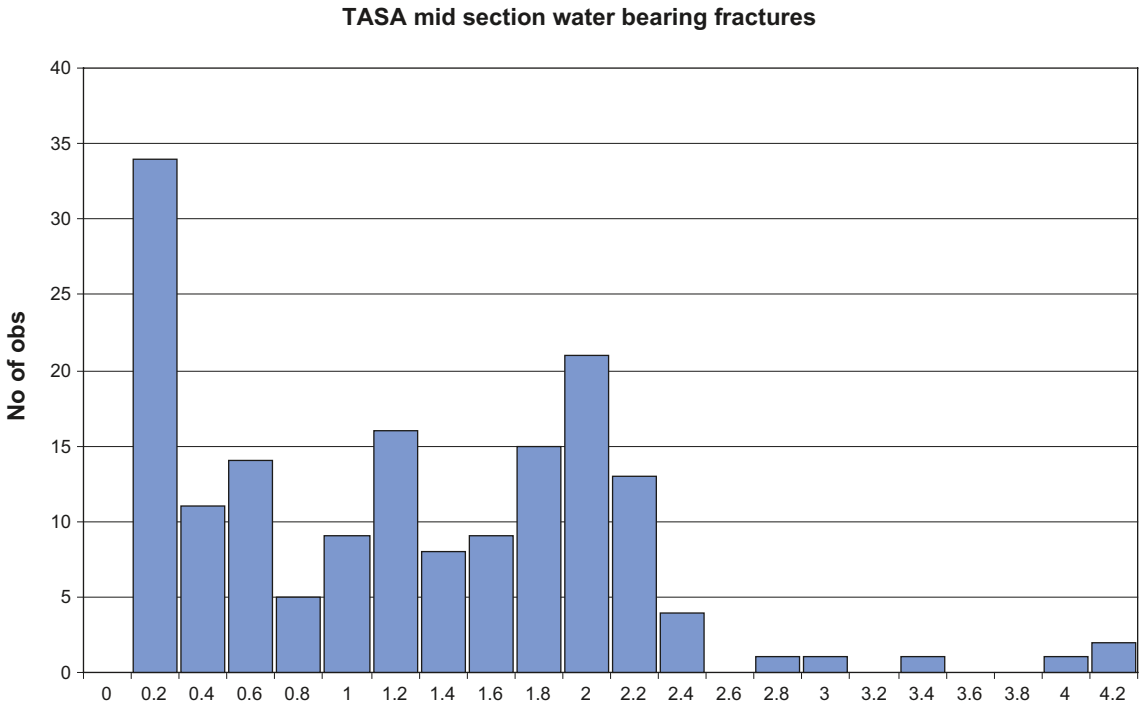

Figure B-27. *Histogram, TASA mid section water bearing fractures search radius 0.5 meters.*

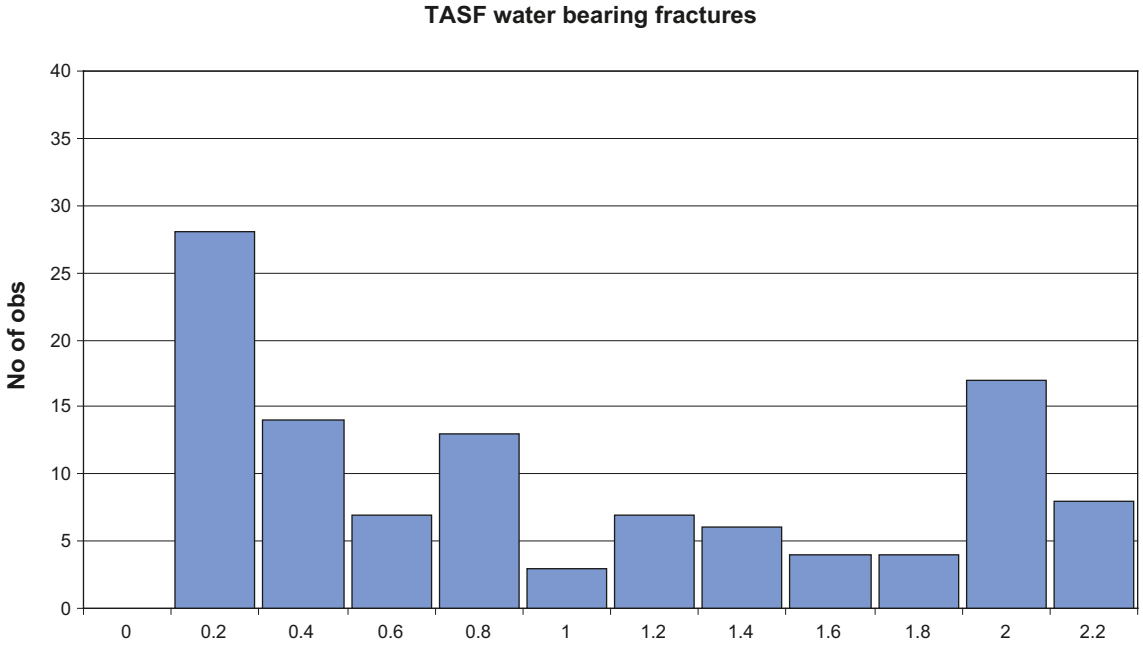

Figure B-28. *Histogram, TASF water bearing fractures search radius 0.5 meters.*

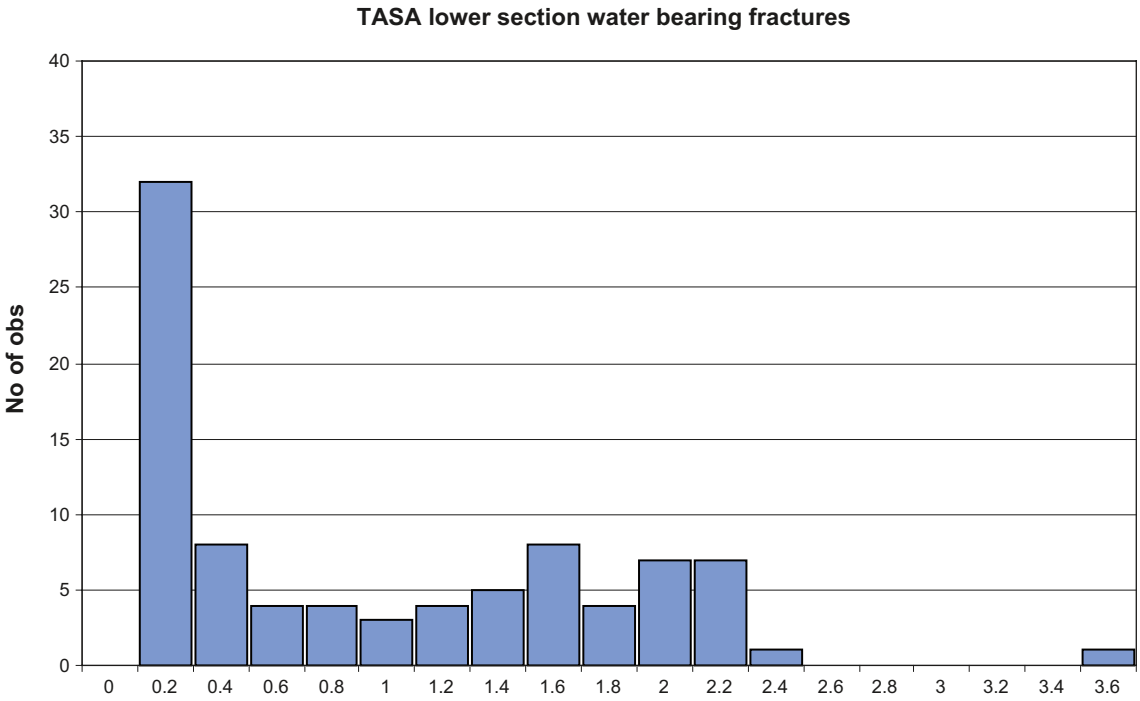

Figure B-29. *Histogram, TASA lower section water bearing fractures search radius 0.5 meters.*

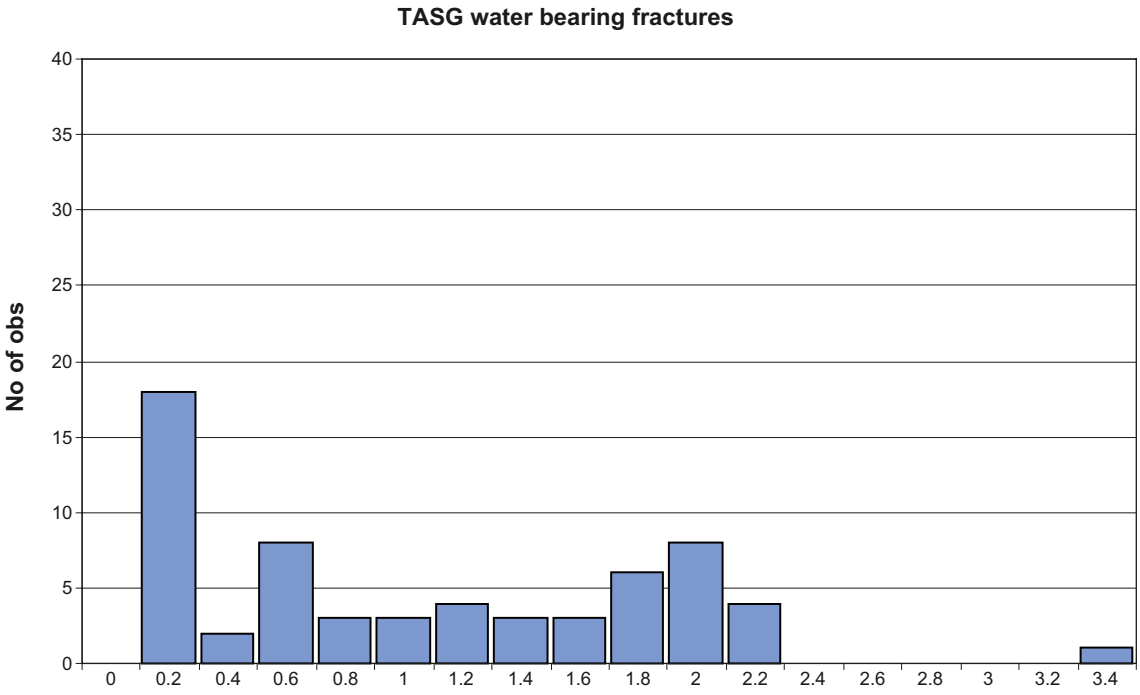

Figure B-30. *Histogram, TASG water bearing fractures search radius 0.5 meters.*

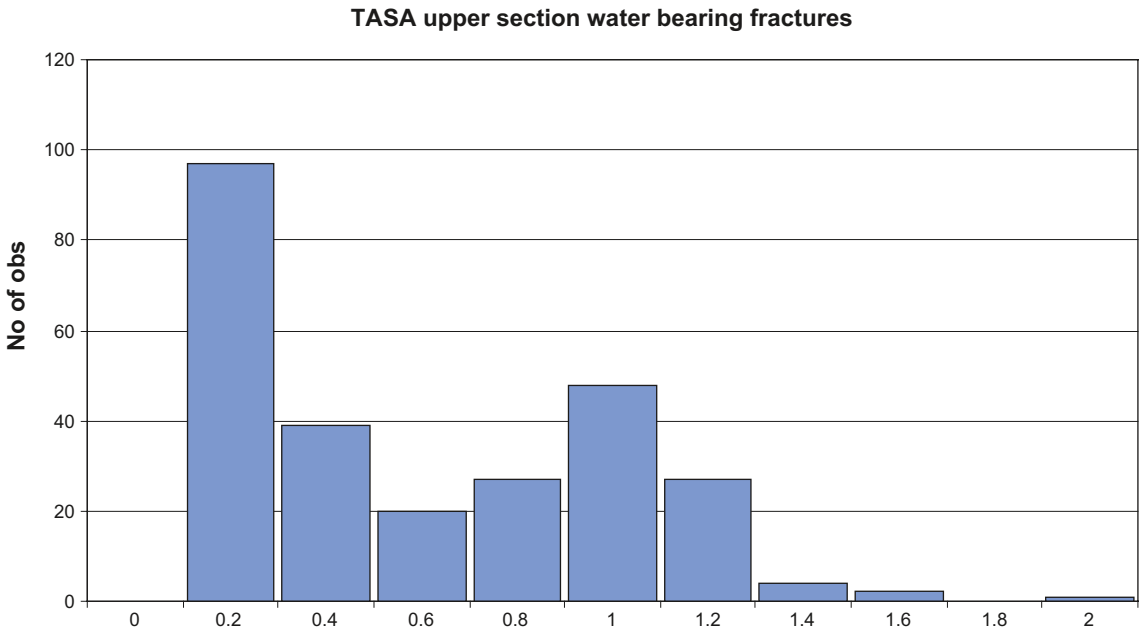

Figure B-31. *Histogram, TASA upper section water bearing fractures search radius 1 meter.*

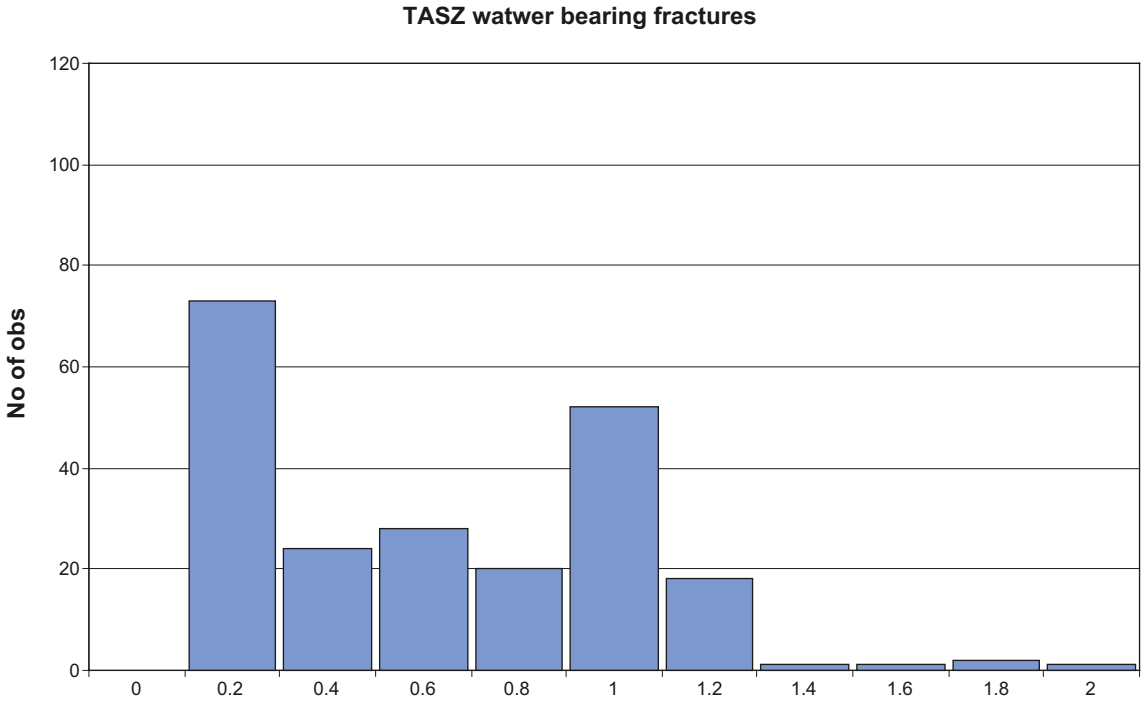

Figure B-32. *Histogram, TASZ water bearing fractures search radius 1 meter.*

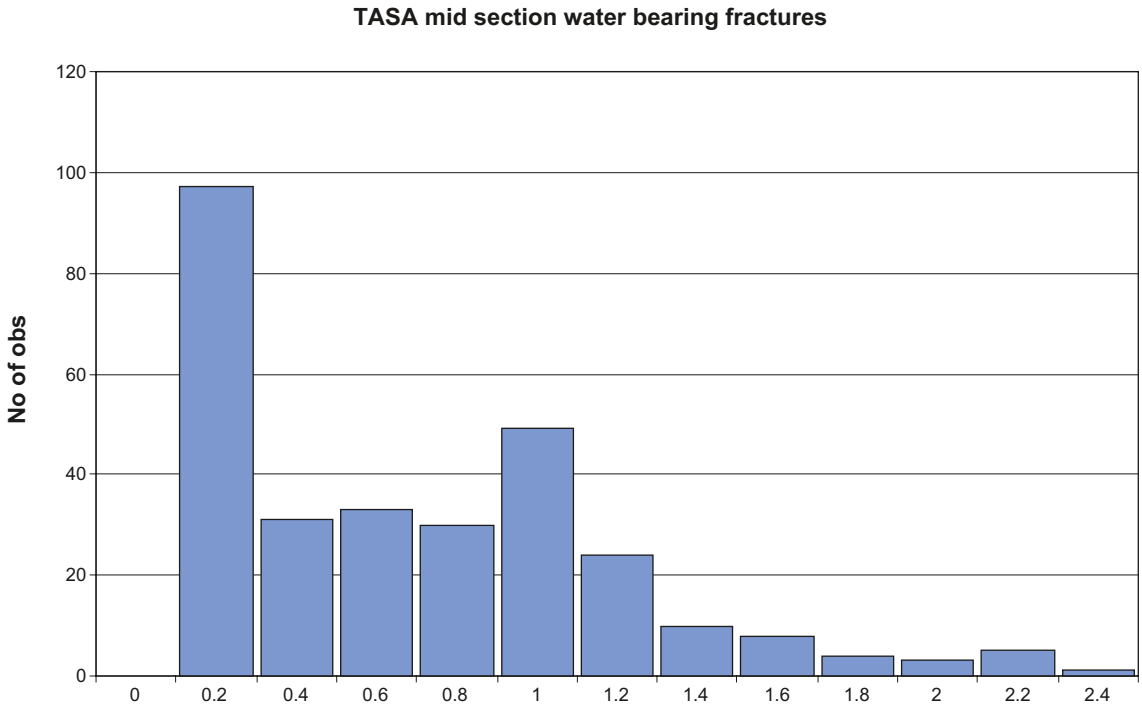

Figure B-33. *Histogram, TASA mid section water bearing fractures search radius 1 meter.*

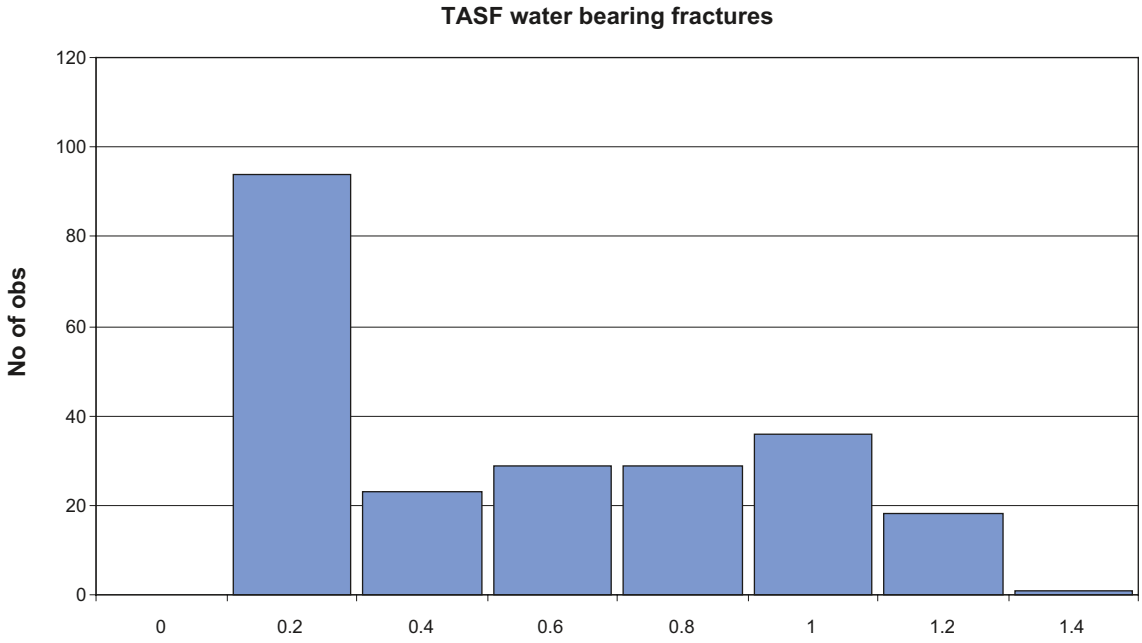

Figure B-34. *Histogram, TASF water bearing fractures search radius 1 meter.*

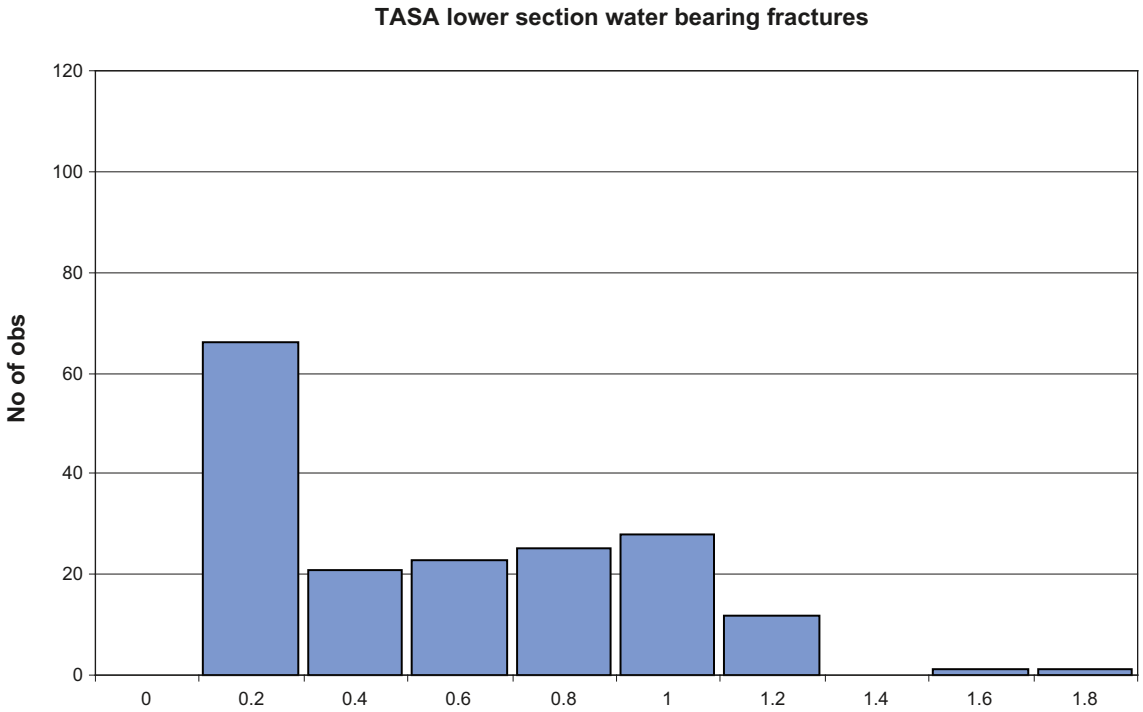

Figure B-35. *Histogram, TASA lower section water bearing fractures search radius 1 meter.*

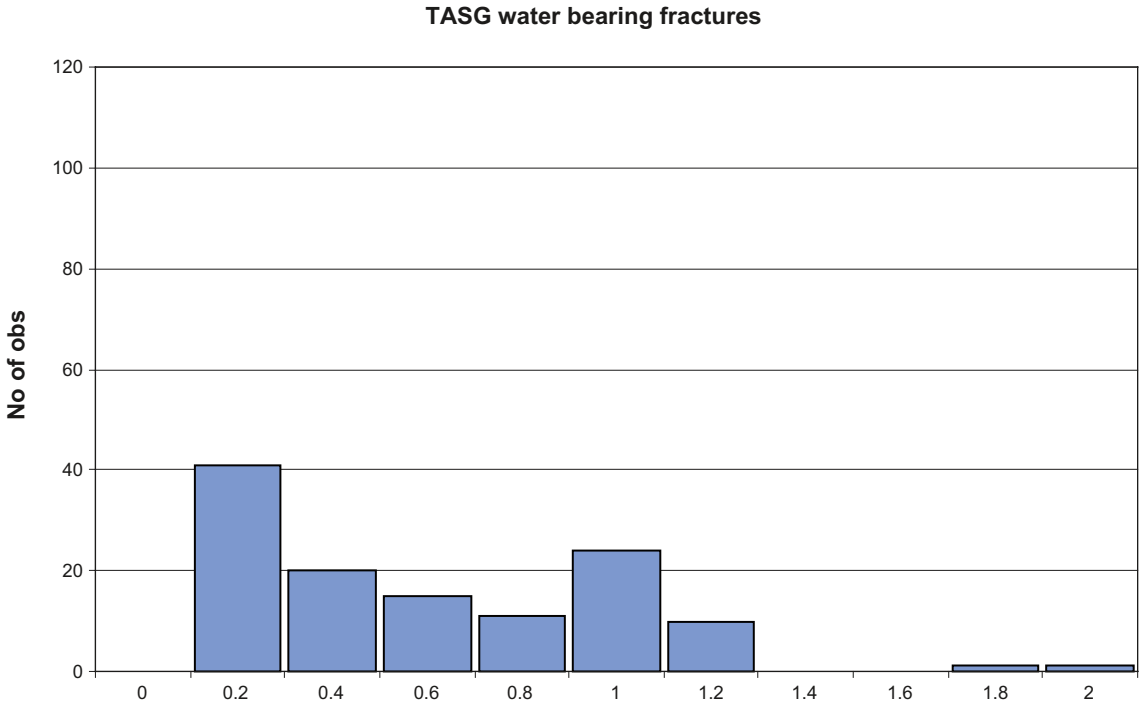

Figure B-36. *Histogram, TASG water bearing fractures search radius 1 meter.*

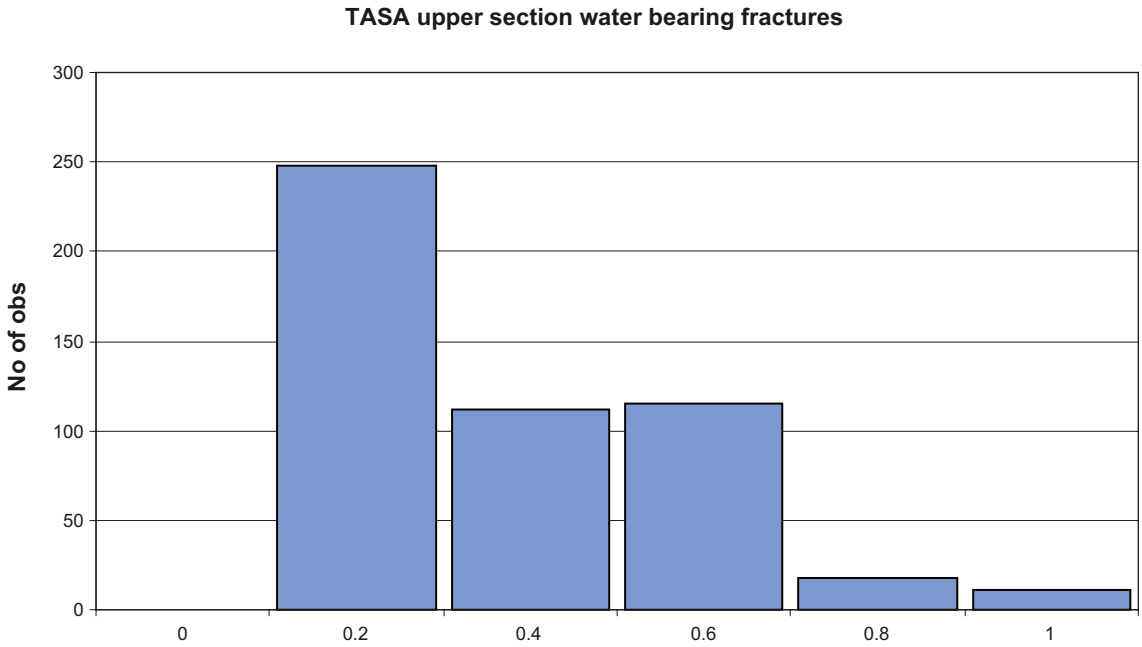

Figure B-37. *Histogram, TASA upper section water bearing fractures search radius 2 meters.*

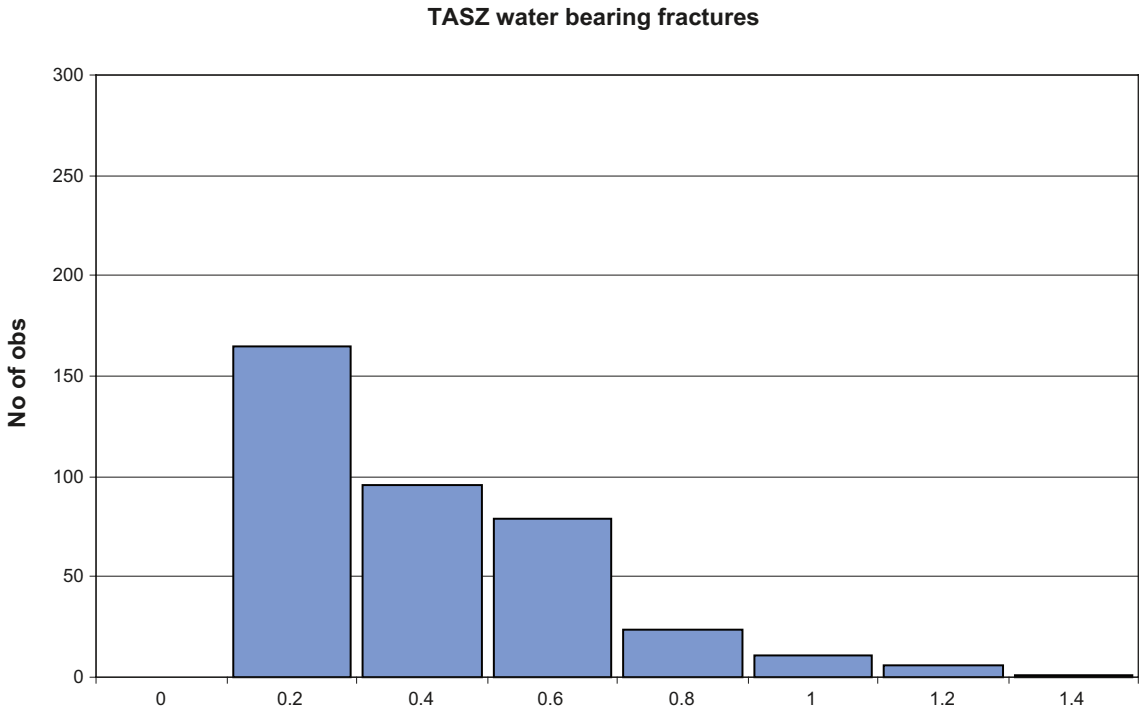

Figure B-38. *Histogram, TASZ water bearing fractures search radius 2 meters.*

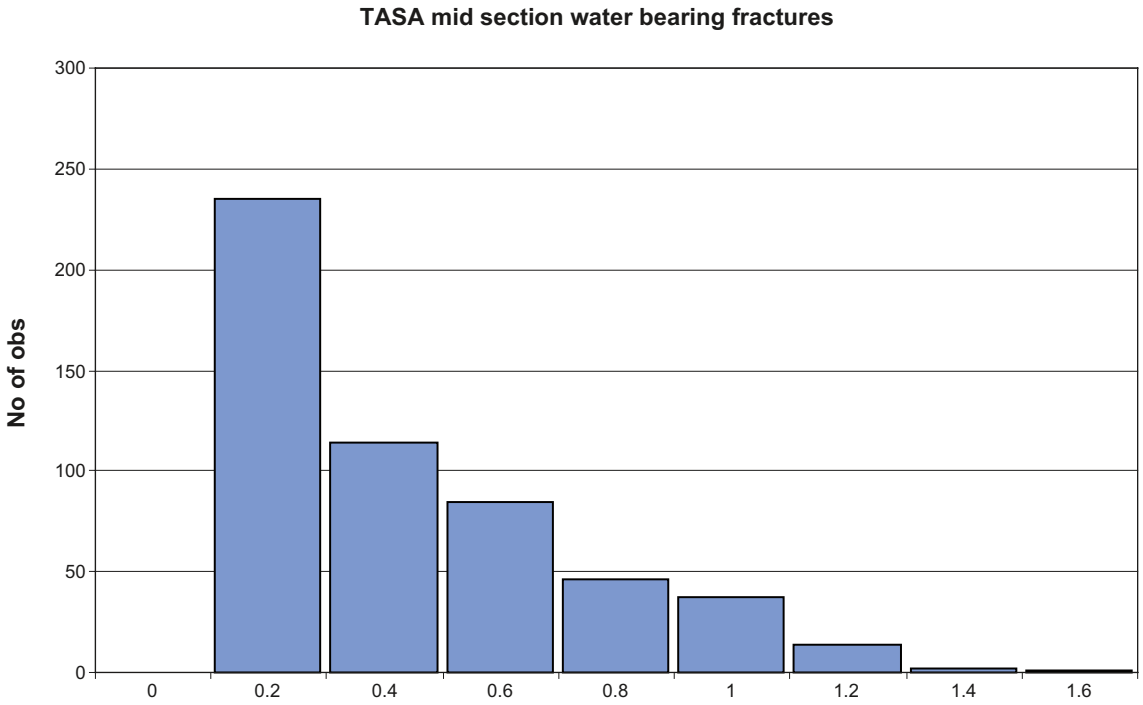

Figure B-39. *Histogram, TASA mid section water bearing fractures search radius 2 meters.*

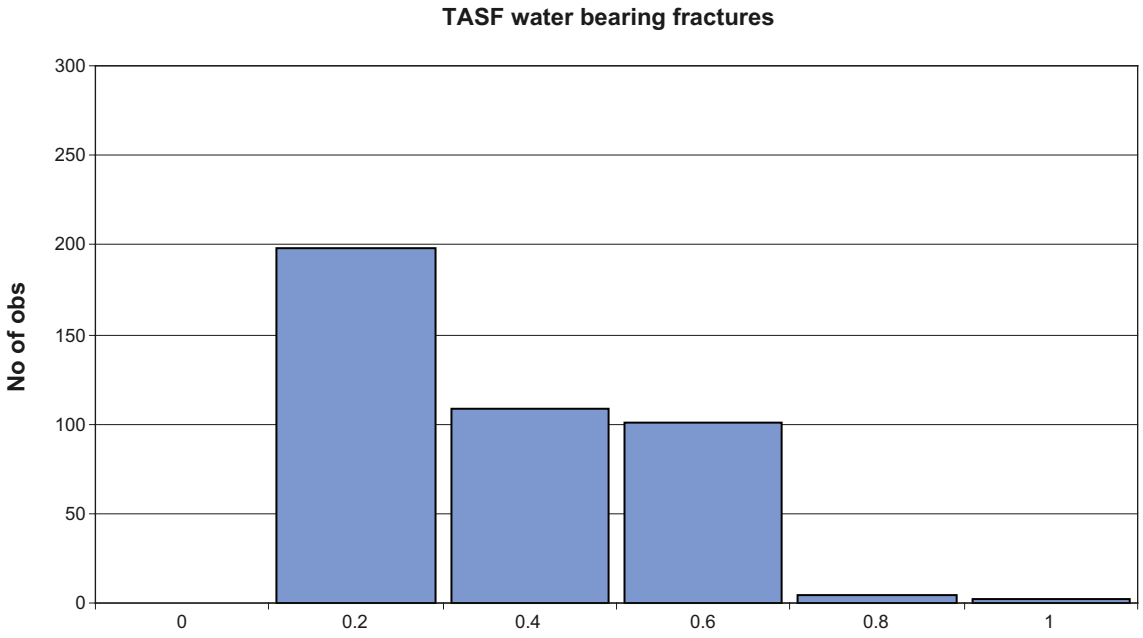

Figure B-40. *Histogram, TASF water bearing fractures search radius 2 meters.*

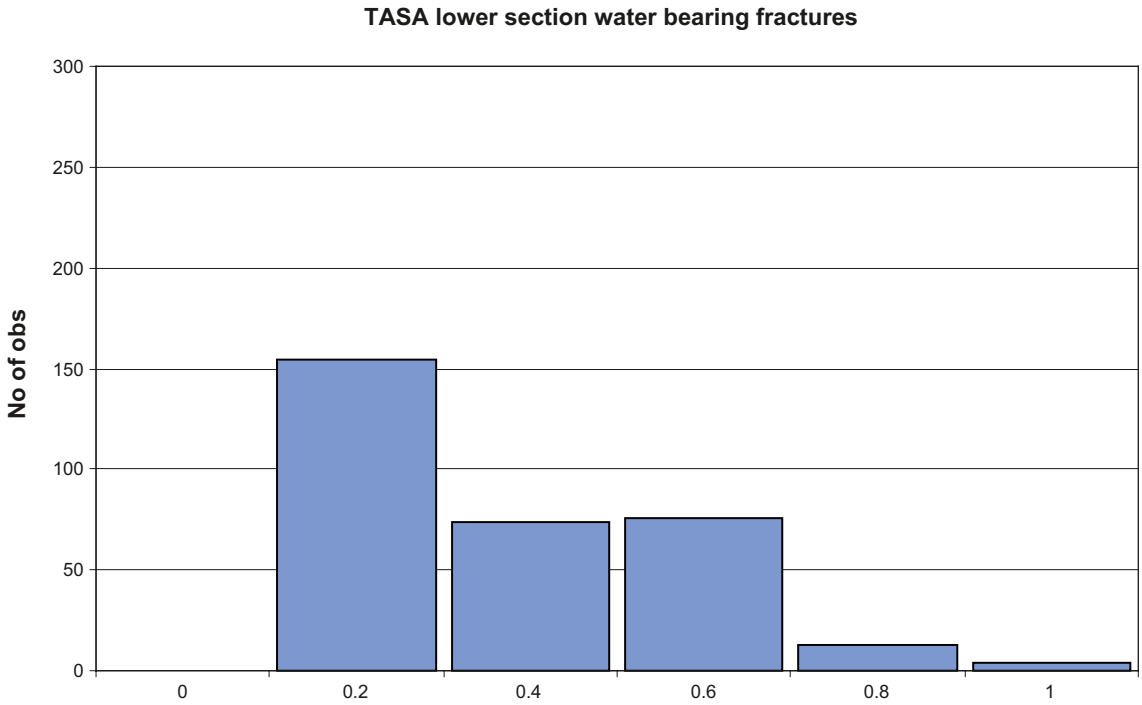

Figure B-41. *Histogram, TASA lower section water bearing fractures search radius 2 meters.*

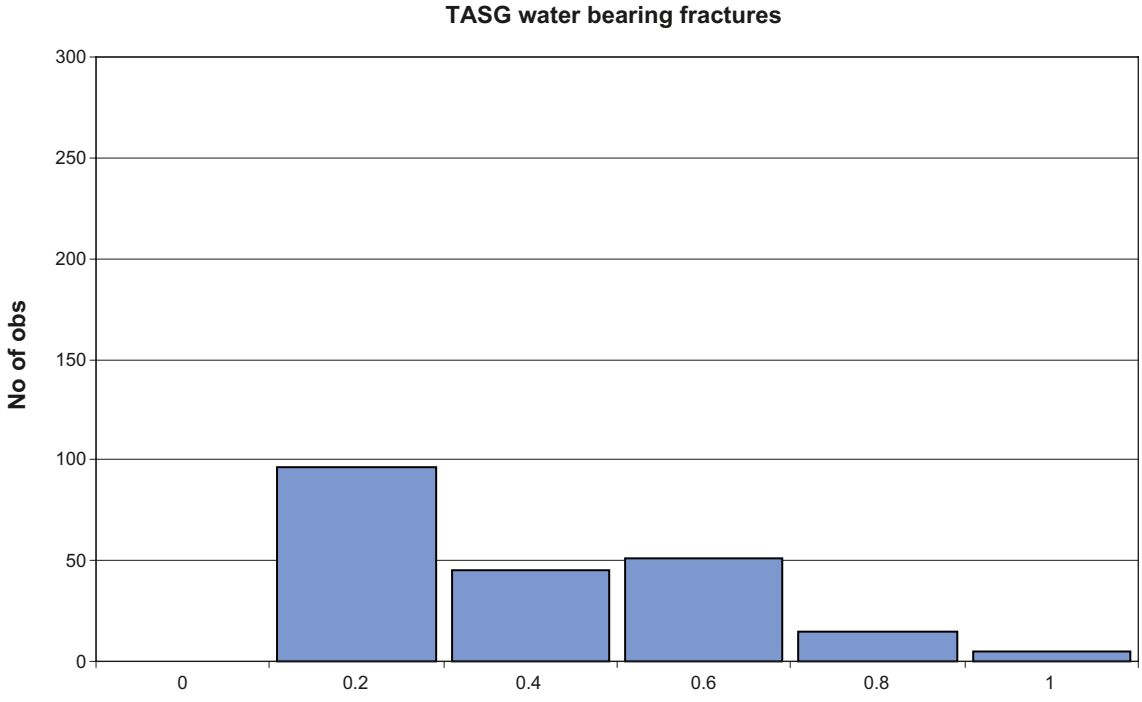

Figure B-42. *Histogram, TASG water bearing fractures search radius 2 meters.*

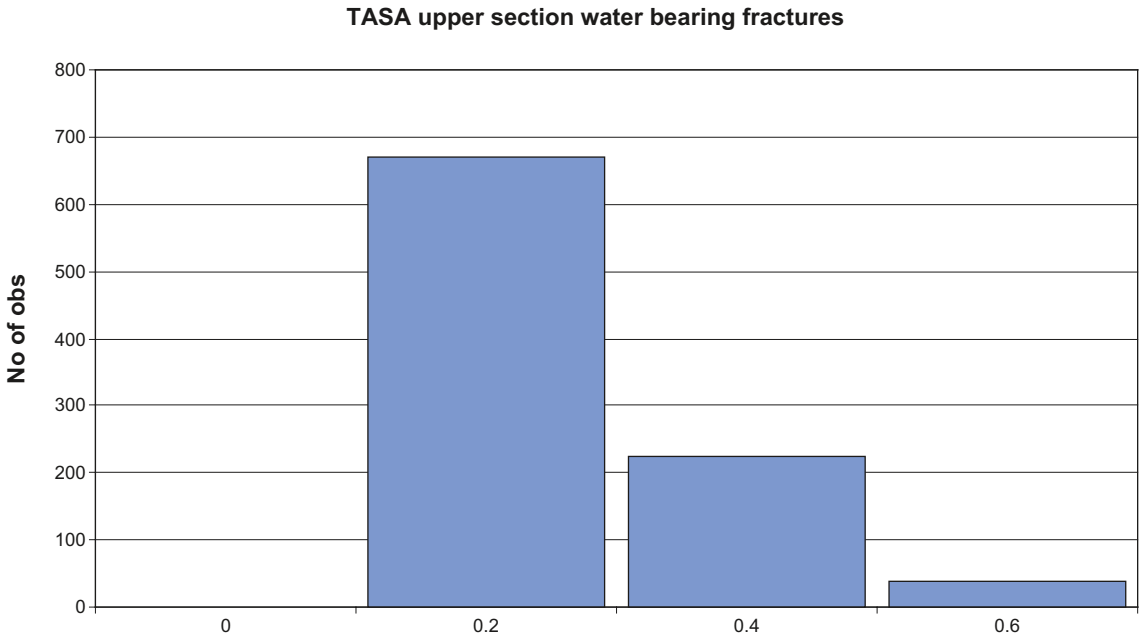

Figure B-43. *Histogram, TASA upper section water bearing fractures search radius 4 meters.*

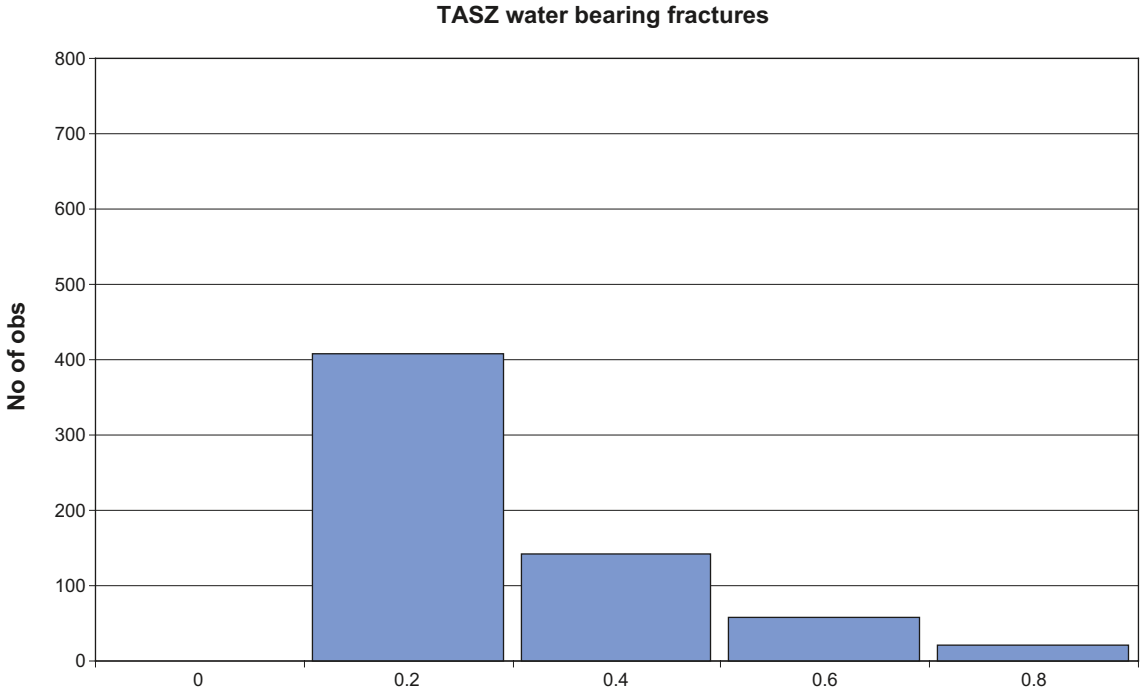

Figure B-44. *Histogram, TASZ water bearing fractures search radius 4 meters.*

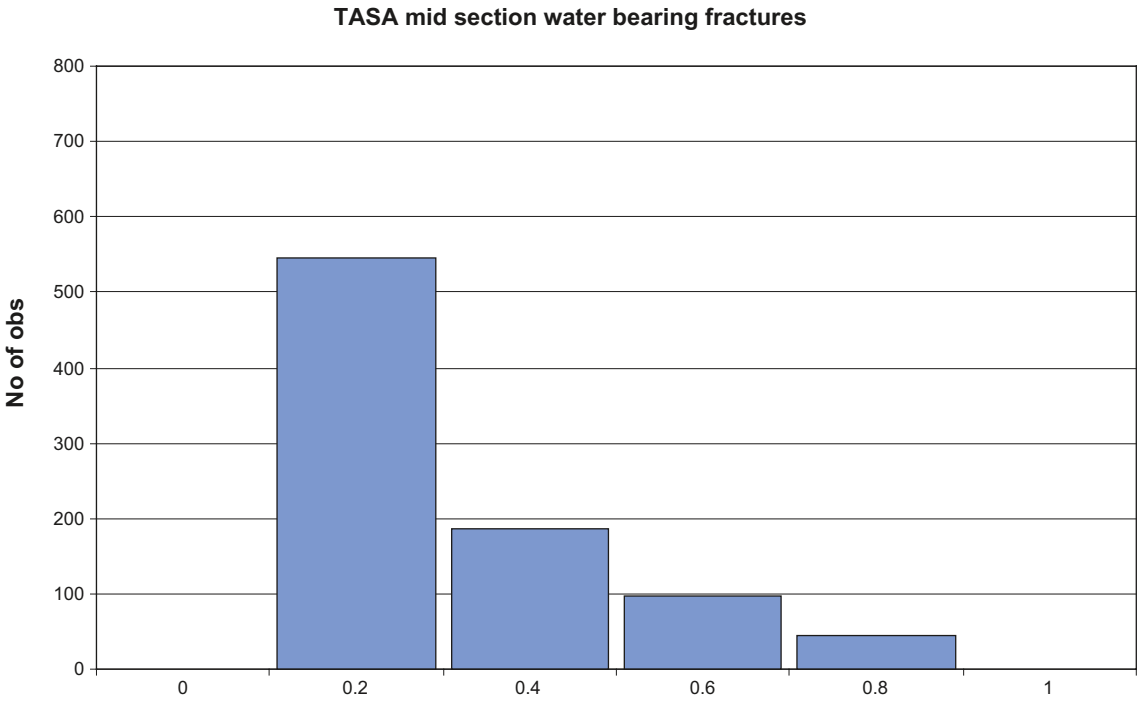

Figure B-45. *Histogram, TASA mid section water bearing fractures search radius 4 meters.*

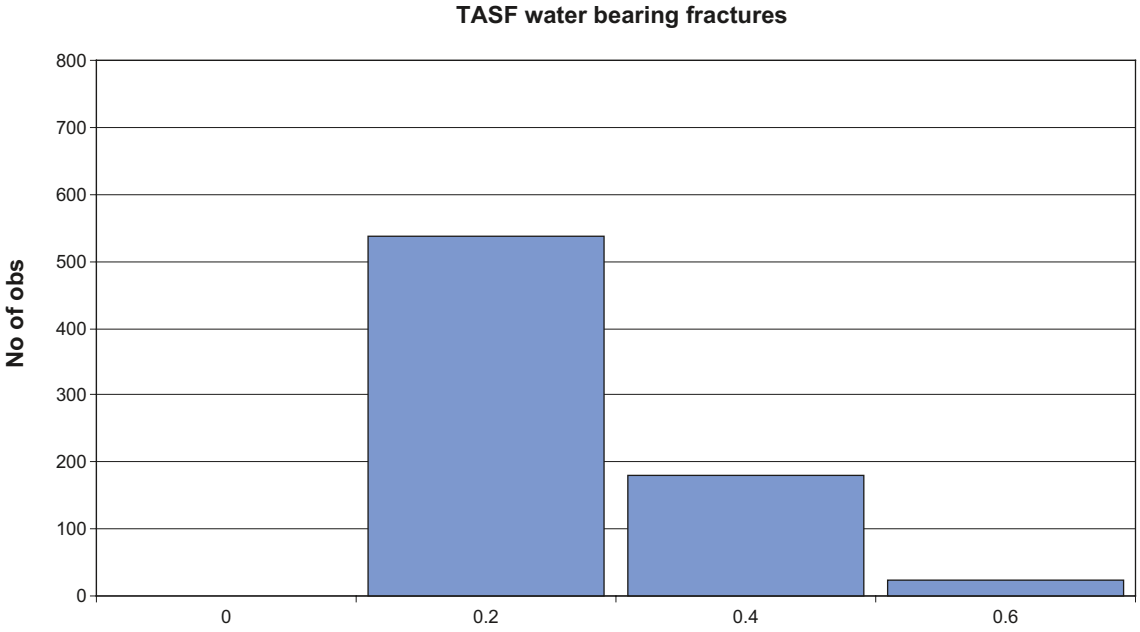

Figure B-46. *Histogram, TASF water bearing fractures search radius 4 meters.*

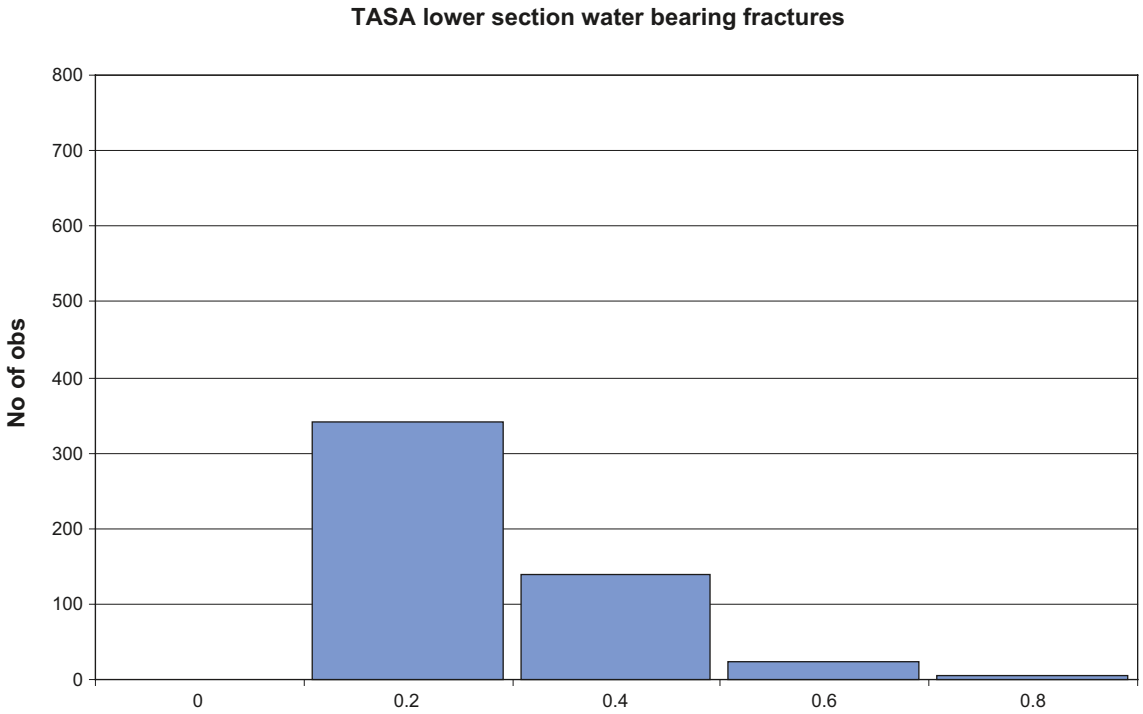

Figure B-47. *Histogram, TASA lower section water bearing fractures search radius 4 meters.*

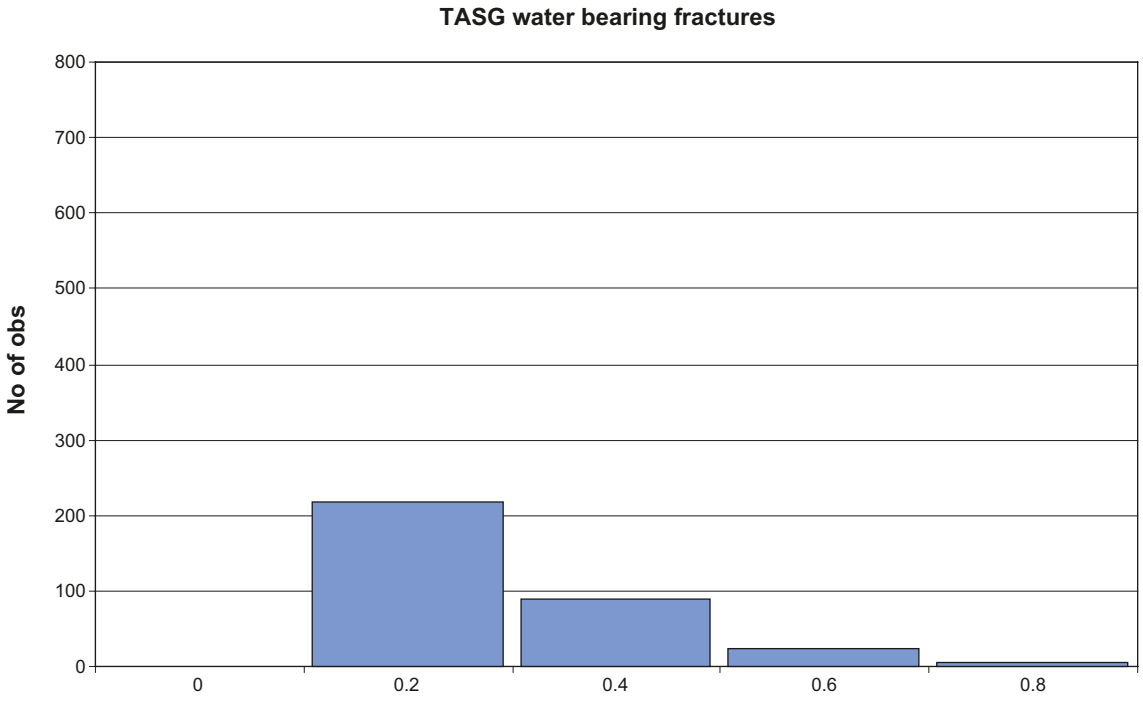

Figure B-48. *Histogram, TASG water bearing fractures search radius 4 meters.*

Appendix C

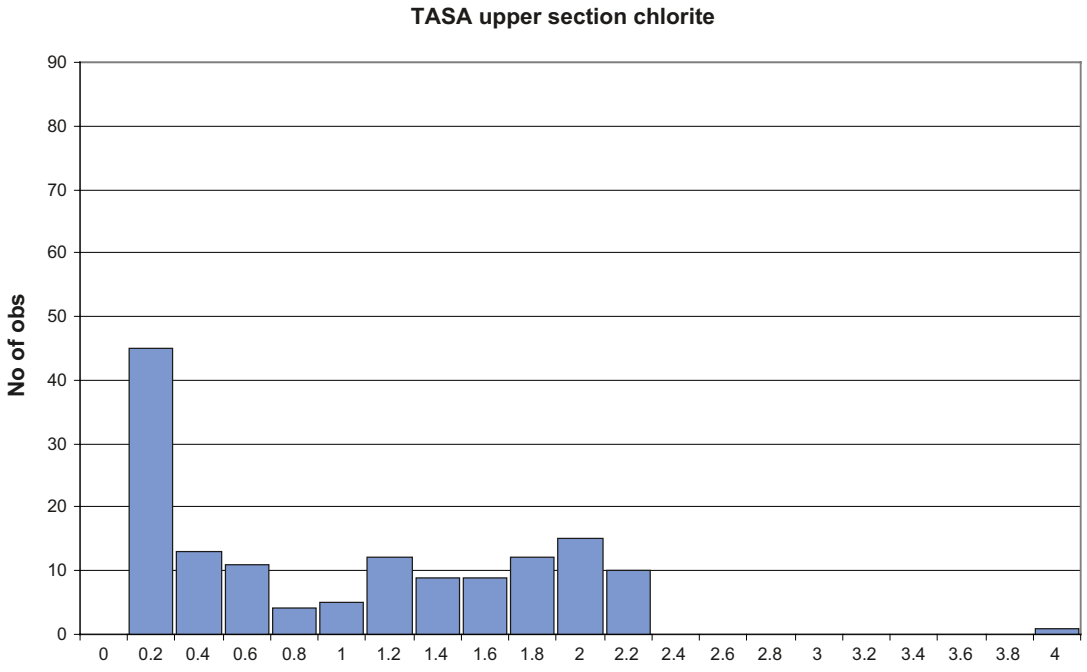

Figure C-1. *Histogram, TASA upper section chlorite search radius 0.5 meters.*

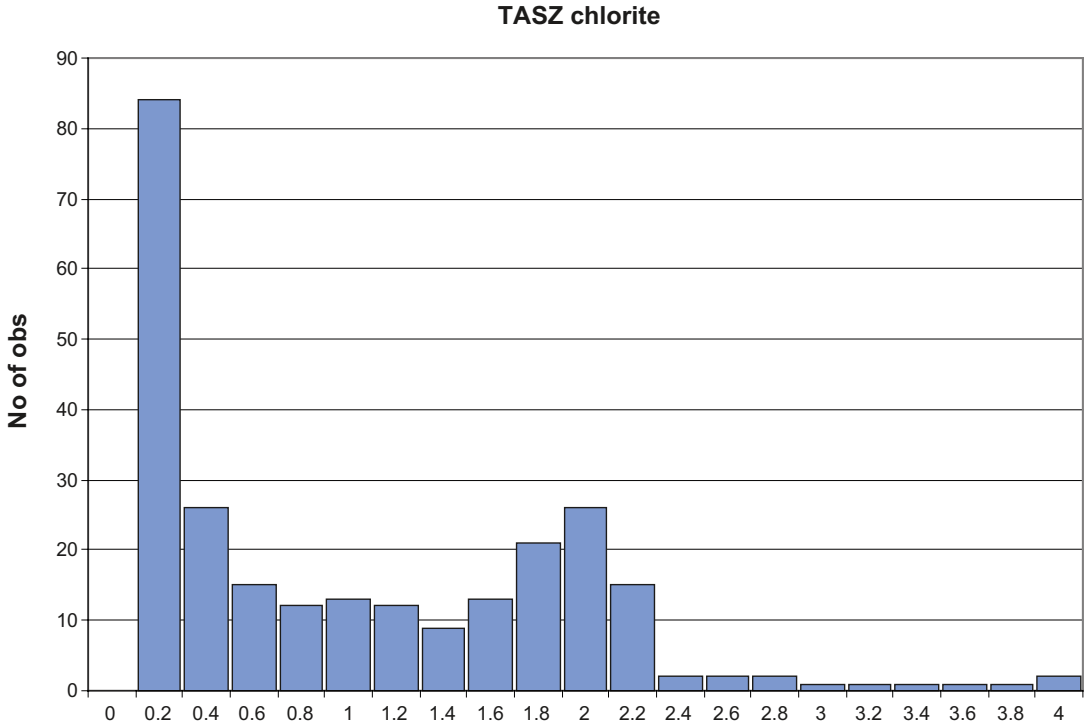

Figure C-2. *Histogram, TASZ chlorite search radius 0.5 meters.*

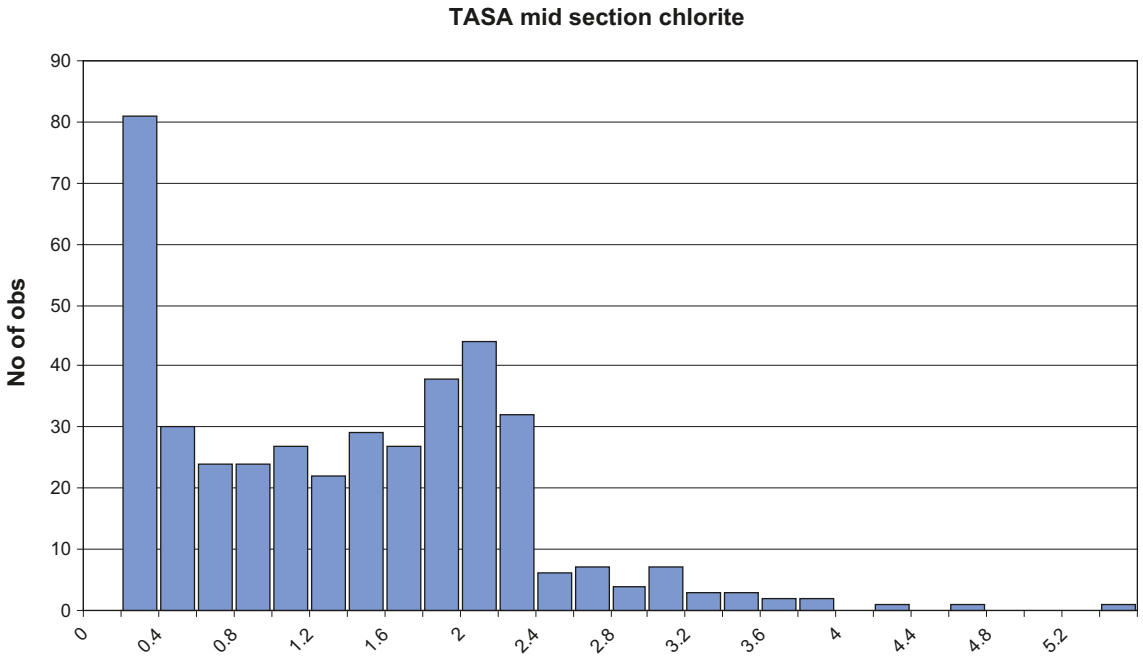

Figure C-3. *Histogram, TASA mid section chlorite search radius 0.5 meters.*

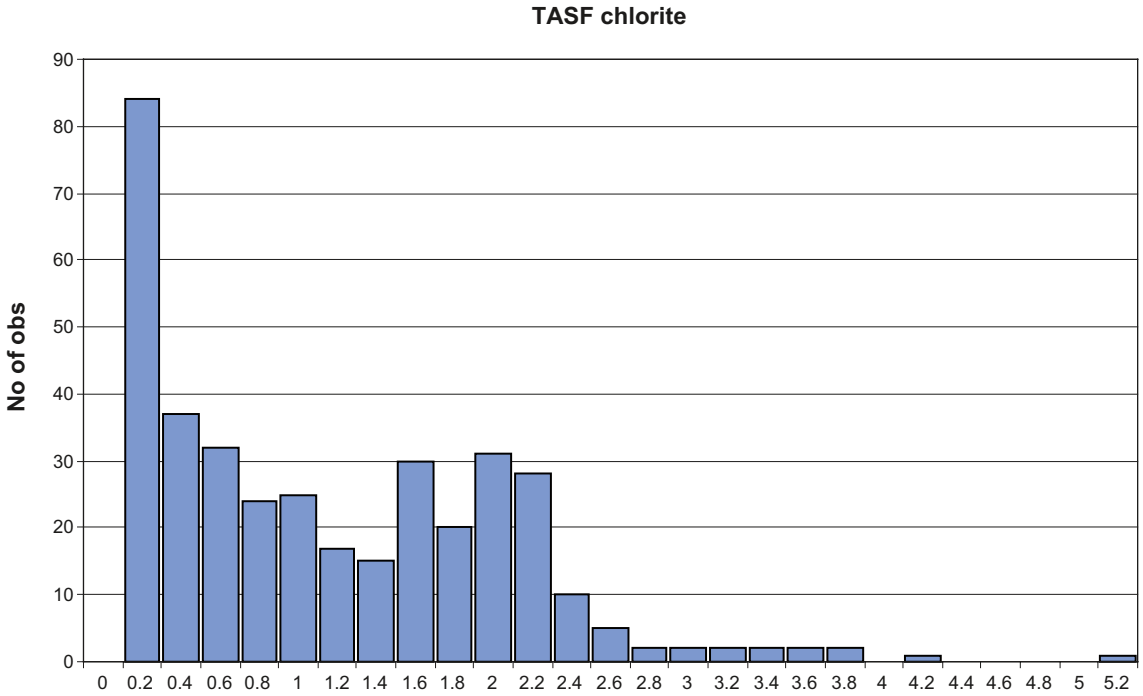

Figure C-4. *Histogram, TASF chlorite search radius 0.5 meters.*

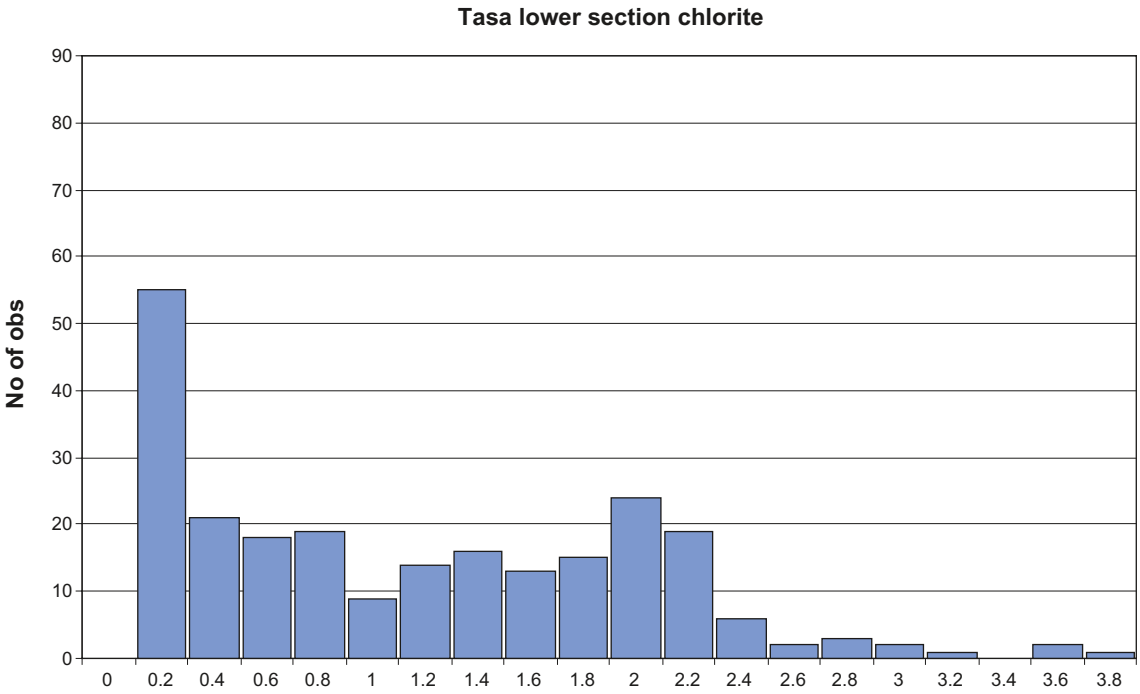

Figure C-5. *Histogram, TASA lower section chlorite search radius 0.5 meters.*

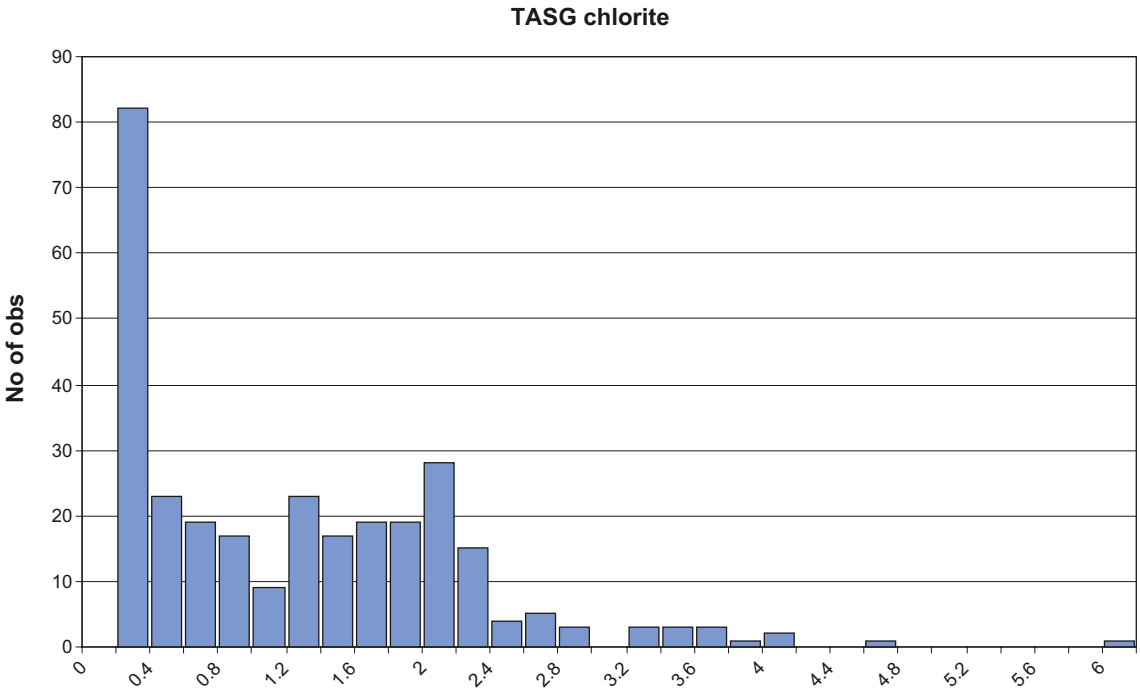

Figure C-6. *Histogram, TASG chlorite search radius 0.5 meters.*

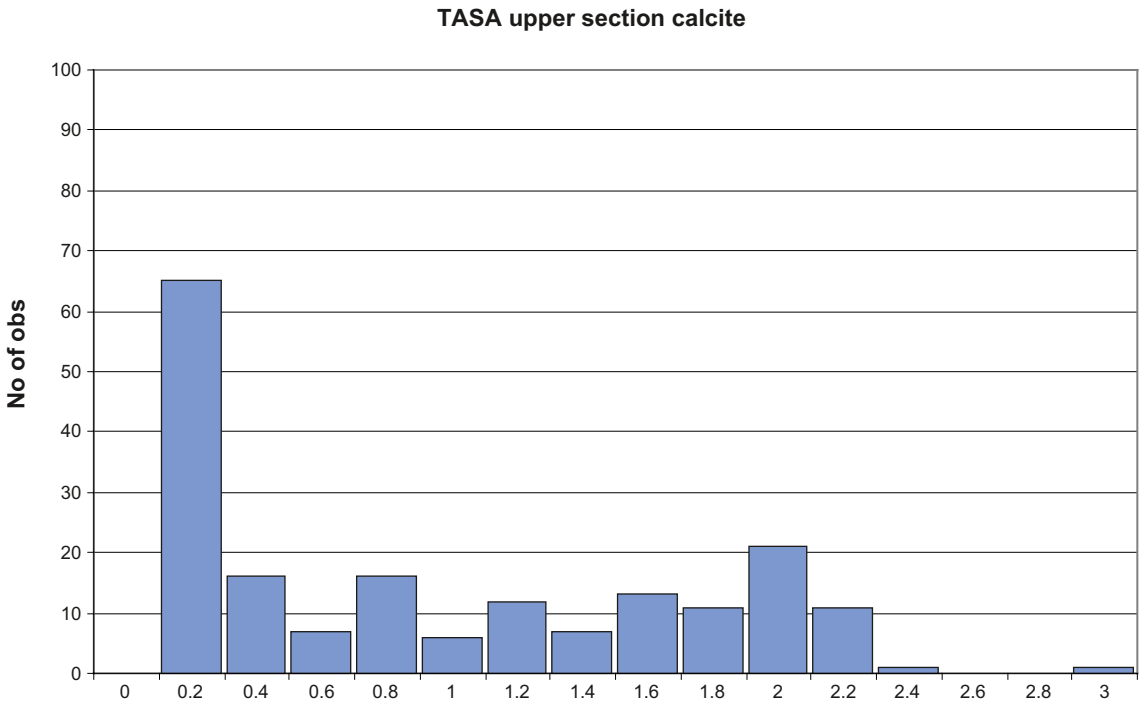

Figure C-7. *Histogram, TASA upper section calcite search radius 0.5 meters.*

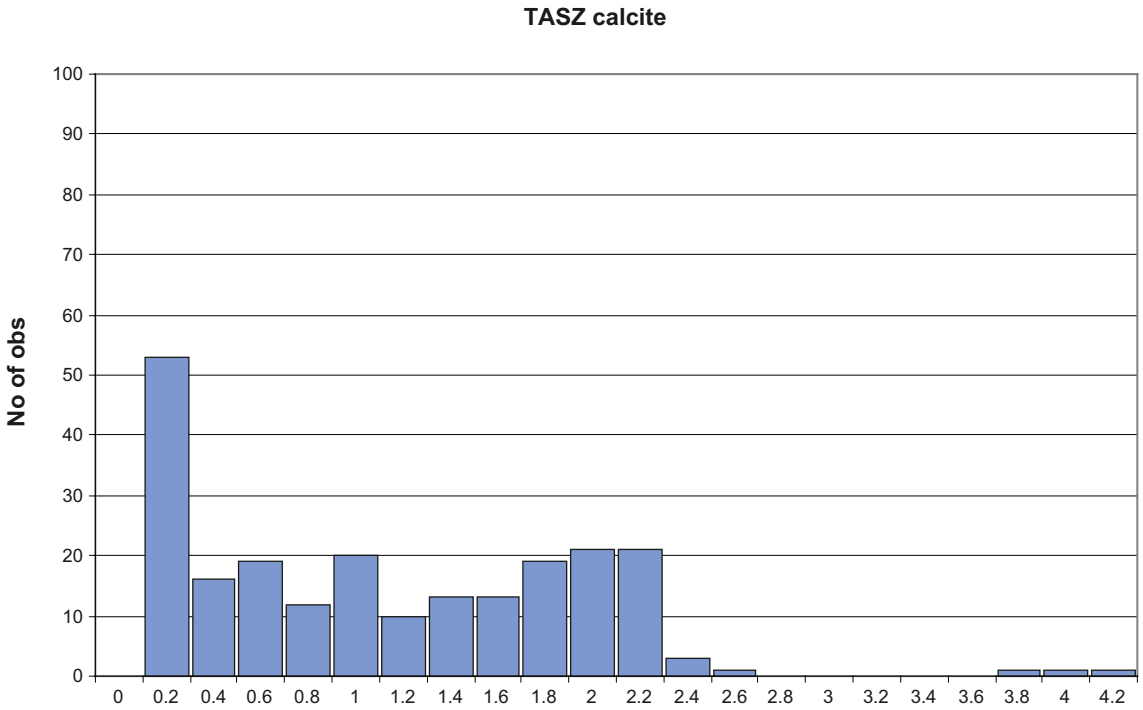

Figure C-8. *Histogram, TASZ calcite search radius 0.5 meters.*

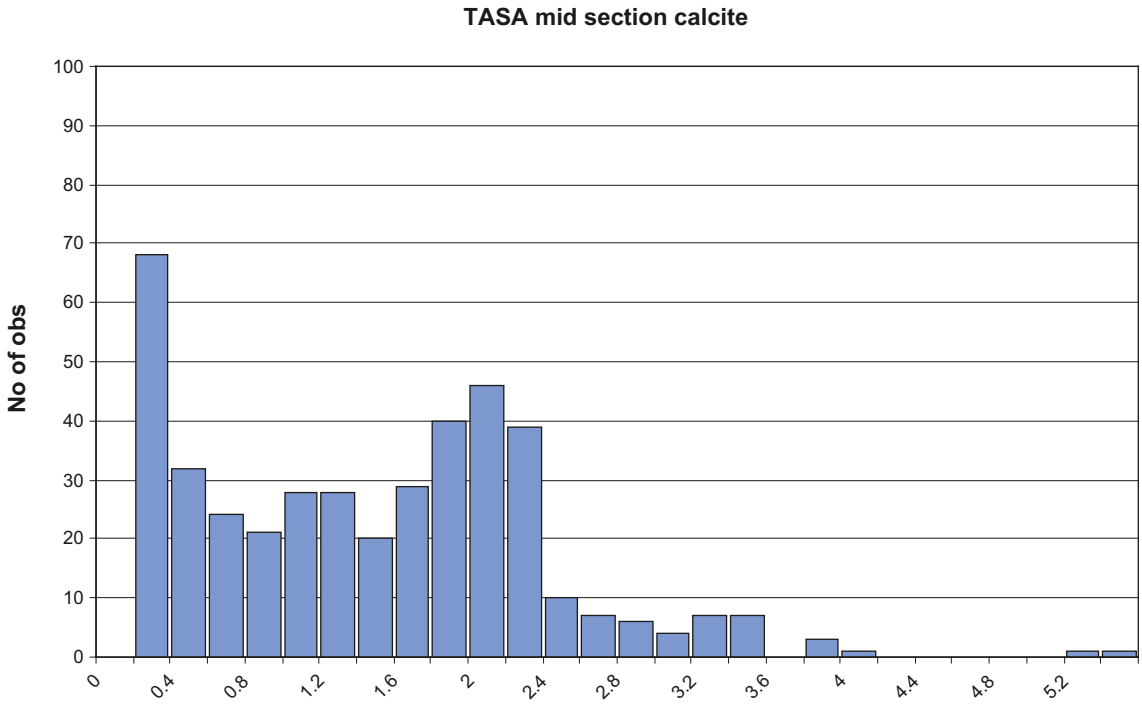

Figure C-9. *Histogram, TASA mid section calcite search radius 0.5 meters.*

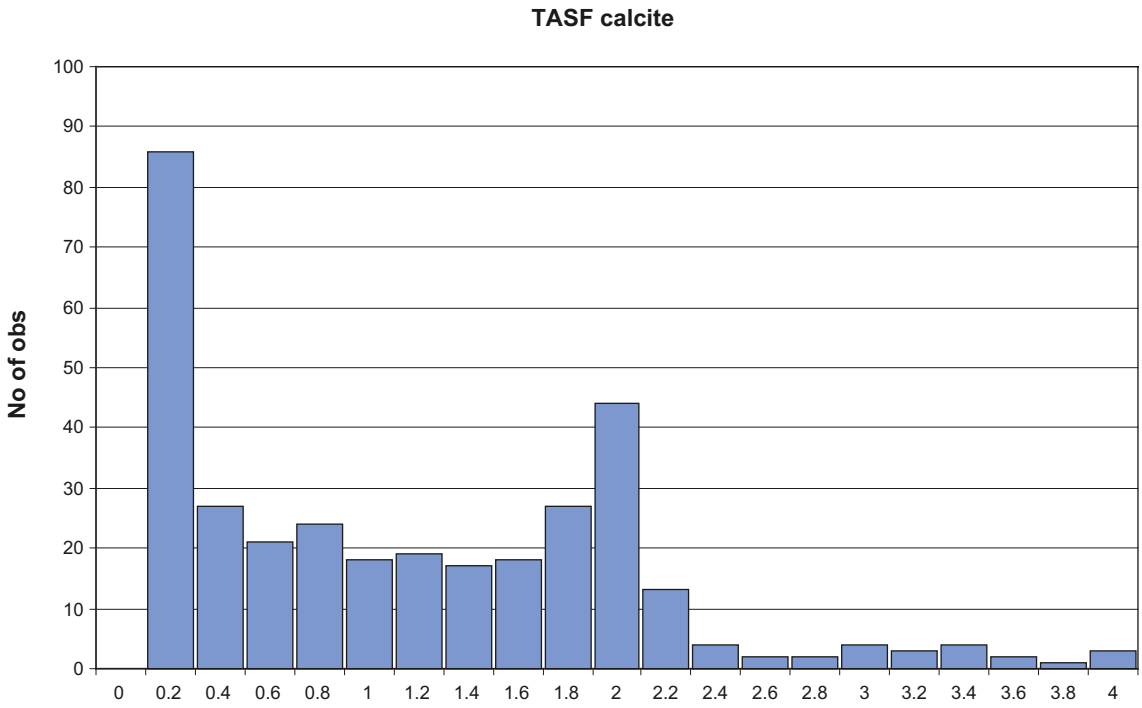

Figure C-10. *Histogram, TASF calcite search radius 0.5 meters.*

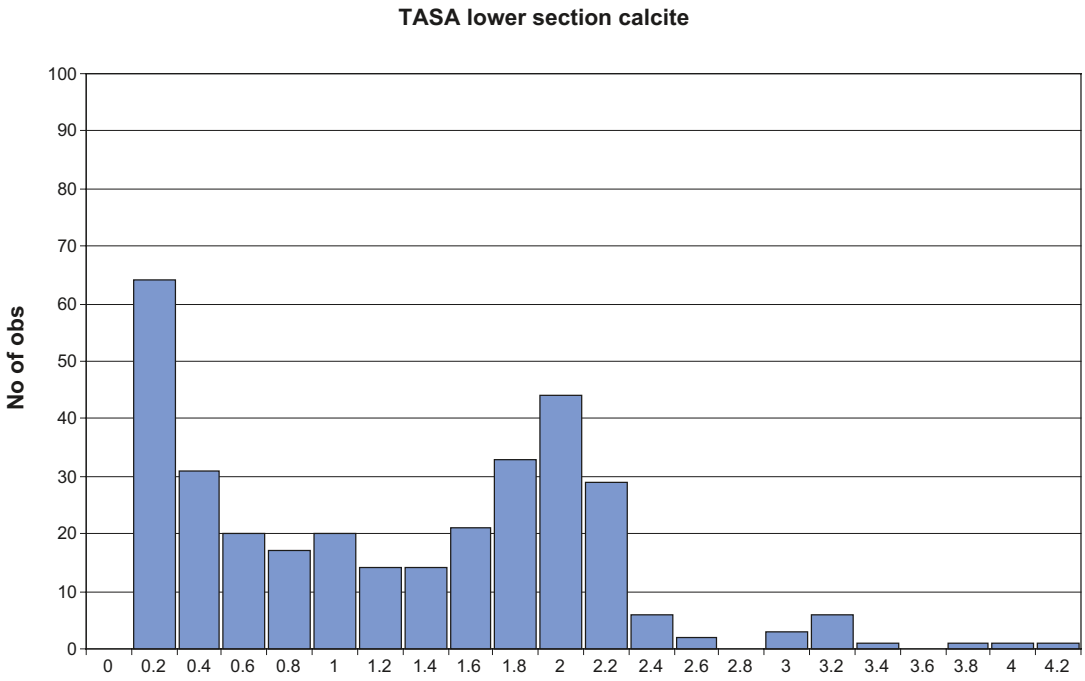

Figure C-11. *Histogram, TASA lower section calcite search radius 0.5 meters.*

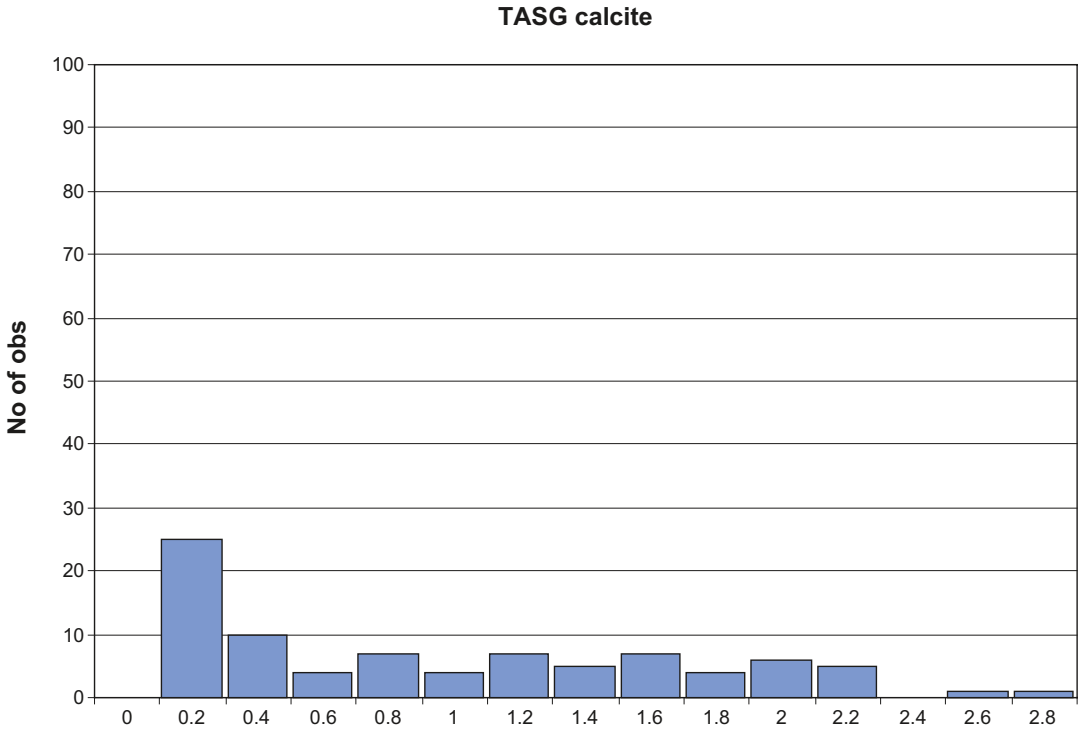

Figure C-12. *Histogram, TASG calcite search radius 0.5 meters.*

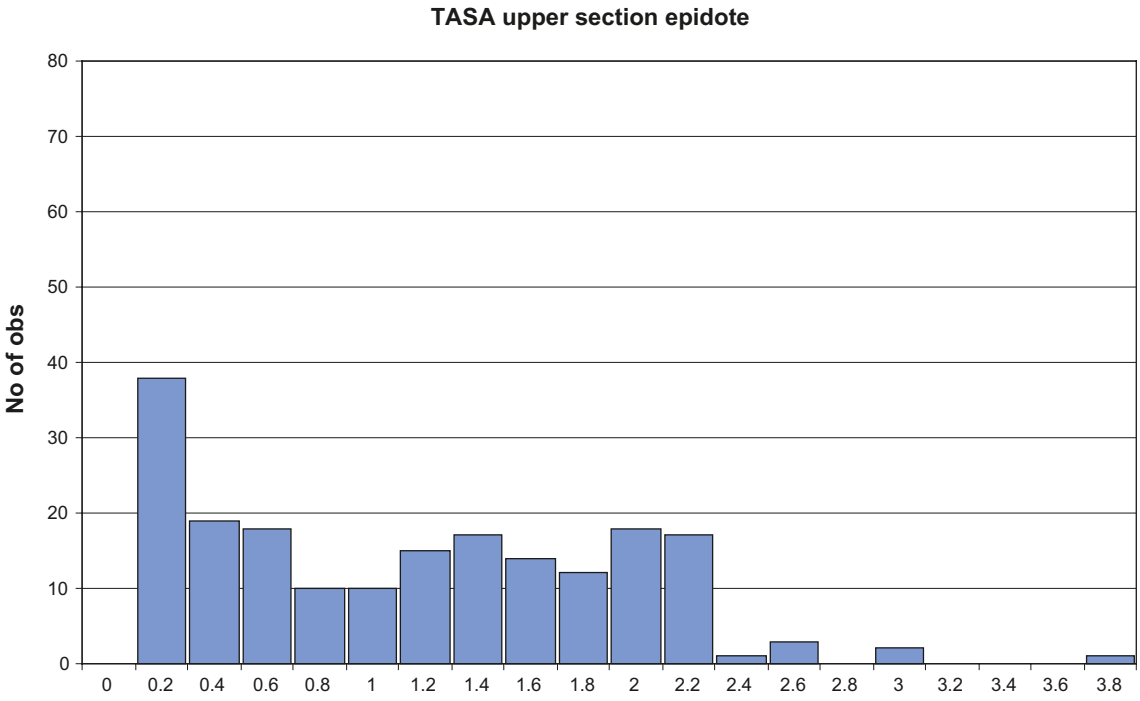

Figure C-13. *Histogram, TASA upper section epidote search radius 0.5 meters.*

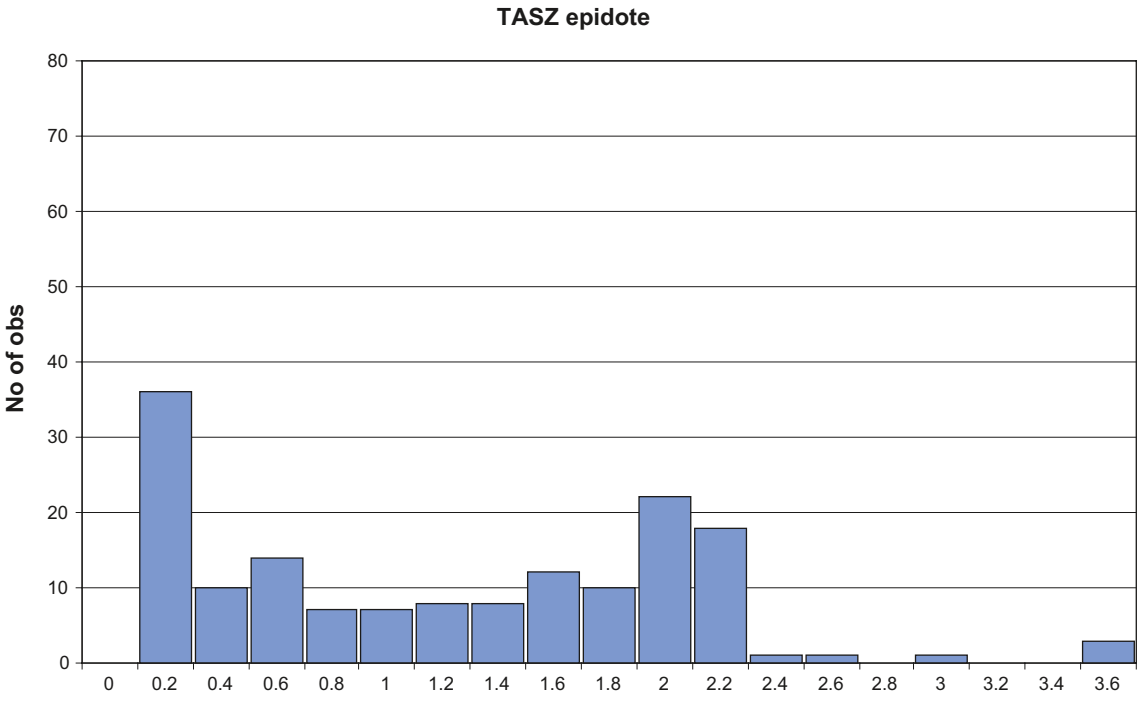

Figure C-14. *Histogram, TASZ epidote search radius 0.5 meters.*

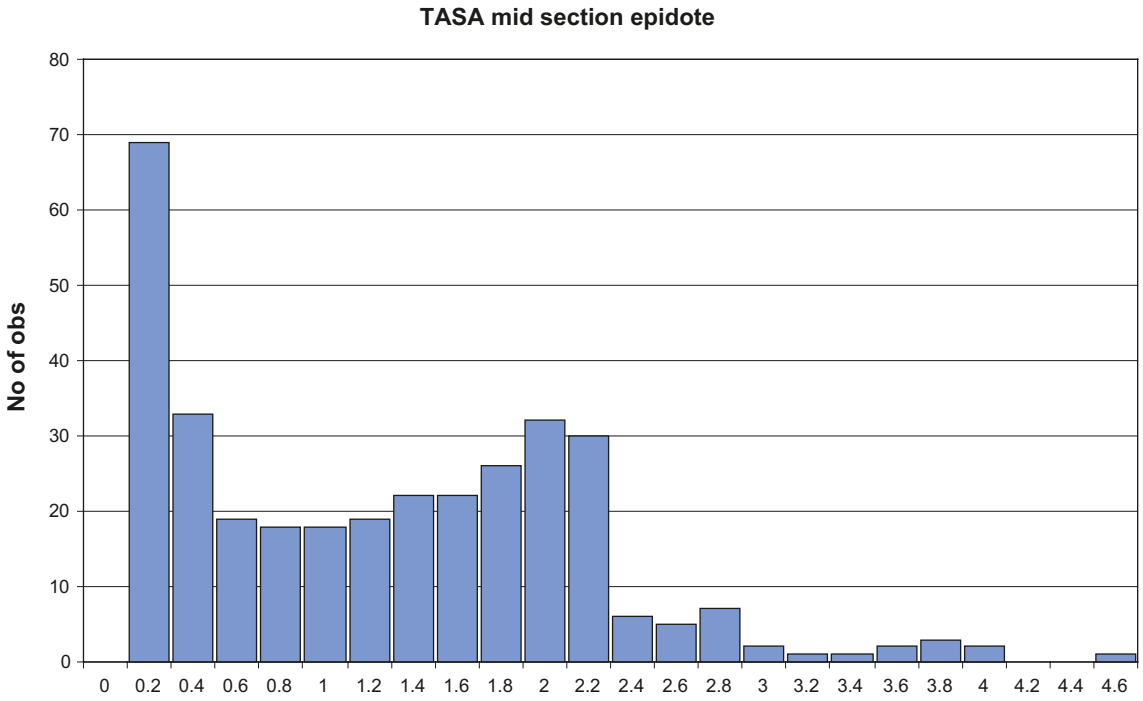

Figure C-15. *Histogram, TASA mid section epidote search radius 0.5 meters.*

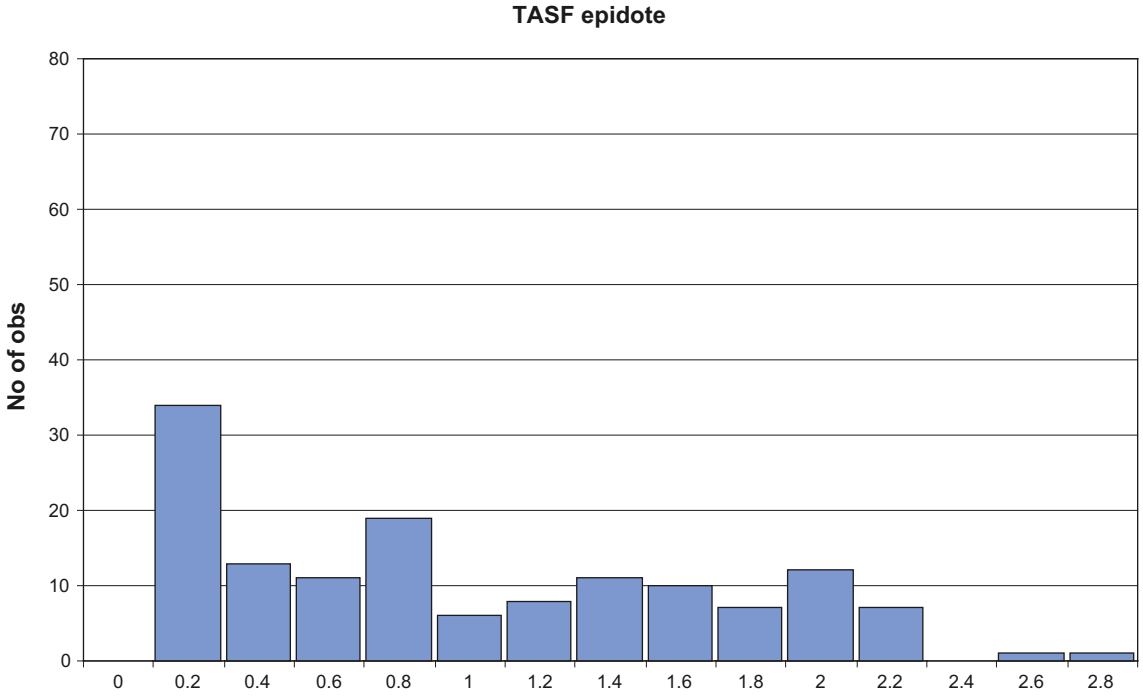

Figure C-16. *Histogram, TASF epidote search radius 0.5 meters.*

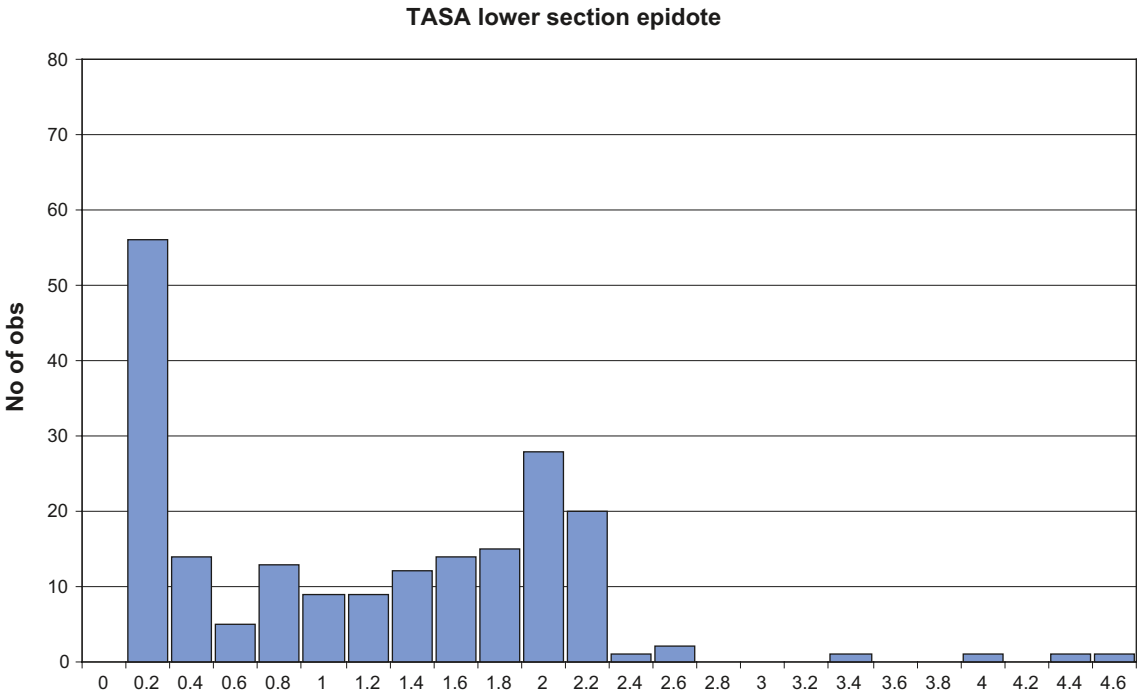

Figure C-17. *Histogram, TASA lower section epidote search radius 0.5 meters.*

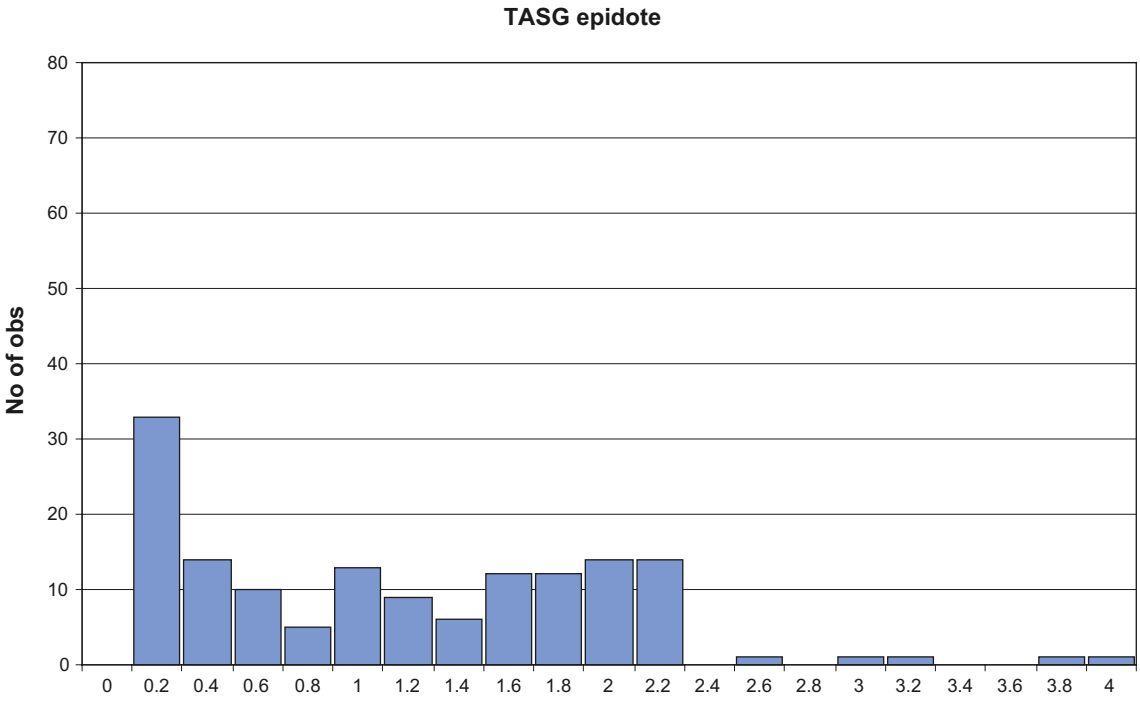

Figure C-18. *Histogram, TASG epidote search radius 0.5 meters.*

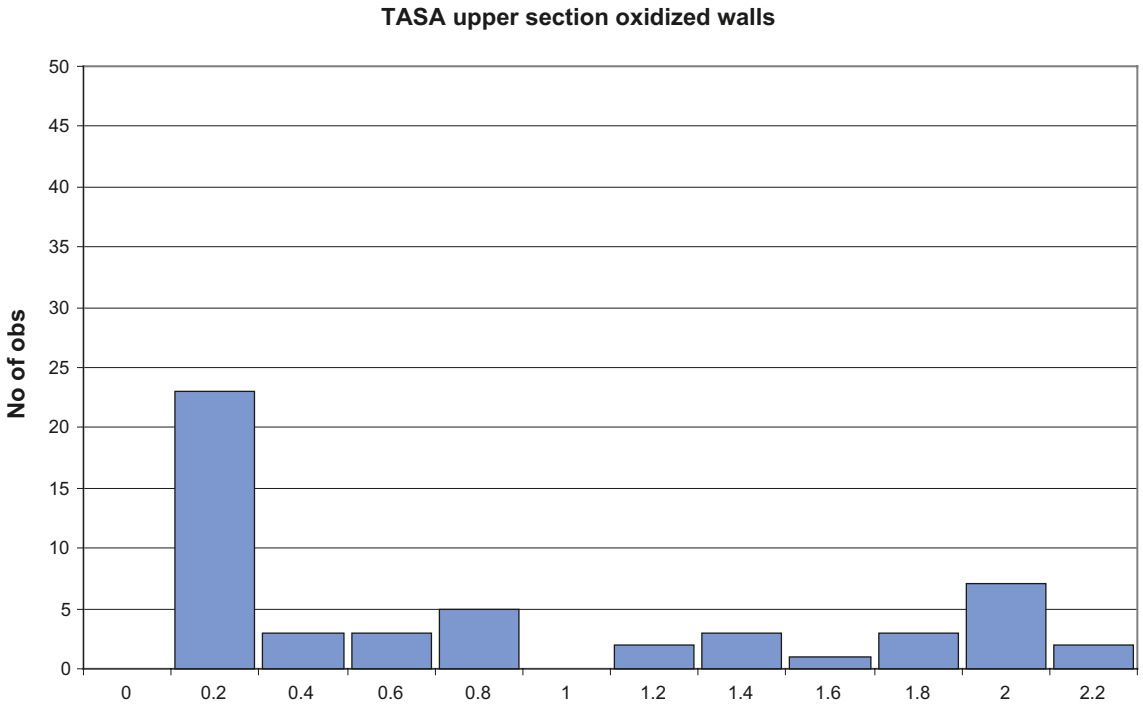

Figure C-19. *Histogram, TASA upper section oxidized walls search radius 0.5 meters.*

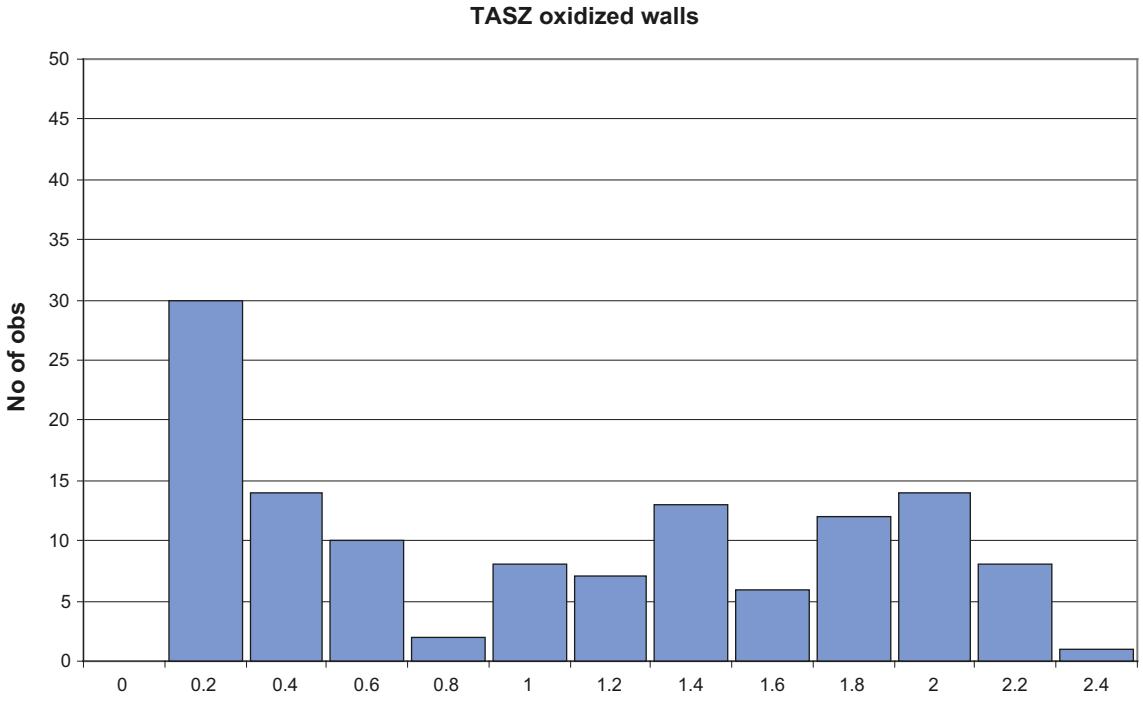

Figure C-20. *Histogram, TASZ oxidized walls search radius 0.5 meters.*

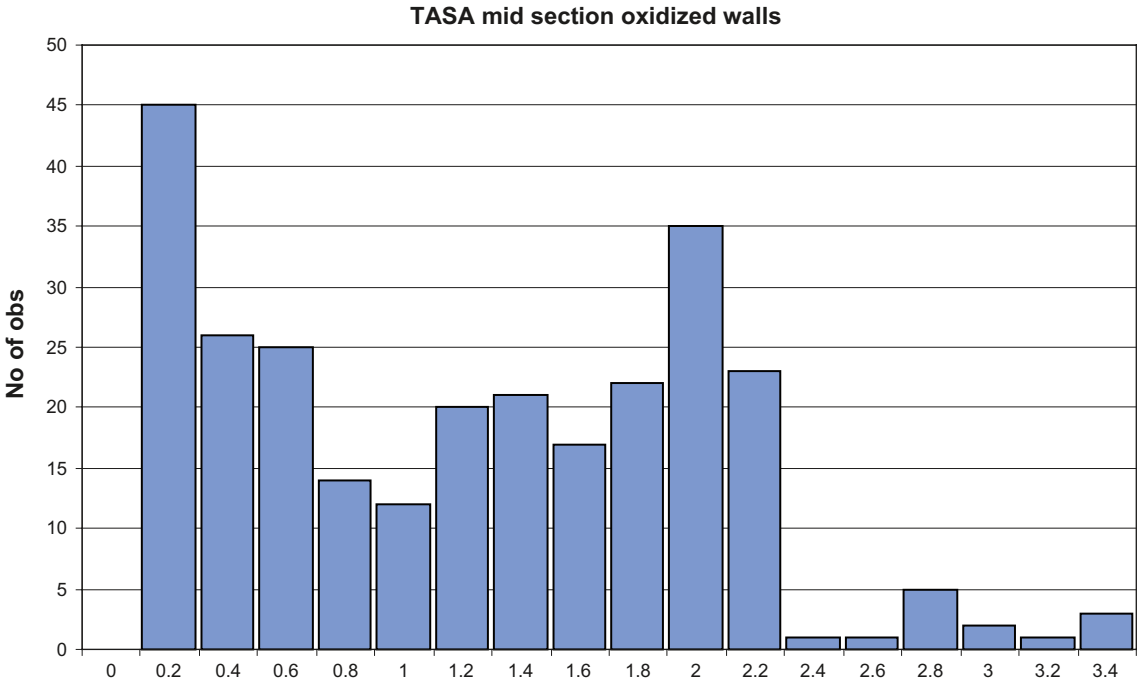

Figure C-21. *Histogram, TASA mid section oxidized walls search radius 0.5 meters.*

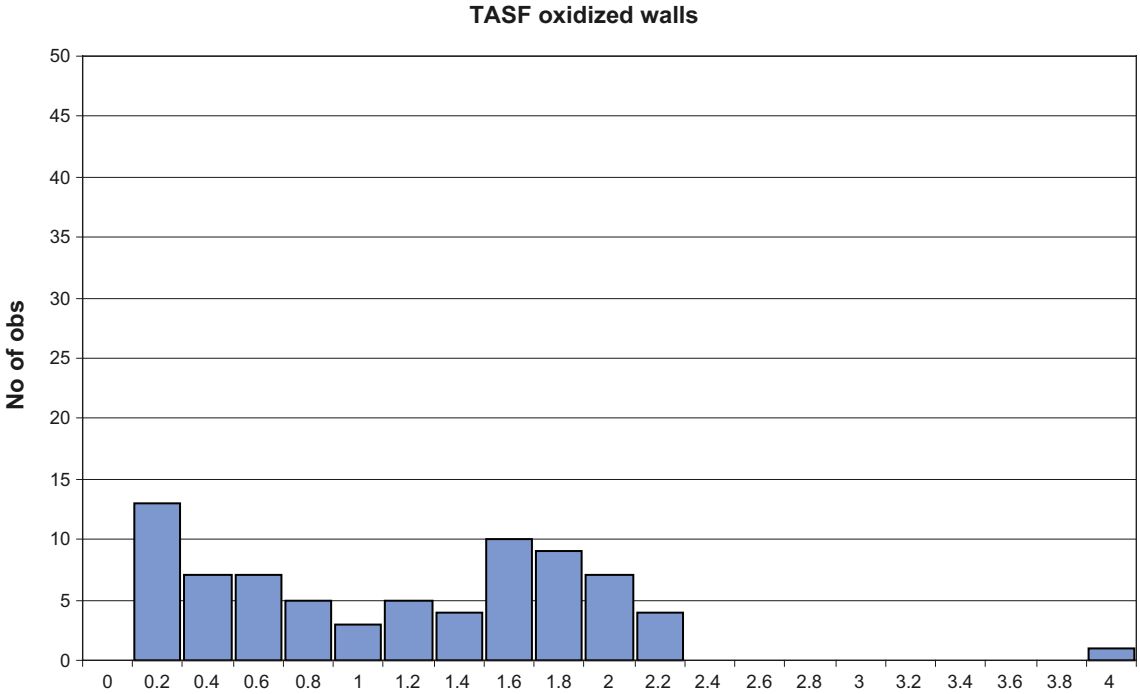

Figure C-22. *Histogram, TASF oxidized walls search radius 0.5 meters.*

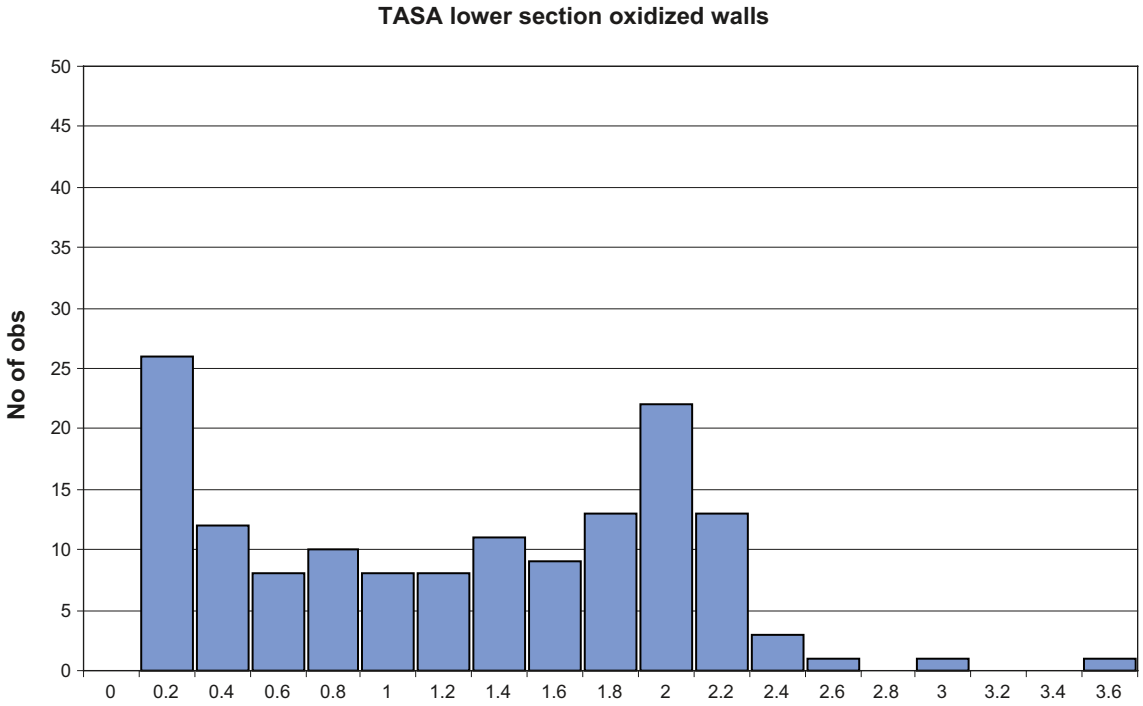

Figure C-23. *Histogram, TASA lower section oxidized walls search radius 0.5 meters.*

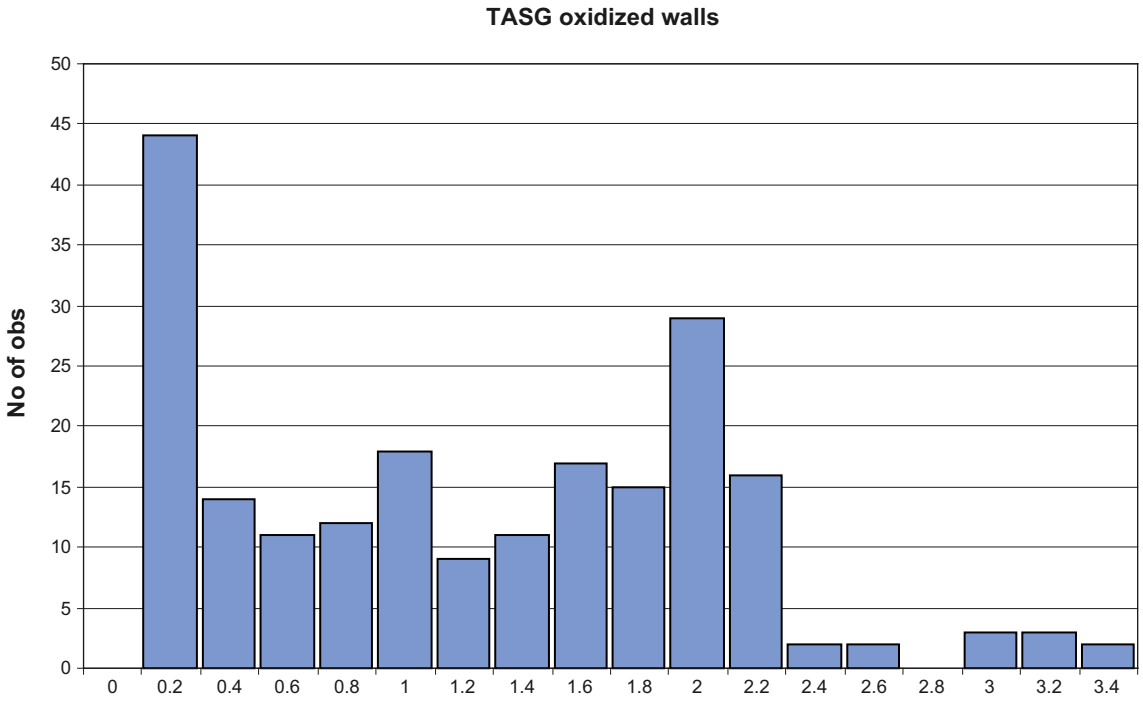

Figure C-24. *Histogram, TASG oxidized walls search radius 0.5 meters.*

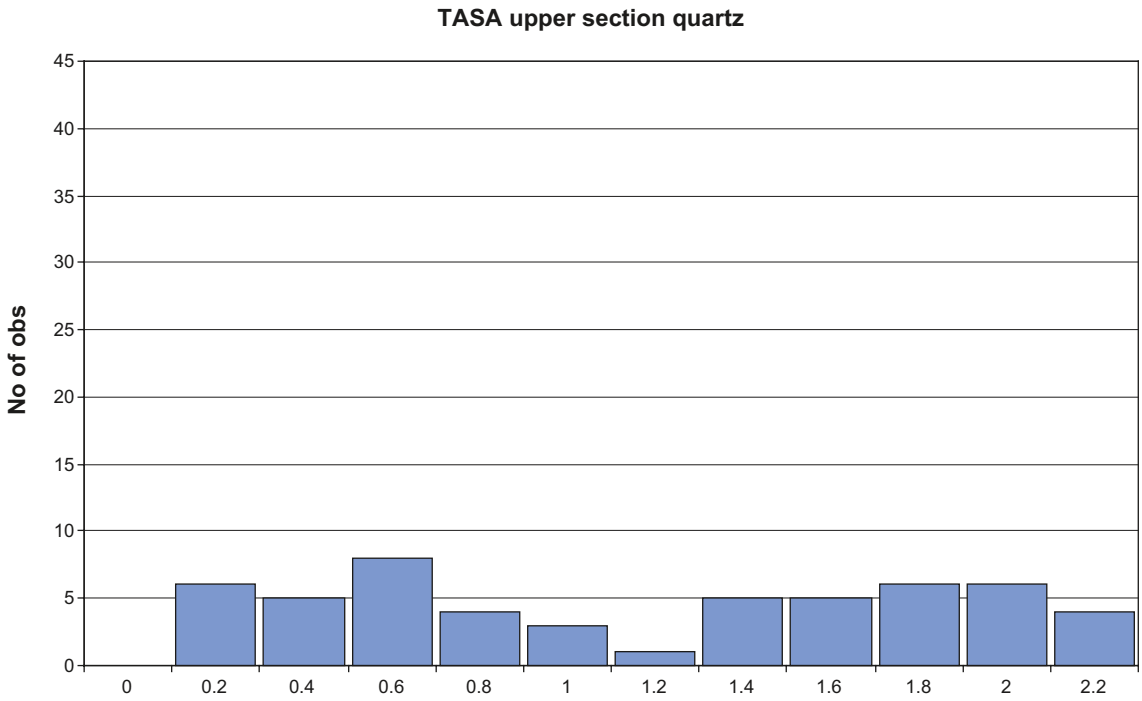

Figure C-25. *Histogram, TASA upper section quartz search radius 0.5 meters.*

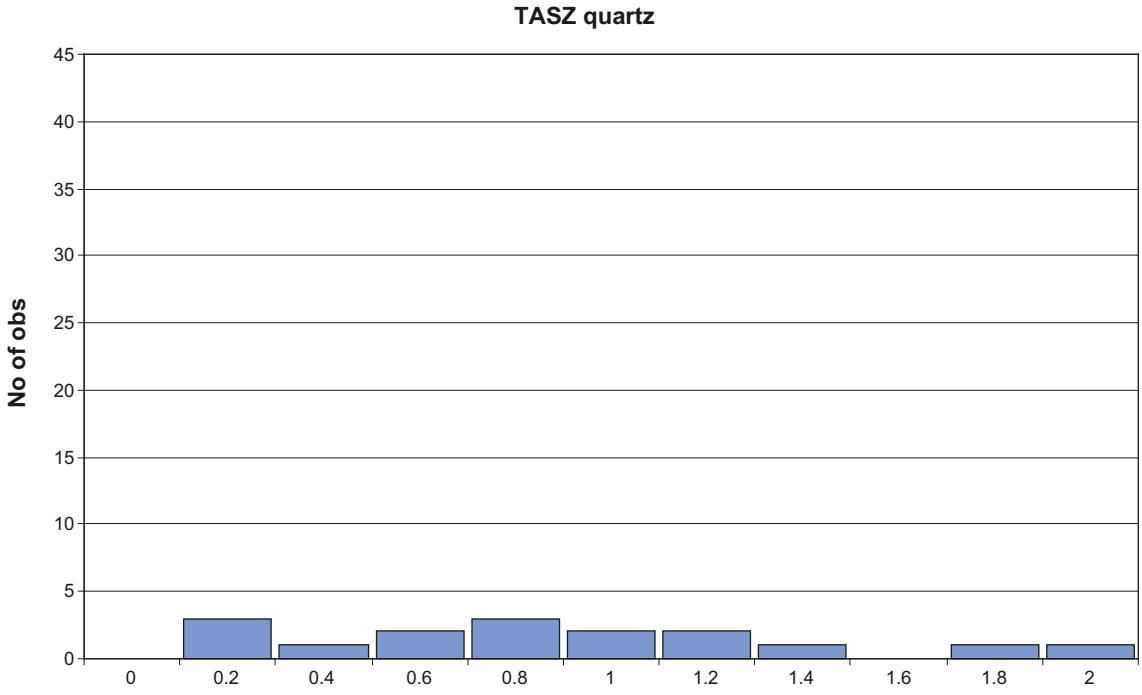

Figure C-26. *Histogram, TASZ quartz search radius 0.5 meters.*

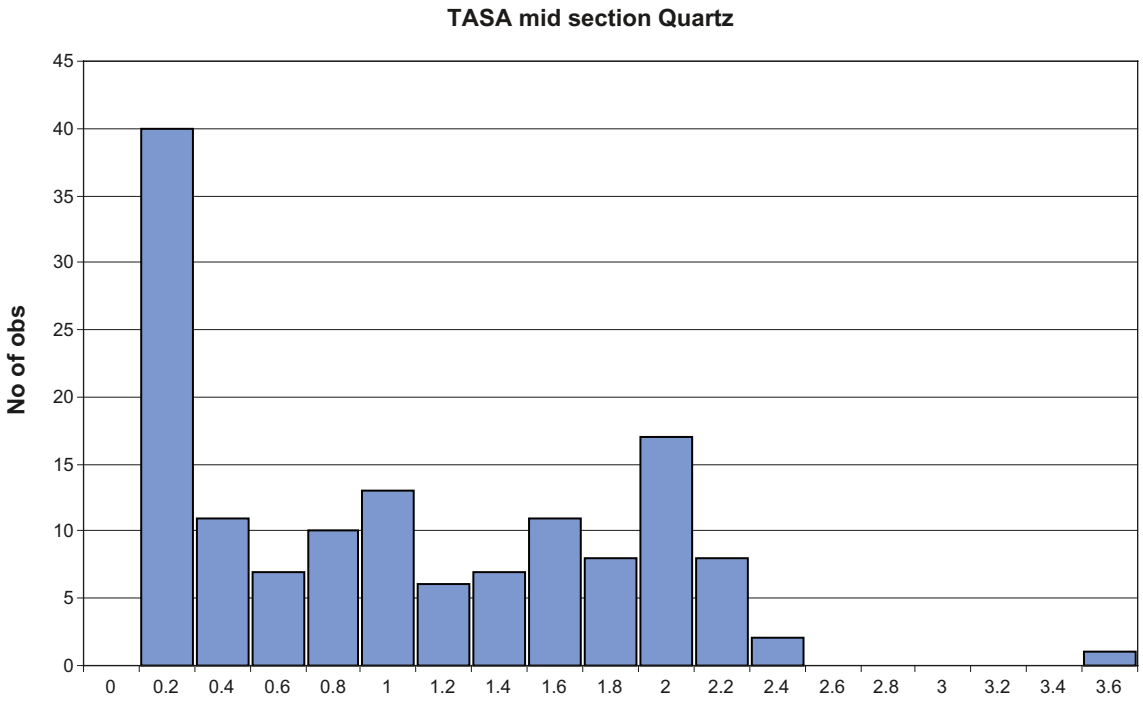

Figure C-27. *Histogram, TASA mid section quartz search radius 0.5 meters.*

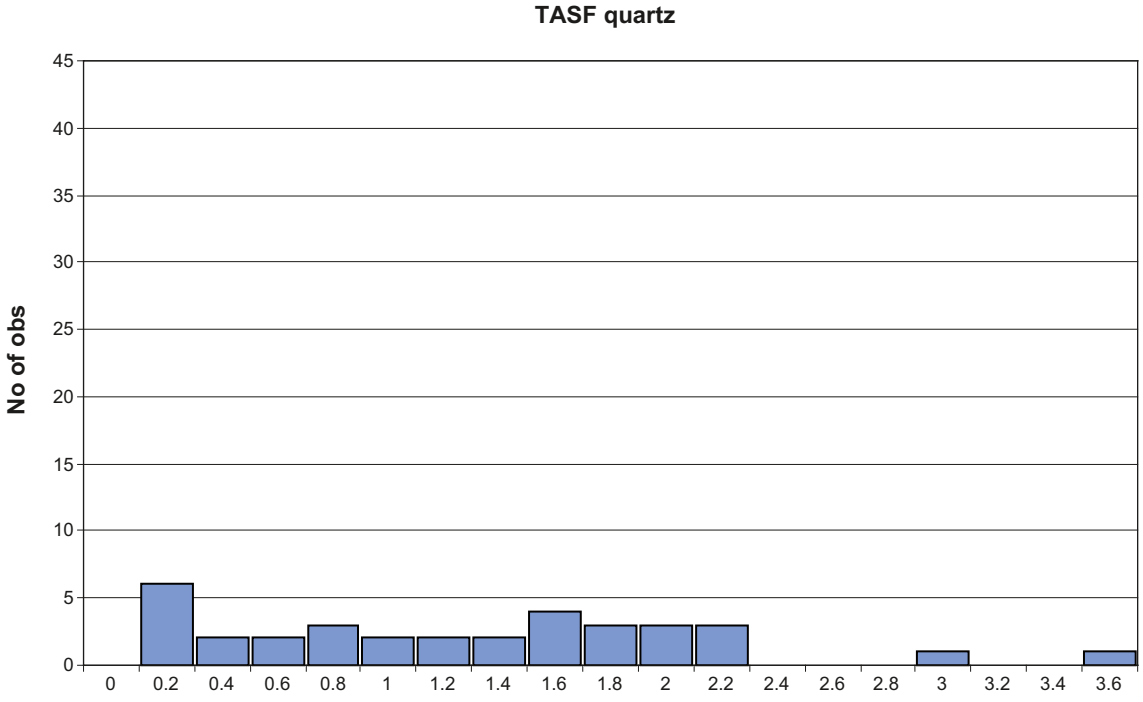

Figure C-28. *Histogram, TASF quartz search radius 0.5 meters.*

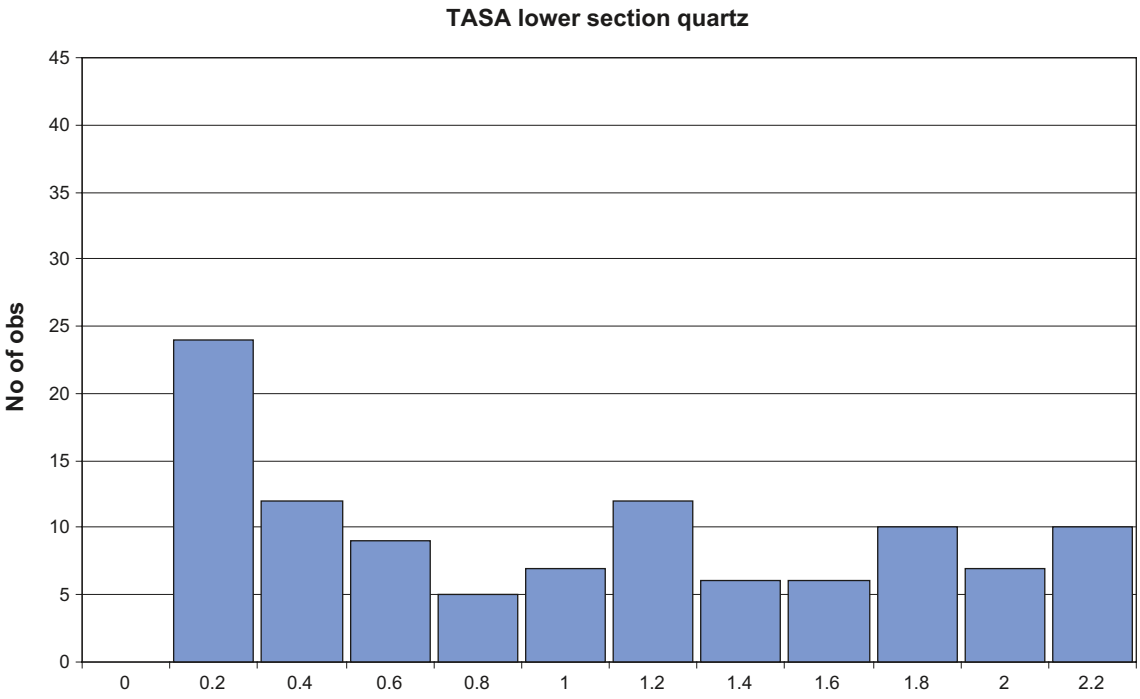

Figure C-29. *Histogram, TASA lower section quartz search radius 0.5 meters.*

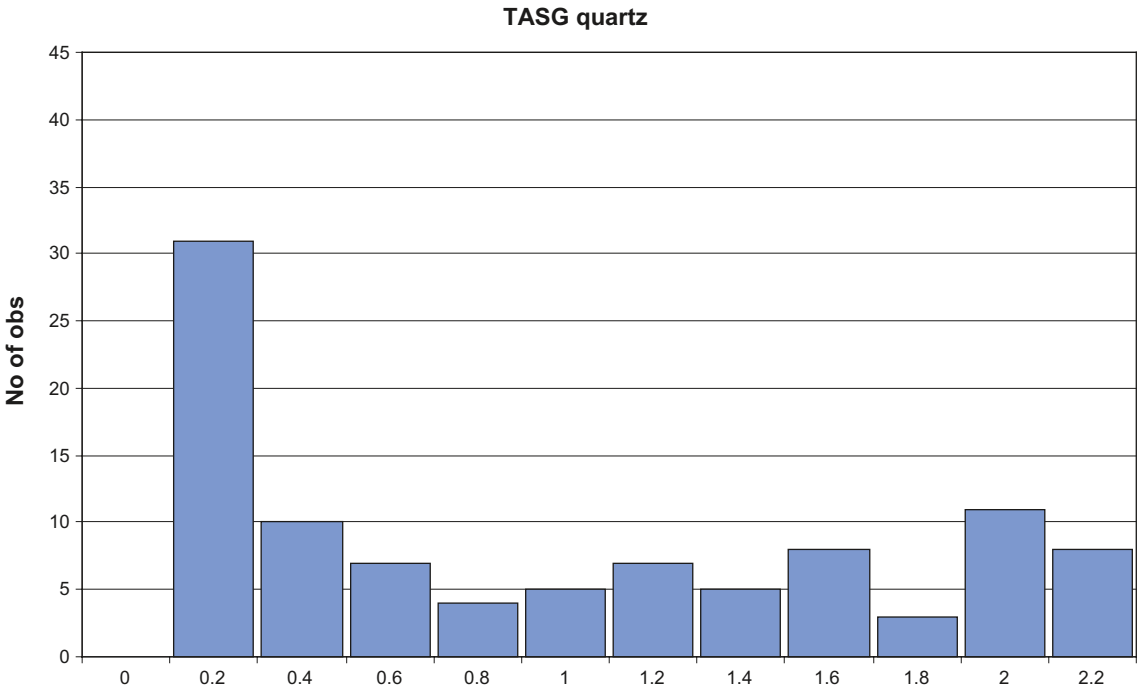

Figure C-30. *Histogram, TASG quartz search radius 0.5 meters.*

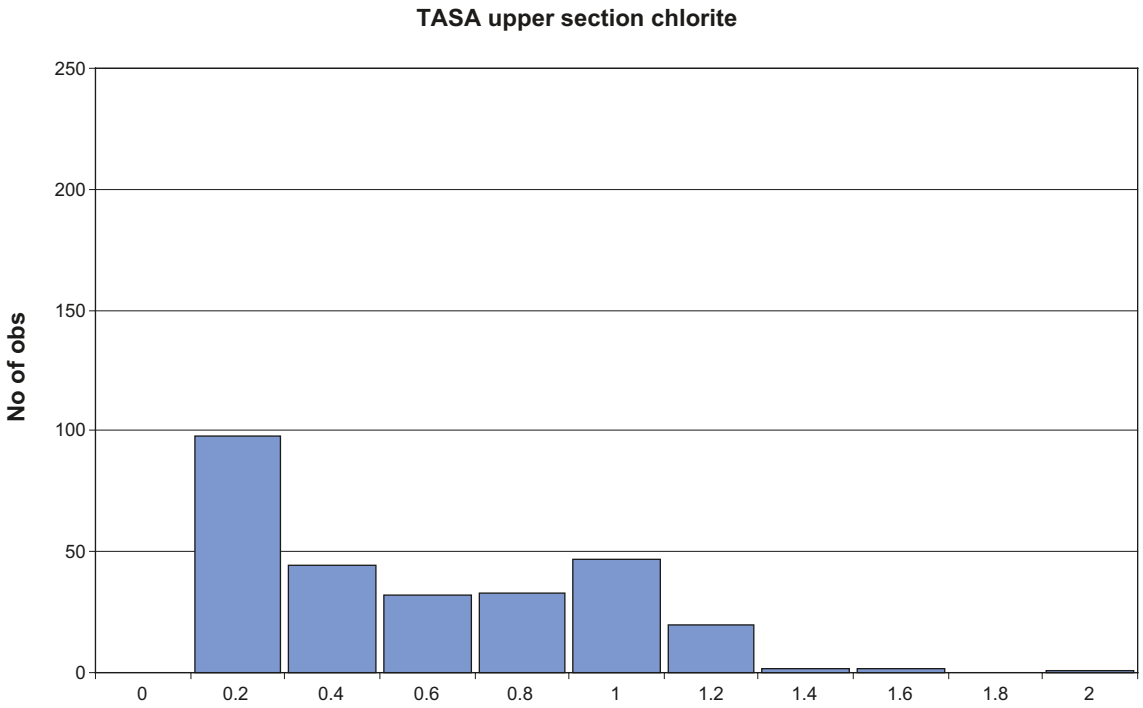

Figure C-31. *Histogram, TASA upper section chlorite search radius 1 meter.*

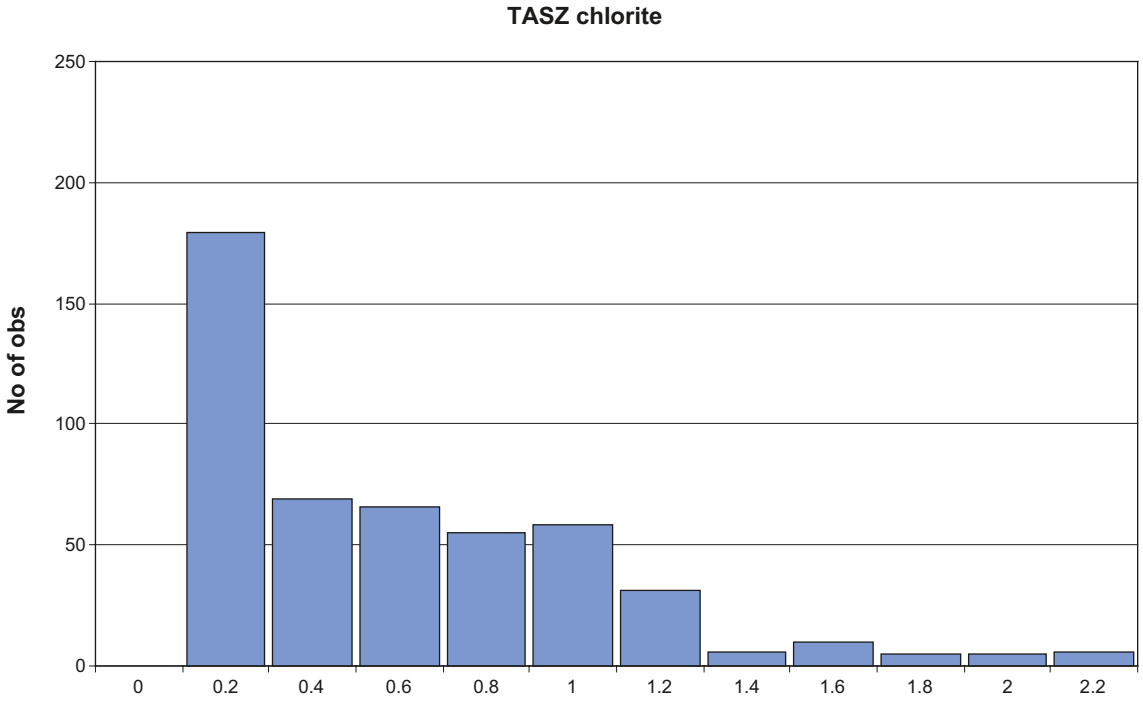

Figure C-32. *Histogram, TASZ chlorite search radius 1 meter.*

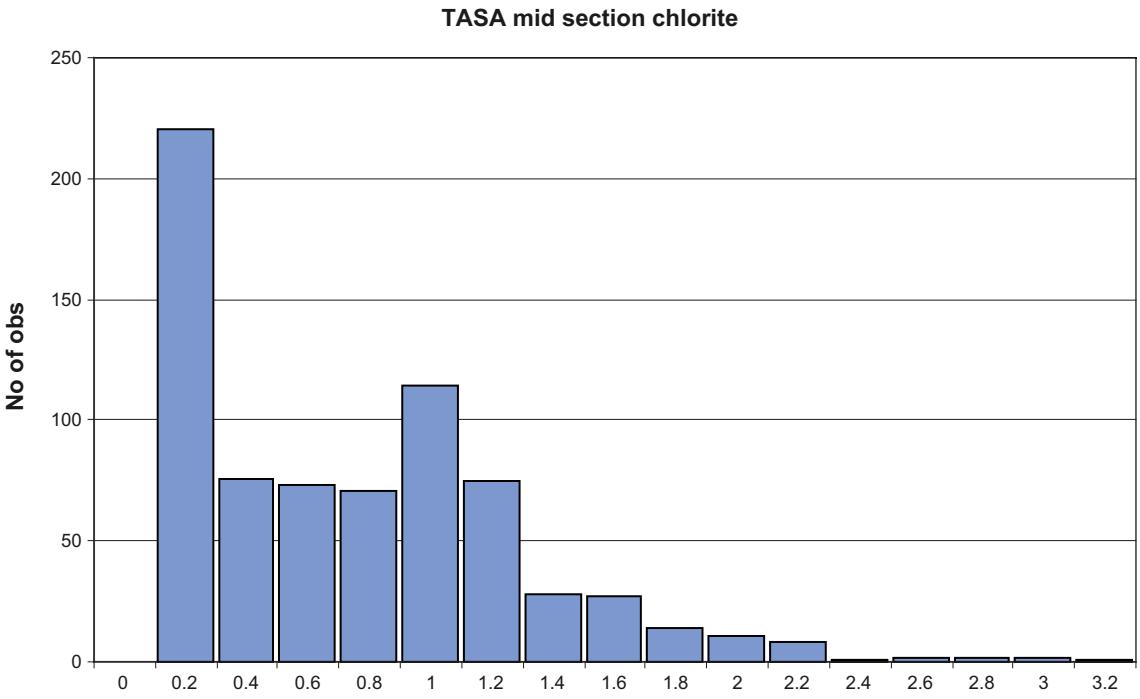

Figure C-33. *Histogram, TASA mid section chlorite search radius 1 meter.*

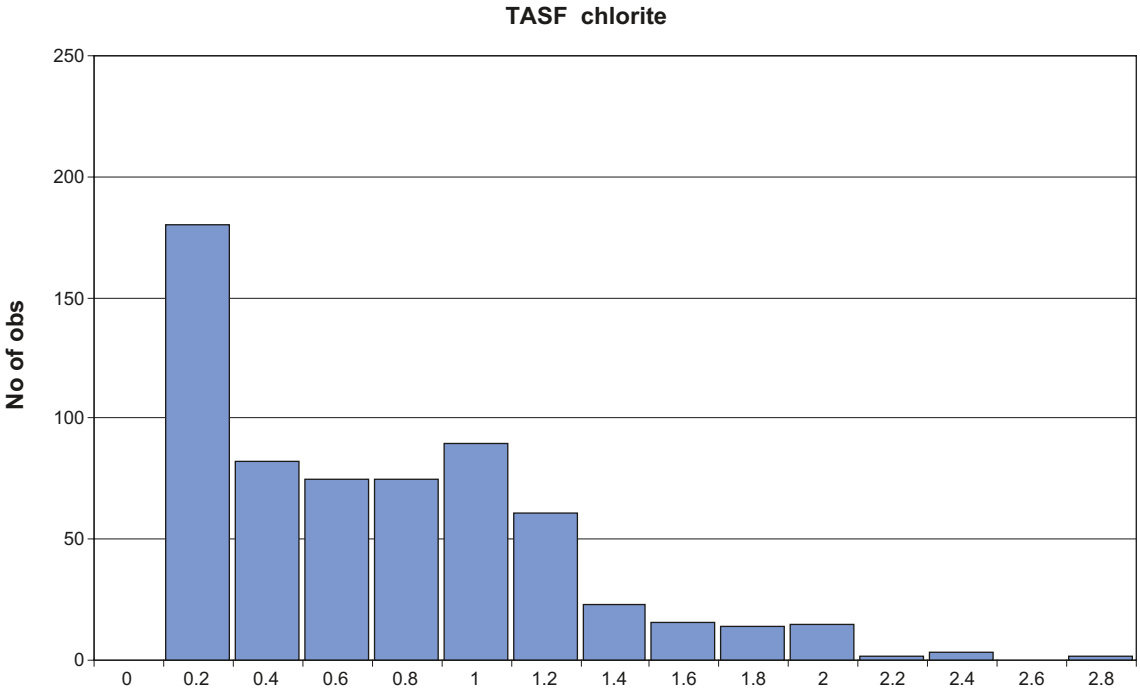

Figure C-34. *Histogram, TASF chlorite search radius 1 meter.*

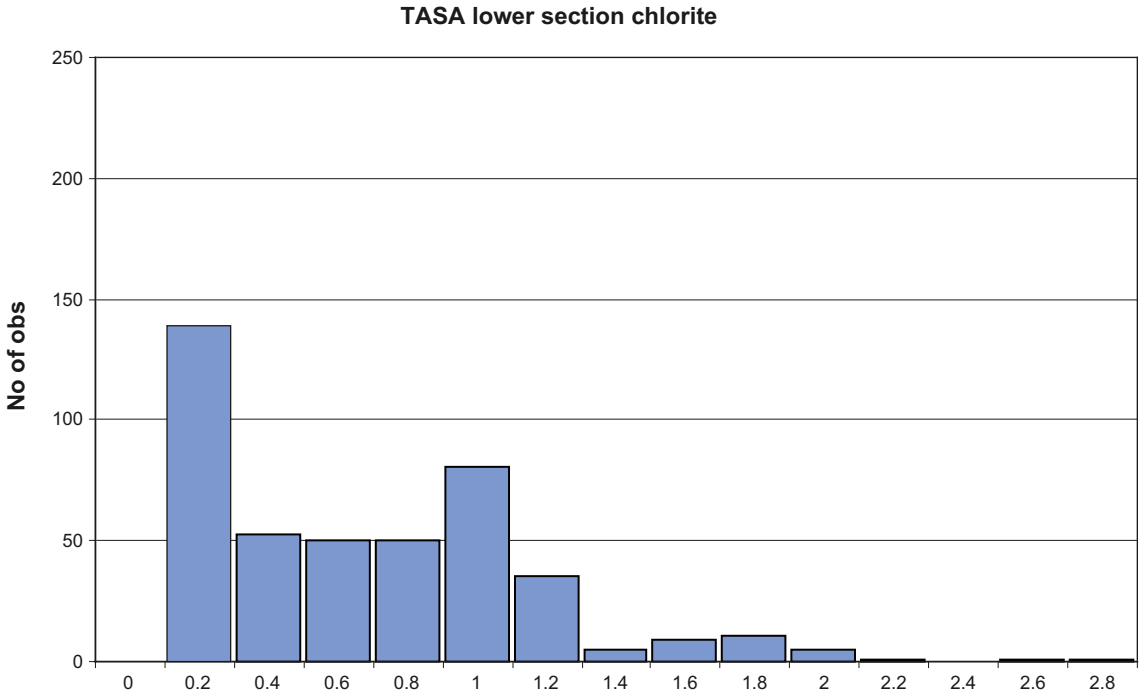

Figure C-35. *Histogram, TASA lower section chlorite search radius 1 meter.*

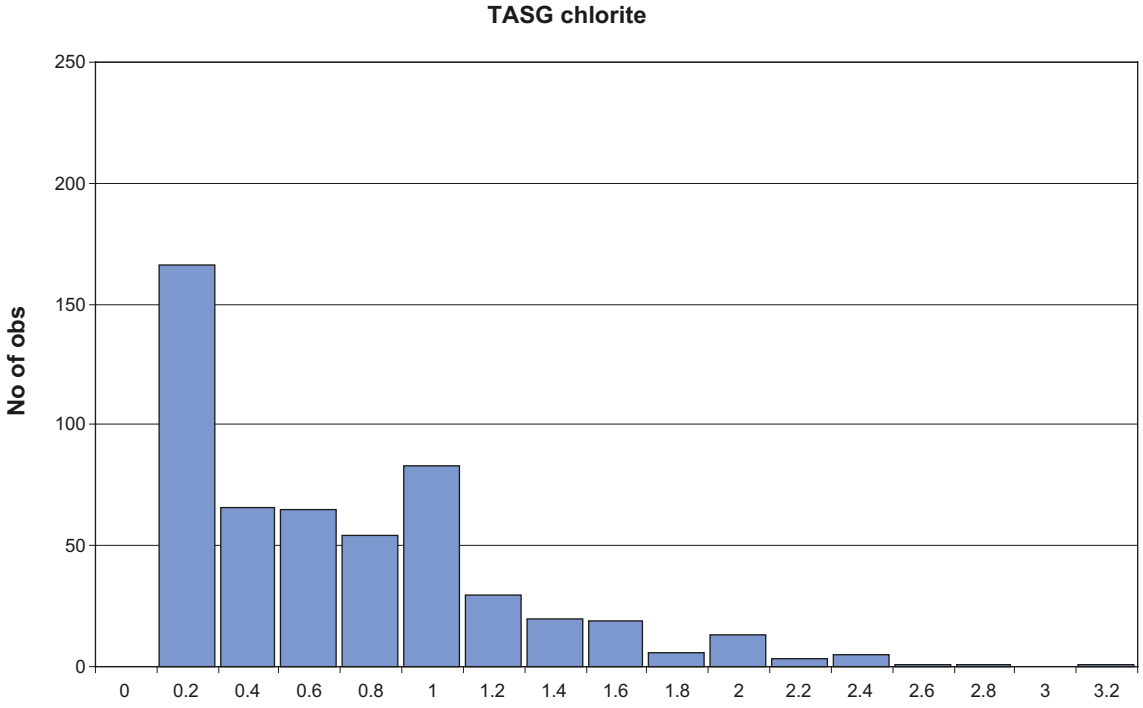

Figure C-36. *Histogram, TASG chlorite search radius 1 meter.*

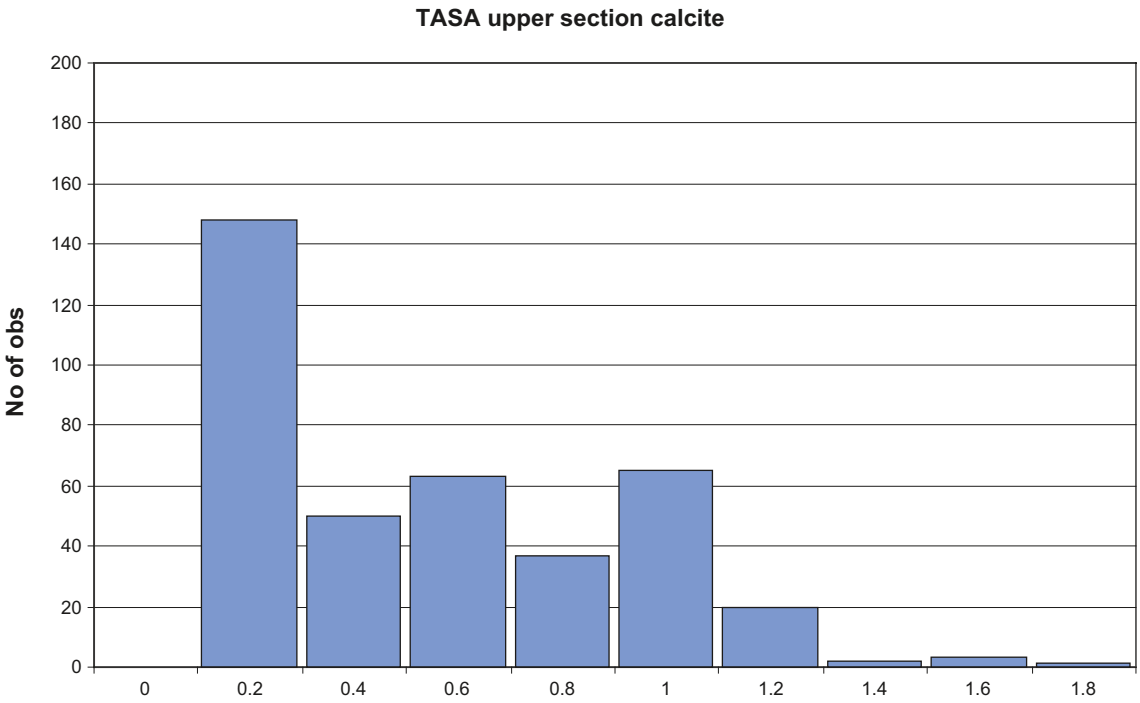

Figure C-37. *Histogram, TASA upper section calcite search radius 1 meter.*

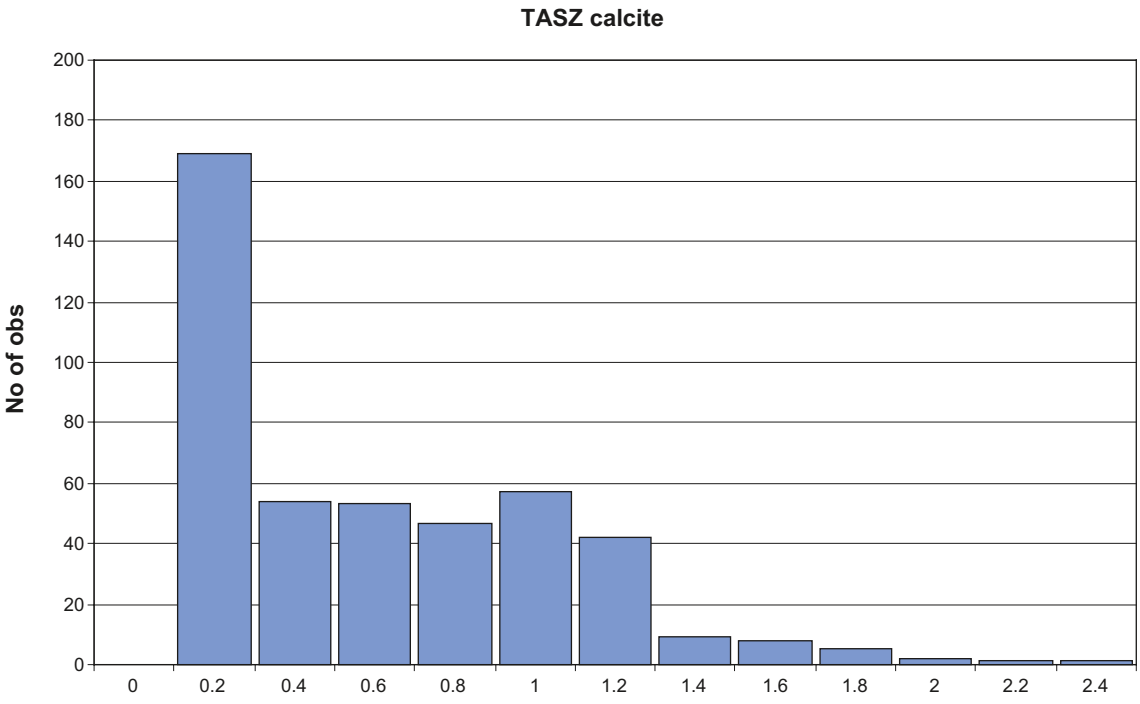

Figure C-38. *Histogram, TASZ calcite search radius 1 meter.*

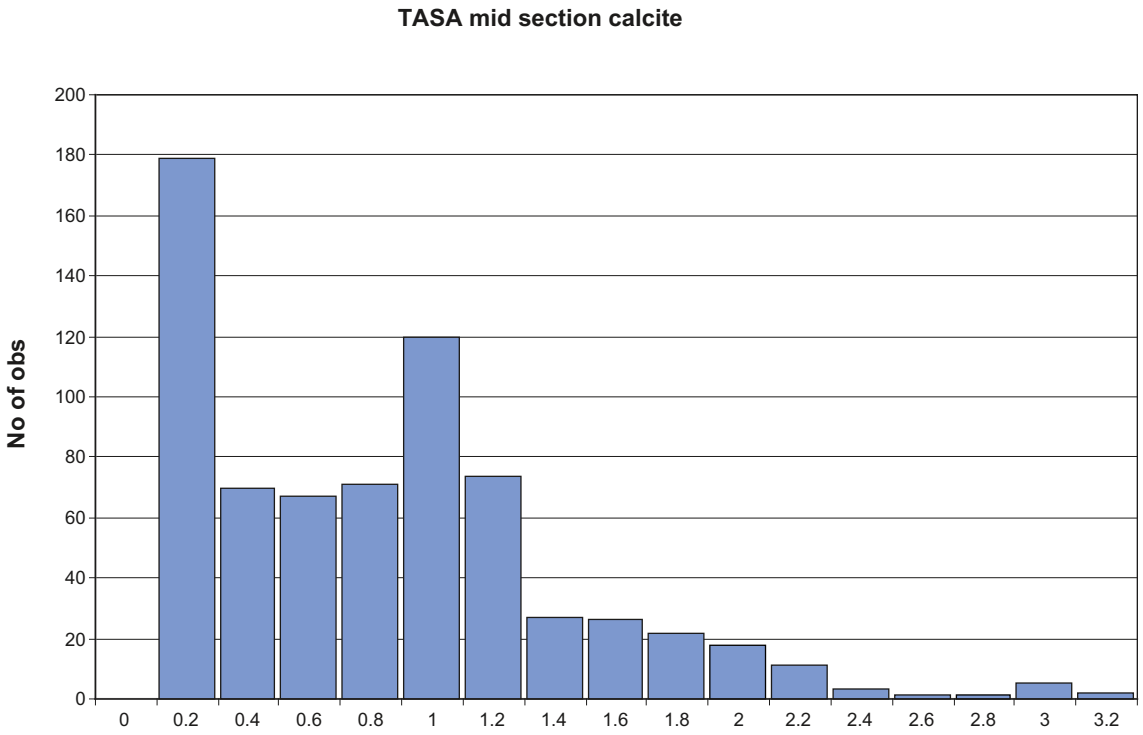

Figure C-39. *Histogram, TASA mid section calcite search radius 1 meter.*

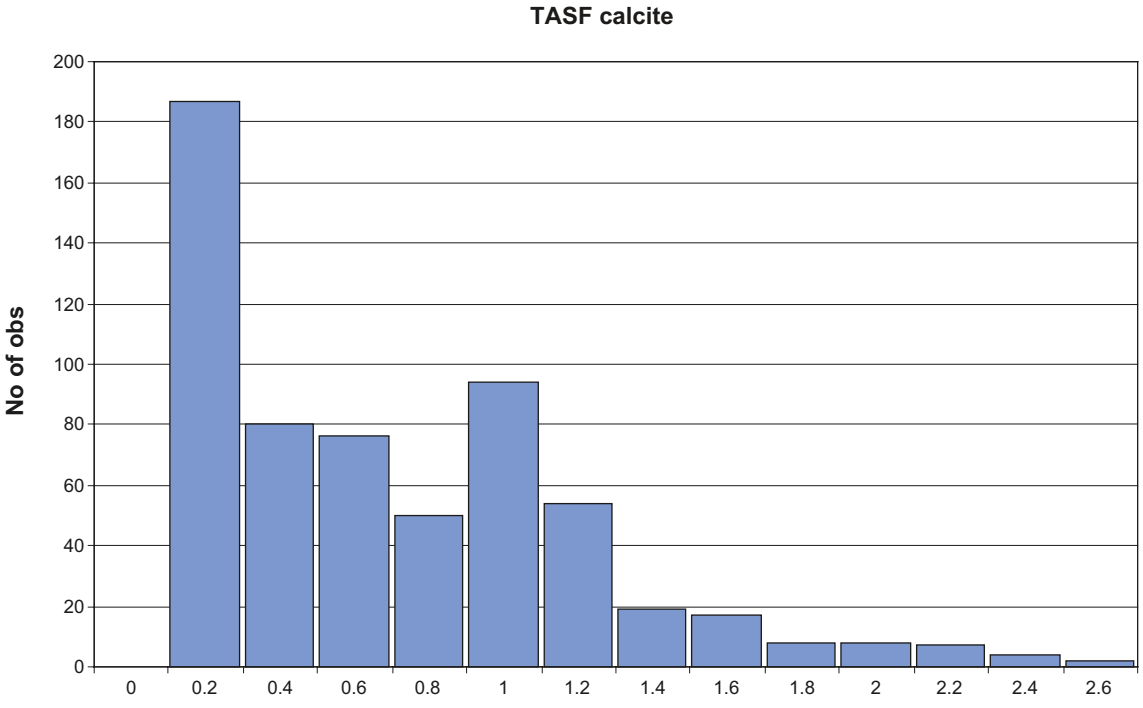

Figure C-40. *Histogram, TASF calcite search radius 1 meter.*

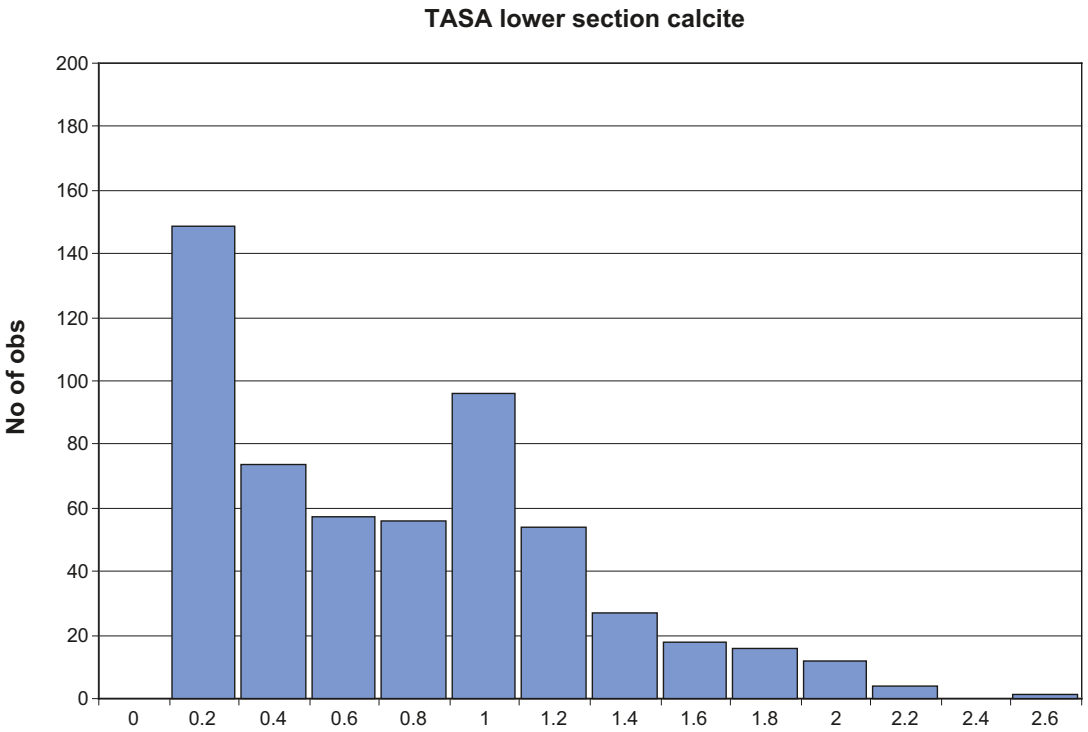

Figure C-41. *Histogram, TASA lower section calcite search radius 1 meter.*

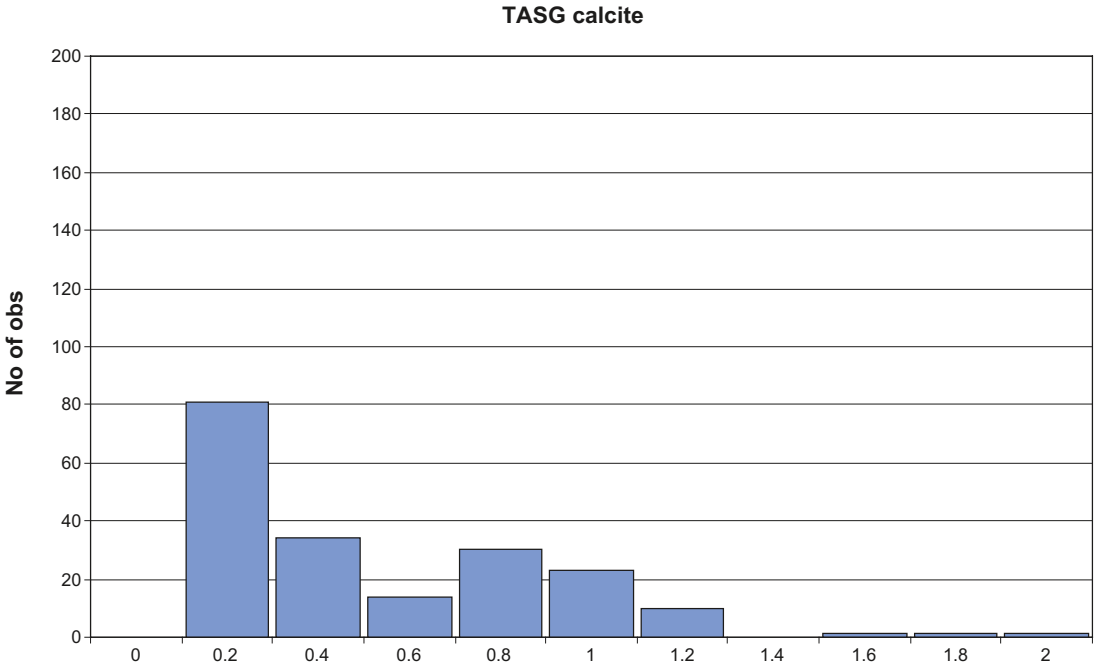

Figure C-42. *Histogram, TASF calcite search radius 1 meter.*

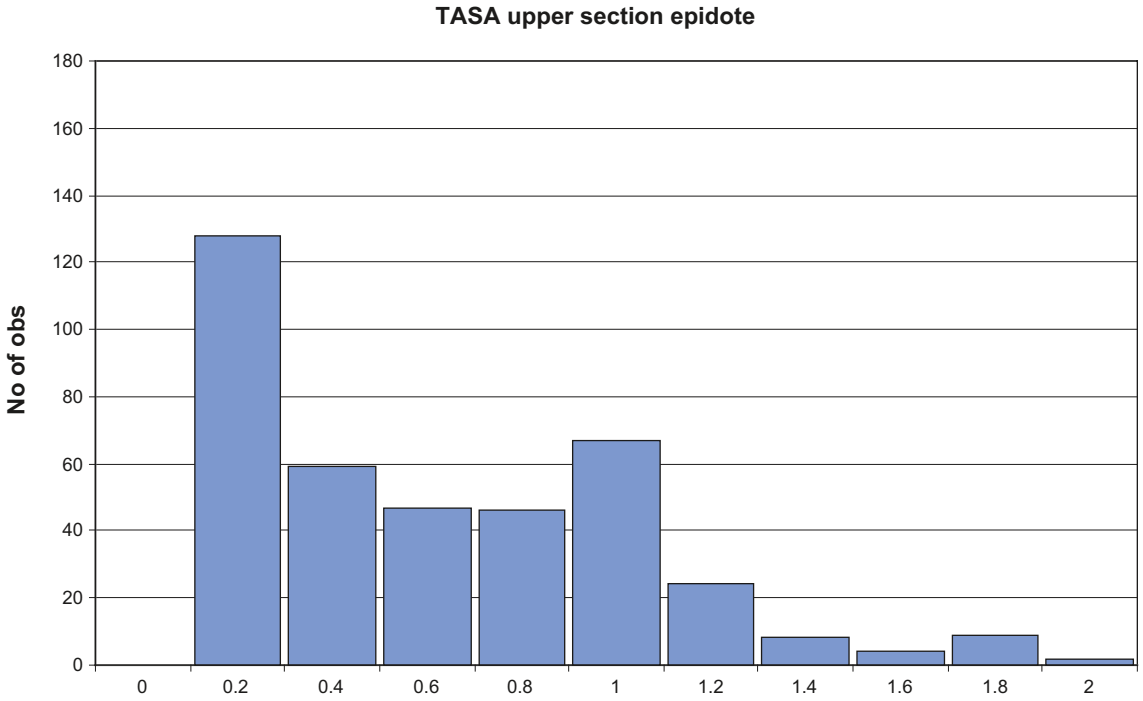

Figure C-43. *Histogram, TASA upper section epidote search radius 1 meter.*

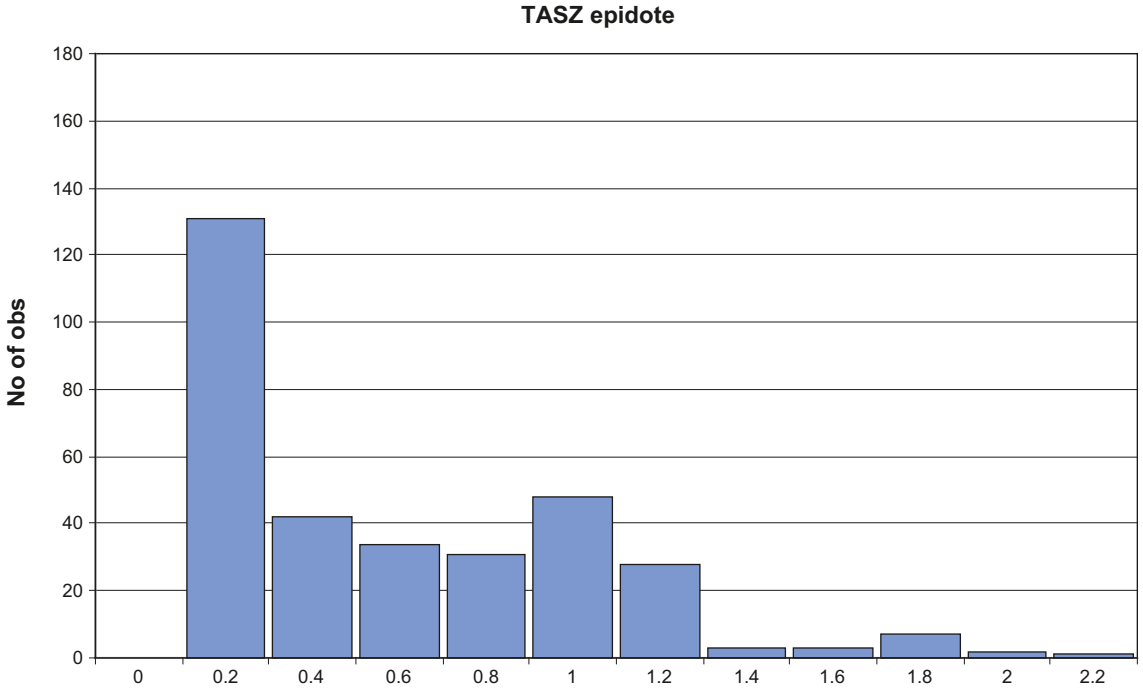

Figure C-44. *Histogram, TASZ epidote search radius 1 meter.*

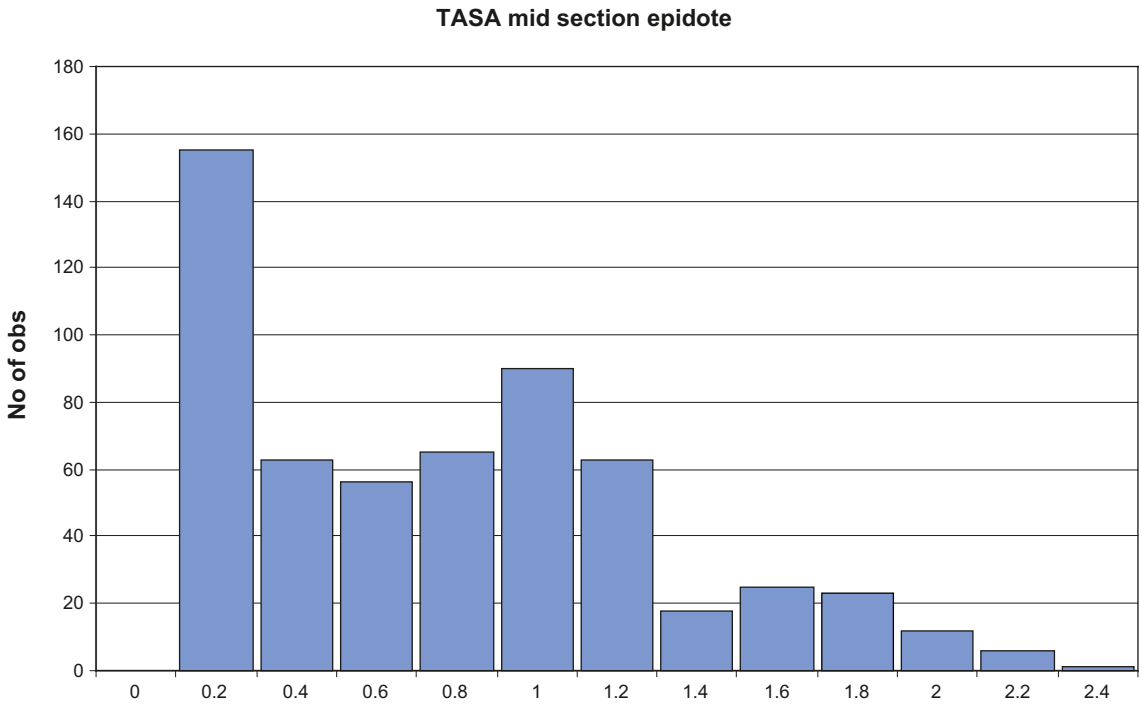

Figure C-45. *Histogram, TASA mid section epidote search radius 1 meter.*

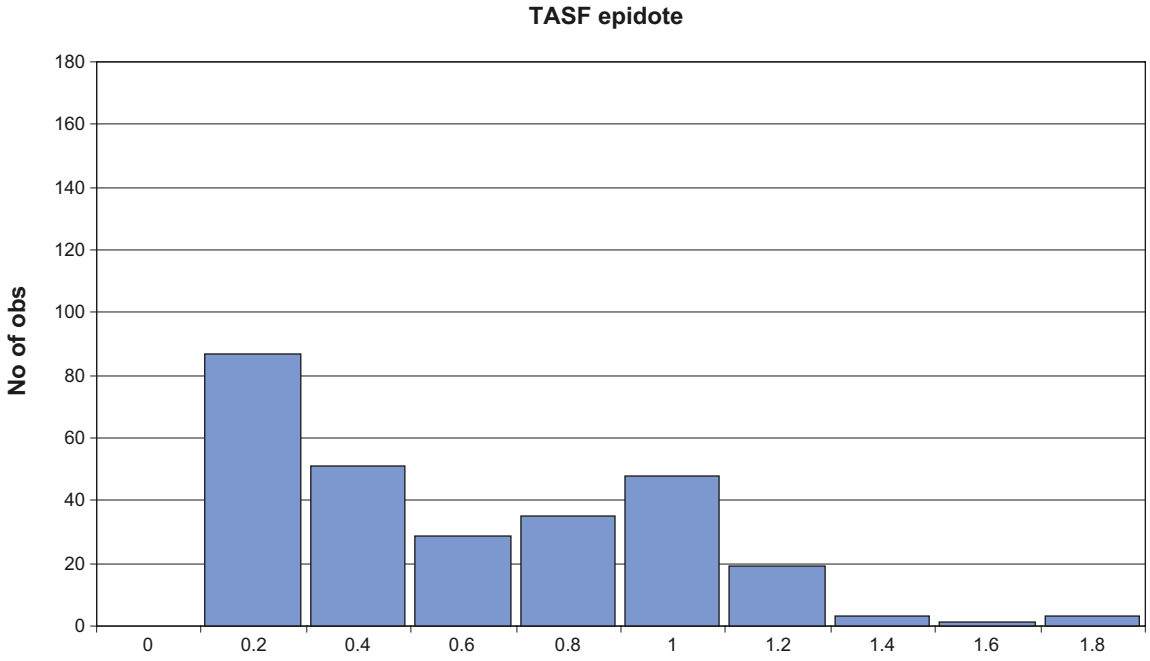

Figure C-46. *Histogram, TASFepidote search radius 1 meter.*

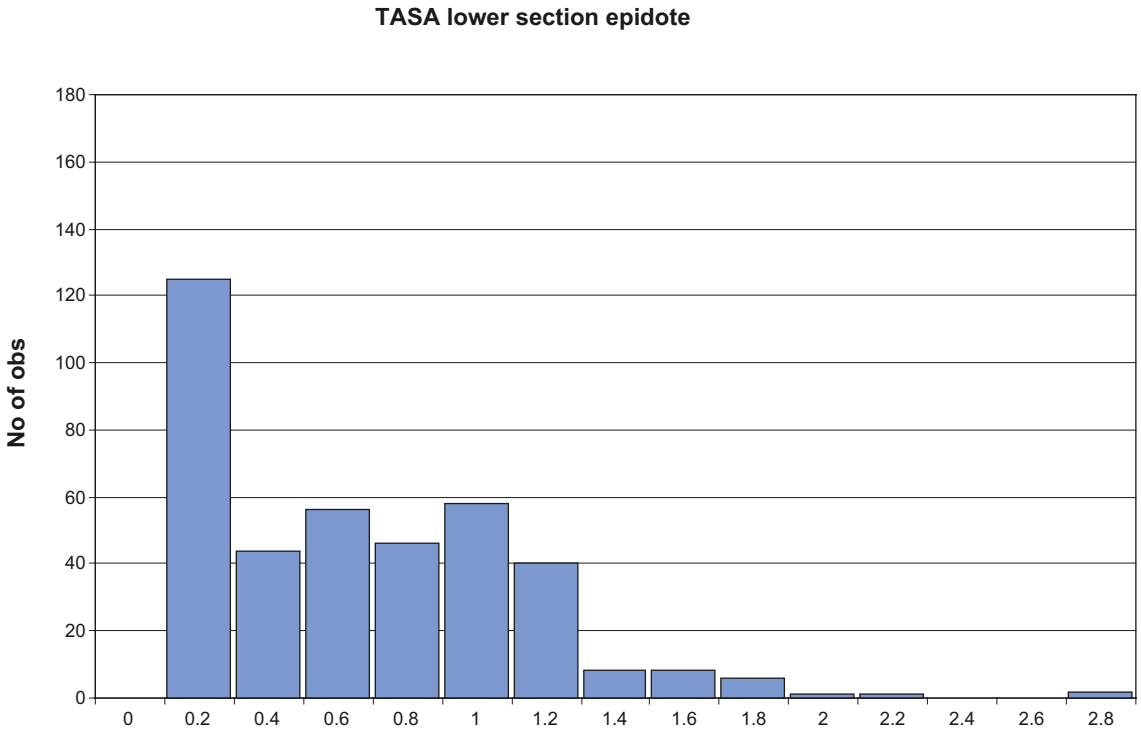

Figure C-47. *Histogram, TASA lower section epidote search radius 1 meter.*

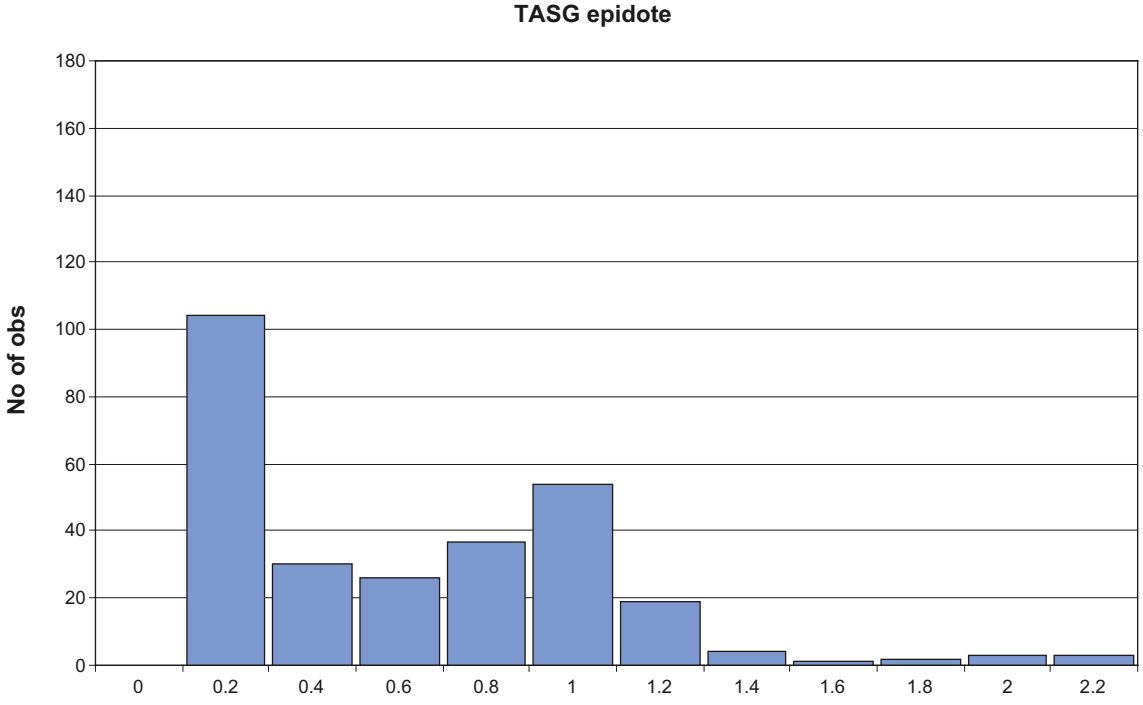

Figure C-48. *Histogram, TASG epidote search radius 1 meter.*

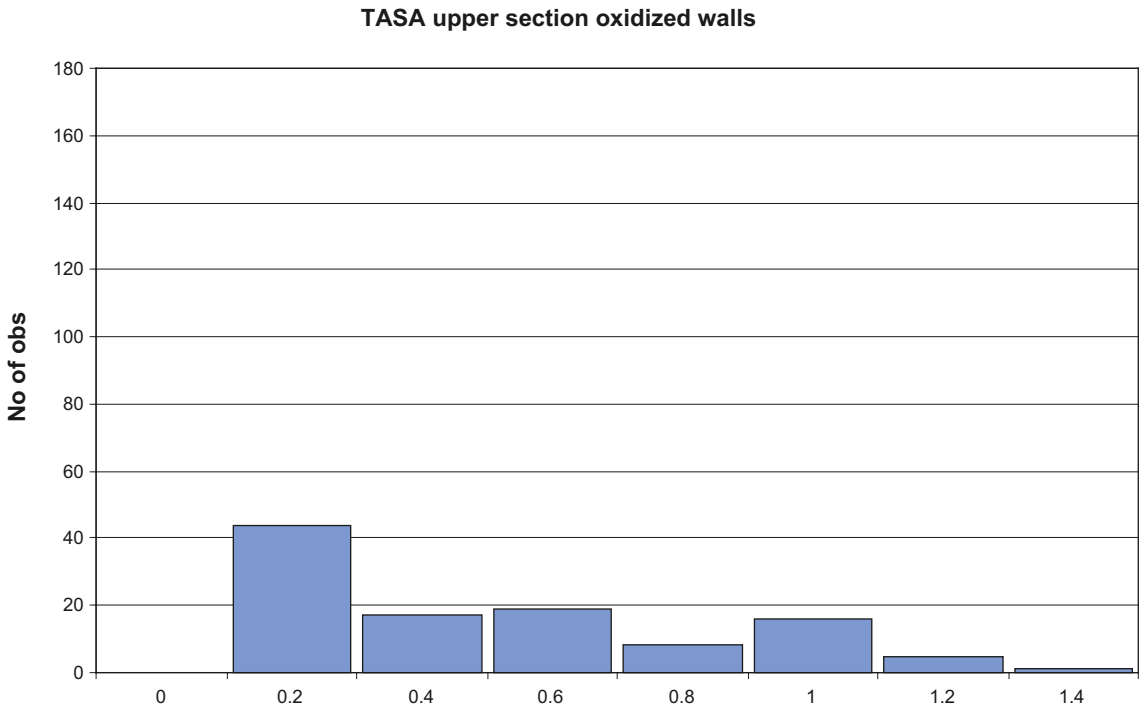

Figure C-49. *Histogram, TASA upper section oxidized walls search radius 1 meter.*

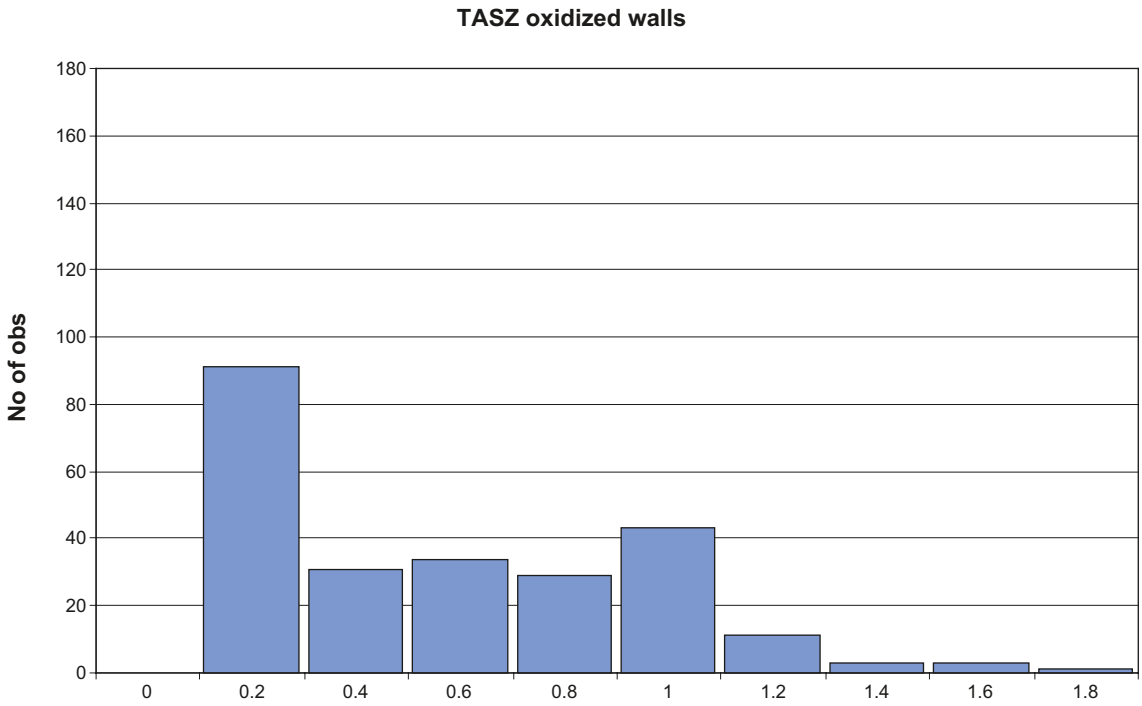

Figure C-50. *Histogram, TASZ oxidized walls search radius 1 meter.*

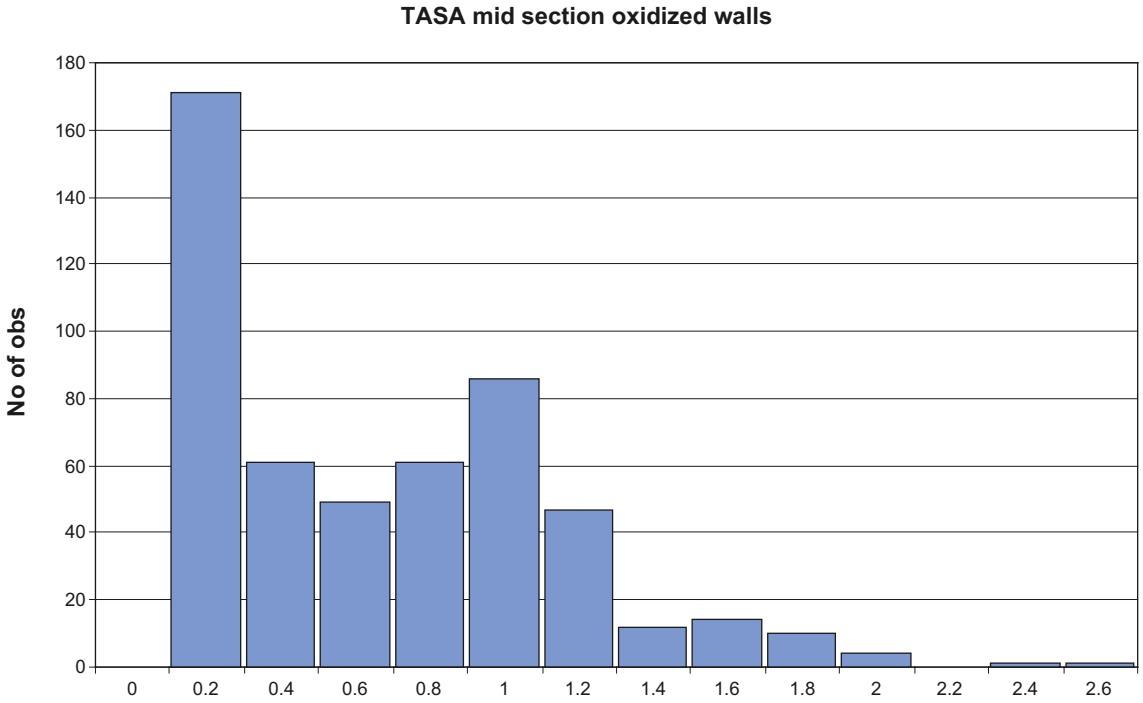

Figure C-51. *Histogram, TASA mid section oxidized walls search radius 1 meter.*

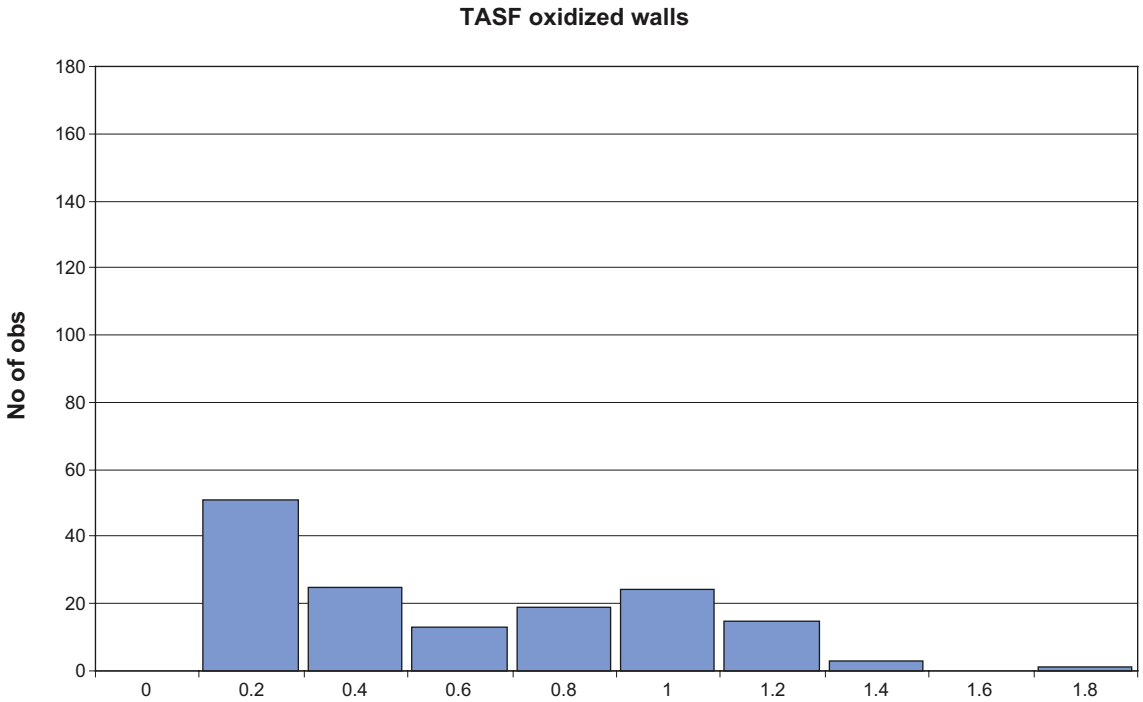

Figure C-52. *Histogram, TASF oxidized walls search radius 1 meter.*

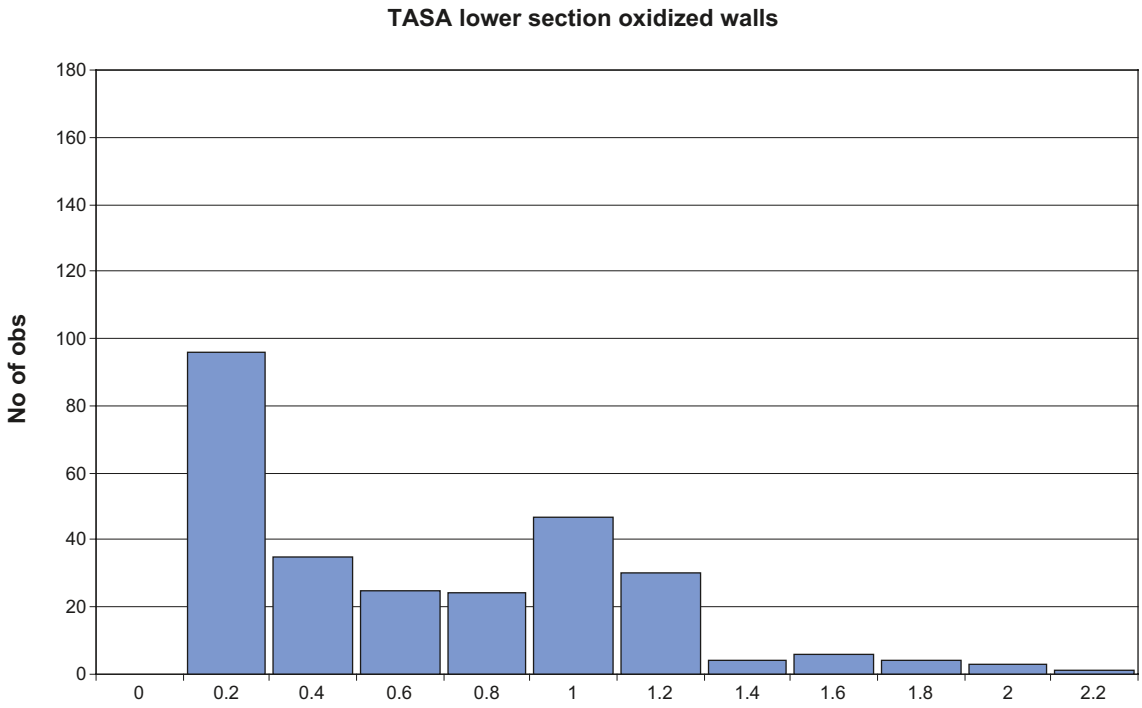

Figure C-53. *Histogram, TASA lower section oxidized walls search radius 1 meter.*

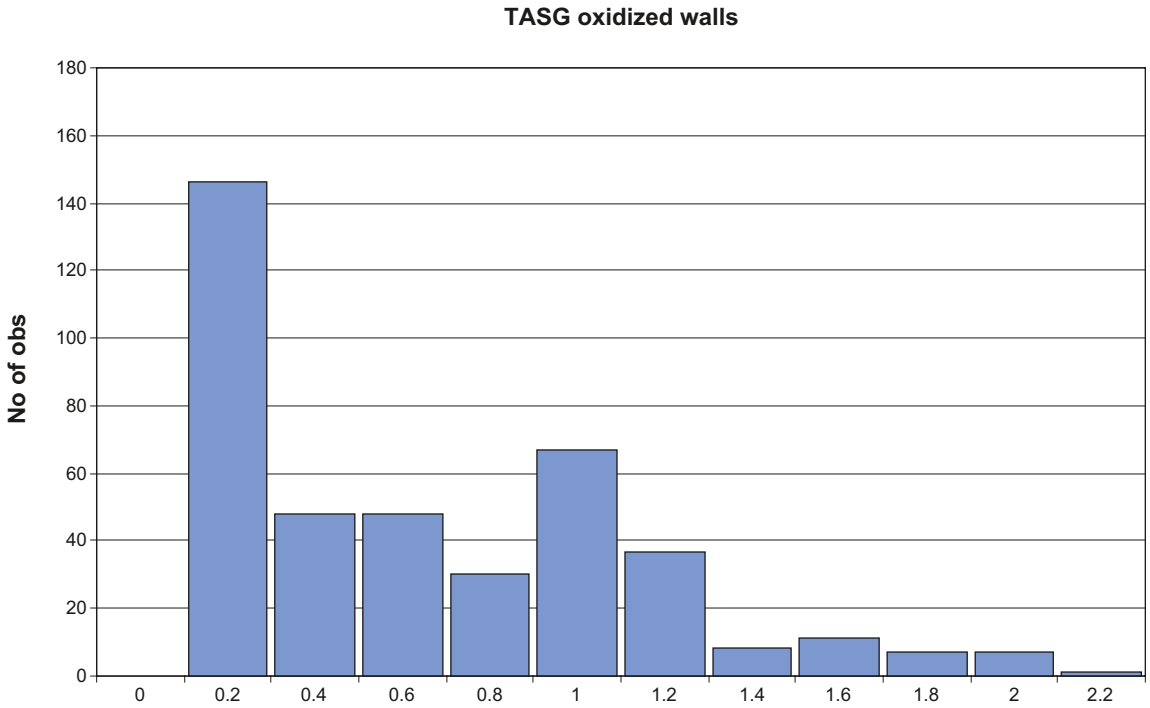

Figure C-54. *Histogram, TASG oxidized walls search radius 1 meter.*

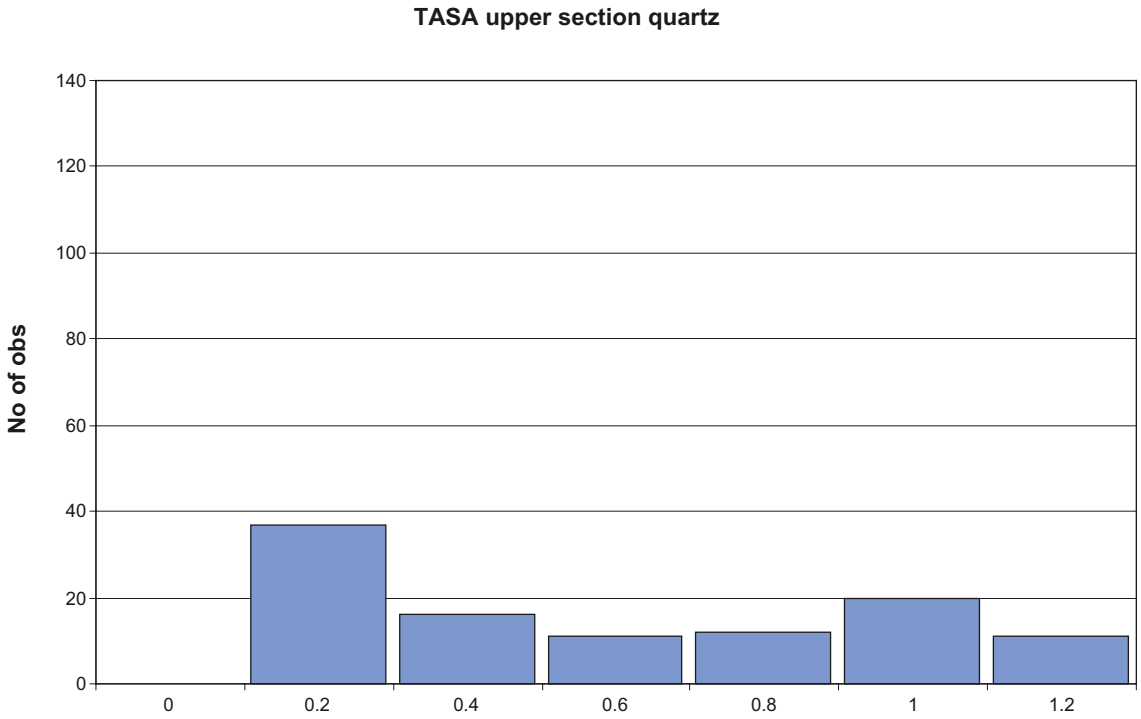

Figure C-55. *Histogram, TASA upper section quartz search radius 1 meter.*

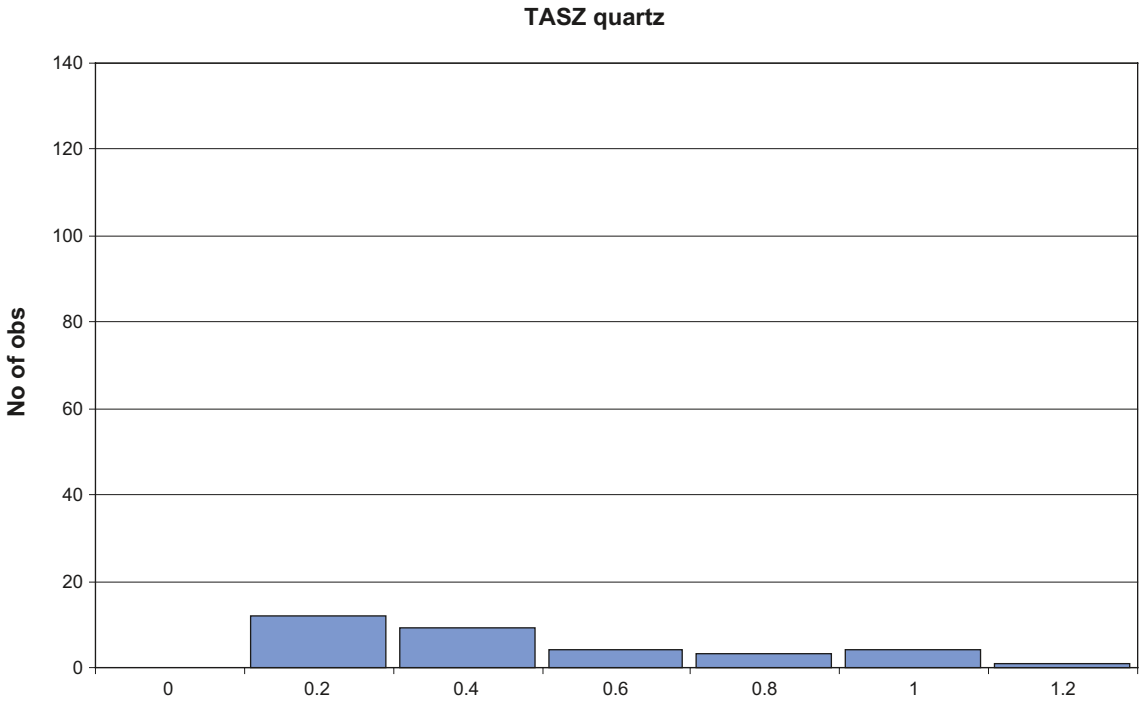

Figure C-56. *Histogram, TASZ quartz search radius 1 meter.*

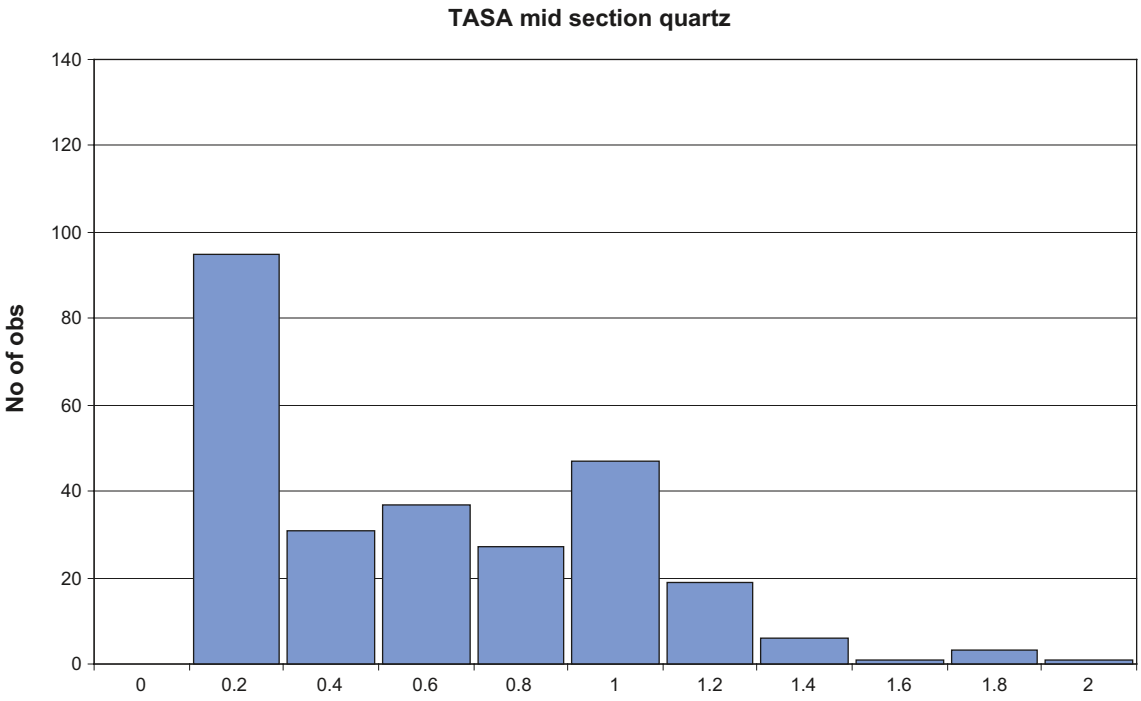

Figure C-57. *Histogram, TASA mid section quartz search radius 1 meter.*

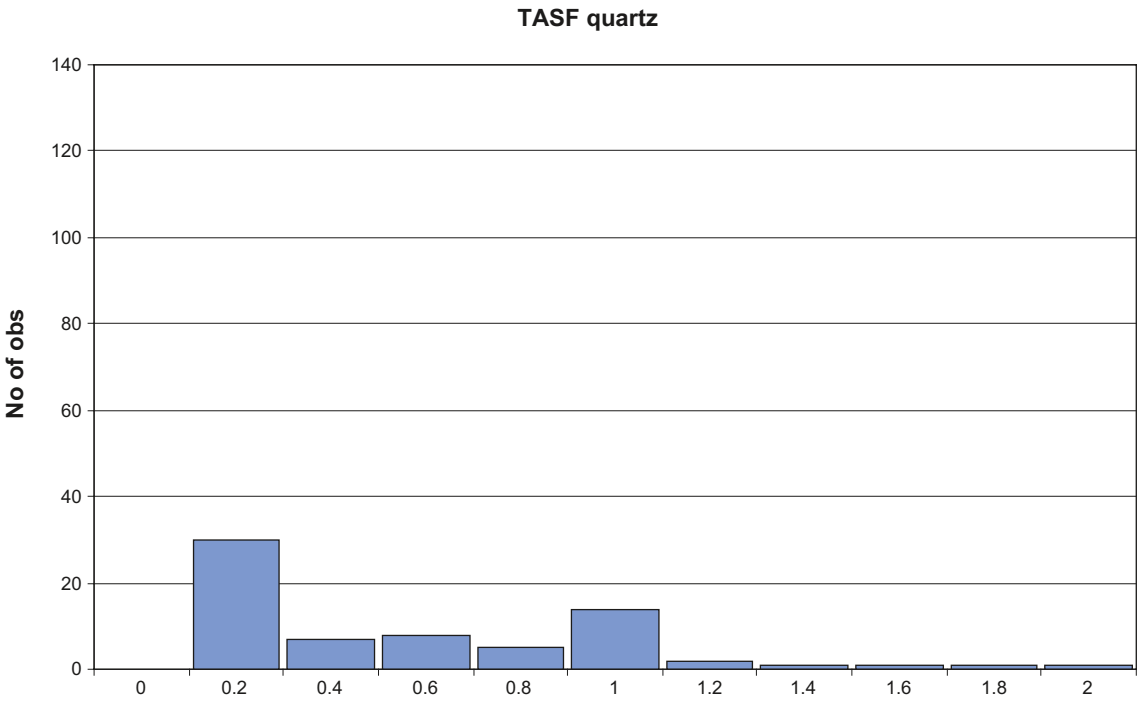

Figure C-58. *Histogram, TASF quartz search radius 1 meter.*

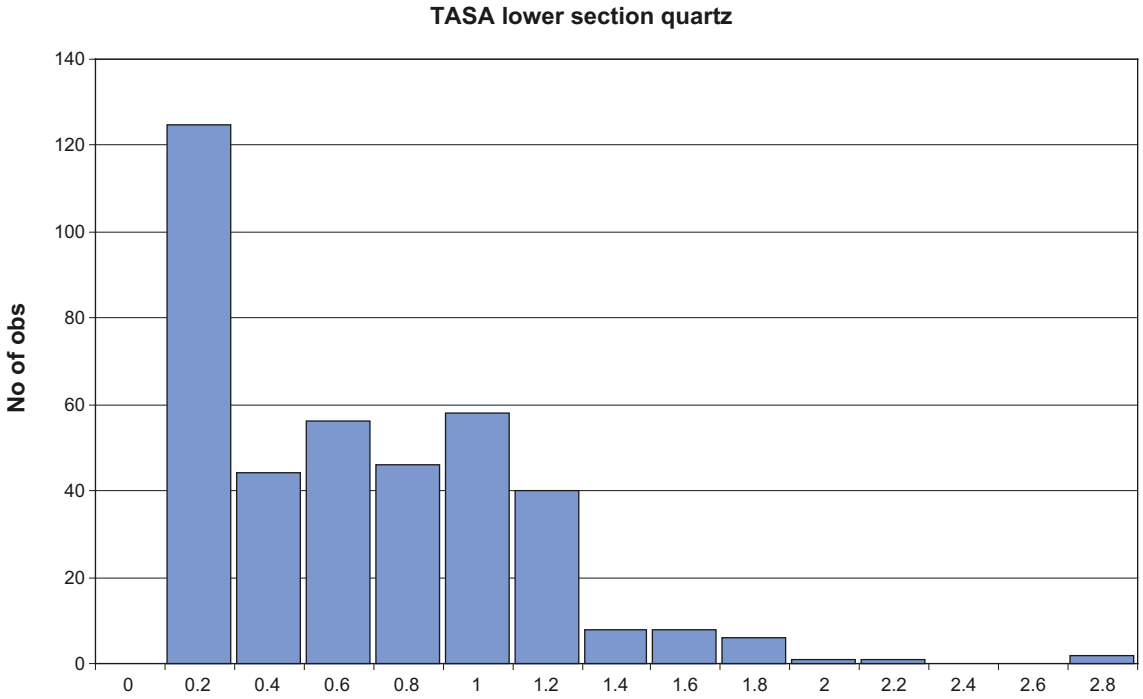

Figure C-59. *Histogram, TASA lower section quartz search radius 1 meter.*

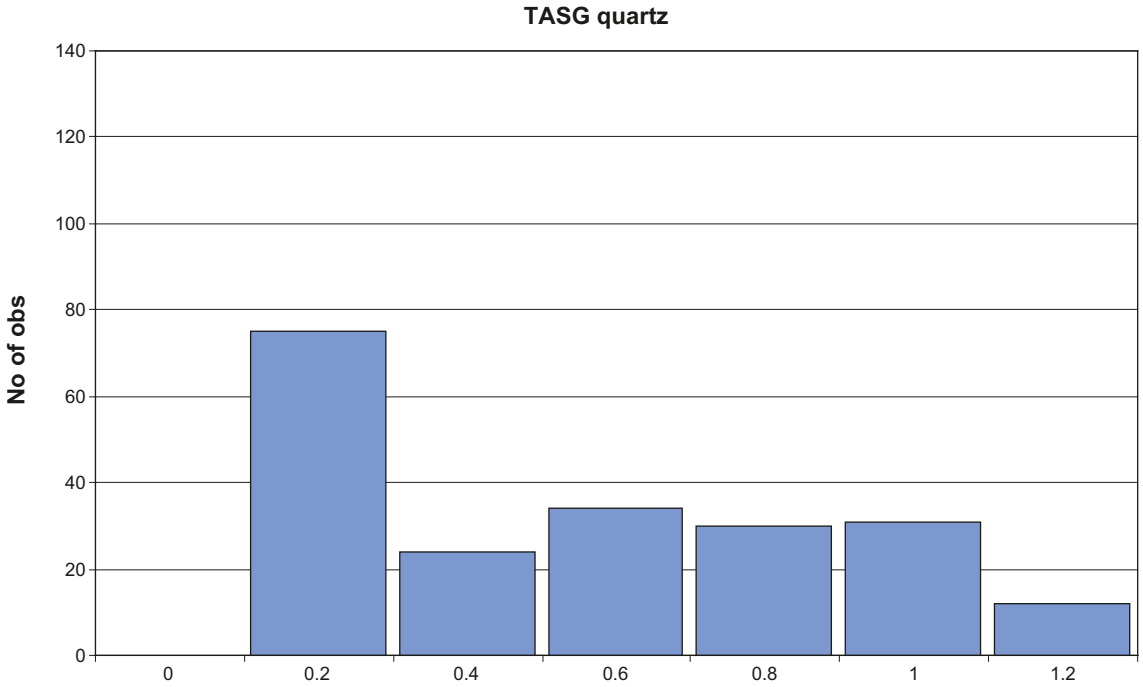

Figure C-60. *Histogram, TASG quartz search radius 1 meter.*

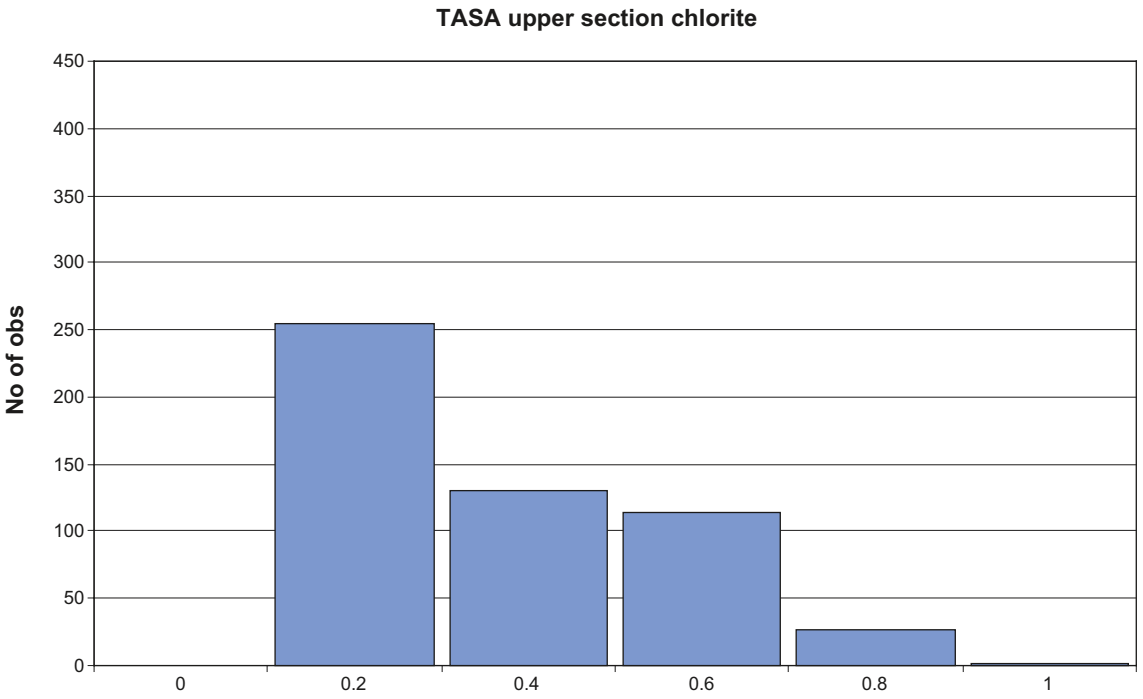

Figure C-61. *Histogram, TASA upper section chlorite search radius 2 meters.*

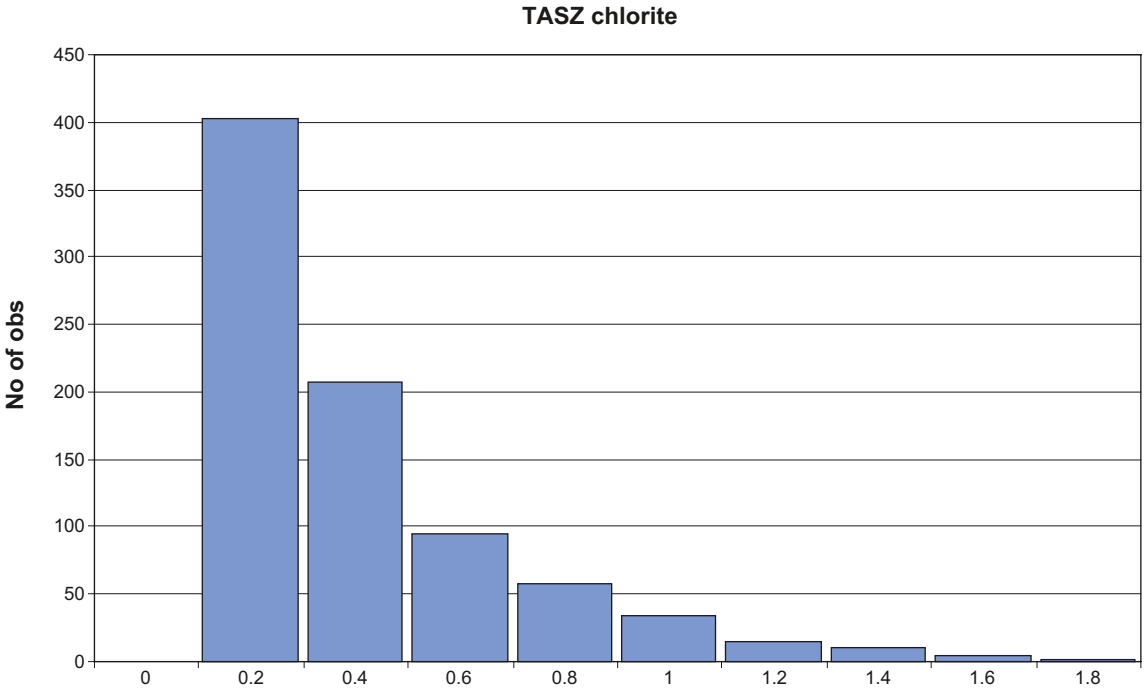

Figure C-62. *Histogram, TASZ chlorite search radius 2 meters.*

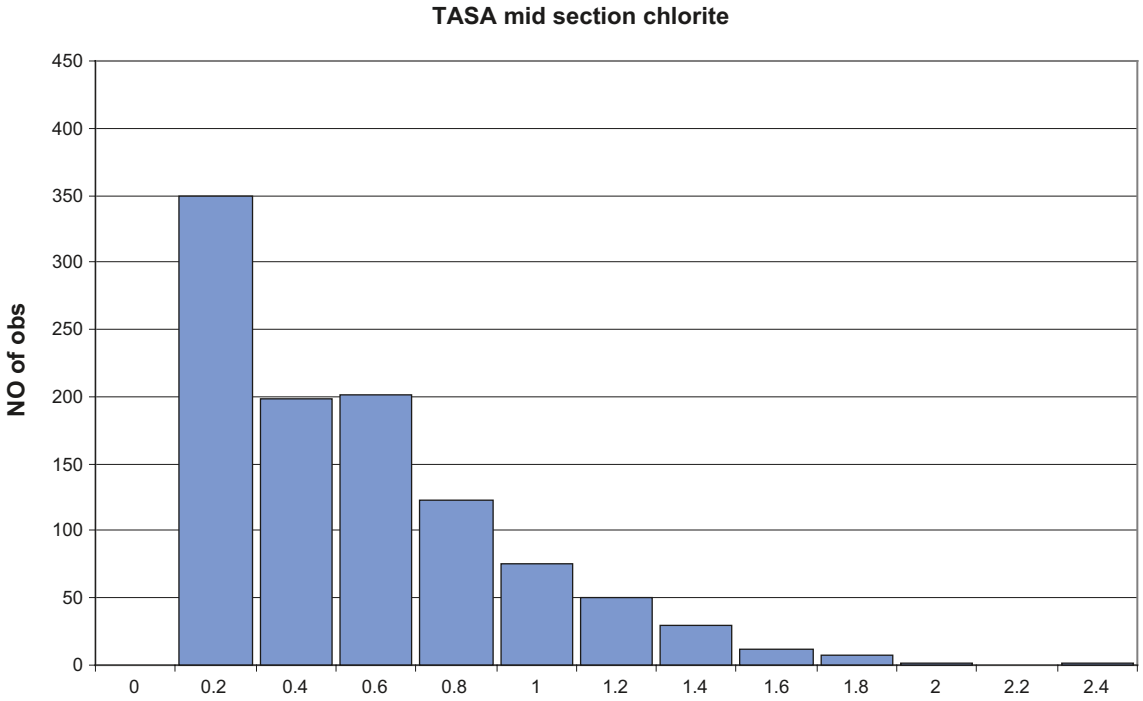

Figure C-63. *Histogram, TASA mid section chlorite search radius 2 meters.*

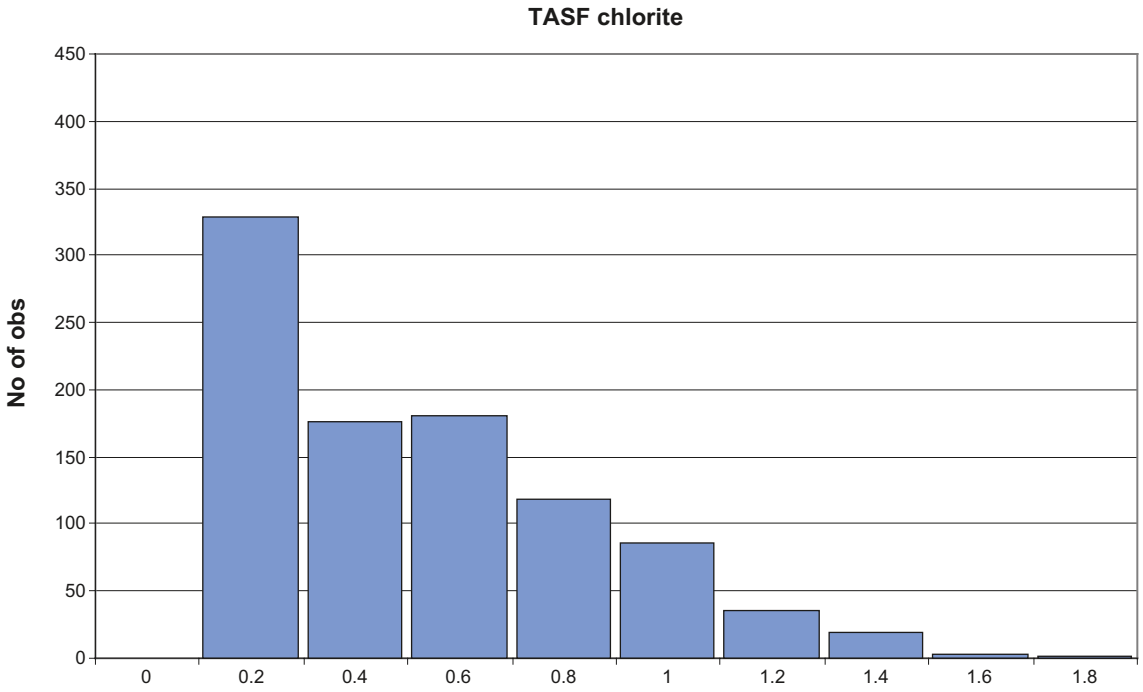

Figure C-64. *Histogram, TASF chlorite search radius 2 meters.*

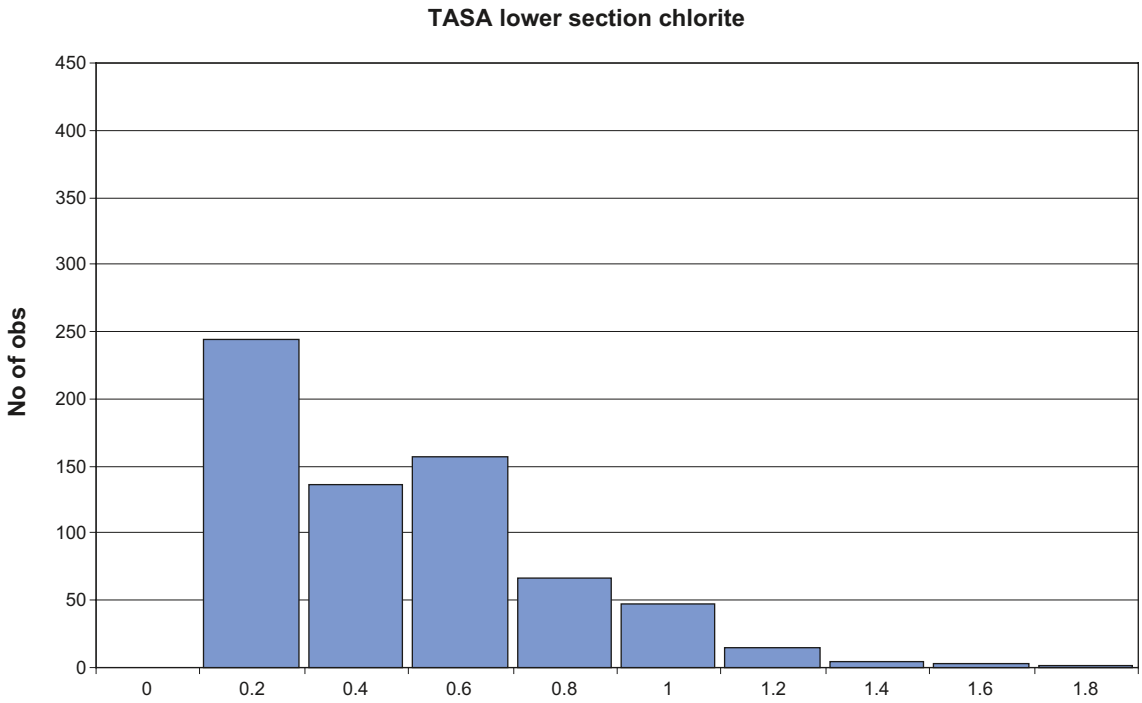

Figure C-65. *Histogram, TASA lower section chlorite search radius 2 meters.*

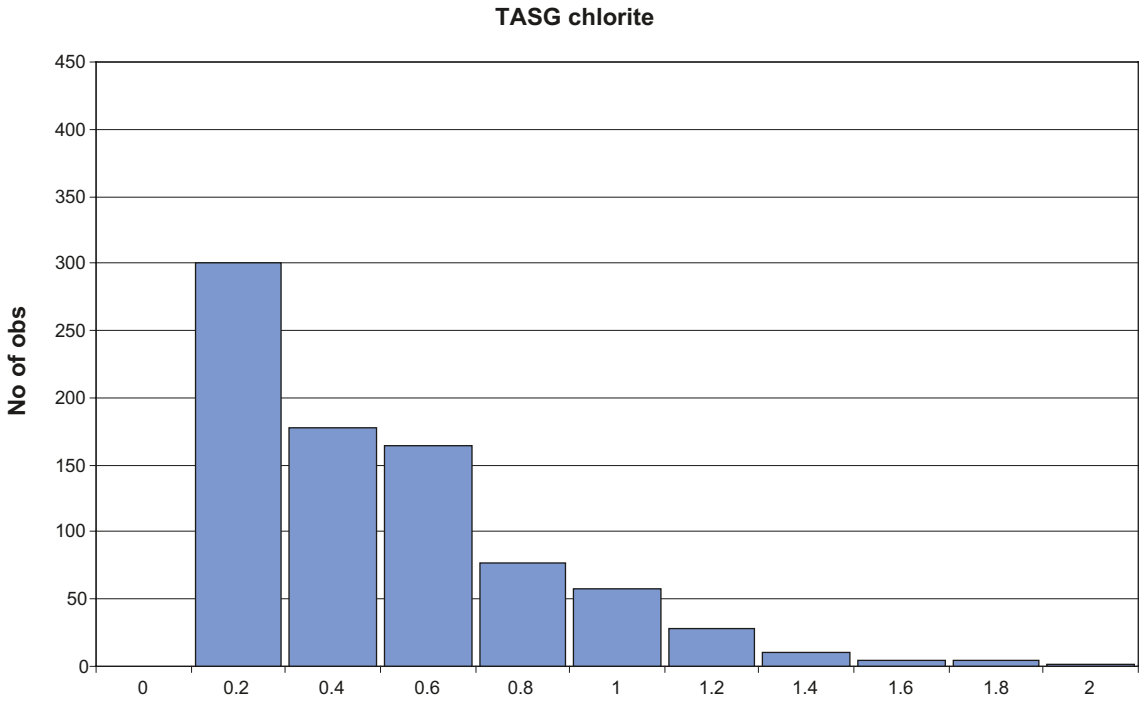

Figure C-66. *Histogram, TASG chlorite search radius 2 meters.*

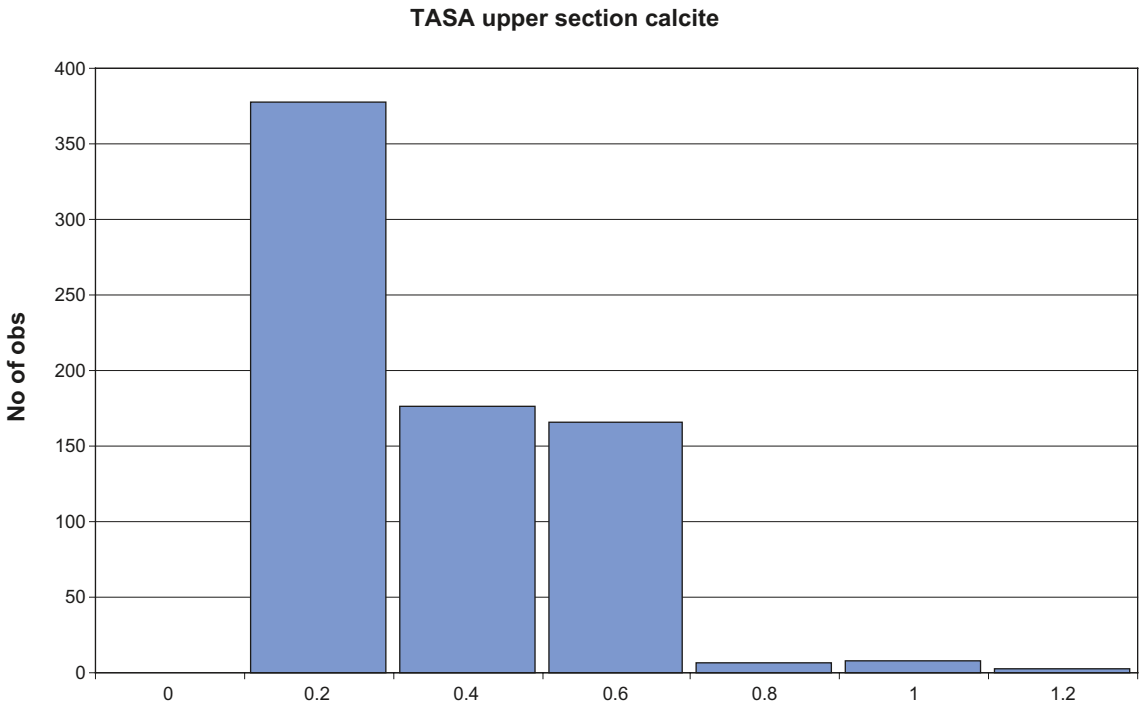

Figure C-67. *Histogram, TASA upper section calcite search radius 2 meters.*

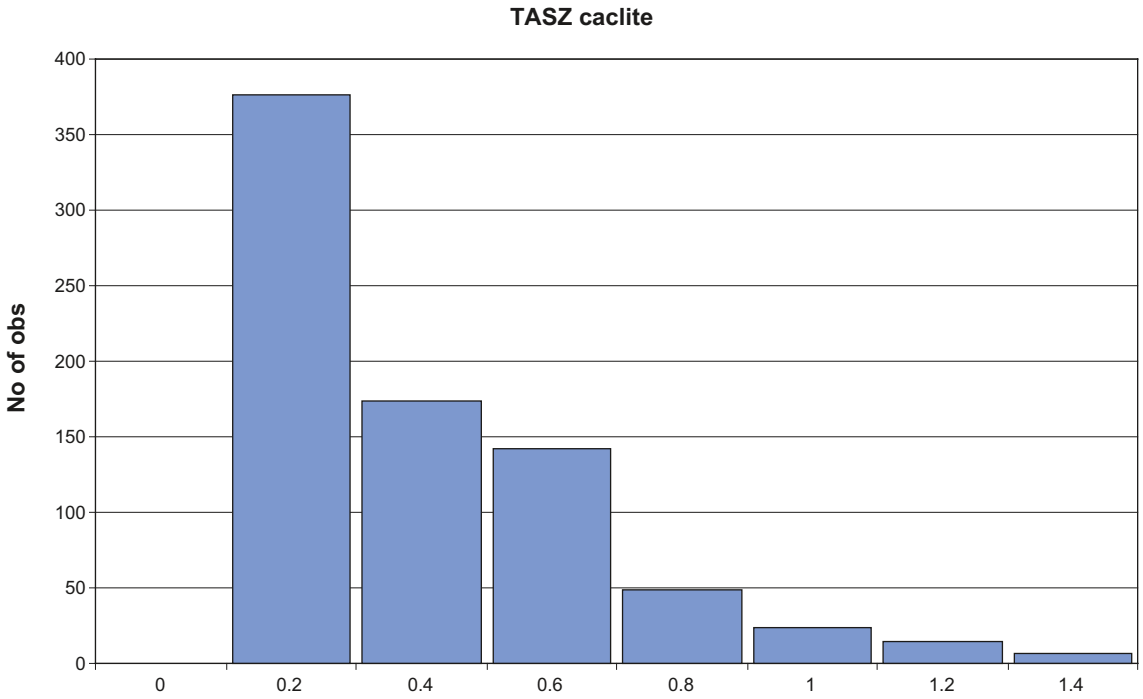

Figure C-68. *Histogram, TASZ calcite search radius 2 meters.*

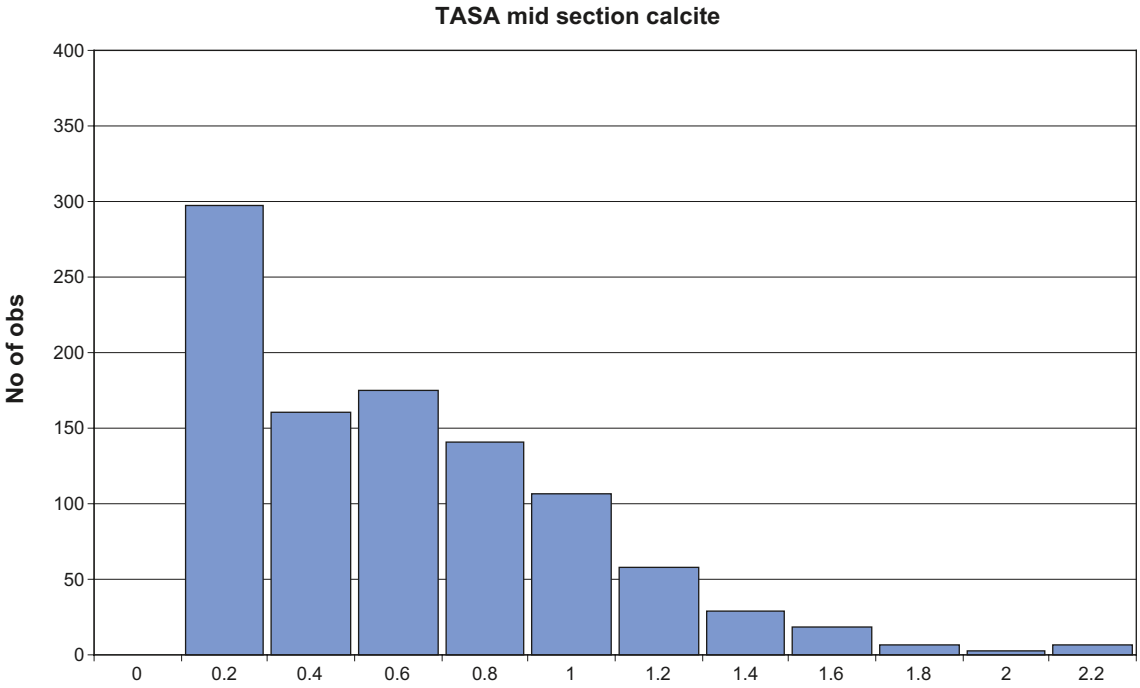

Figure C-69. *Histogram, TASA mid section calcite search radius 2 meters.*

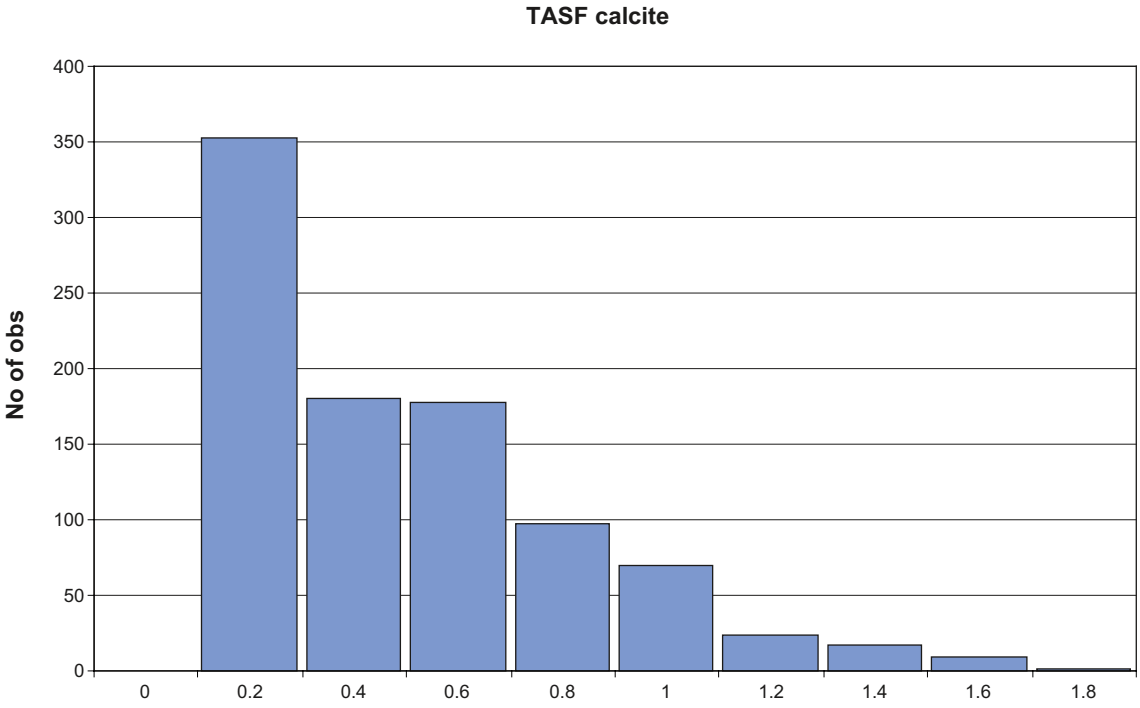

Figure C-70. *Histogram, TASF calcite search radius 2 meters.*

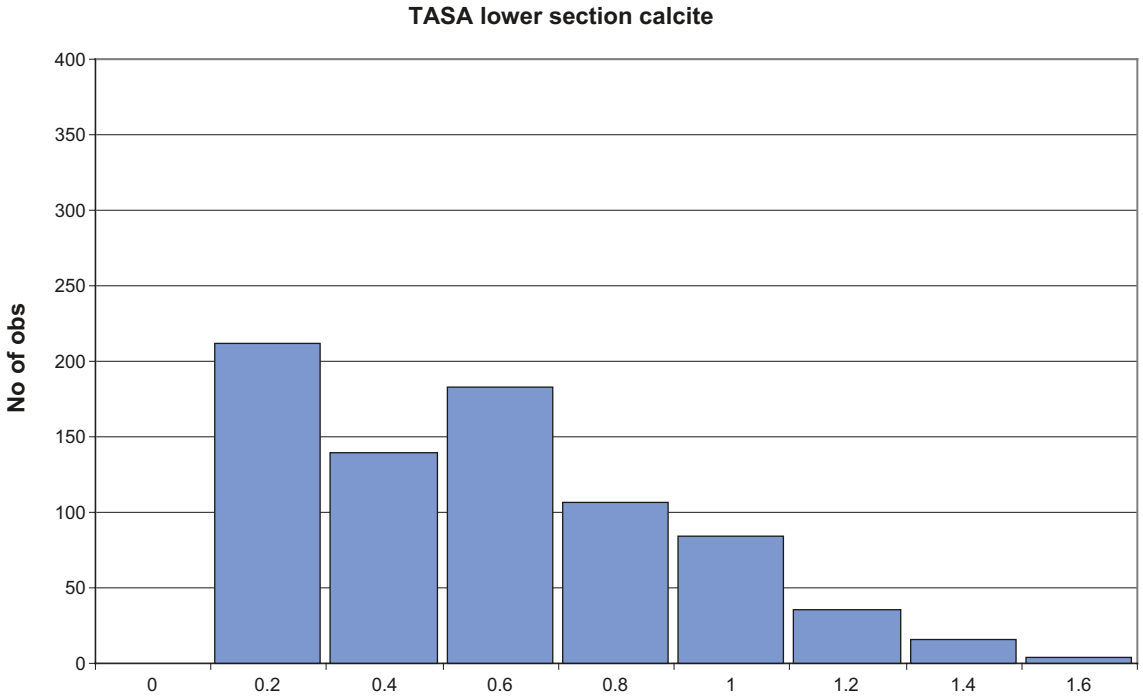

Figure C-71. *Histogram, TASA lower section calcite search radius 2 meters.*

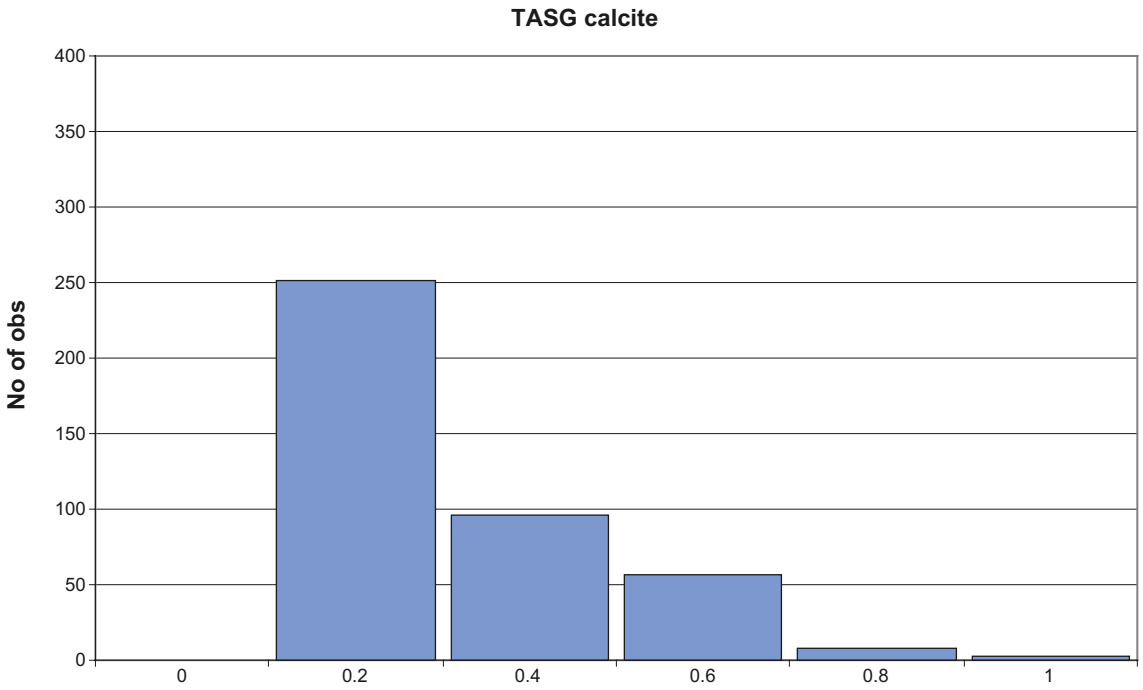

Figure C-72. *Histogram, TASG calcite search radius 2 meters.*

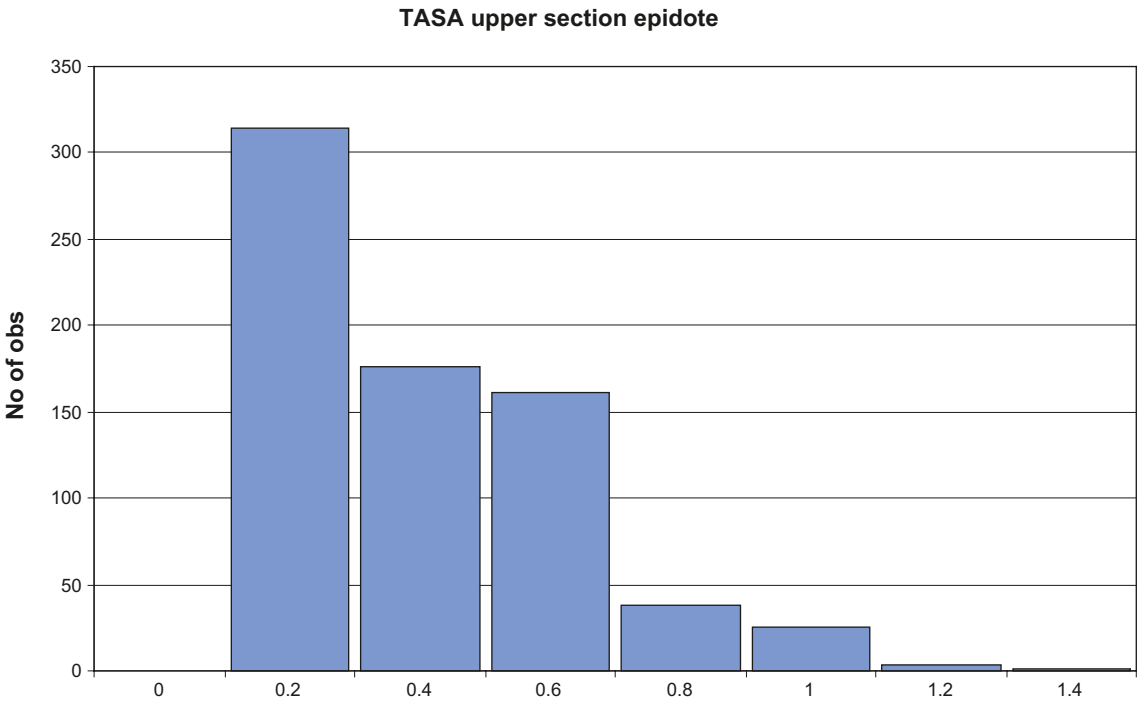

Figure C-73. *Histogram, TASA upper section epidote search radius 2 meters.*

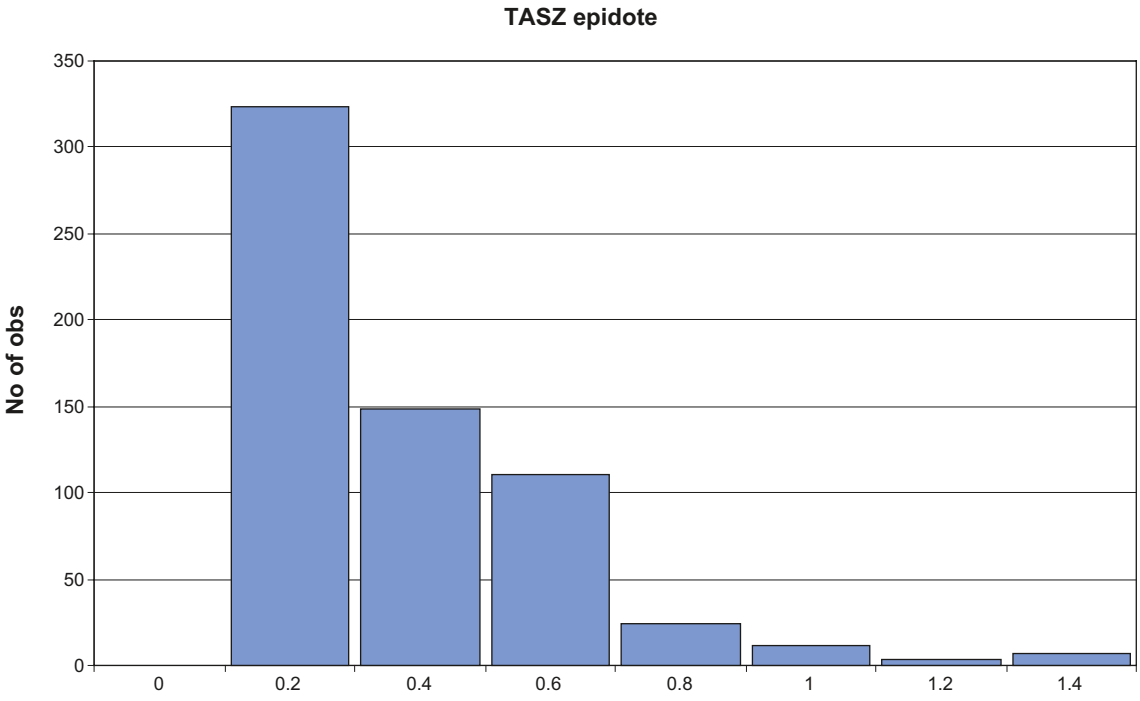

Figure C-74. *Histogram, TASZ epidote search radius 2 meters.*

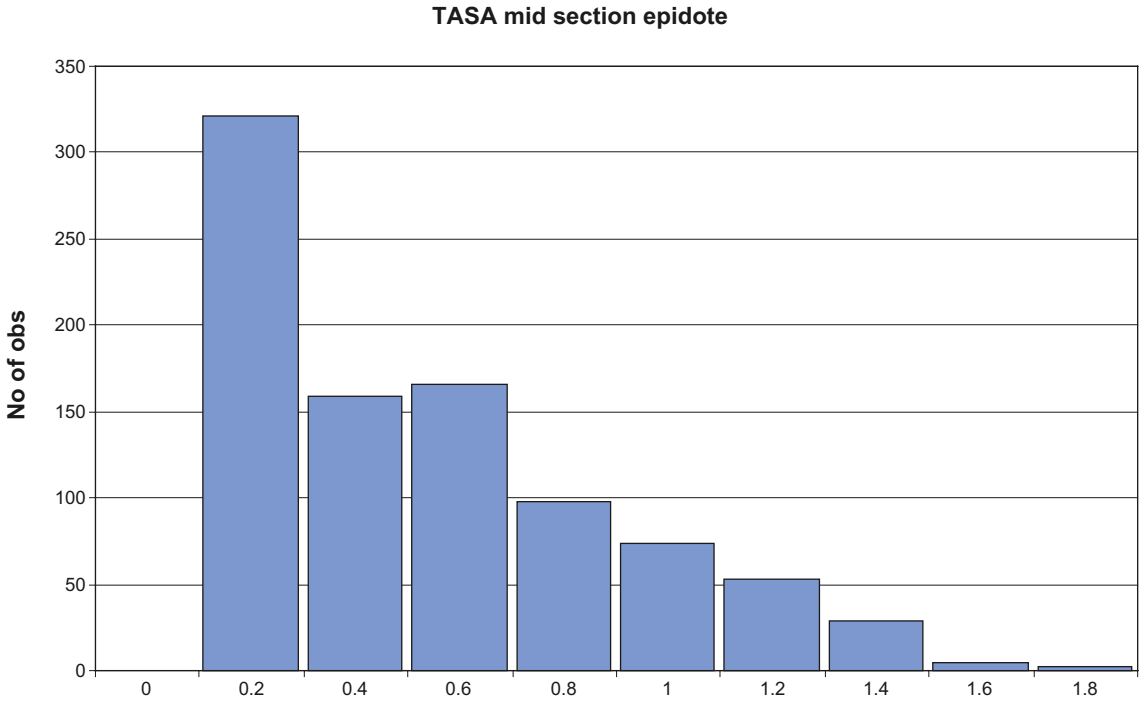

Figure C-75. *Histogram, TASA mid section epidote search radius 2 meters.*

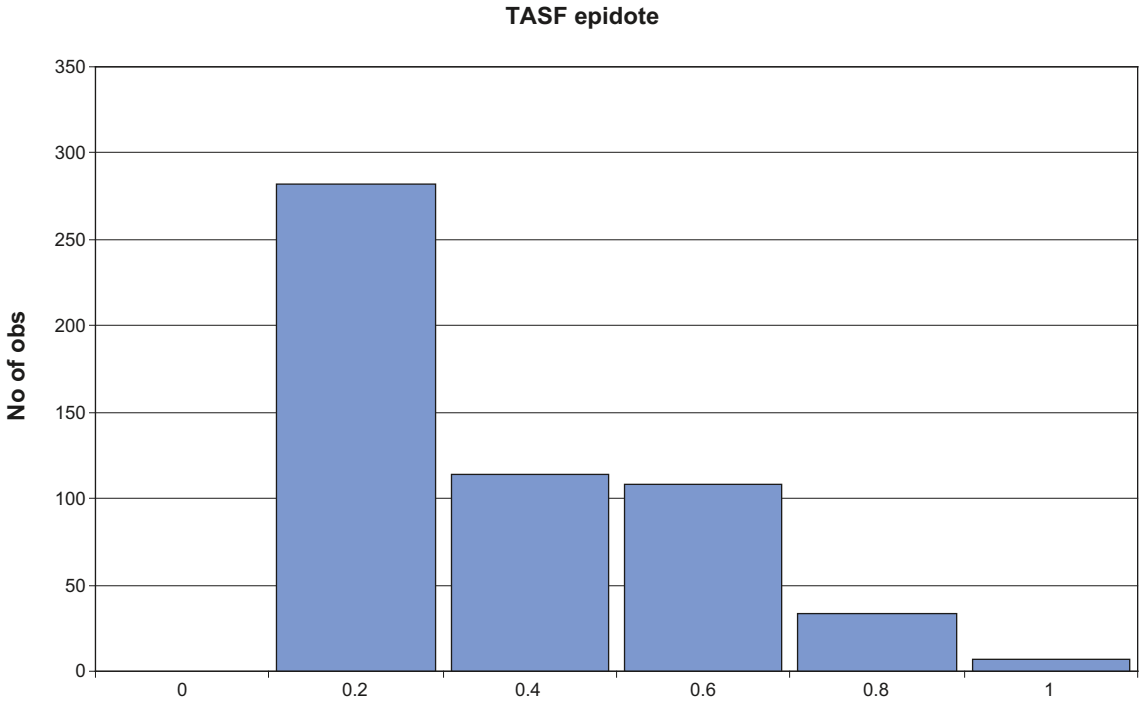

Figure C-76. *Histogram, TASF epidote search radius 2 meters.*

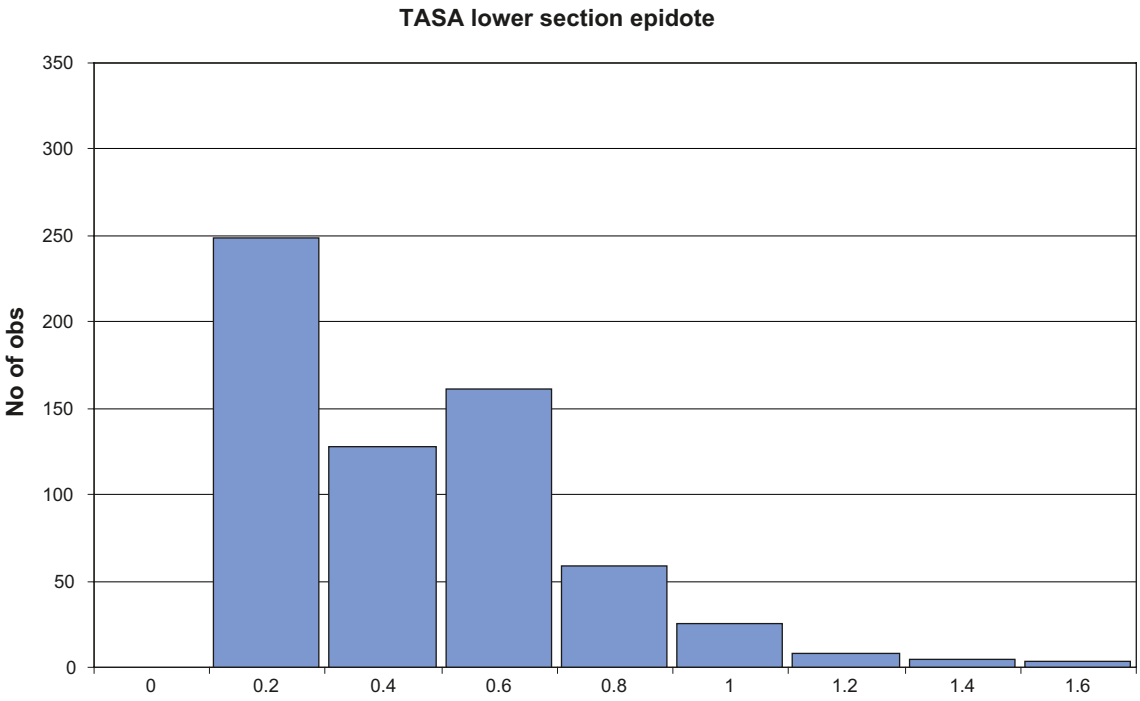

Figure C-77. *Histogram, TASA lower section epidote search radius 2 meters.*

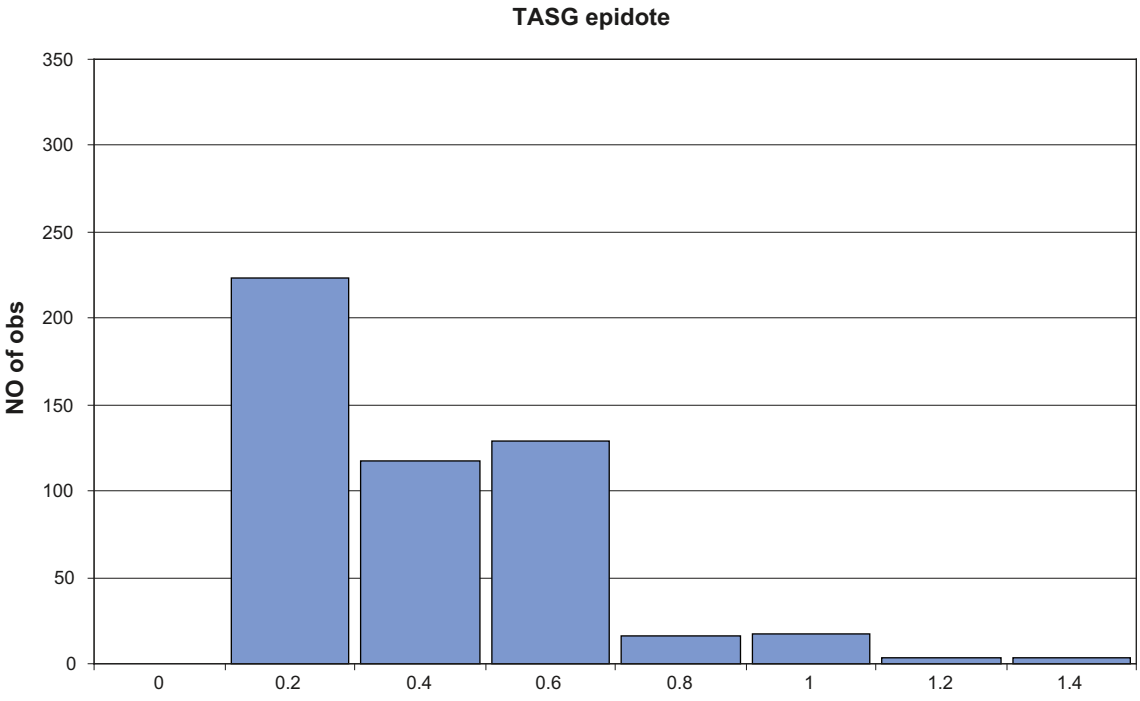

Figure C-78. *Histogram, TASG epidote search radius 2 meters.*

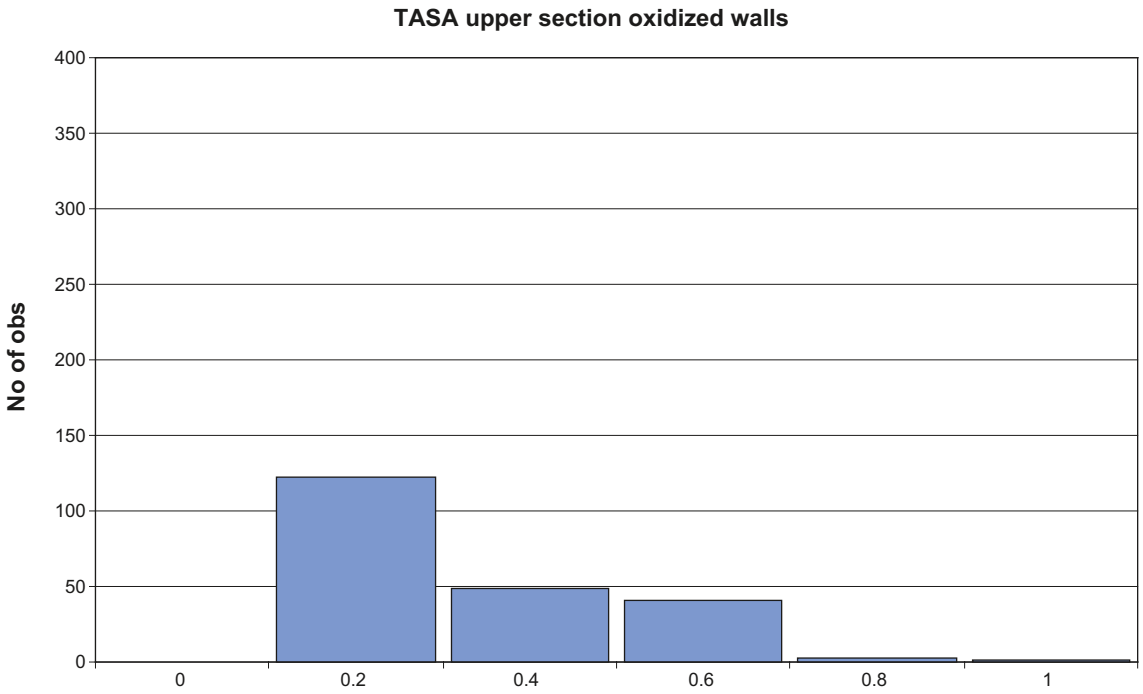

Figure C-79. *Histogram, TASA upper section oxidized walls search radius 2 meters.*

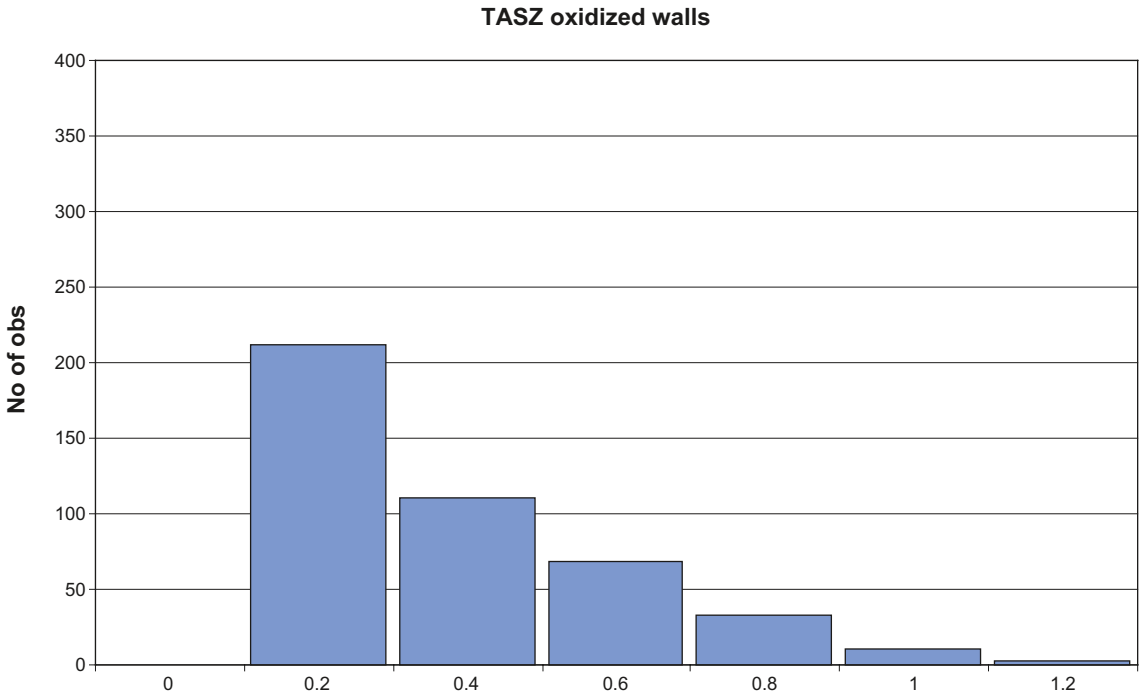

Figure C-80. *Histogram, TASZ oxidized walls search radius 2 meters.*

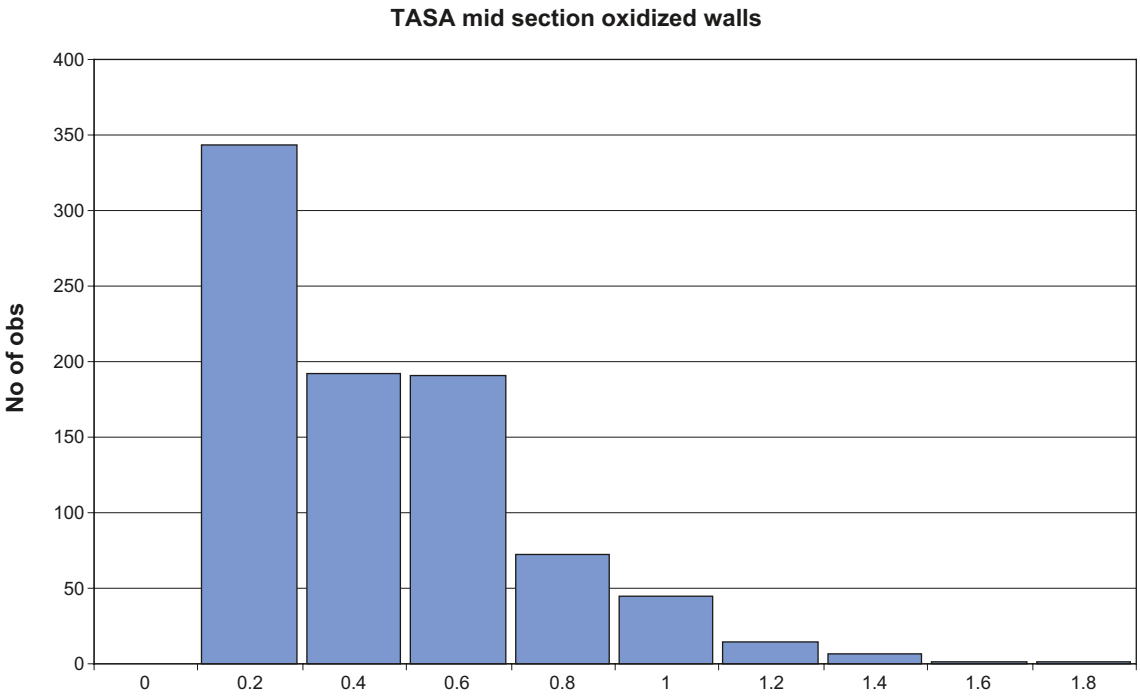

Figure C-81. *Histogram, TASA mid section oxidized walls search radius 2 meters.*

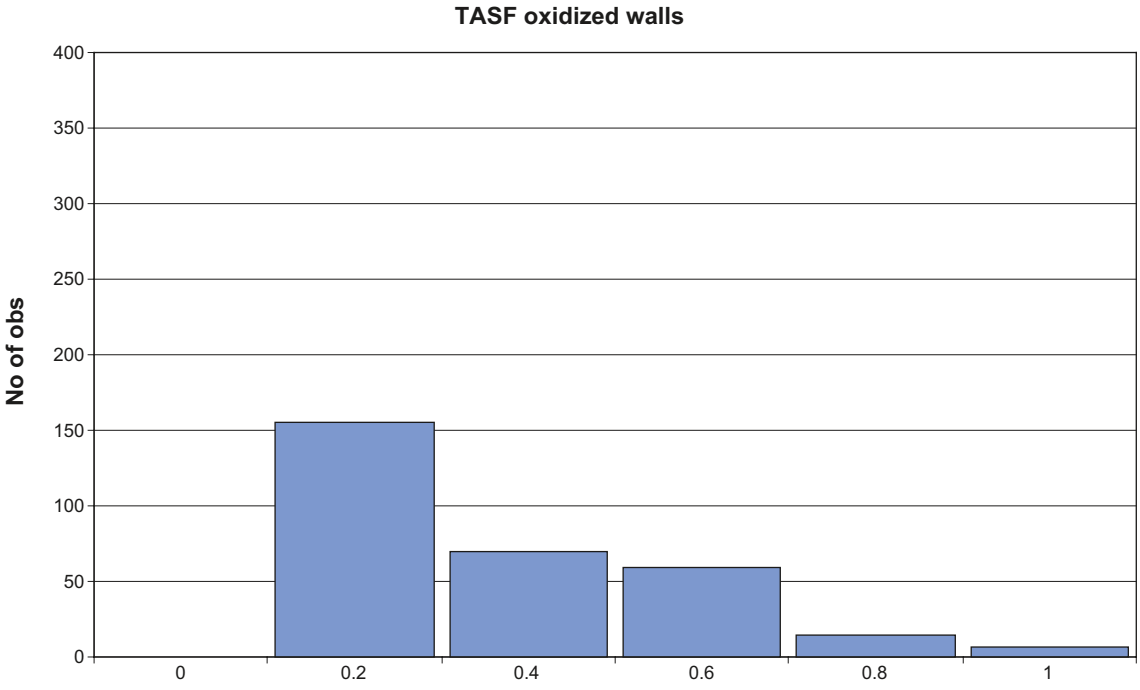

Figure C-82. *Histogram, TASF oxidized walls search radius 2 meters.*

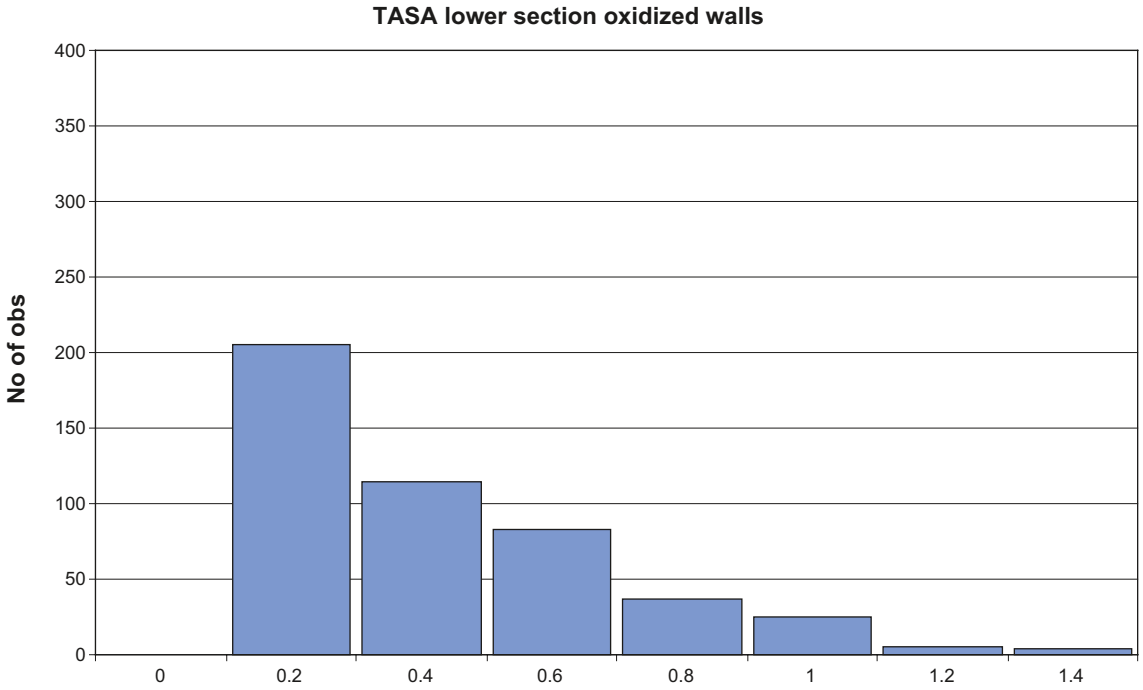

Figure C-83. *Histogram, TASA lower section oxidized walls search radius 2 meters.*

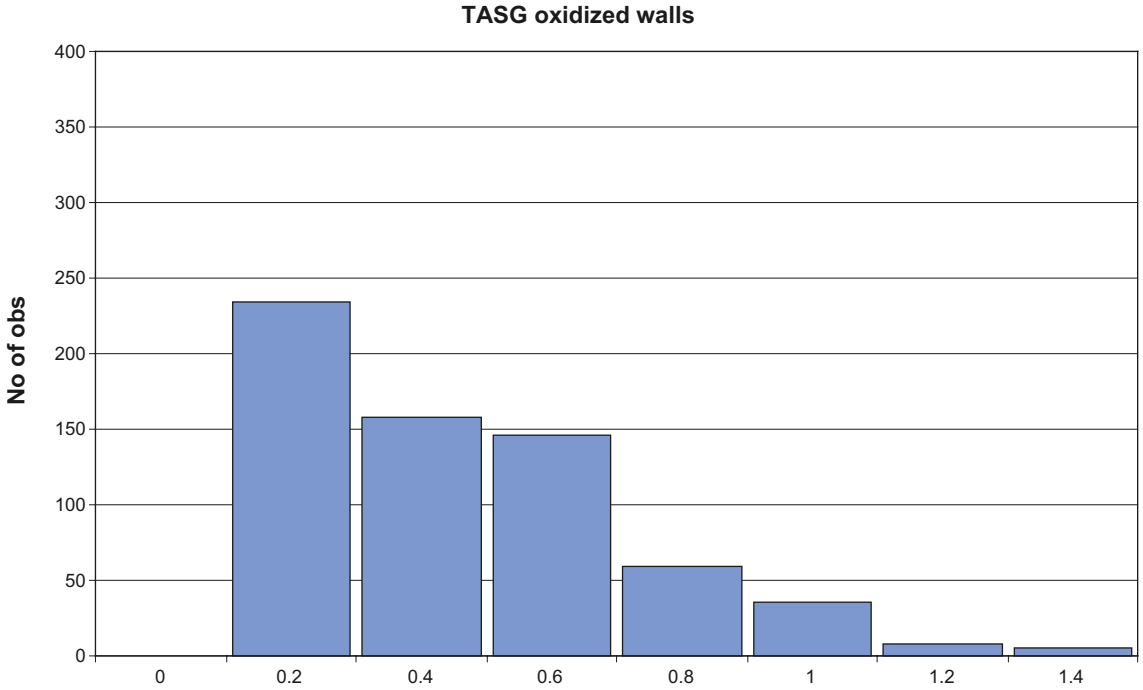

Figure C-84. *Histogram, TASG oxidized walls search radius 2 meters.*

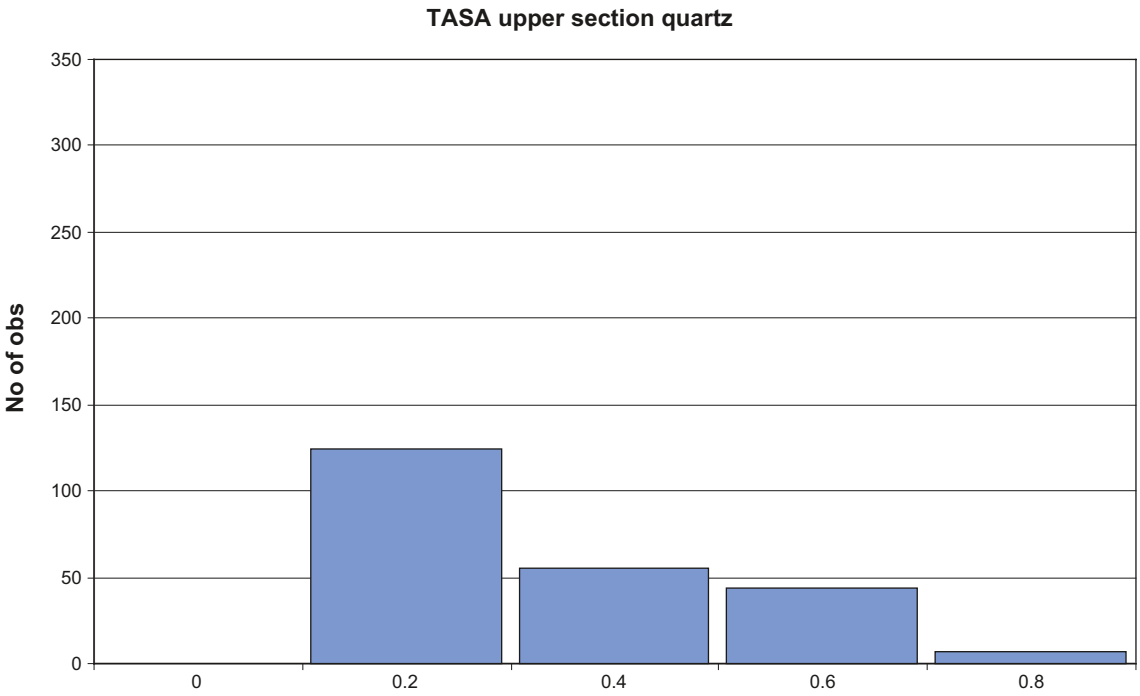

Figure C-85. *Histogram, TASA upper section quartz search radius 2 meters.*

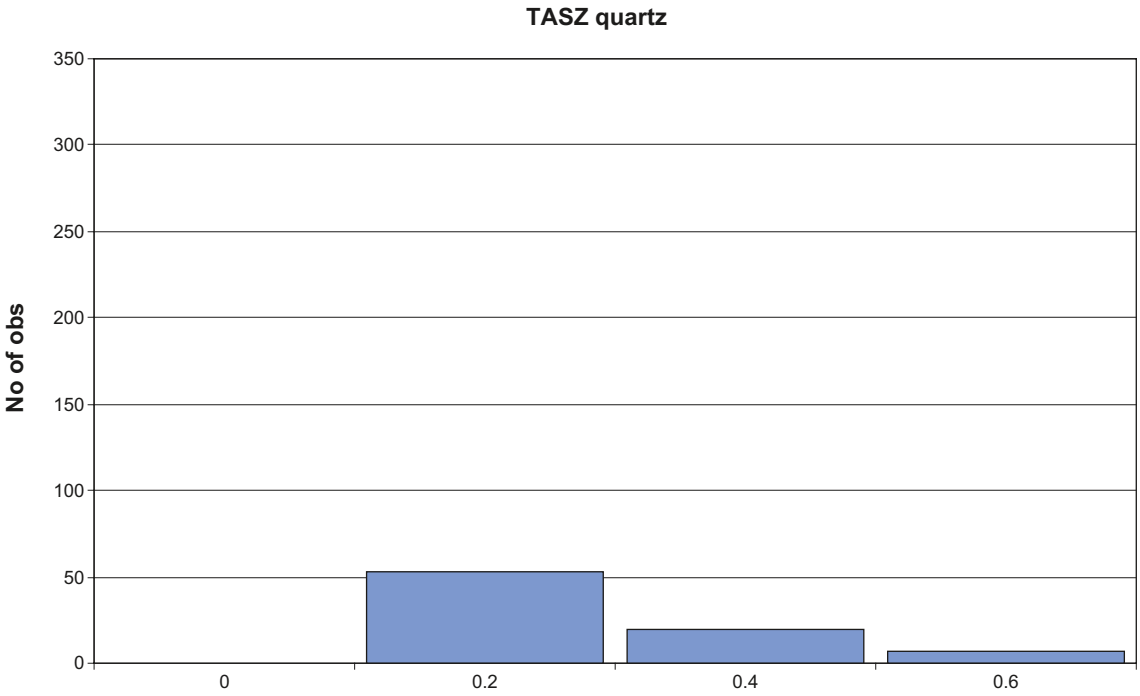

Figure C-86. *Histogram, TASZ quartz search radius 2 meters.*

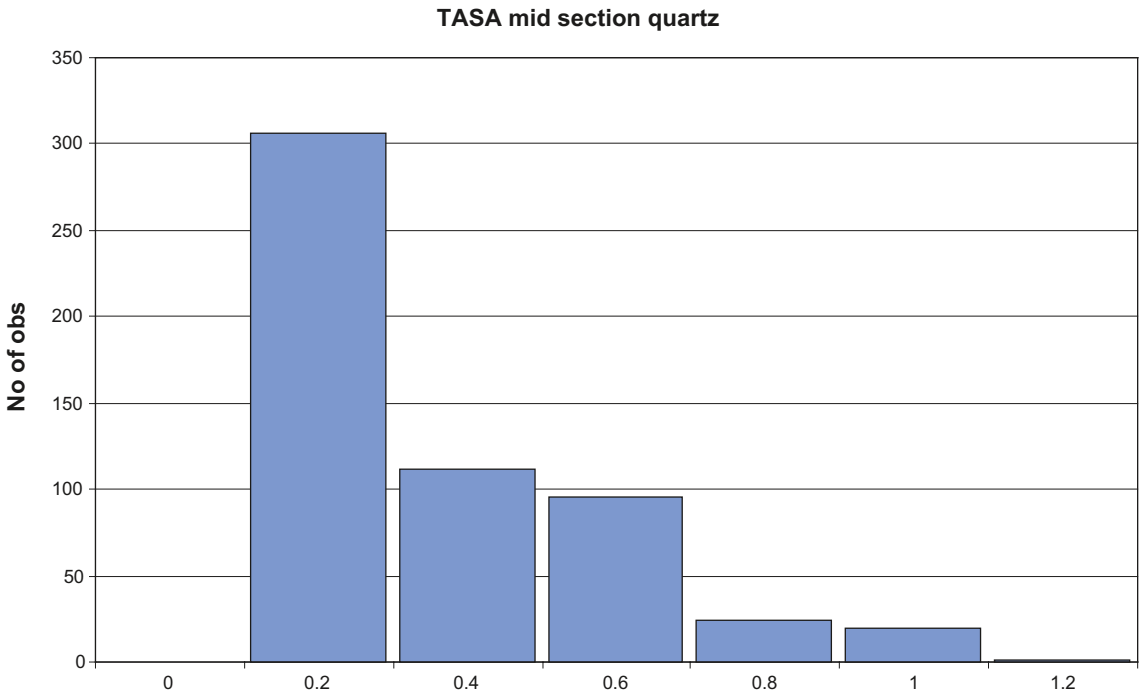

Figure C-87. *Histogram, TASA mid section quartz search radius 2 meters.*

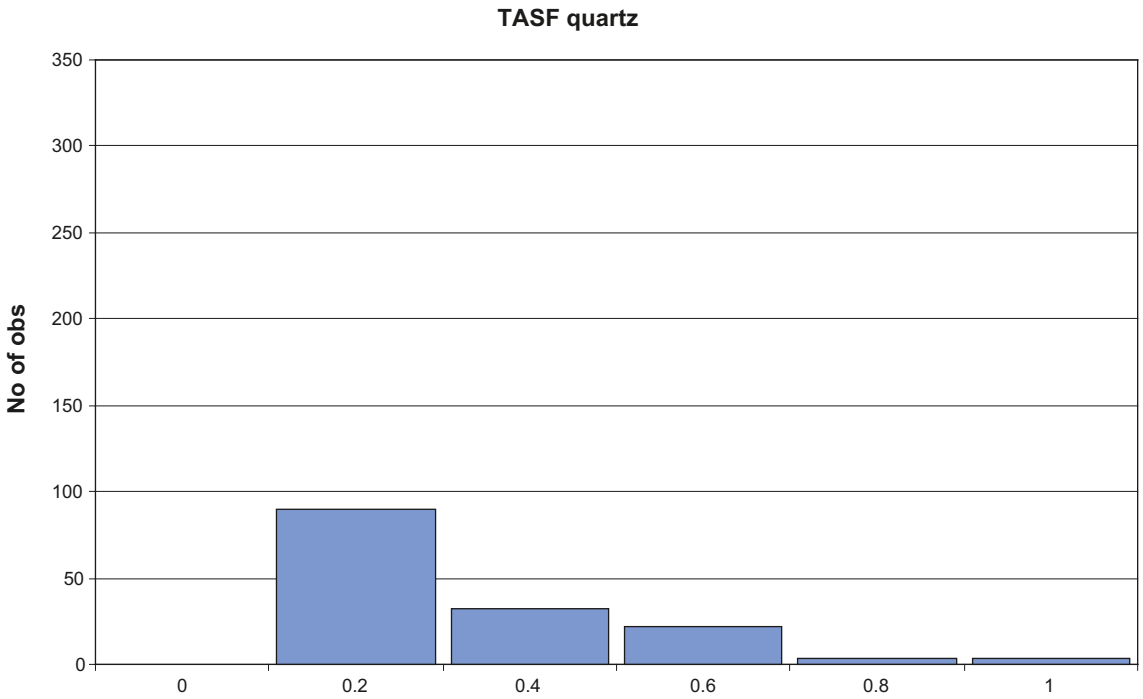

Figure C-88. *Histogram, TASF quartz search radius 2 meters.*

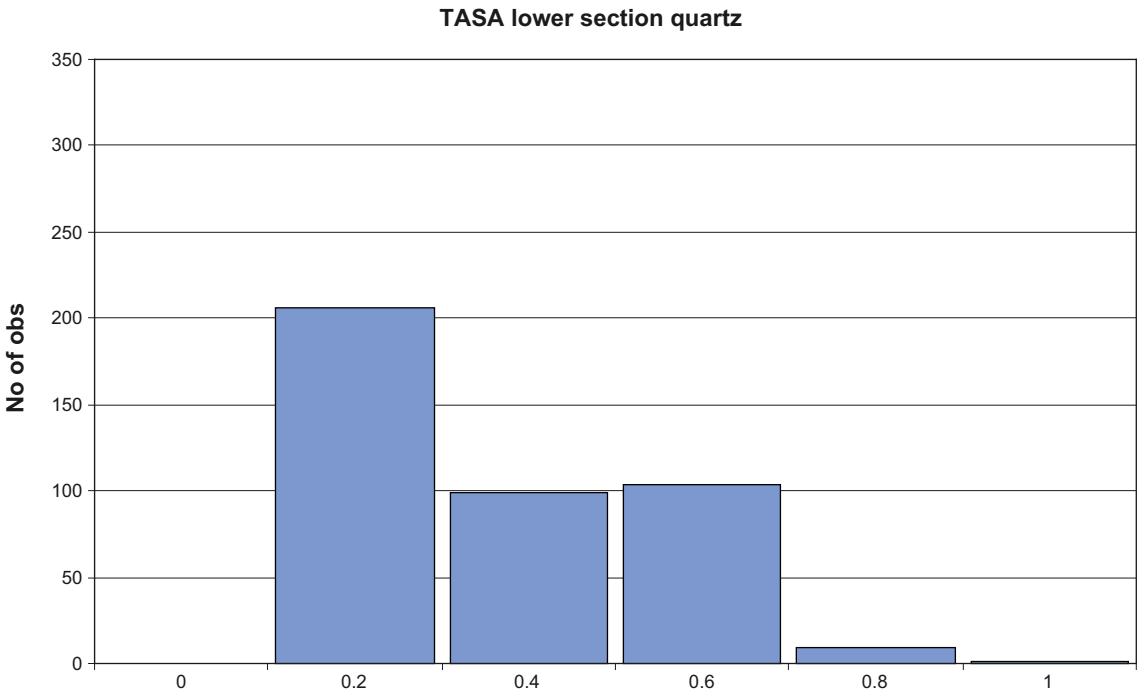

Figure C-89. *Histogram, TASA lower section quartz search radius 2 meters.*

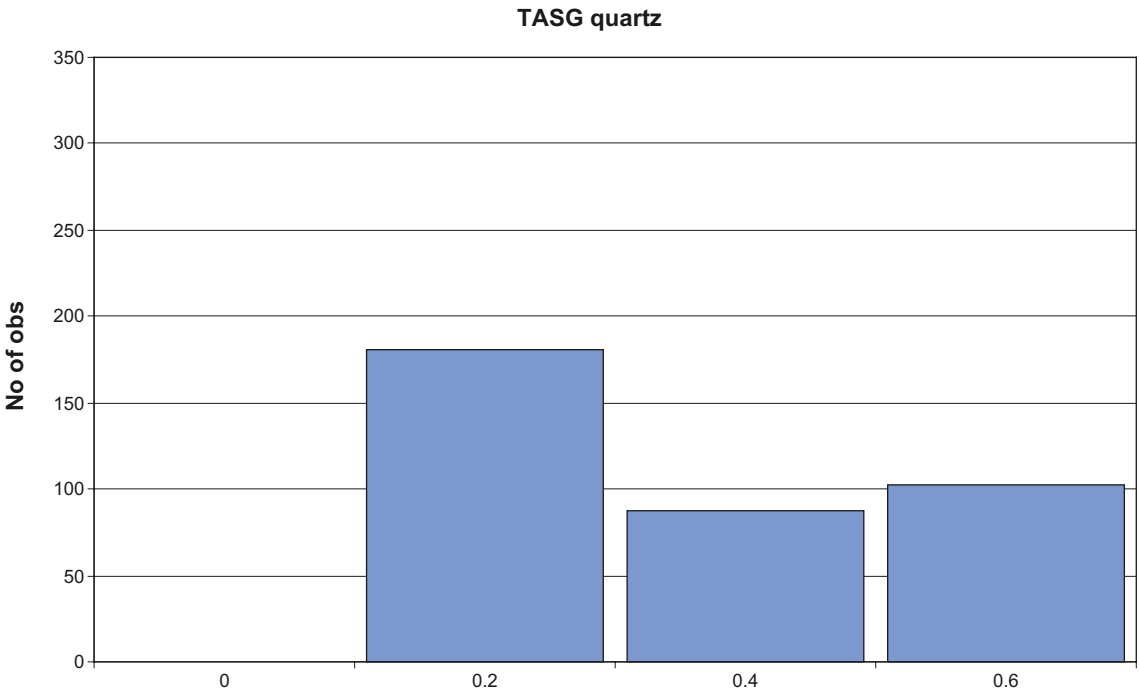

Figure C-90. *Histogram, TASG quartz search radius 2 meters.*

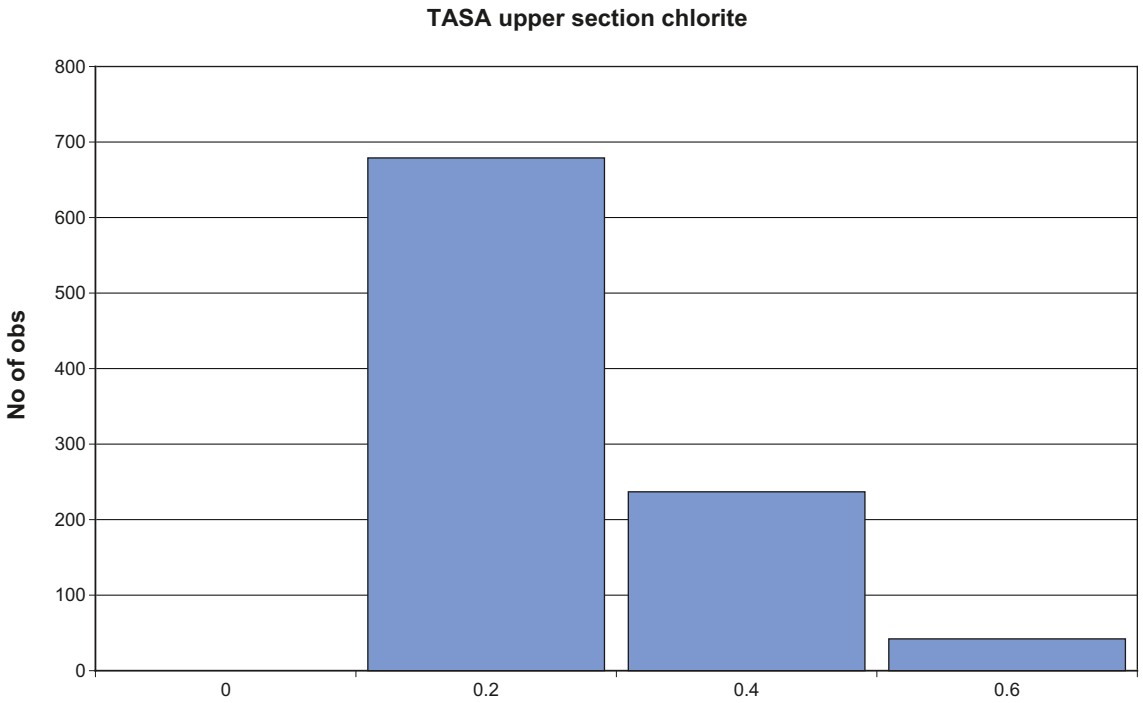

Figure C-91. *Histogram, TASA upper section chlorite search radius 4 meters.*

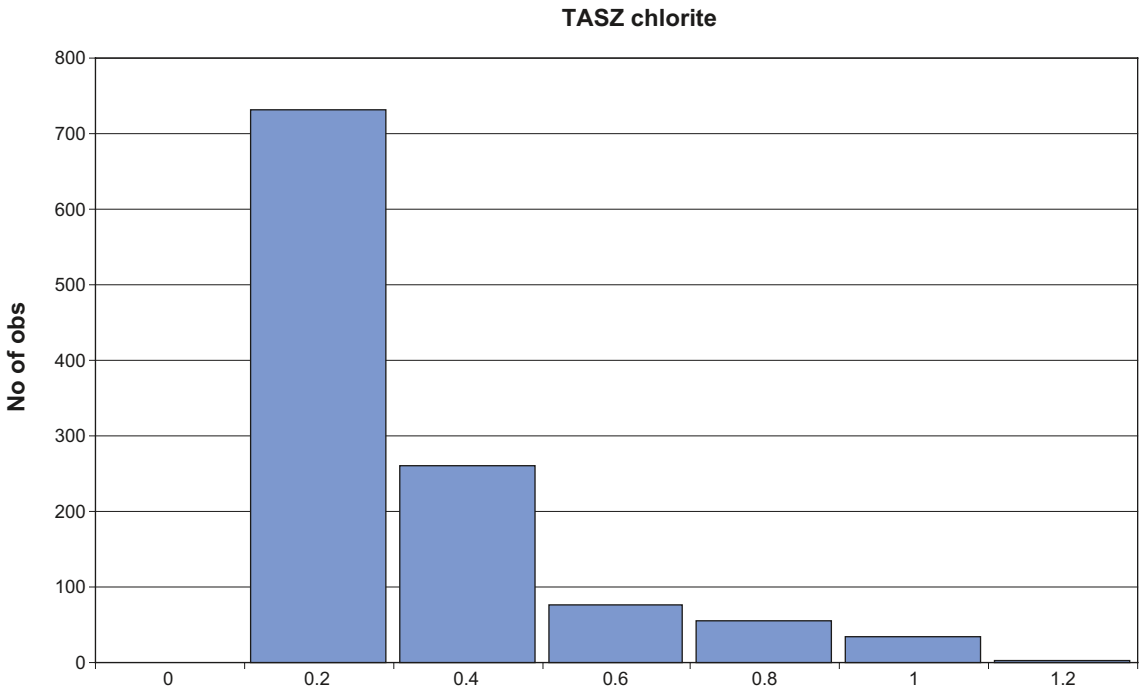

Figure C-92. *Histogram, TASZ chlorite search radius 4 meters.*

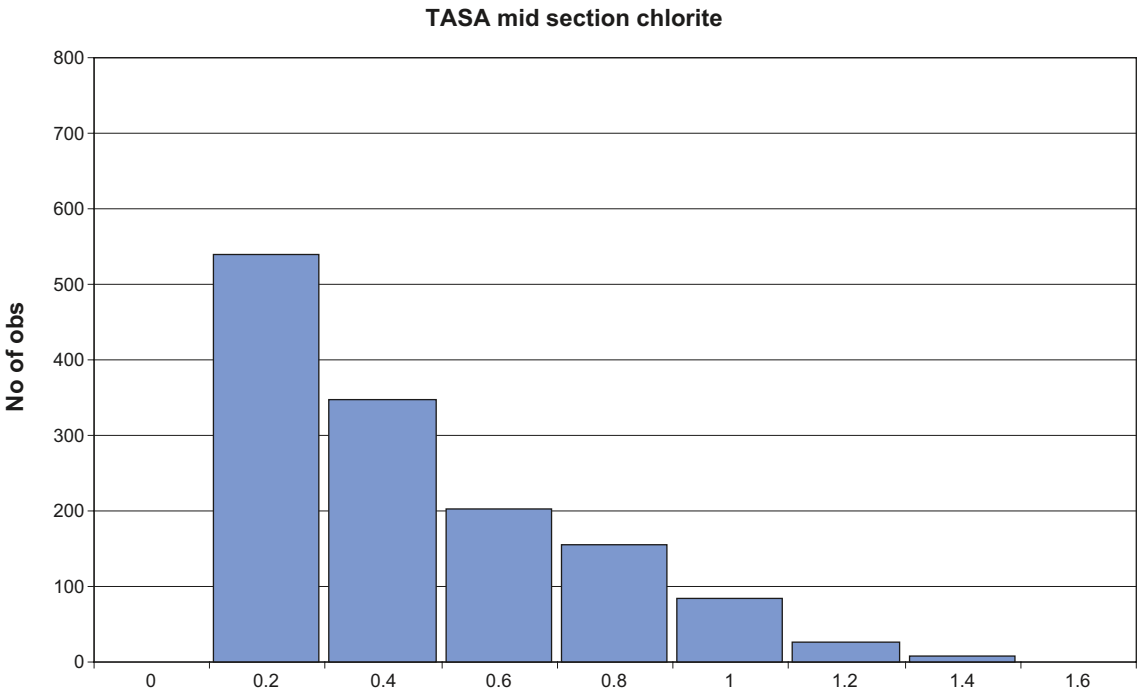

Figure C-93. *Histogram, TASA mid section chlorite search radius 4 meters.*

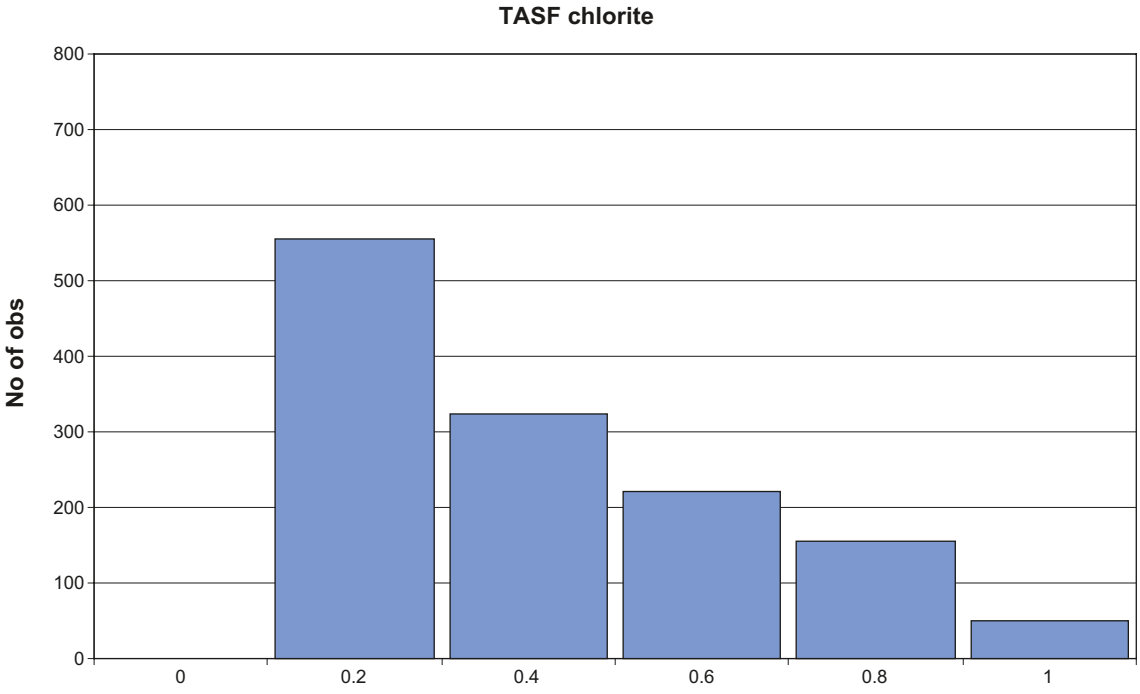

Figure C-94. *Histogram, TASF chlorite search radius 4 meters.*

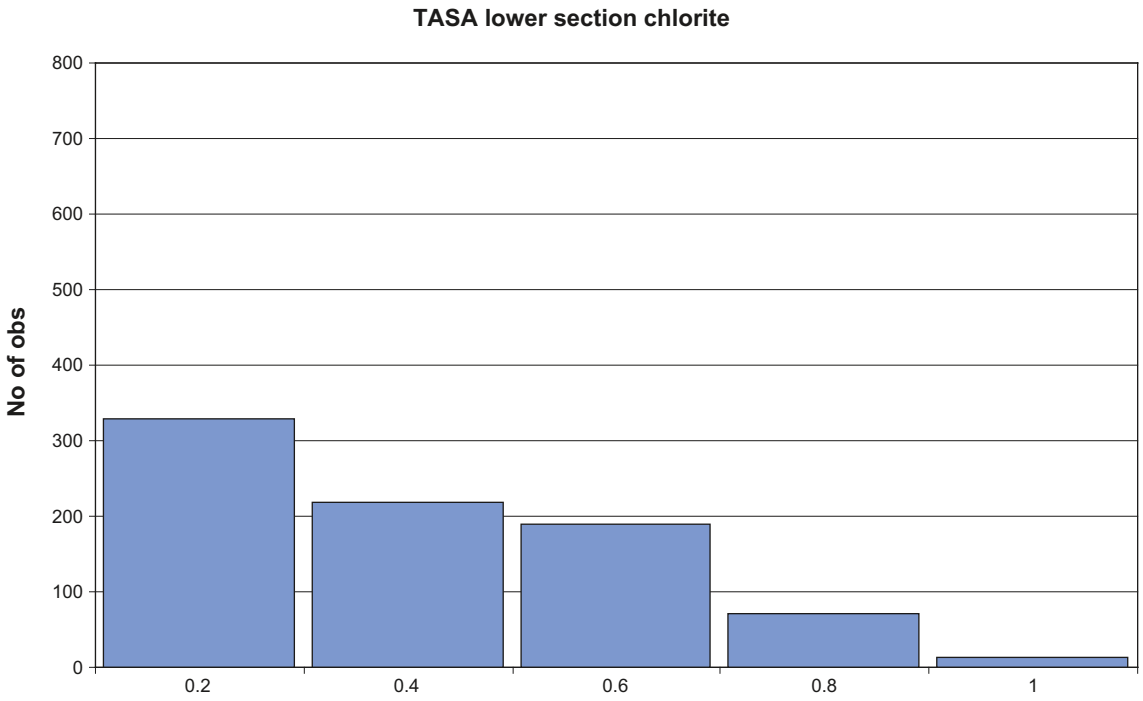

Figure C-95. *Histogram, TASA lower section chlorite search radius 4 meters.*

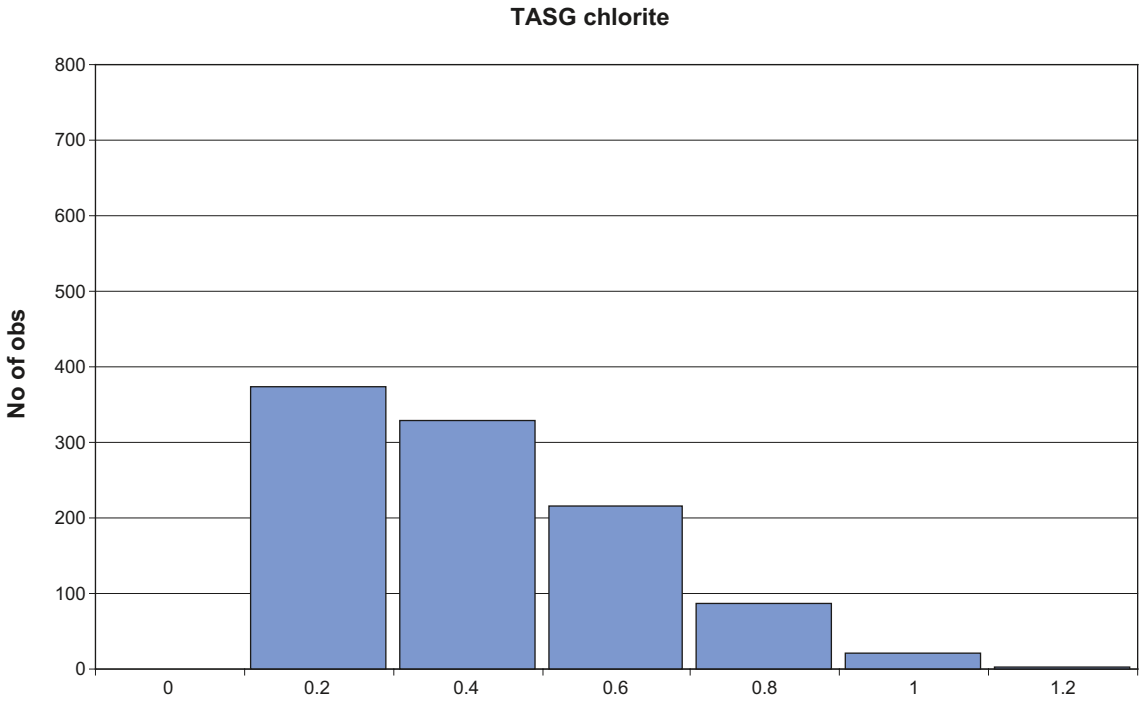

Figure C-96. *Histogram, TASG chlorite search radius 4 meters.*

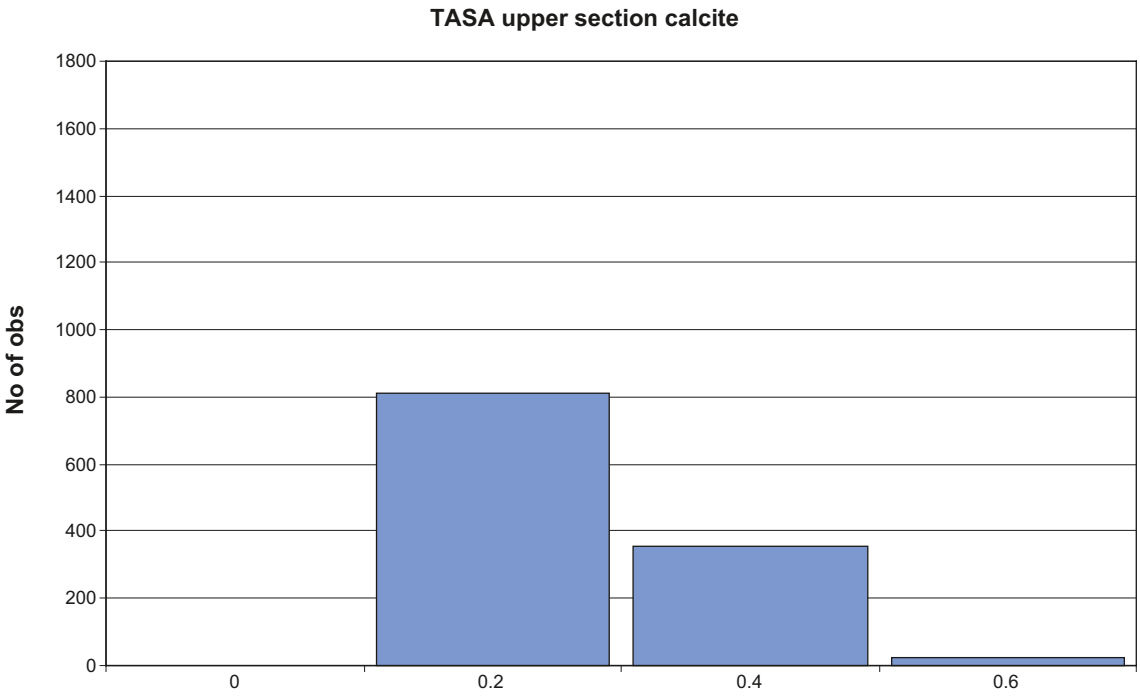

Figure C-97. *Histogram, TASA upper section calcite search radius 4 meters.*

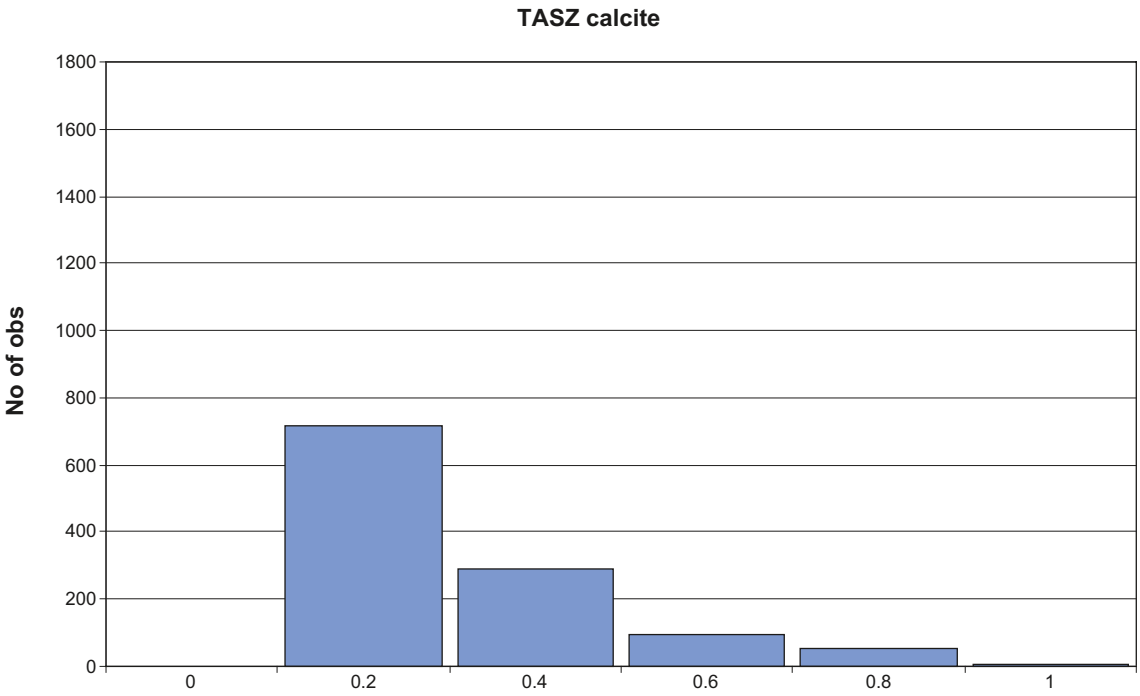

Figure C-98. *Histogram, TASZ calcite search radius 4 meters.*

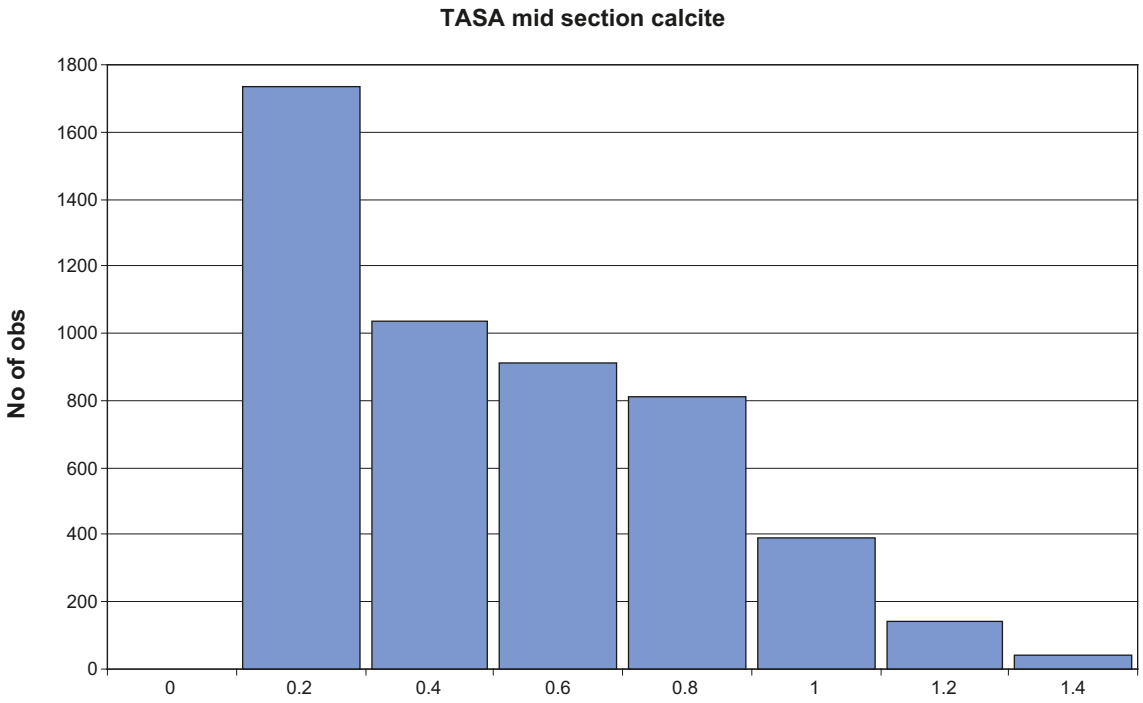

Figure C-99. *Histogram, TASA mid section calcite search radius 4 meters.*

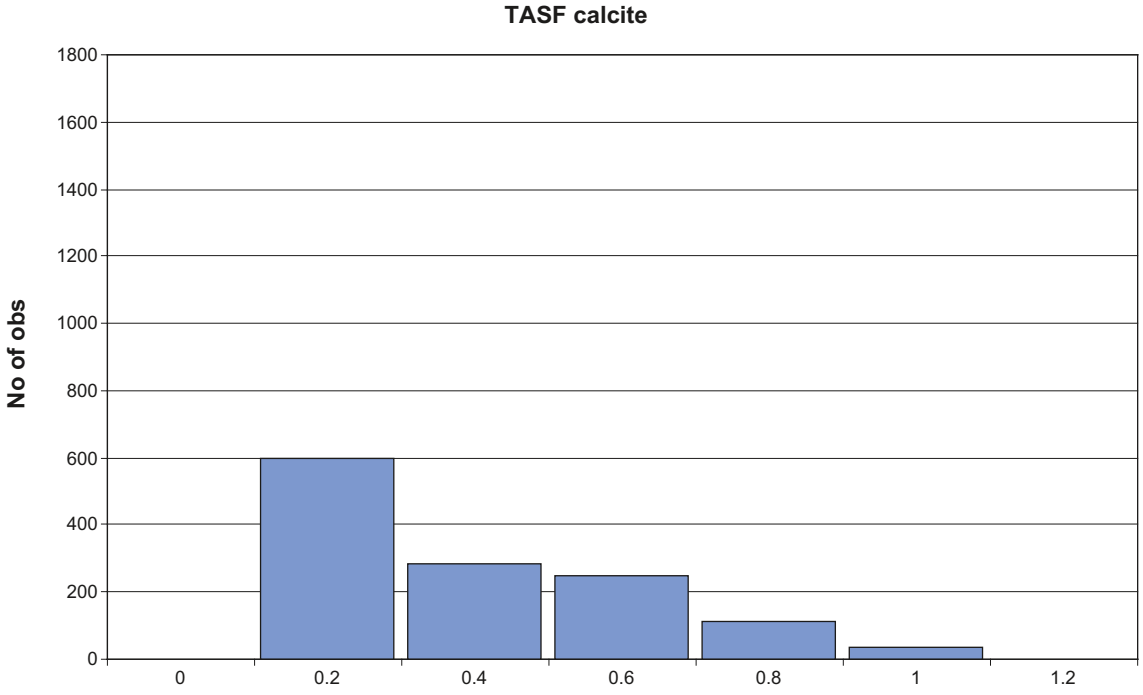

Figure C-100. *Histogram, TASF calcite search radius 4 meters.*

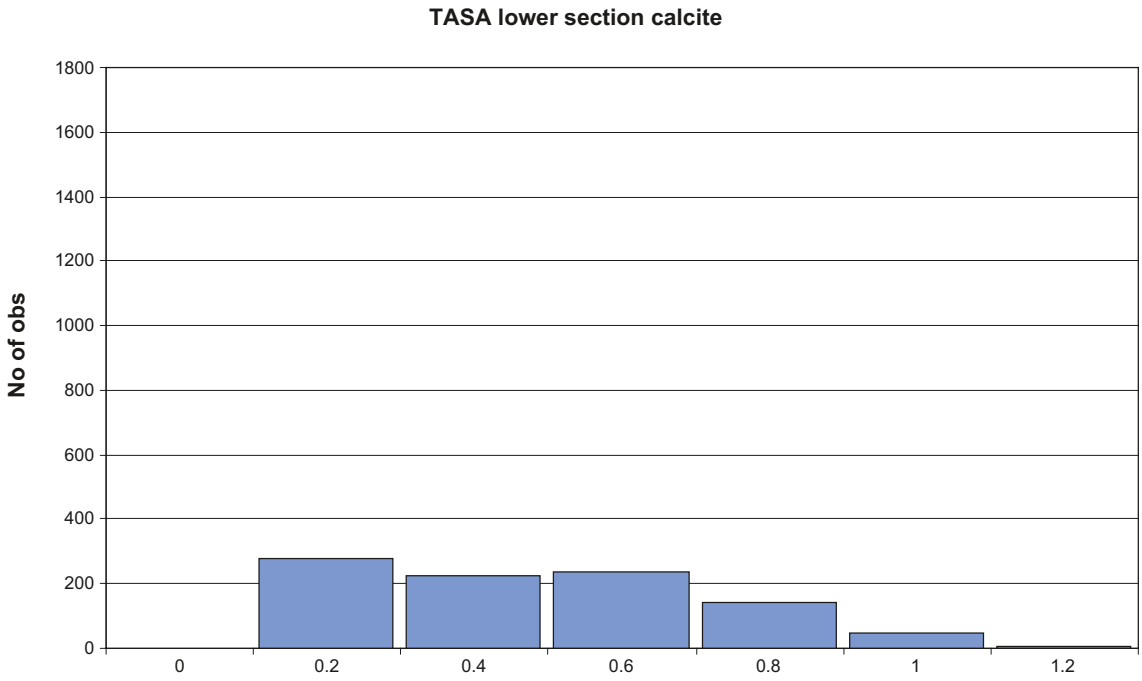

Figure C-101. *Histogram, TASA lower section calcite search radius 4 meters.*

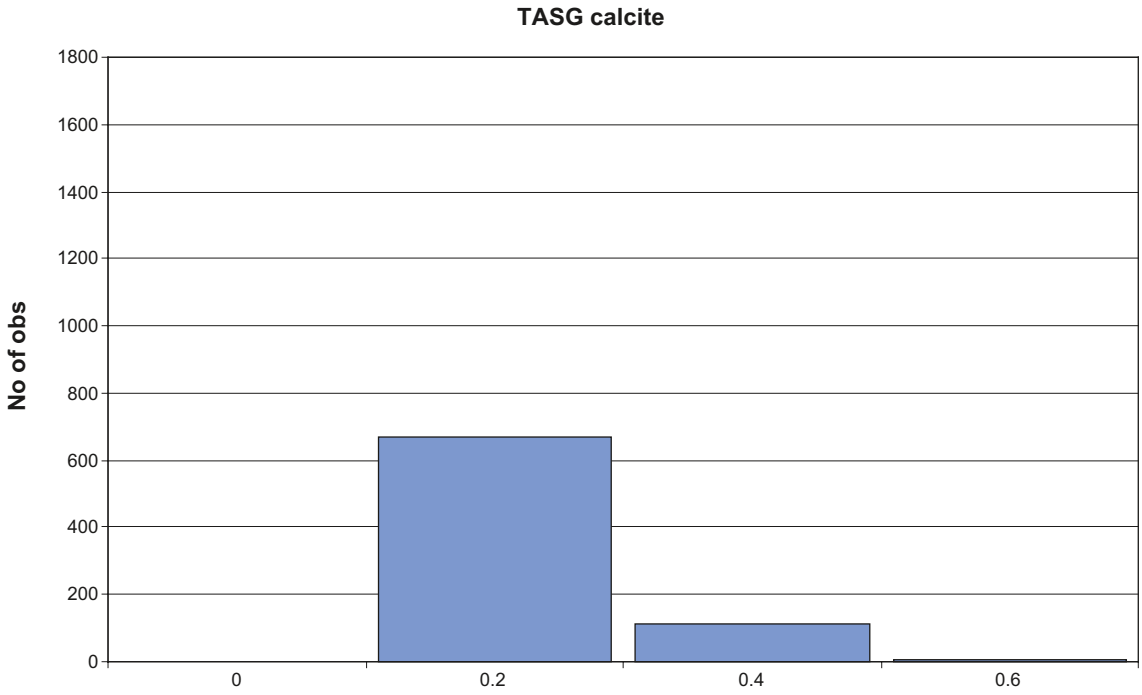

Figure C-102. *Histogram, TASG calcite search radius 4 meters.*

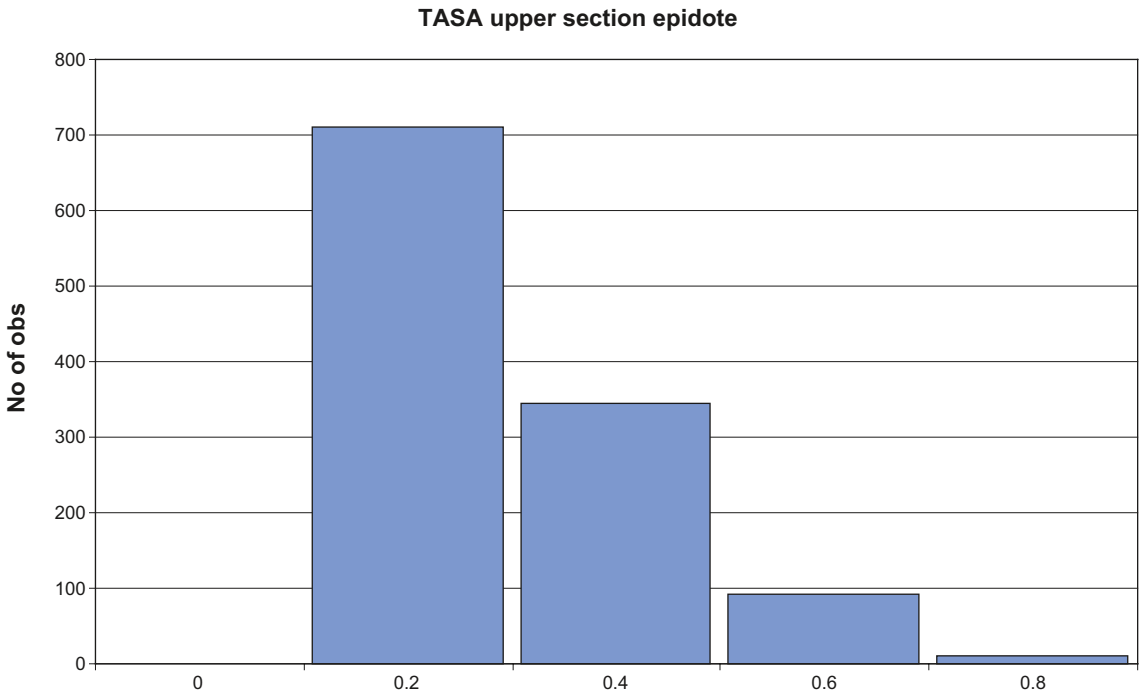

Figure C-103. *Histogram, TASA upper section epidote search radius 4 meters.*

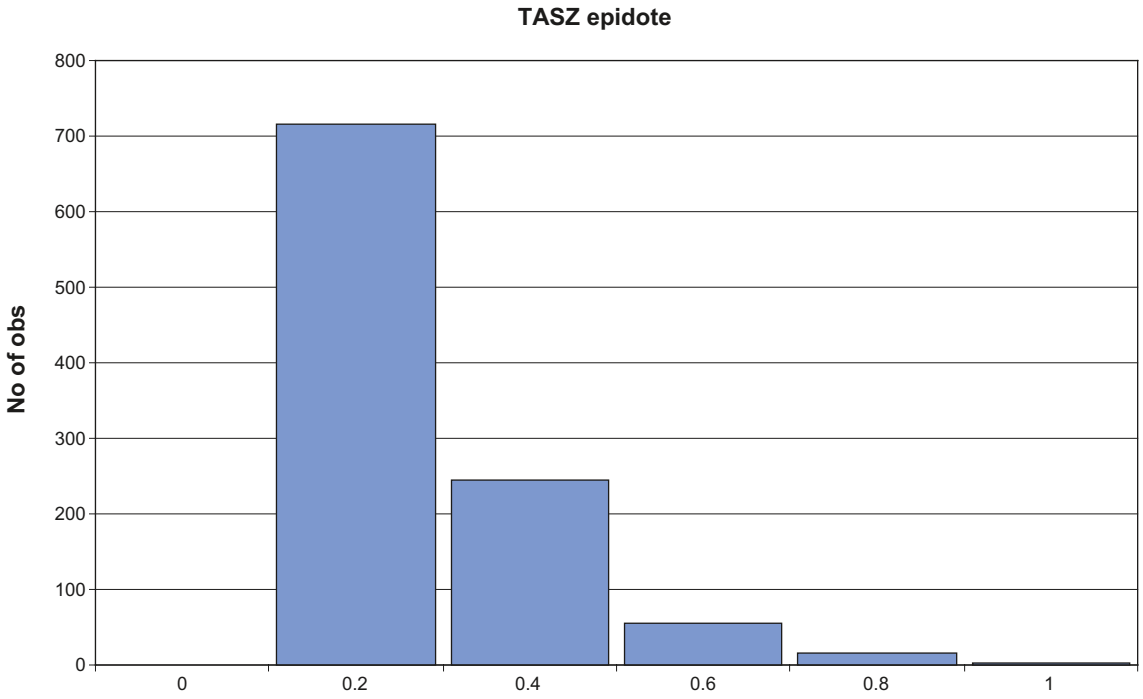

Figure C-104. *Histogram, TASZ epidote search radius 4 meters.*

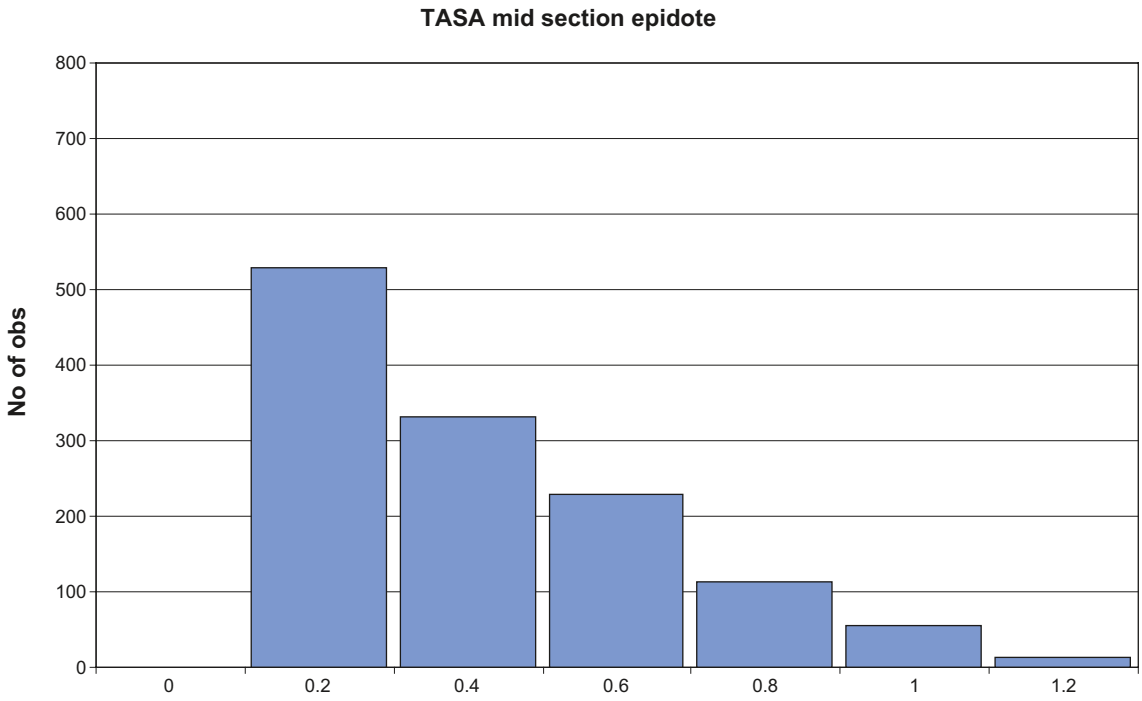

Figure C-105. *Histogram, TASA mid section epidote search radius 4 meters.*

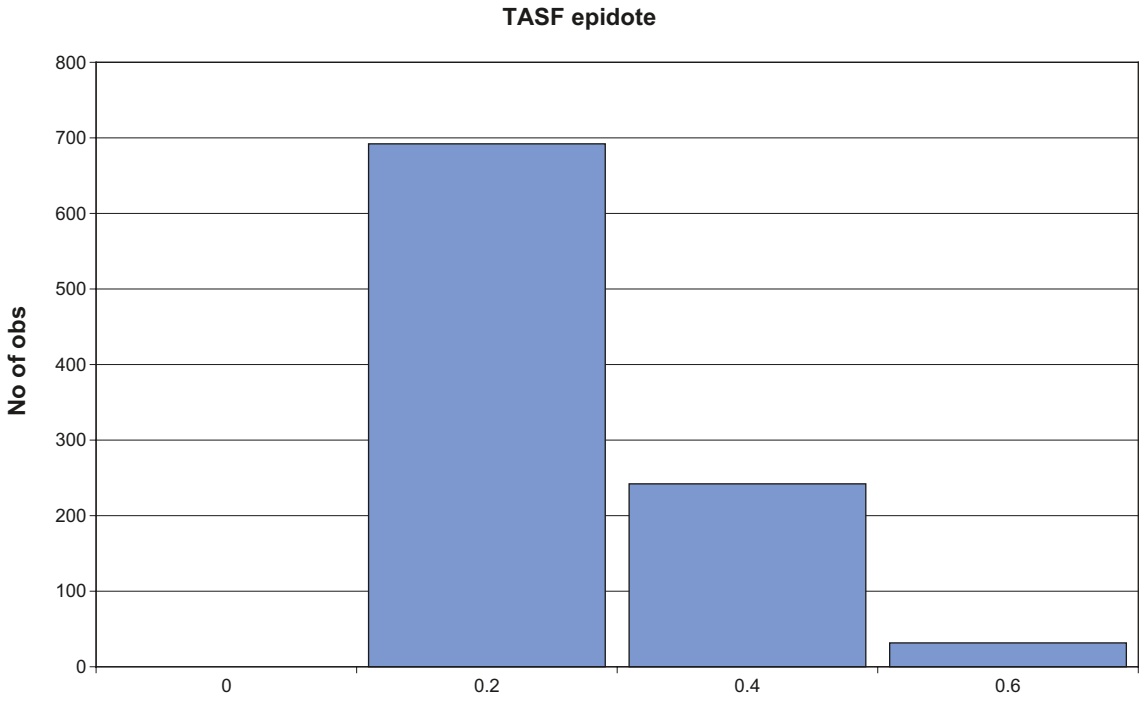

Figure C-106. *Histogram, TASF epidote search radius 4 meters.*

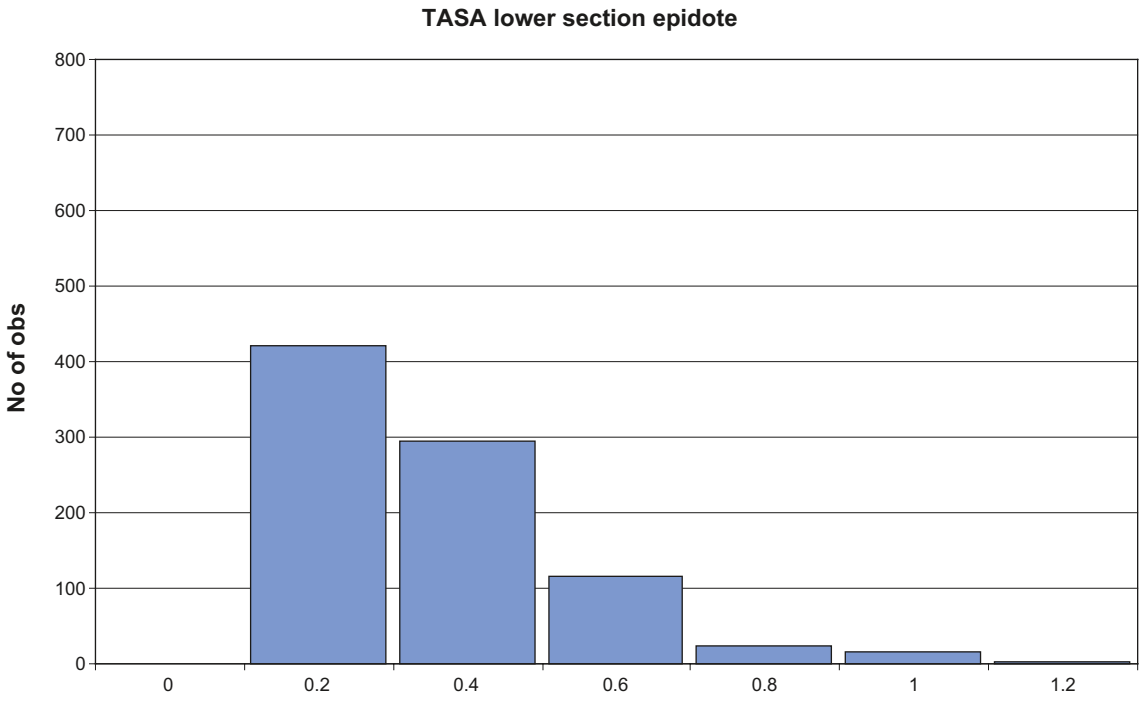

Figure C-107. *Histogram, TASA lower section epidote search radius 4 meters.*

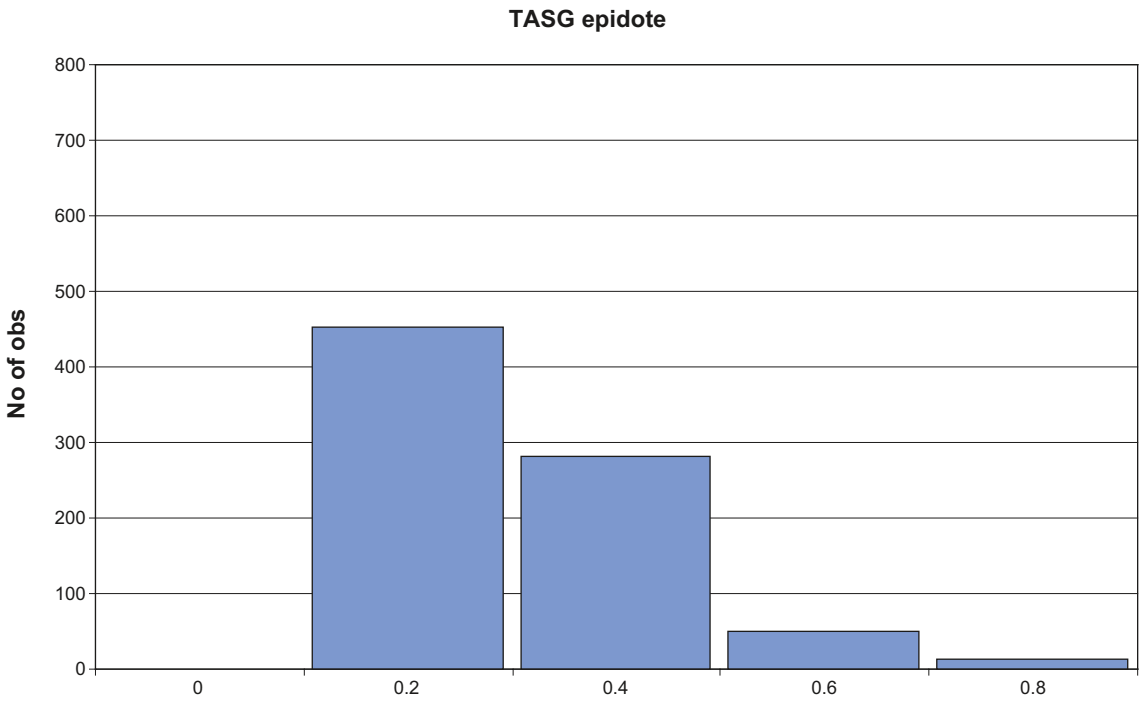

Figure C-108. *Histogram, TASG epidote search radius 4 meters.*

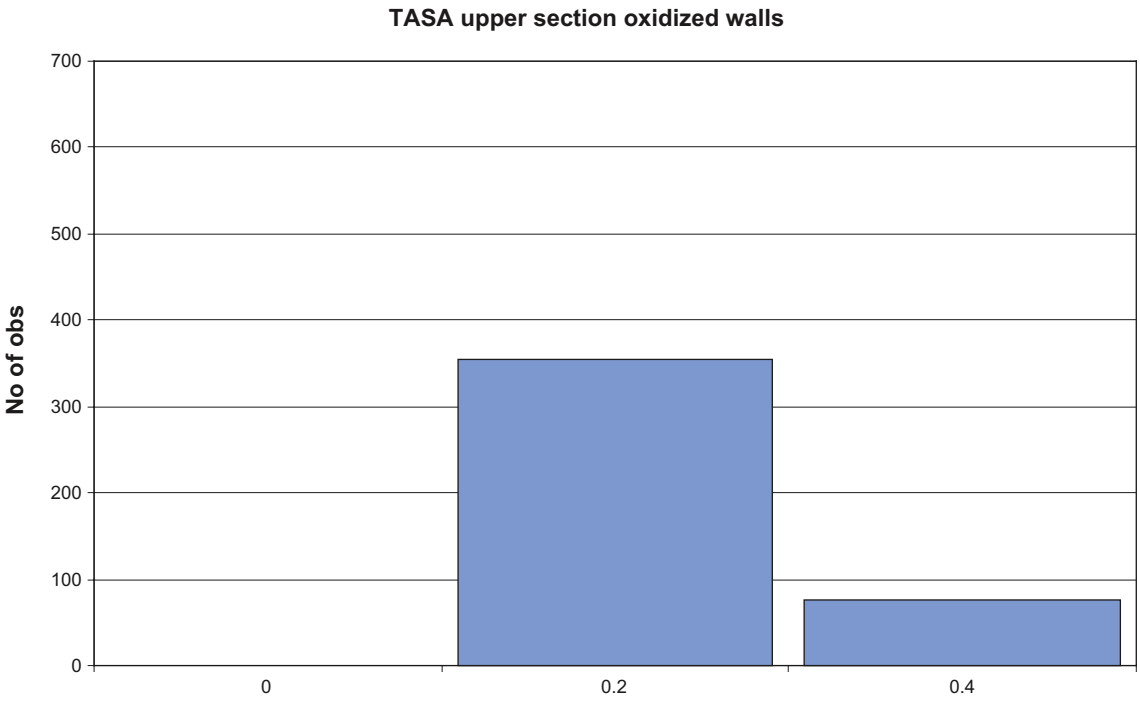

Figure C-109. *Histogram, TASA upper section oxidized walls search radius 4 meters.*

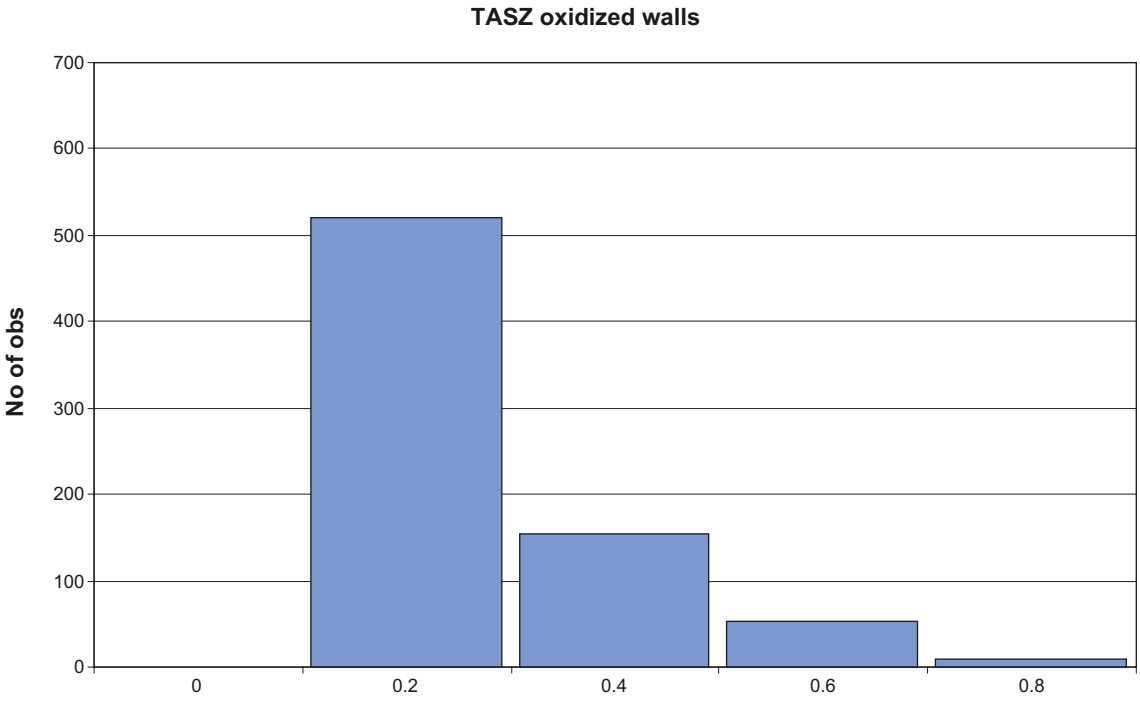

Figure C-110. *Histogram, TASZ oxidized walls search radius 4 meters.*

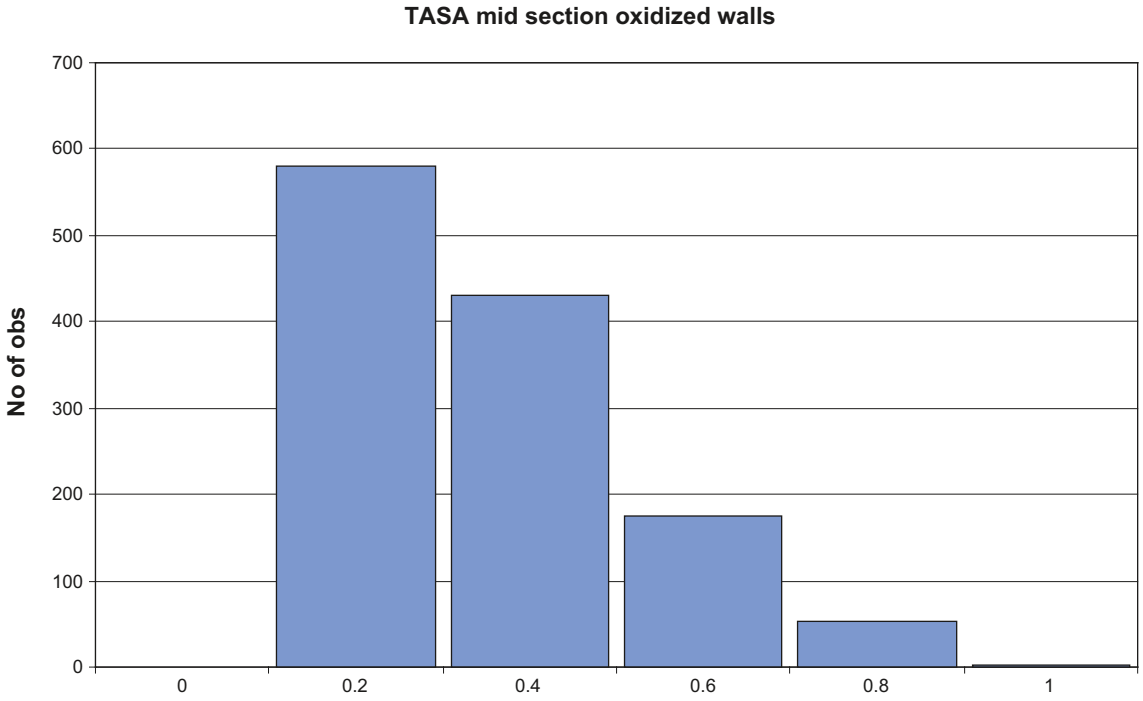

Figure C-111. *Histogram, TASA mid section oxidized walls search radius 4 meters.*

Figure C-112. *Histogram, TASF oxidized walls search radius 4 meters.*

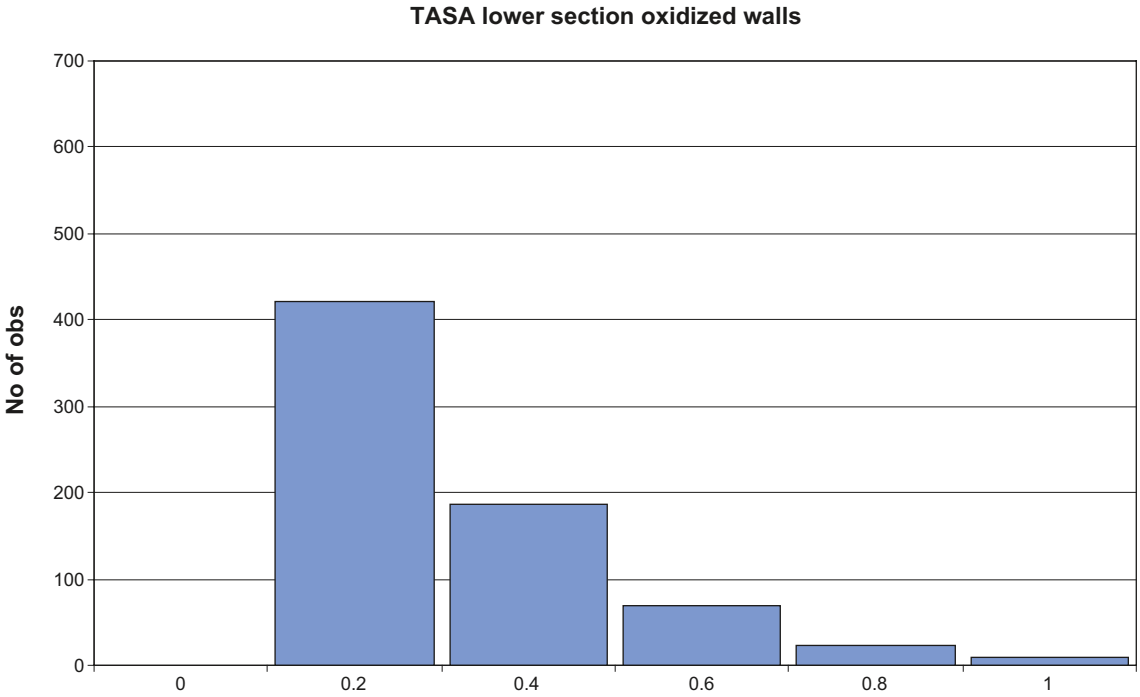

Figure C-113. *Histogram, TASA lower section oxidized walls search radius 4 meters.*

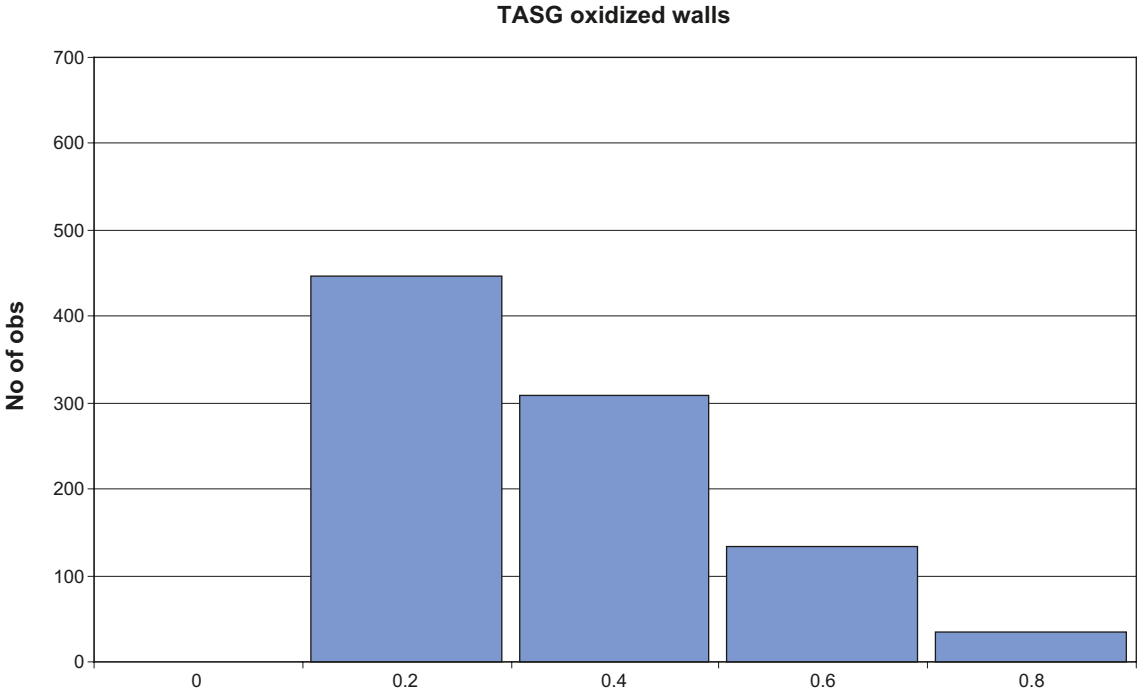

Figure C-114. *Histogram, TASG oxidized walls search radius 4 meters.*

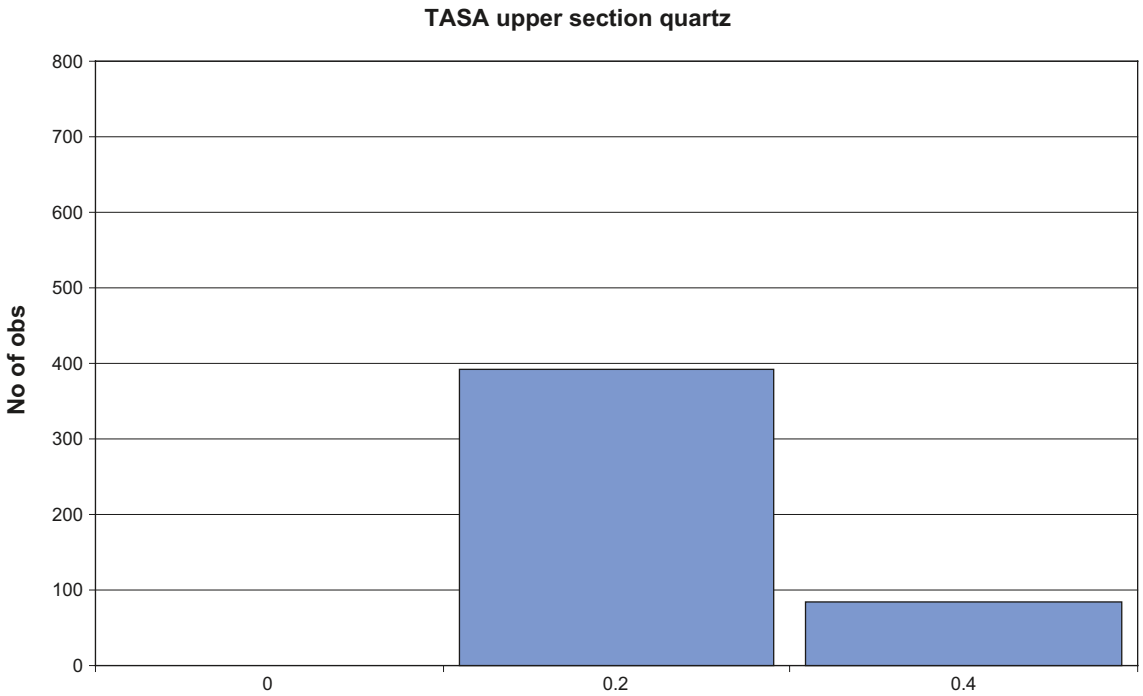

Figure C-115. *Histogram, TASA upper section quarts search radius 4 meters.*

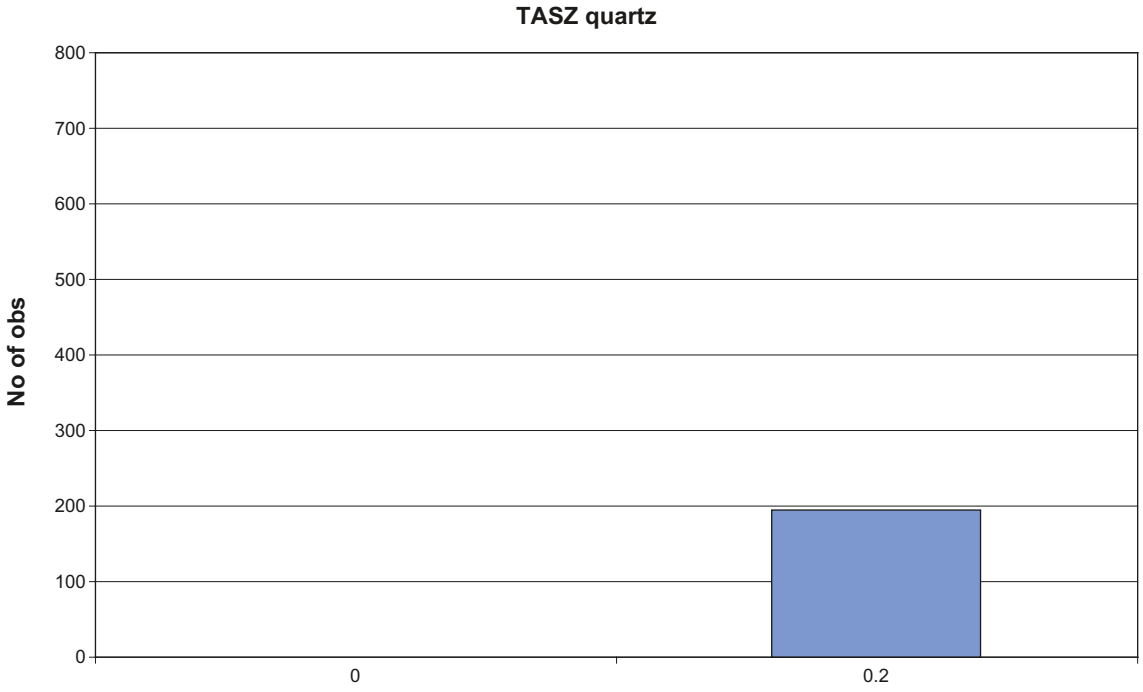

Figure C-116. *Histogram, TASZ quarts search radius 4 meters.*

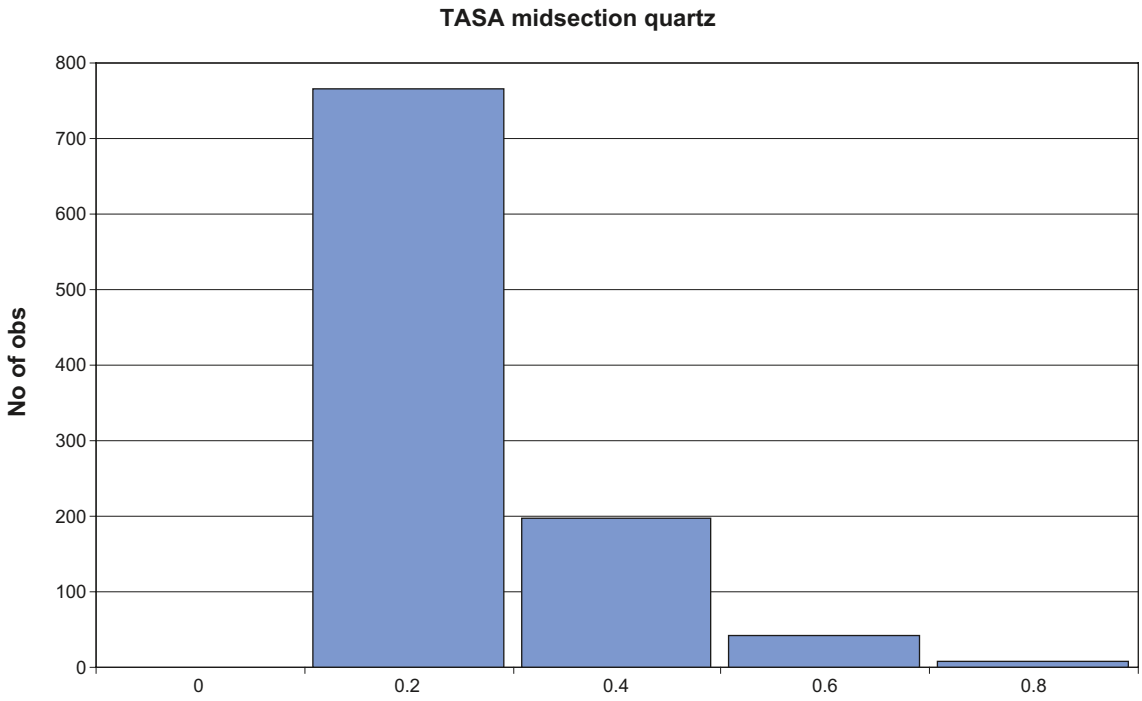

Figure C-117. *Histogram, TASA mid section quarts search radius 4 meters.*

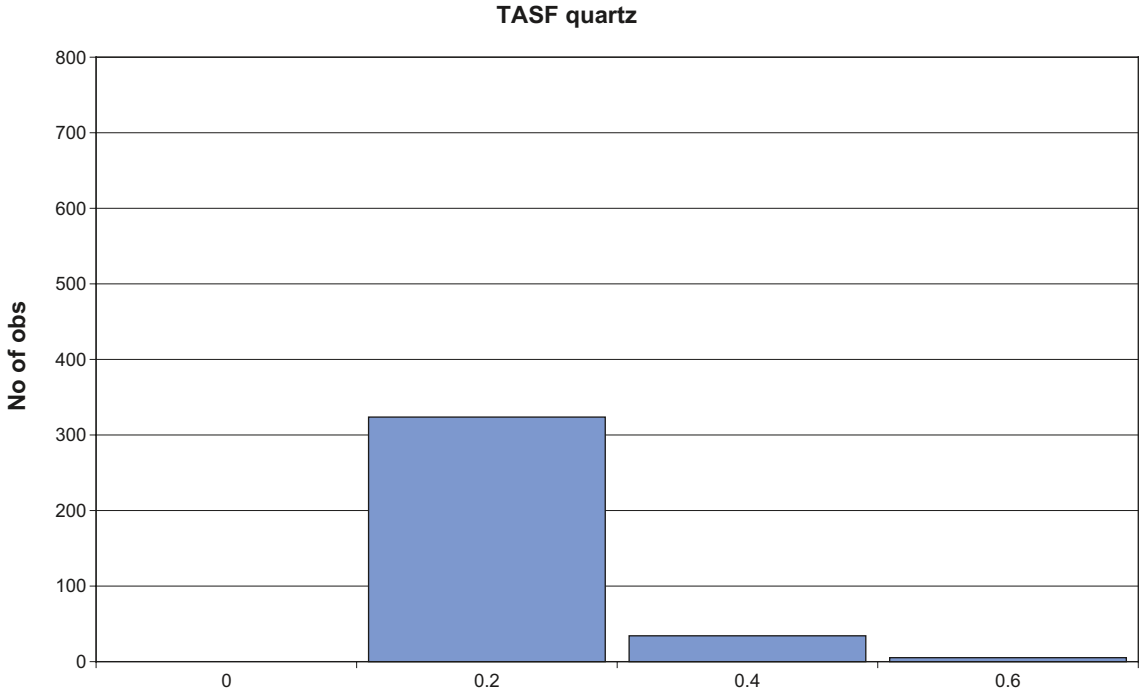

Figure C-118. *Histogram, TASF quarts search radius 4 meters.*

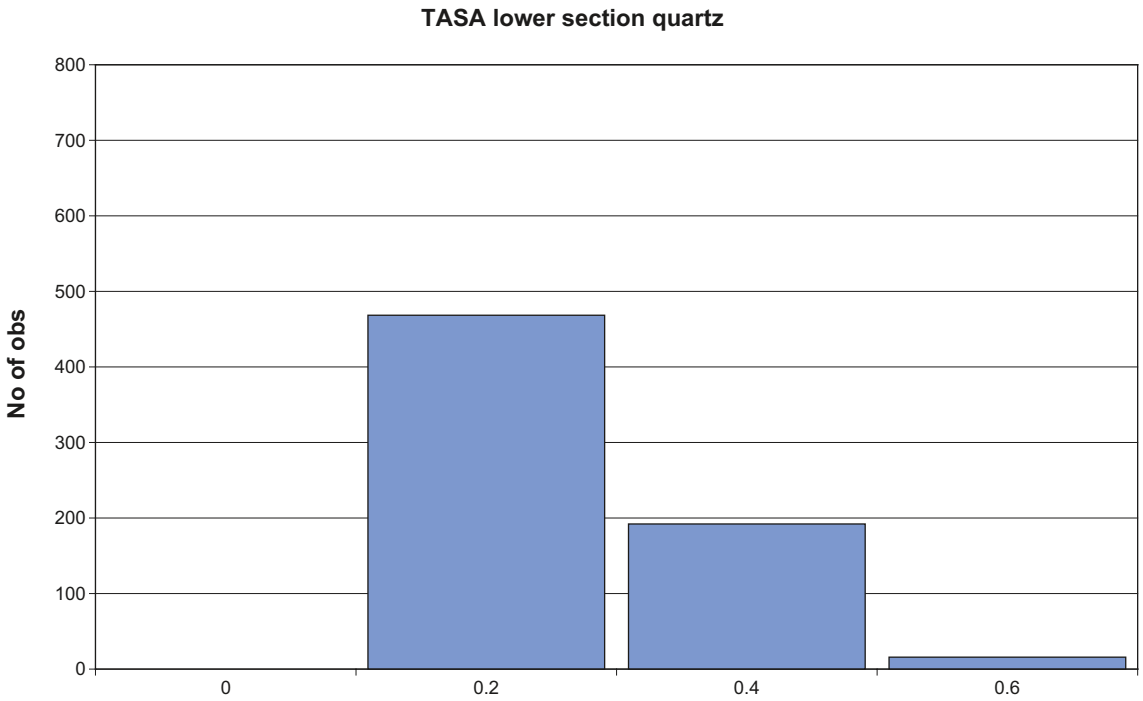

Figure C-119. *Histogram, TASA lower section quarts search radius 4 meters.*

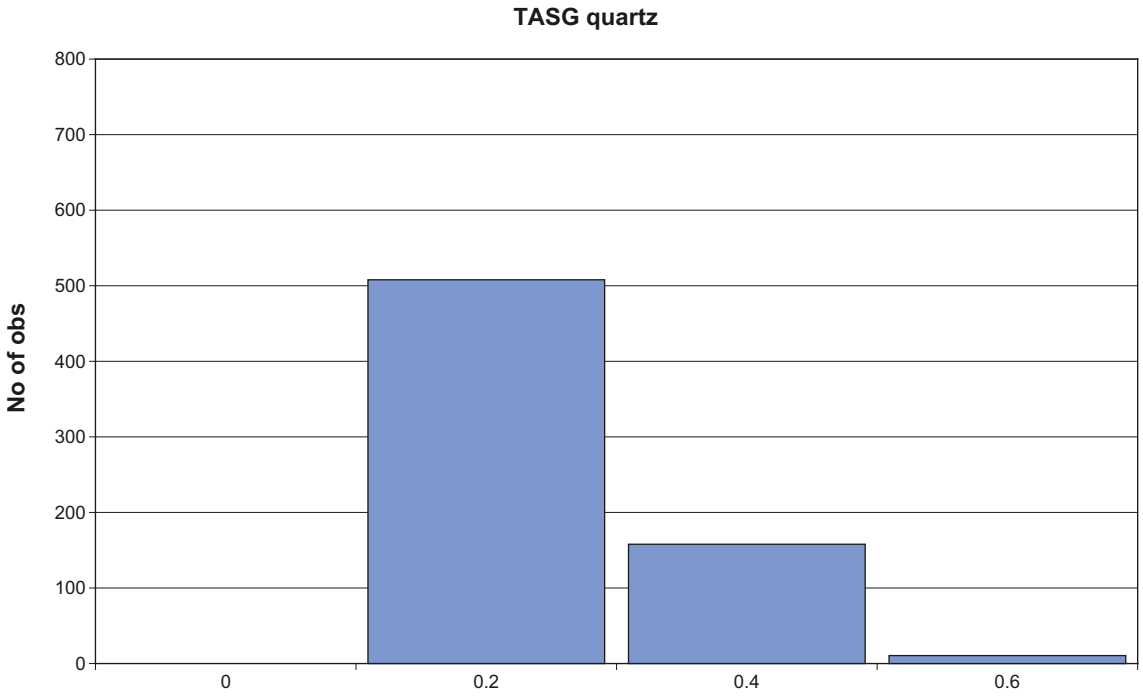

Figure C-120. *Histogram, TASG quarts search radius 4 meters.*

Appendix D

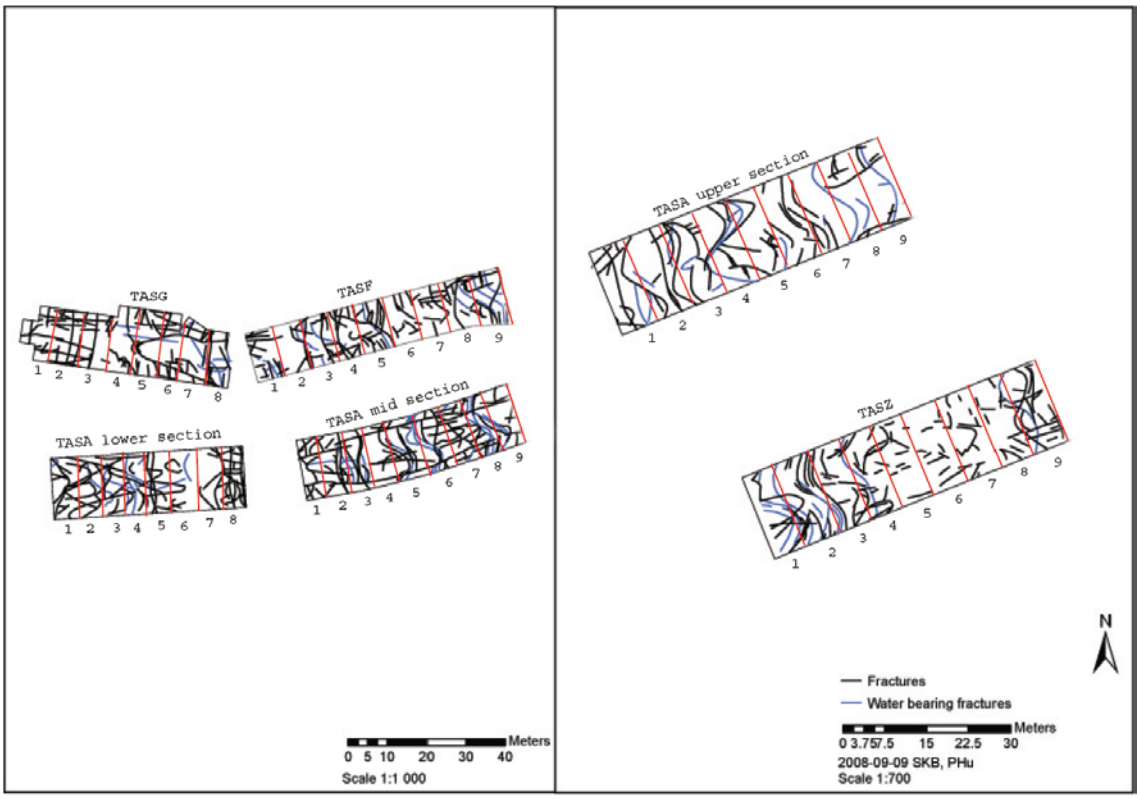

Figure D-1. *Each Tunnel section divided into minor sections, approximately 100 m².*

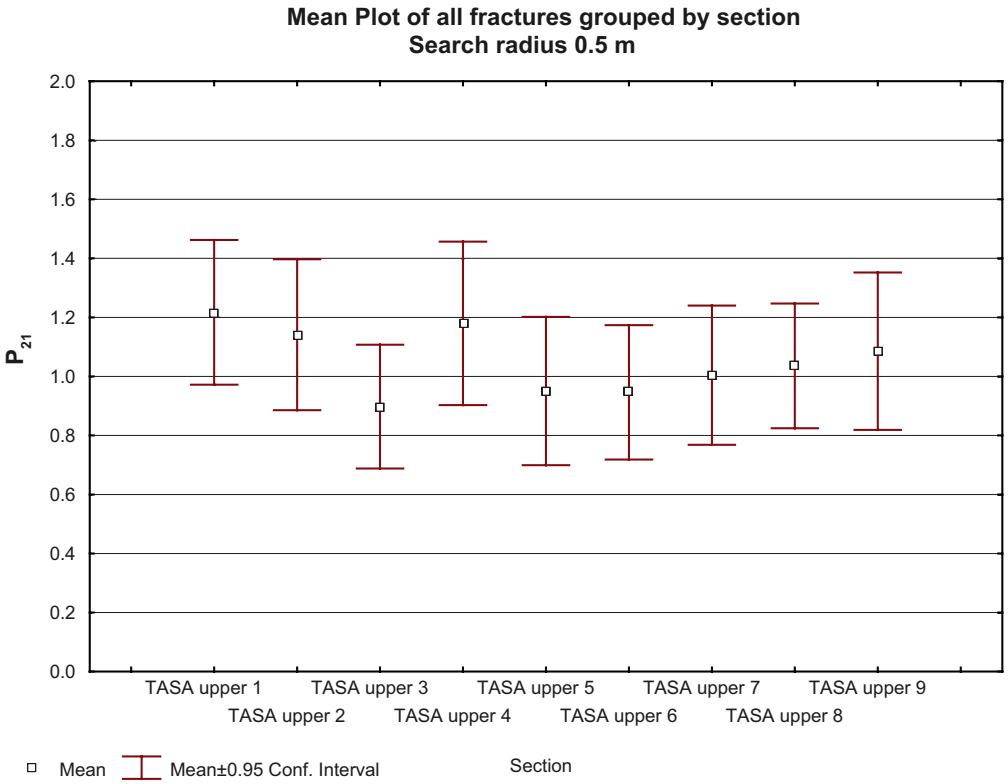

Figure D-2. *Mean plot of all fractures grouped by section, search radius 0.5 m.*

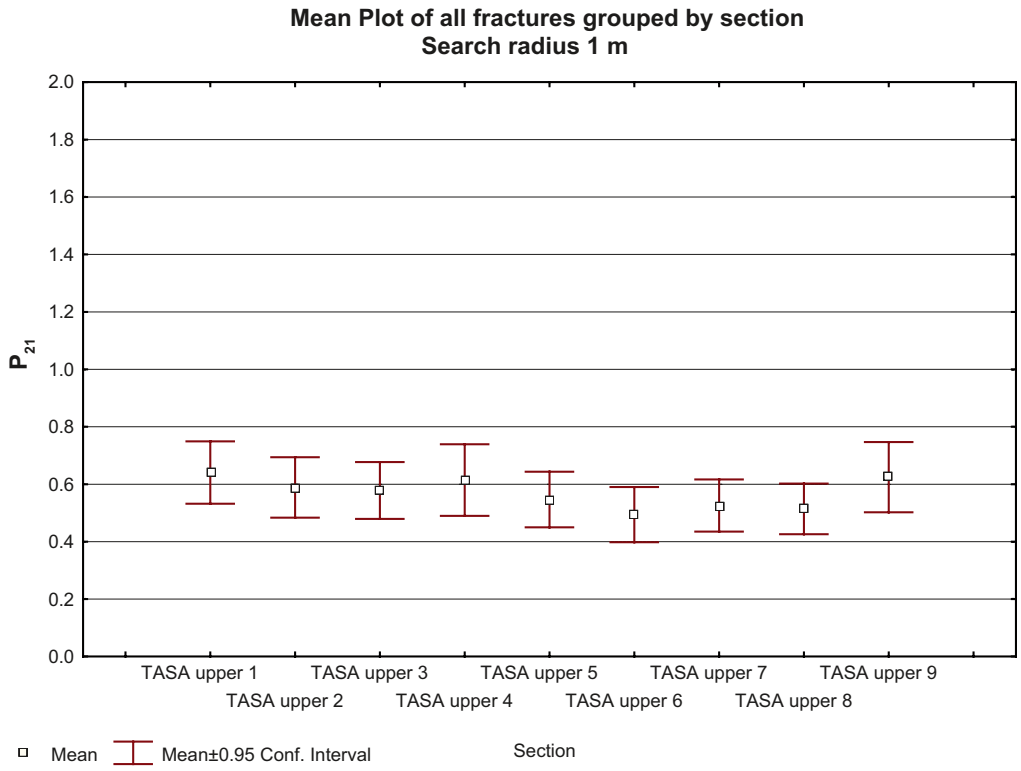

Figure D-3. *Mean plot of all fractures grouped by section, search radius 1 m.*

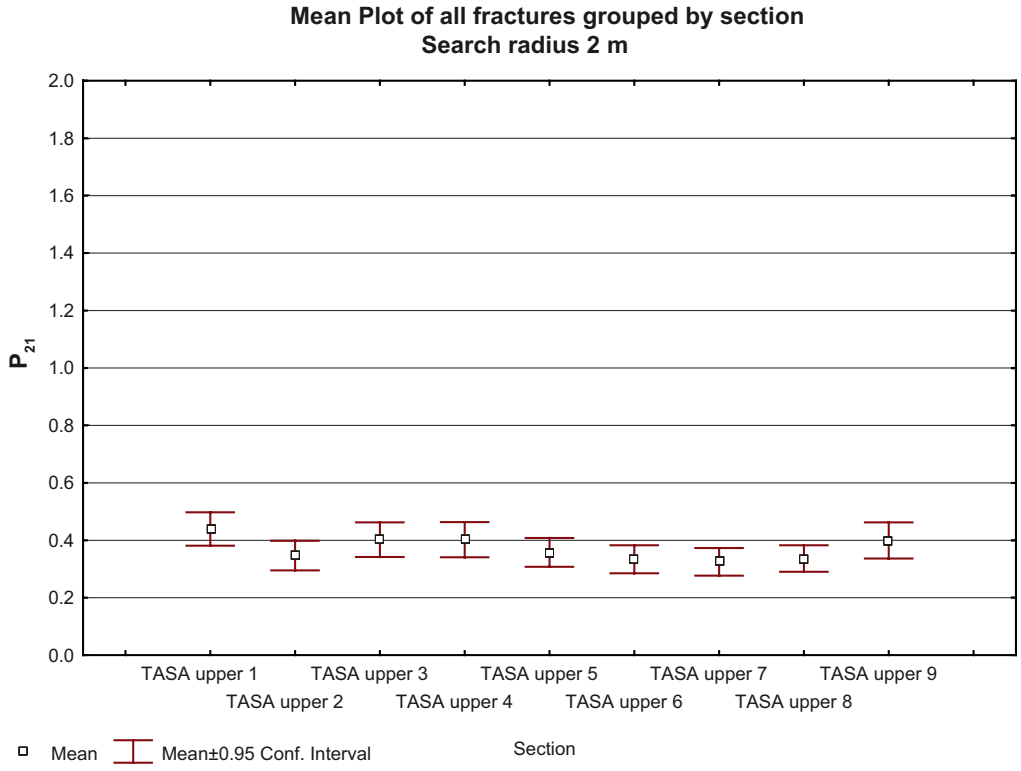

Figure D-4. *Mean plot of all fractures grouped by section, search radius 2 m.*

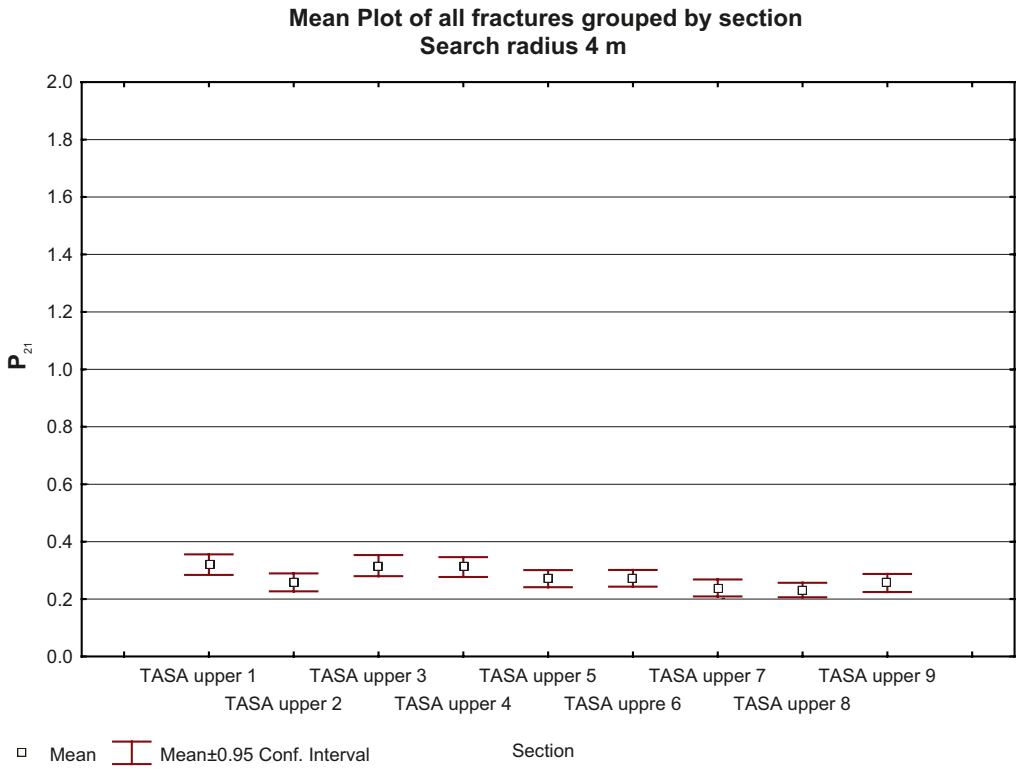

Figure D-5. *Mean plot of all fractures grouped by section, search radius 4 m.*

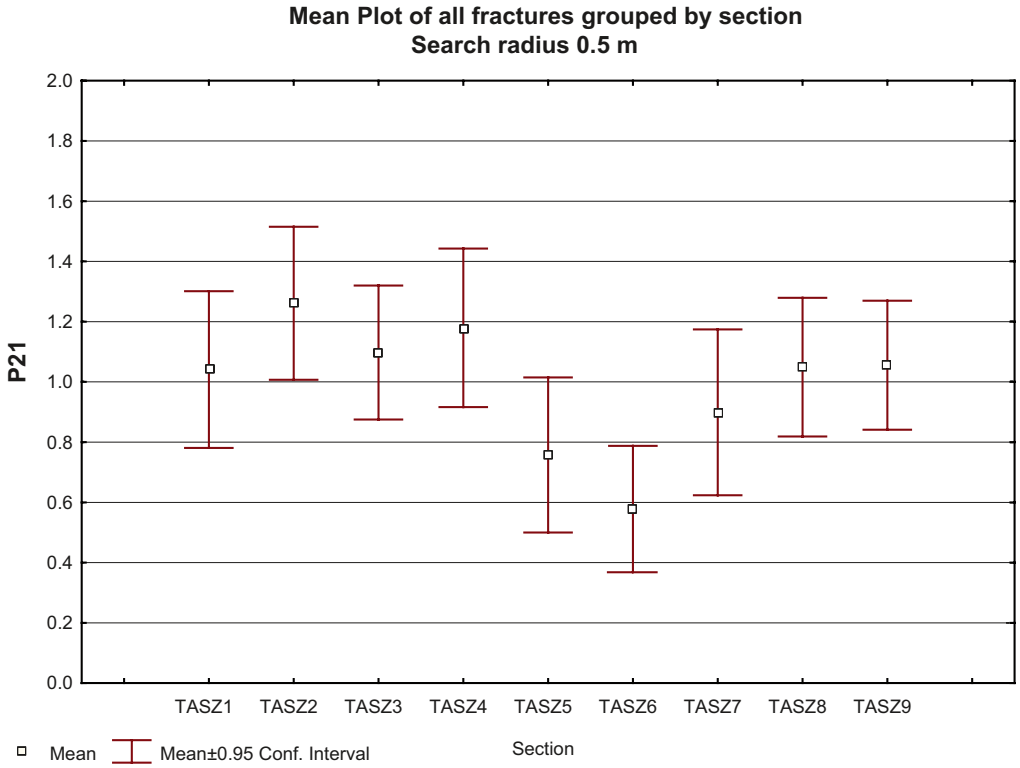

Figure D-6. *Mean plot of all fractures grouped by section, search radius 0.5 m.*

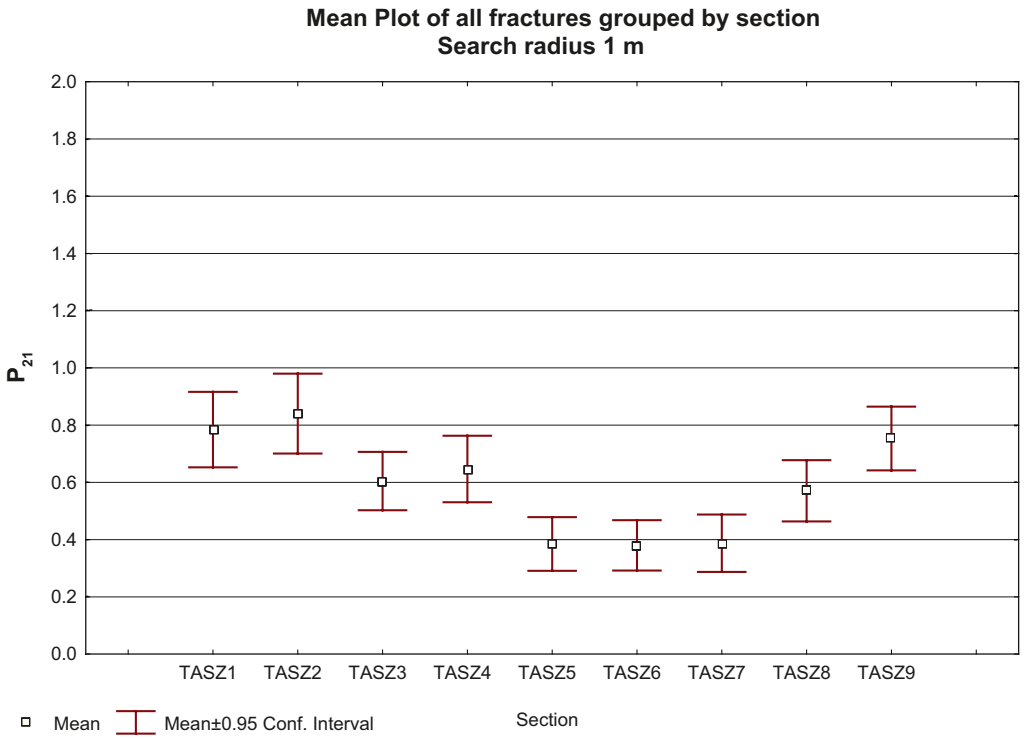

Figure D-7. *Mean plot of all fractures grouped by section, search radius 1 m.*

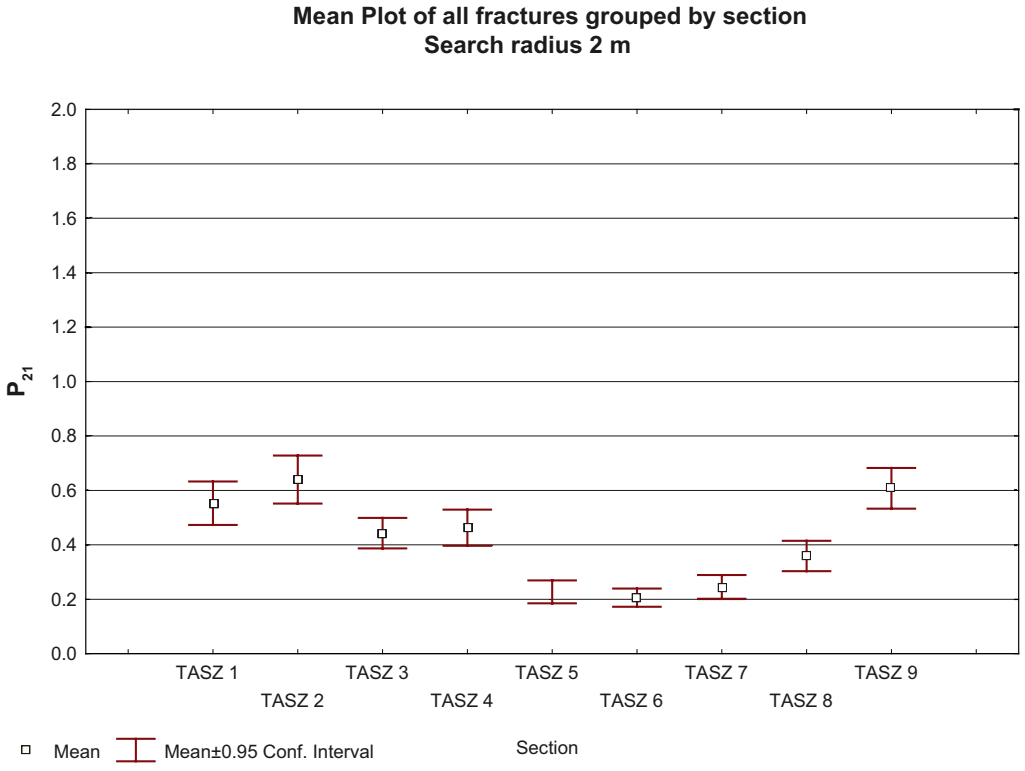

Figure D-8. *Mean plot of all fractures grouped by section, search radius 2 m.*

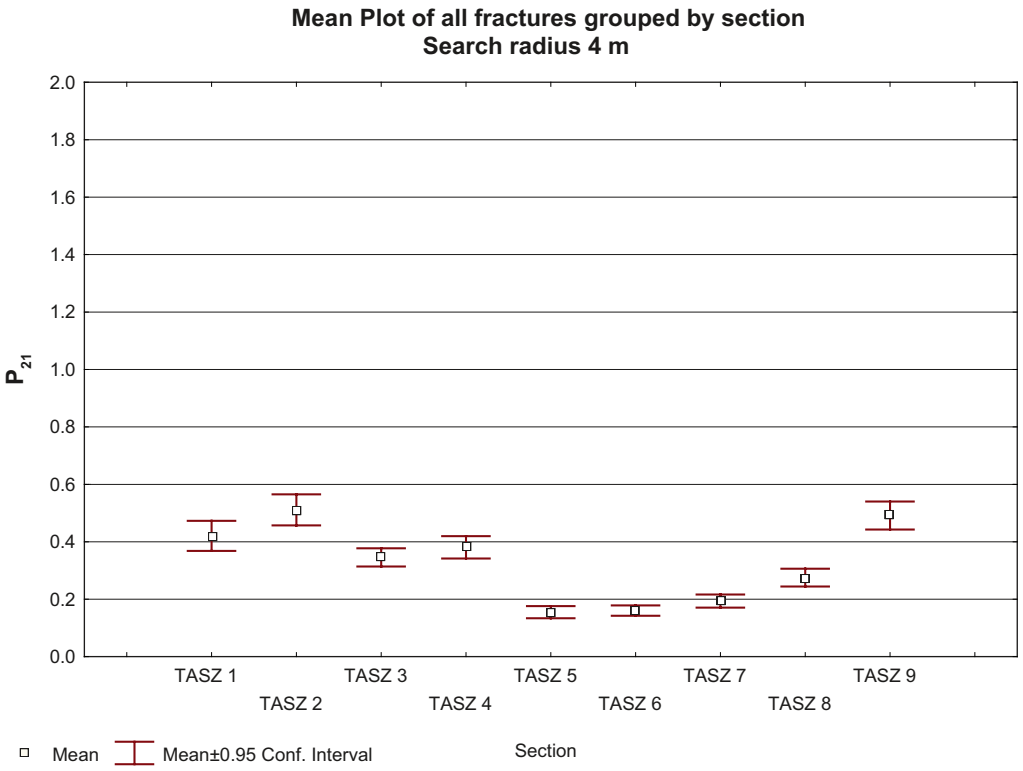

Figure D-9. *Mean plot of all fractures grouped by section, search radius 4 m.*

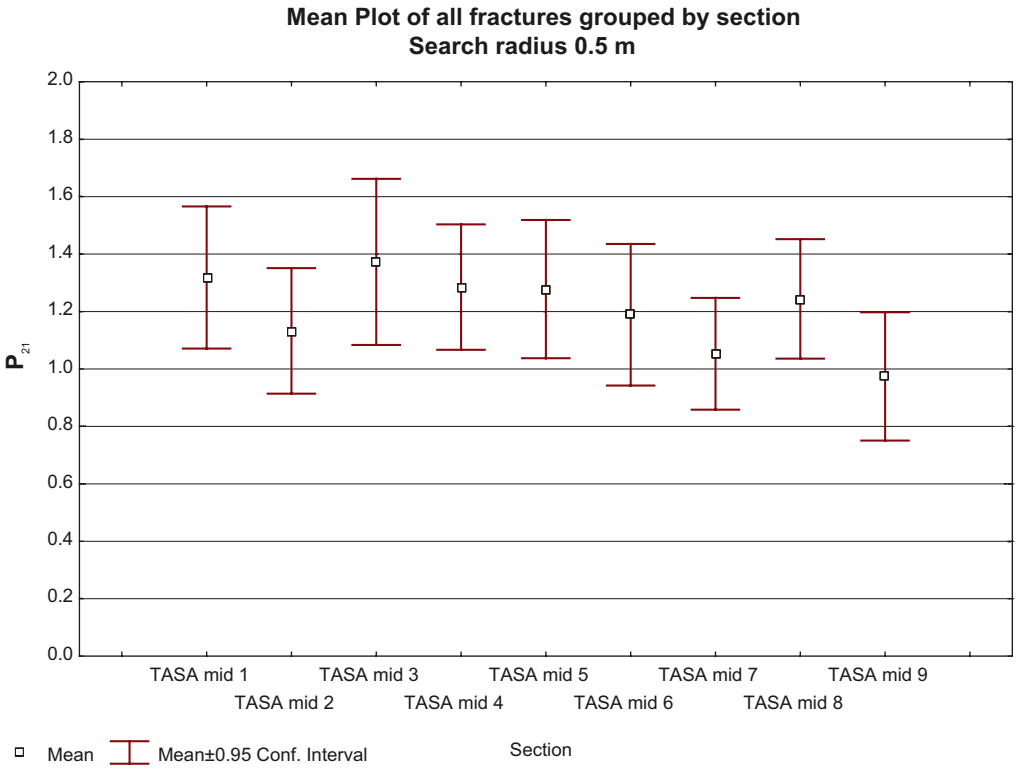

Figure D-10. *Mean plot of all fractures grouped by section, search radius 0.5 m.*

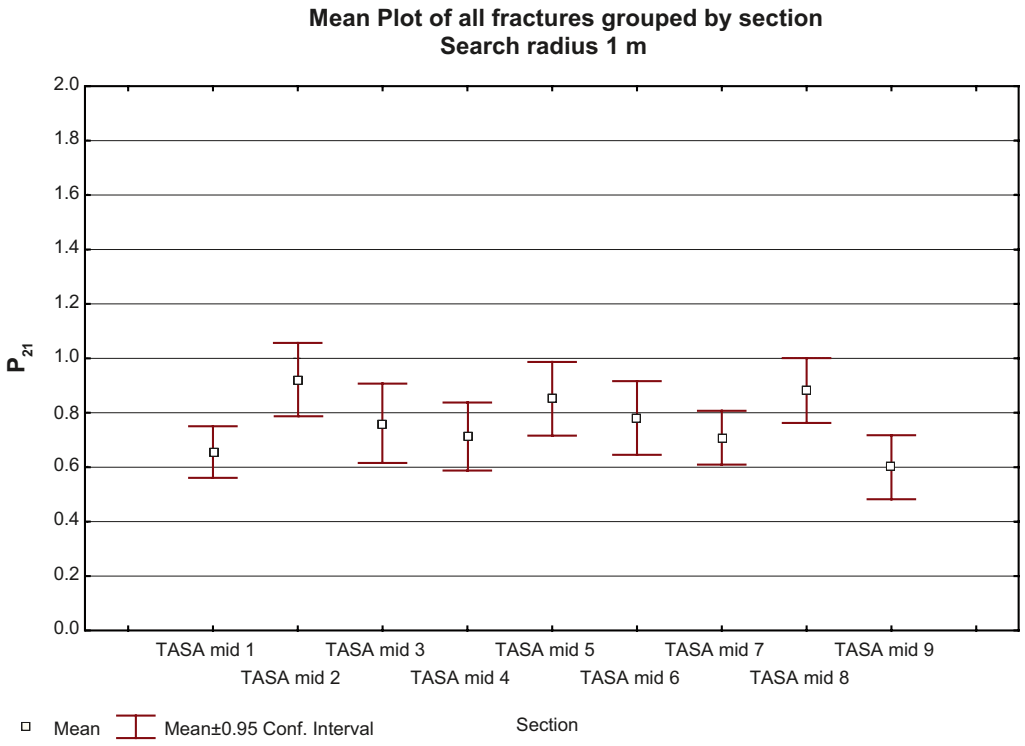

Figure D-11. *Mean plot of all fractures grouped by section, search radius 1 m.*

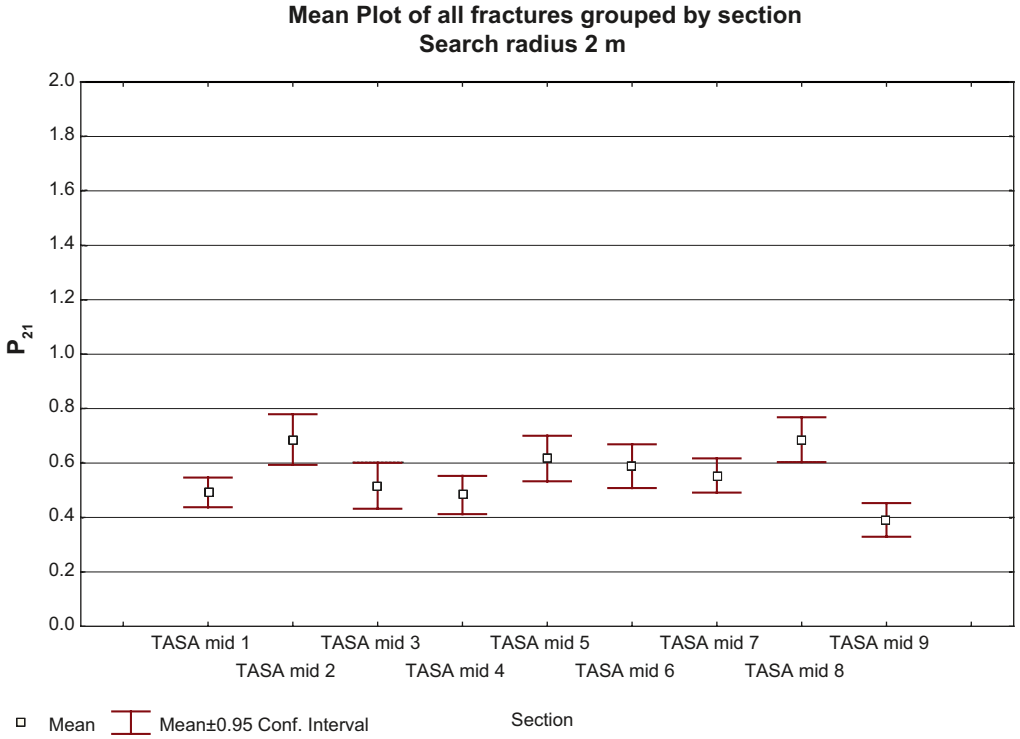

Figure D-12. *Mean plot of all fractures grouped by section, search radius 2 m.*

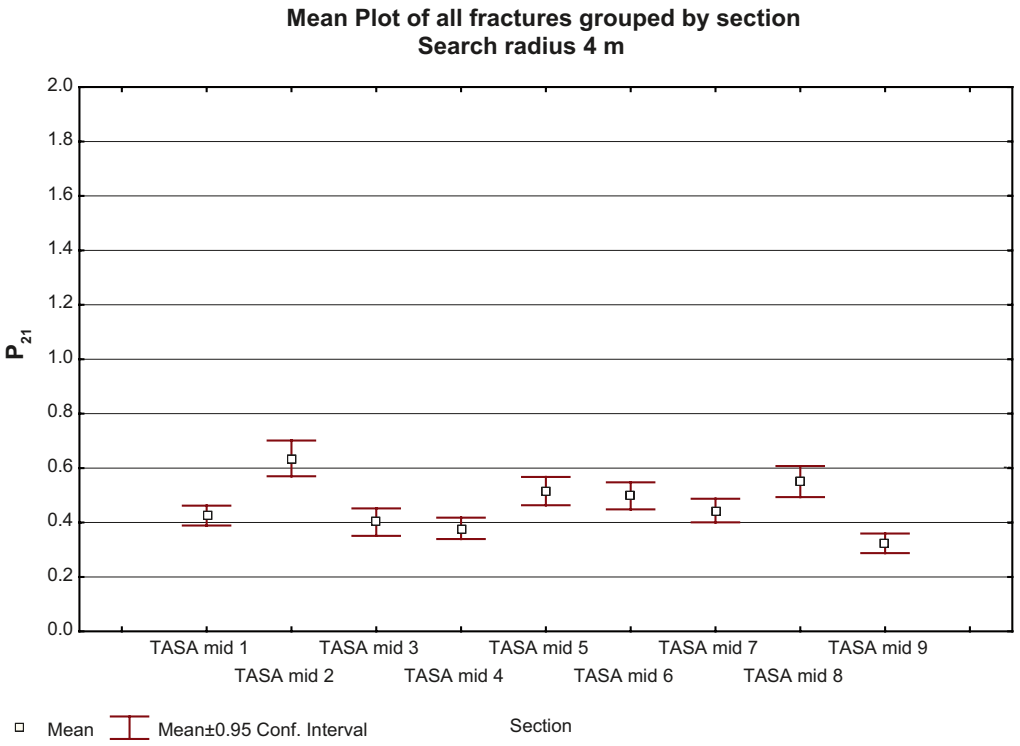

Figure D-13. *Mean plot of all fractures grouped by section, search radius 4 m.*

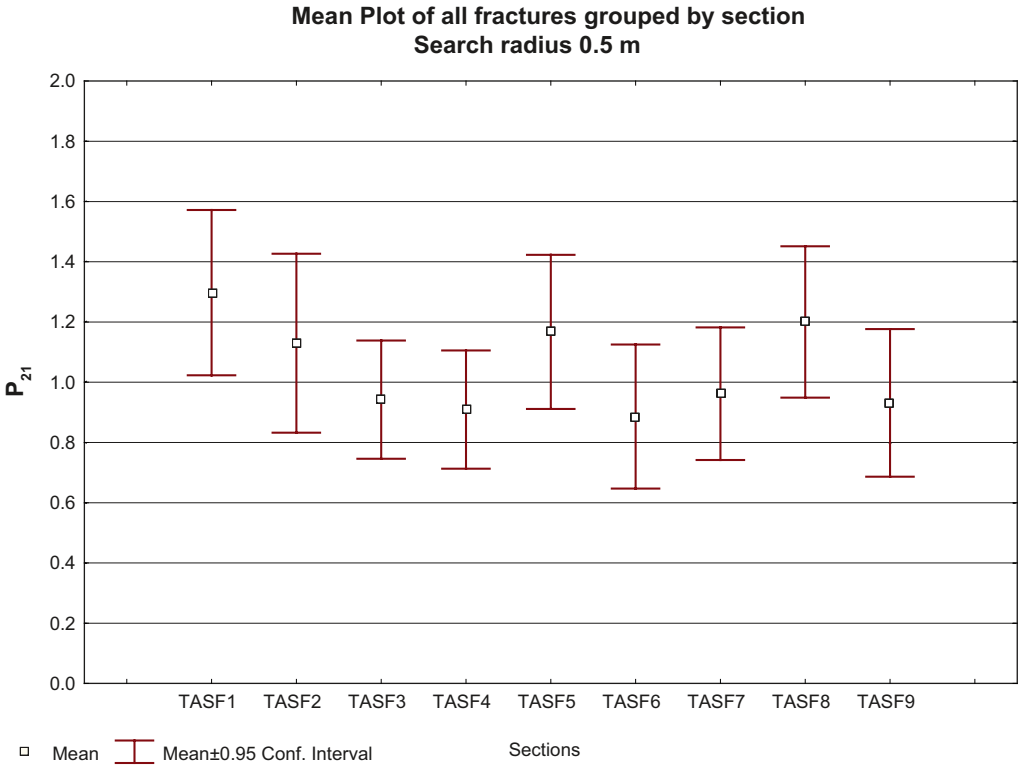

Figure D-14. *Mean plot of all fractures grouped by section, search radius 0.5 m.*

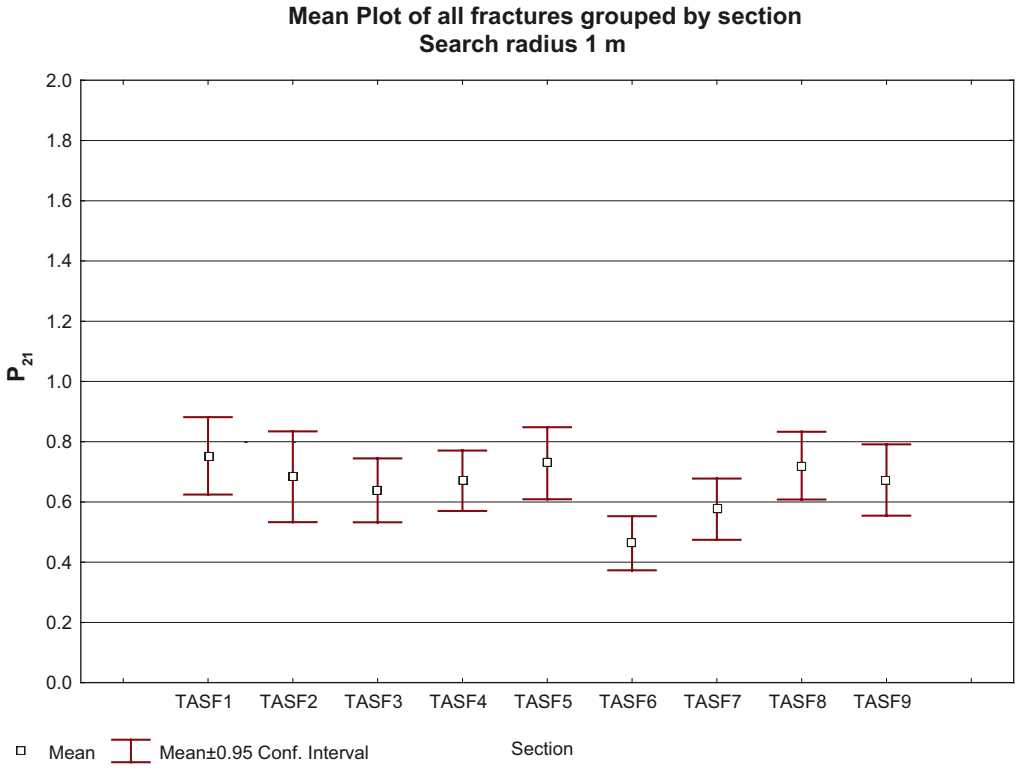

Figure D-15. *Mean plot of all fractures grouped by section, search radius 1 m.*

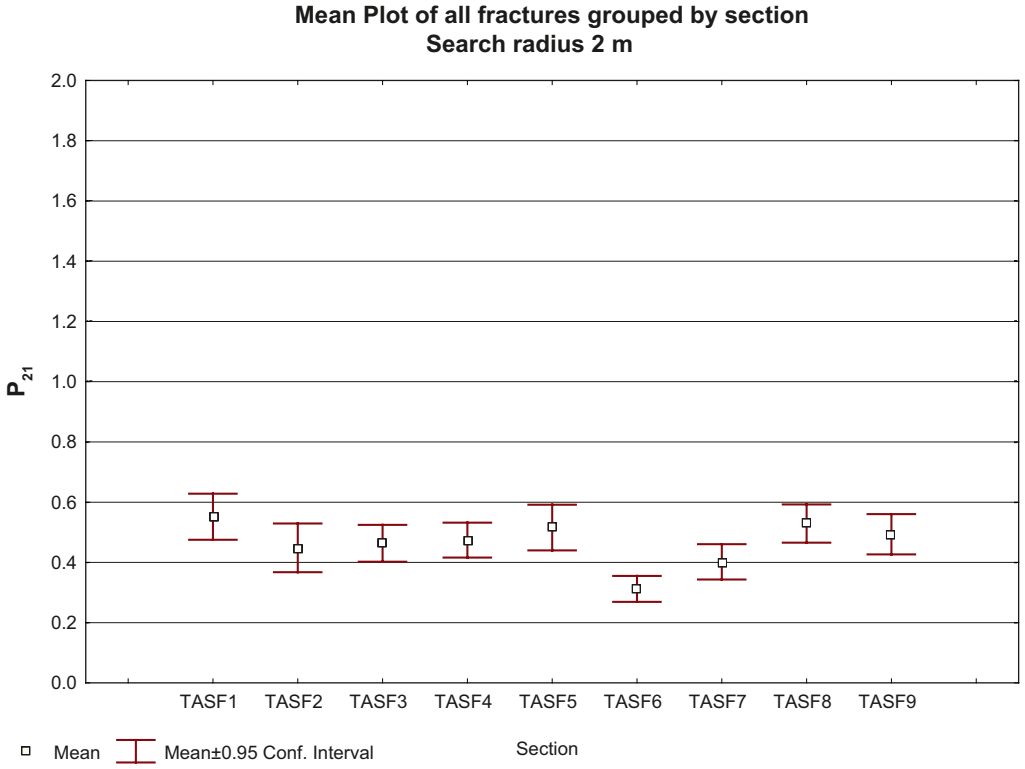

Figure D-16. *Mean plot of all fractures grouped by section, search radius 2 m.*

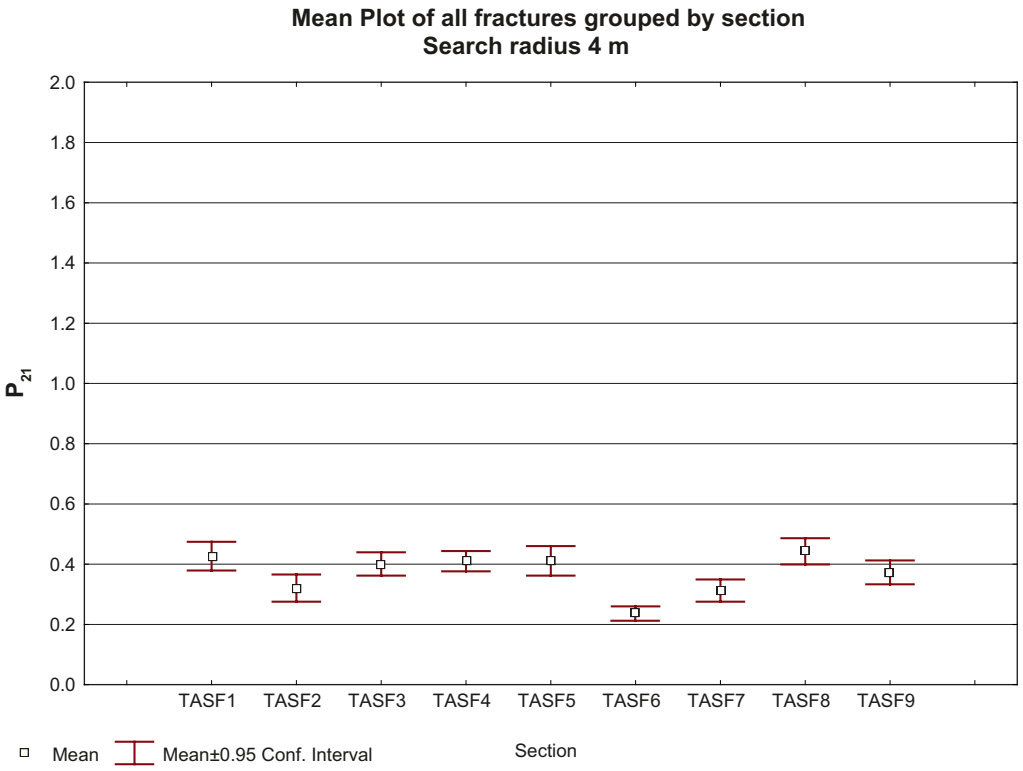

Figure D-17. *Mean plot of all fractures grouped by section, search radius 4 m.*

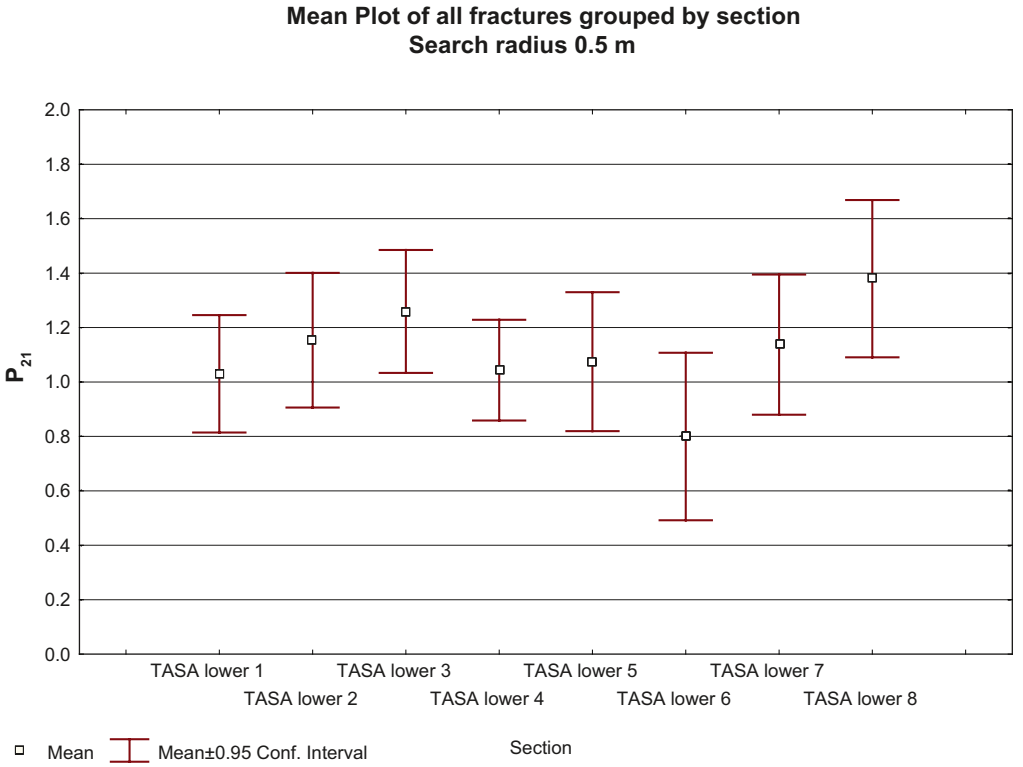

Figure D-18. *Mean plot of all fractures grouped by section, search radius 0.5 m.*

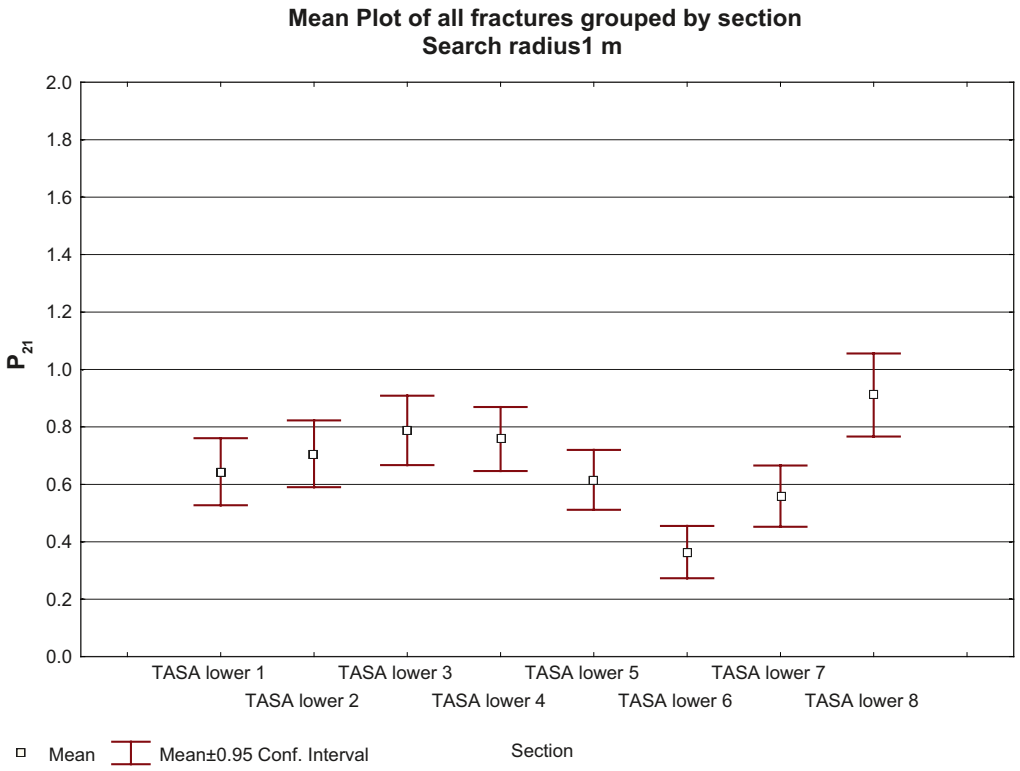

Figure D-19. *Mean plot of all fractures grouped by section, search radius 1 m.*

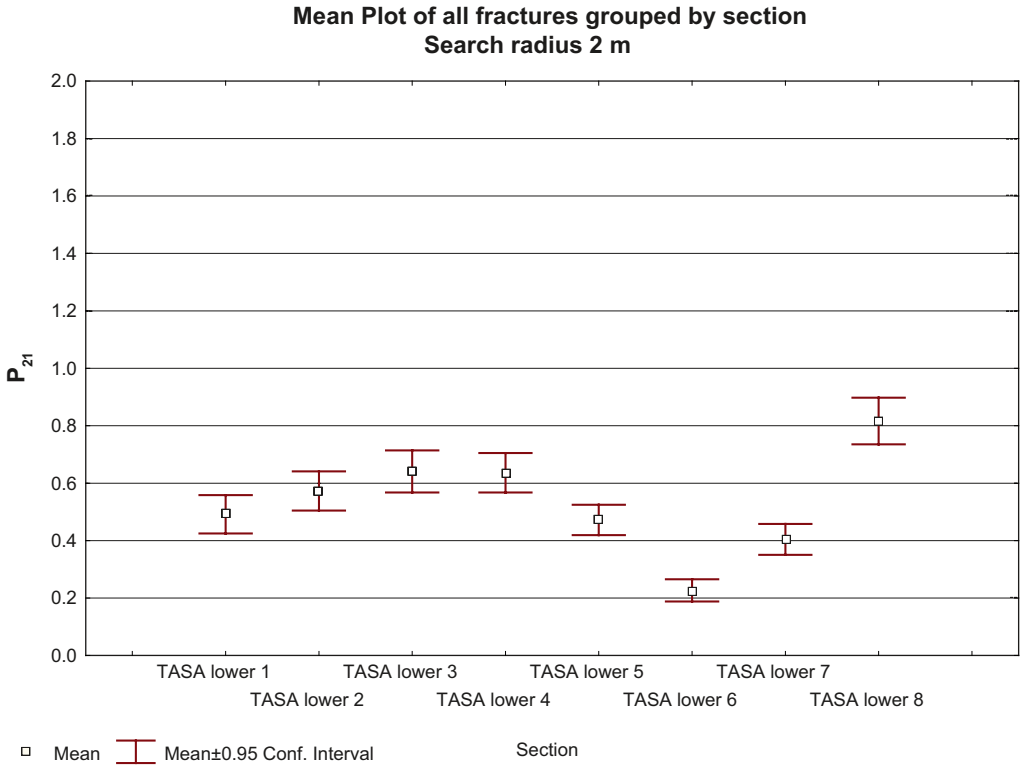

Figure D-20. *Mean plot of all fractures grouped by section, search radius 2 m.*

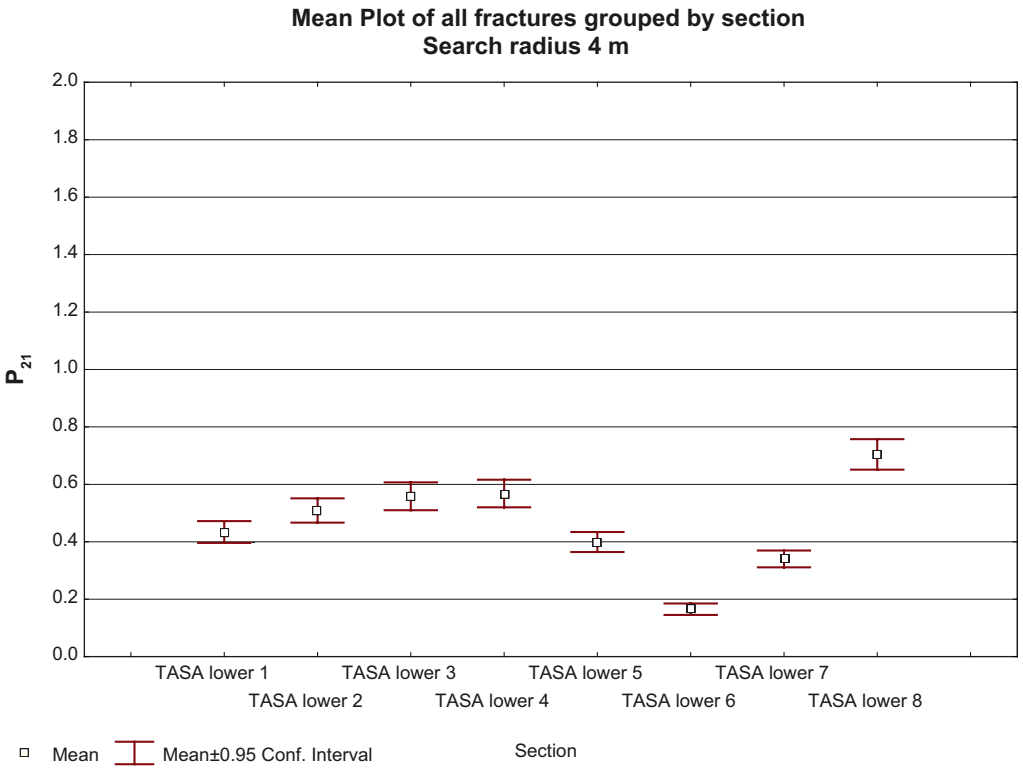

Figure D-21. *Mean plot of all fractures grouped by section, search radius 4 m.*

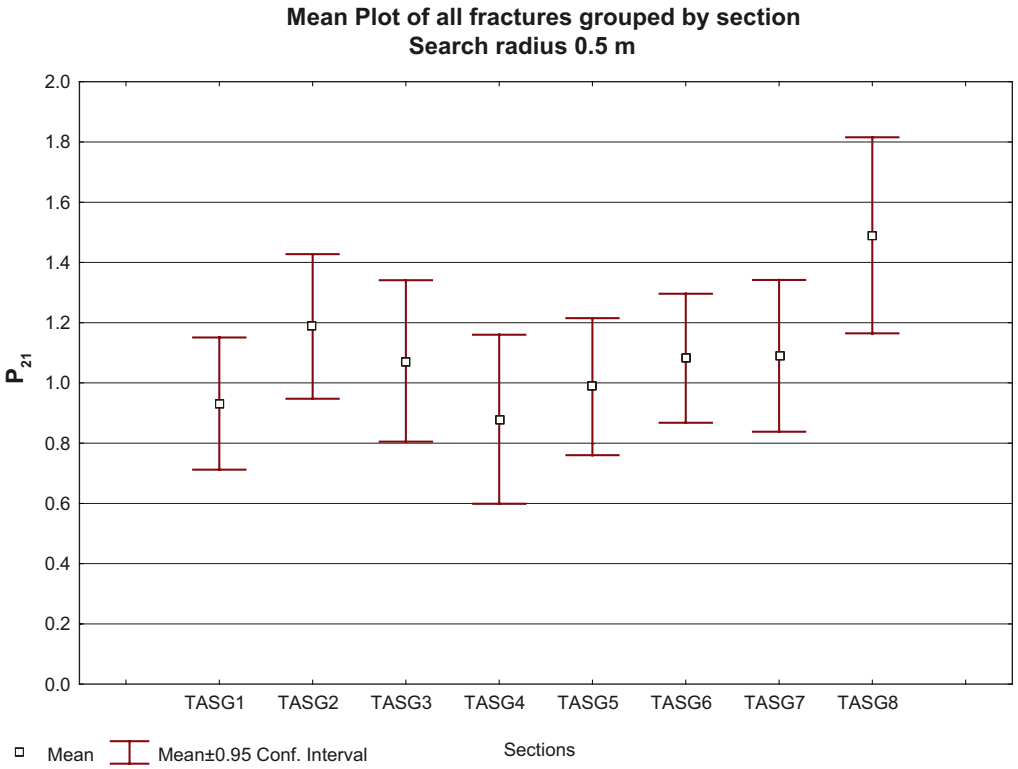

Figure D-22. *Mean plot of all fractures grouped by section, search radius 0.5 m.*

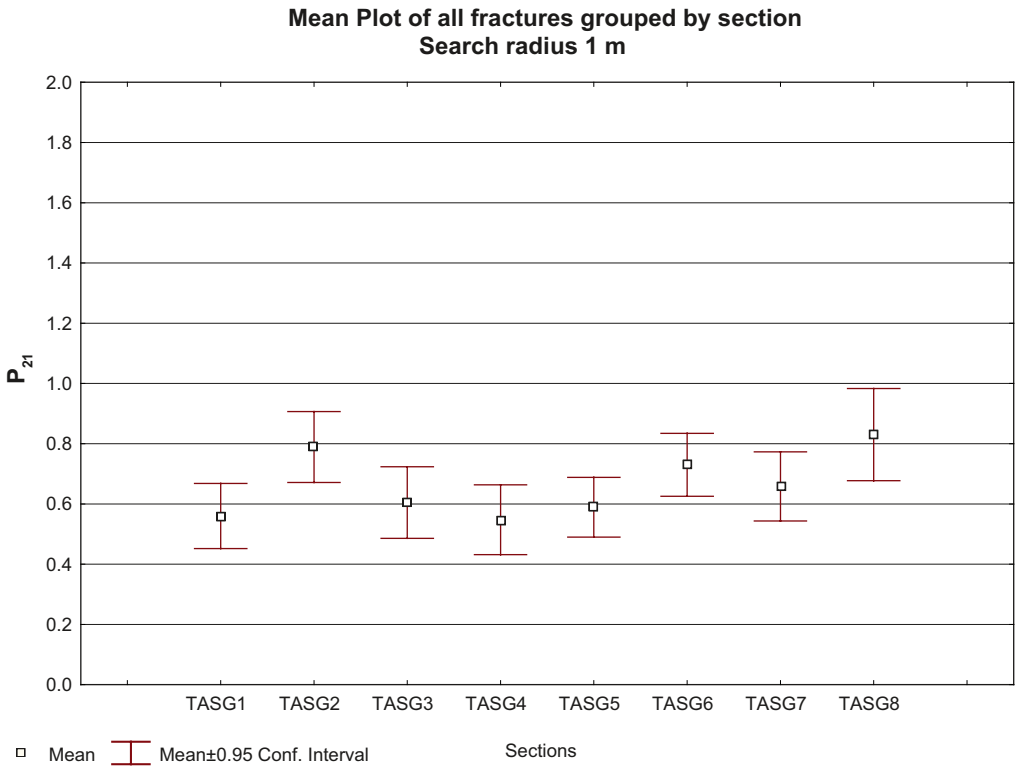

Figure D-23. *Mean plot of all fractures grouped by section, search radius 1 m.*

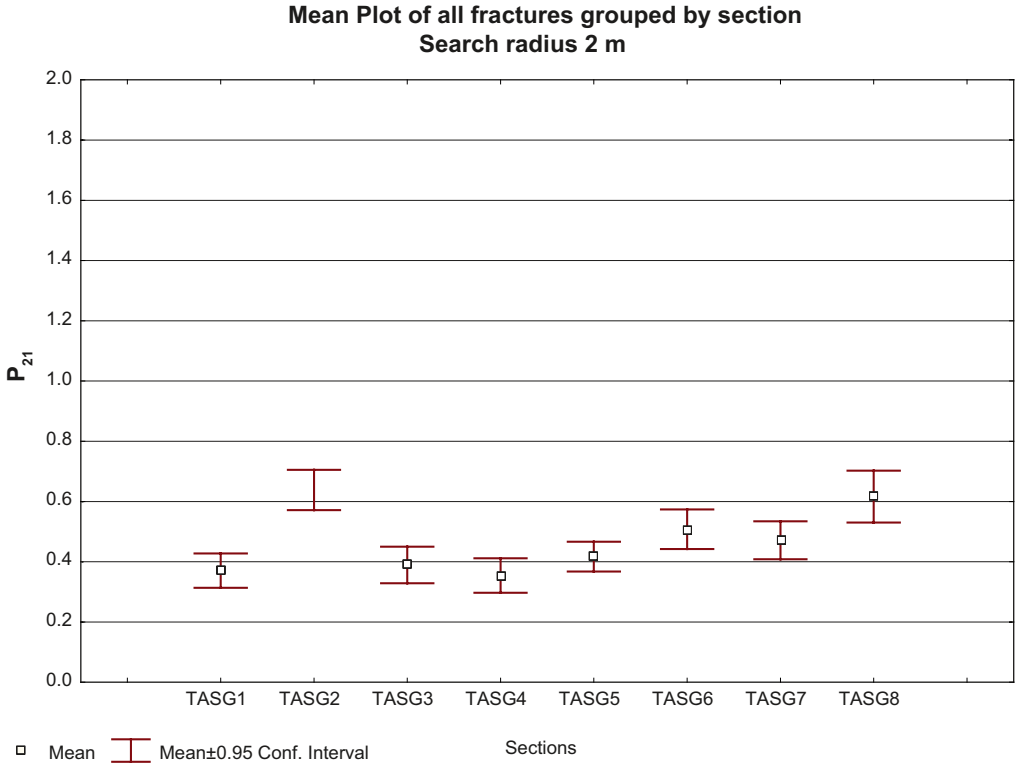

Figure D-24. *Mean plot of all fractures grouped by section, search radius 2 m.*

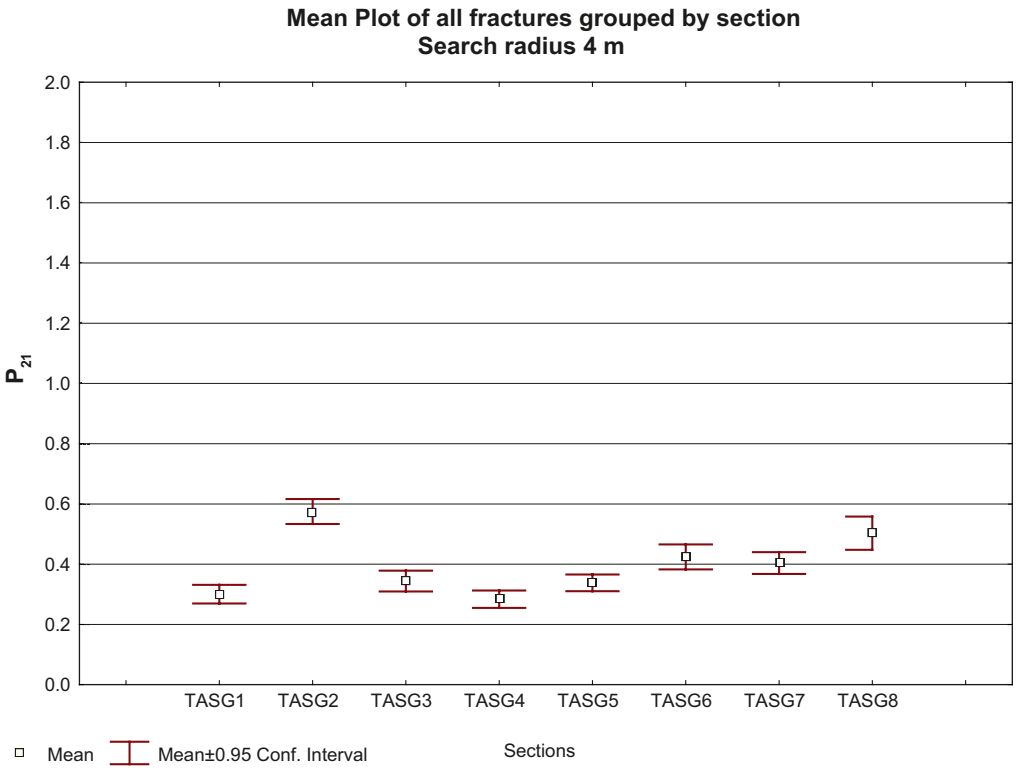

Figure D-25. *Mean plot of all fractures grouped by section, search radius 4 m.*

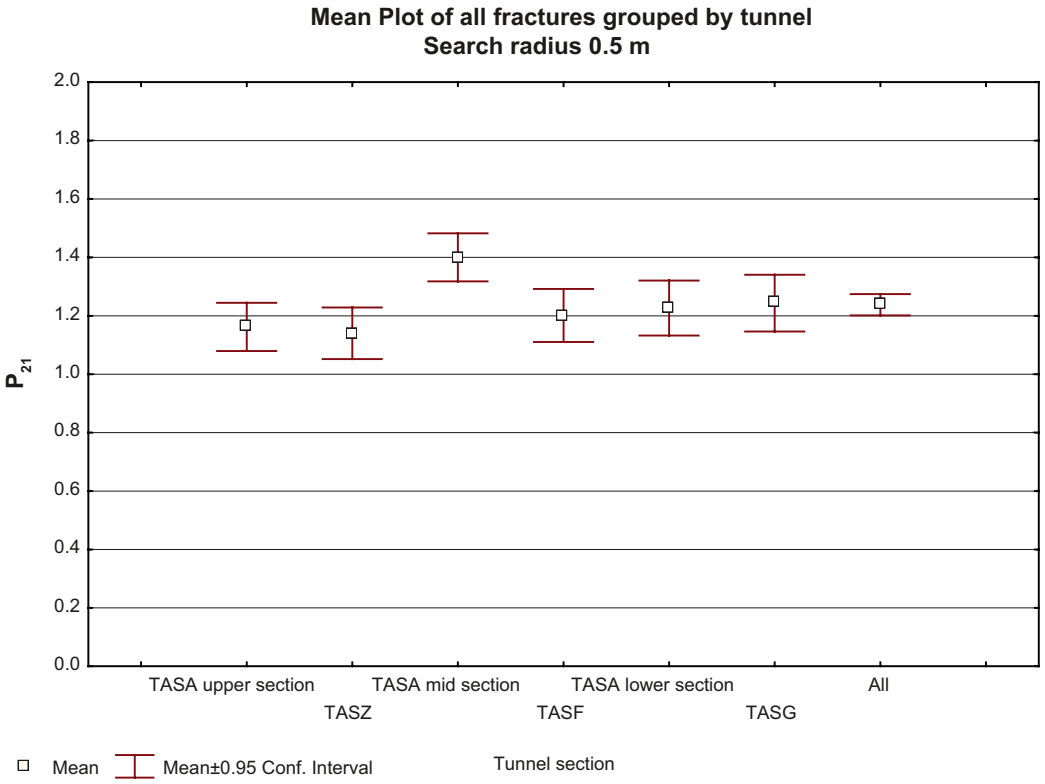

Figure D-26. *Mean plot of all fractures search radius 0.5 meters.*

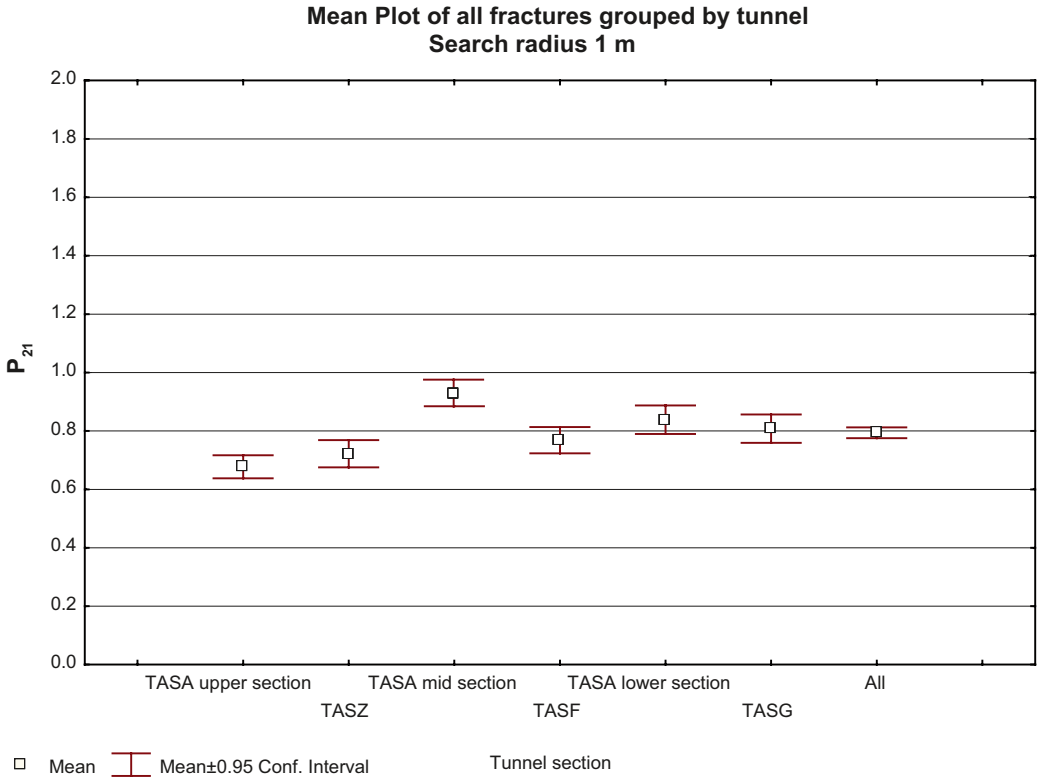

Figure D-27. *Mean plot of all fractures search radius 1 meter.*

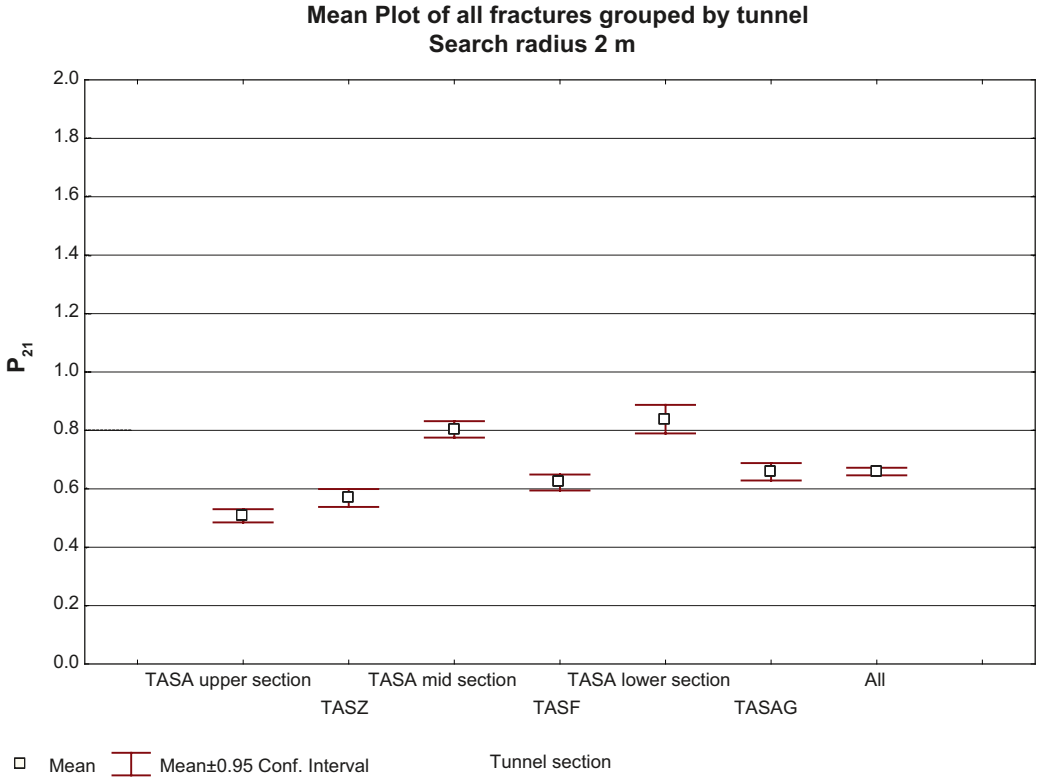

Figure D-28. *Mean plot of all fractures search radius 2 meters.*

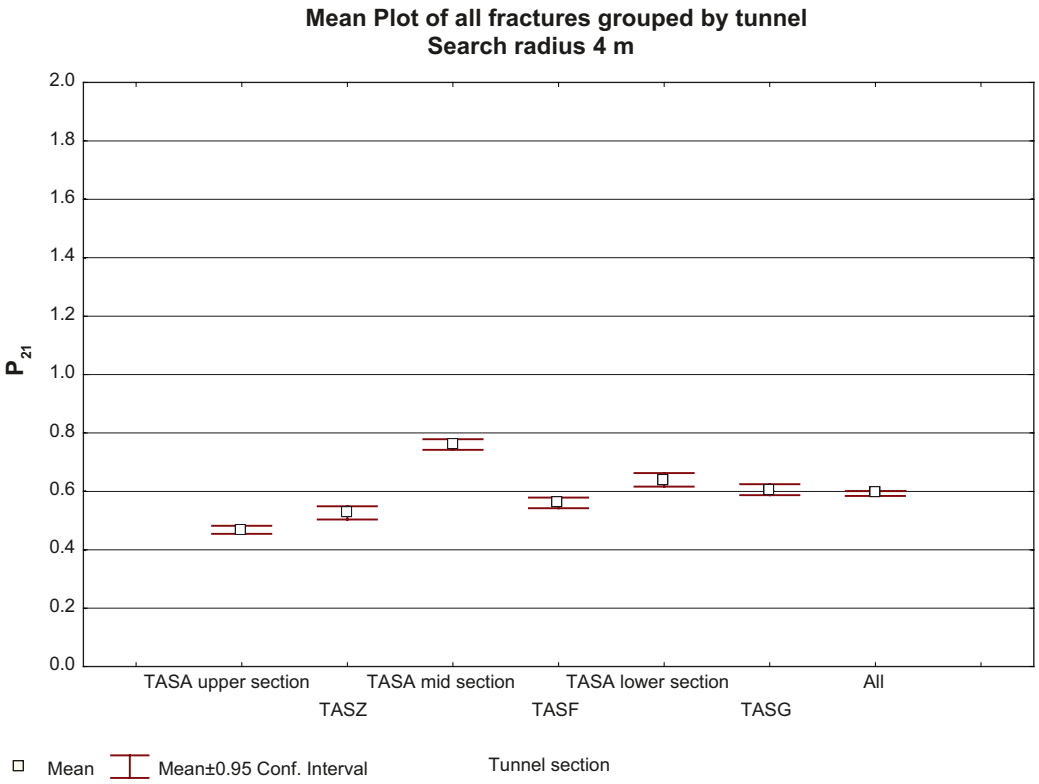

Figure D-29. *Mean plot of all fractures search radius 4 meters.*

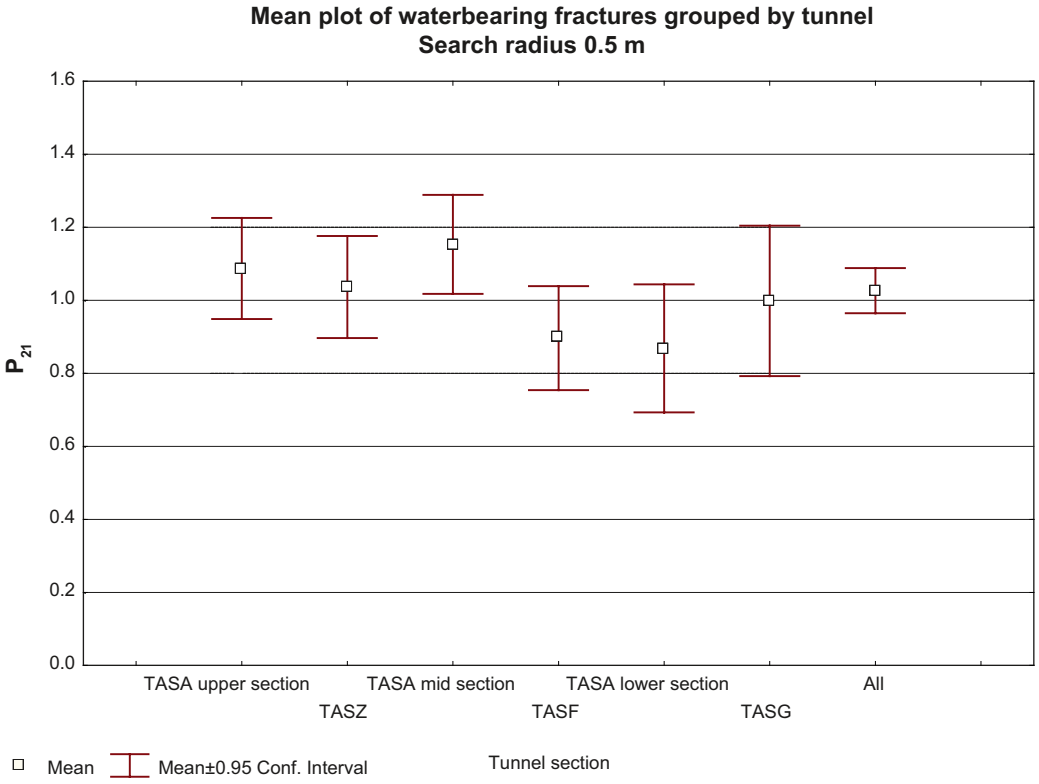

Figure D-30. *Mean plot of waterbearing fractures search radius 0.5 meters.*

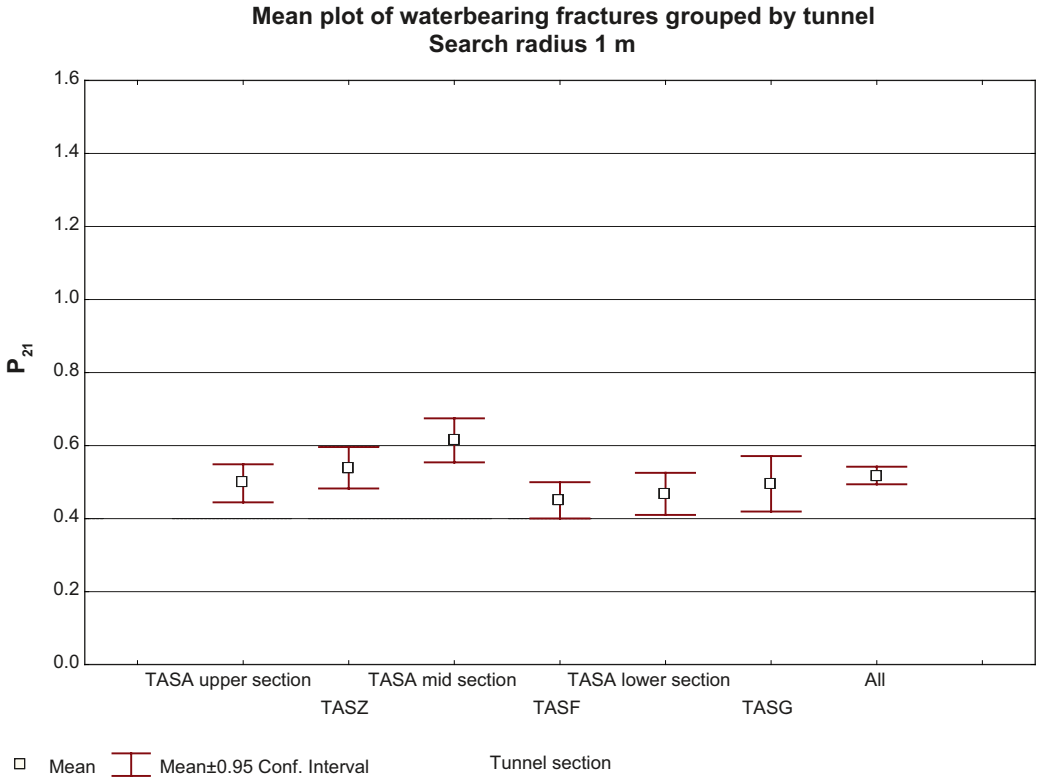

Figure D-31. *Mean plot of waterbearing fractures search radius 1 meter.*

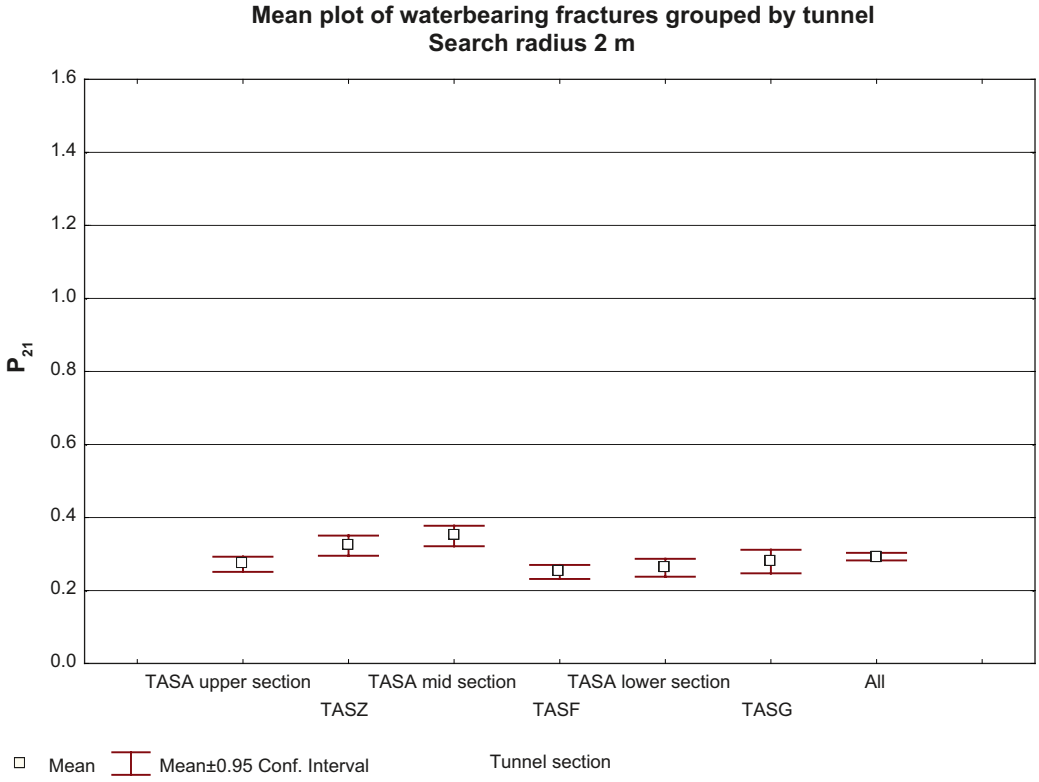

Figure D-32. *Mean plot of waterbearing fractures search radius 2 meters.*

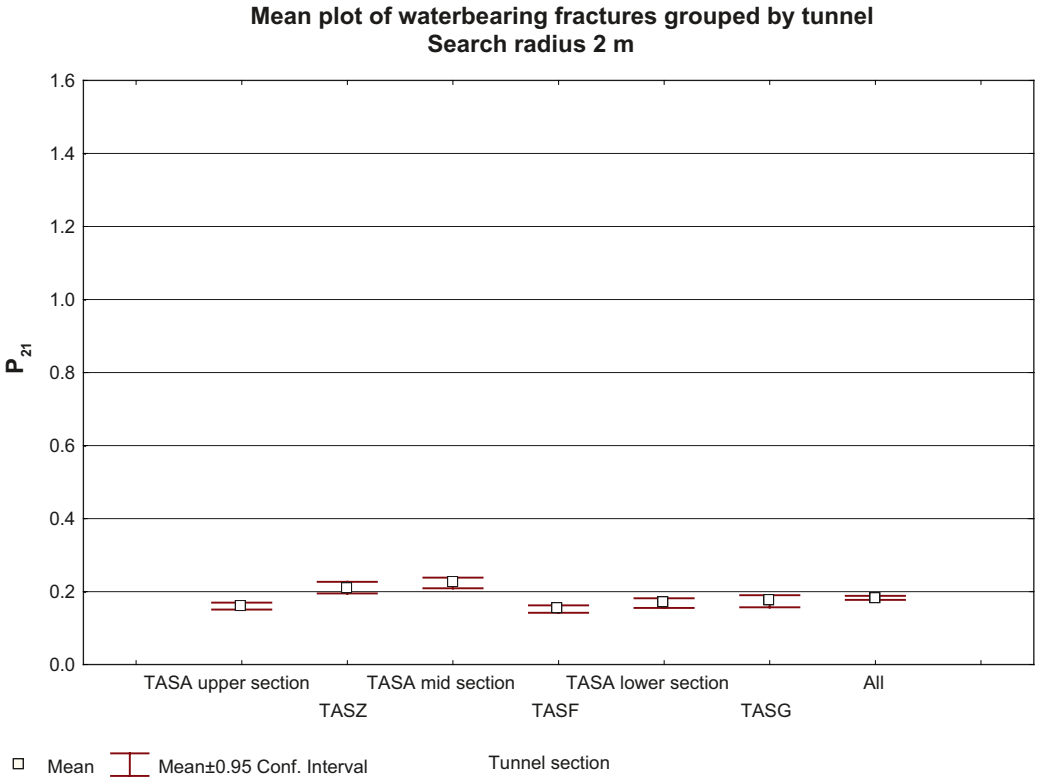

Figure D-33. *Mean plot of waterbearing fractures search radius 4 meters.*

Appendix E

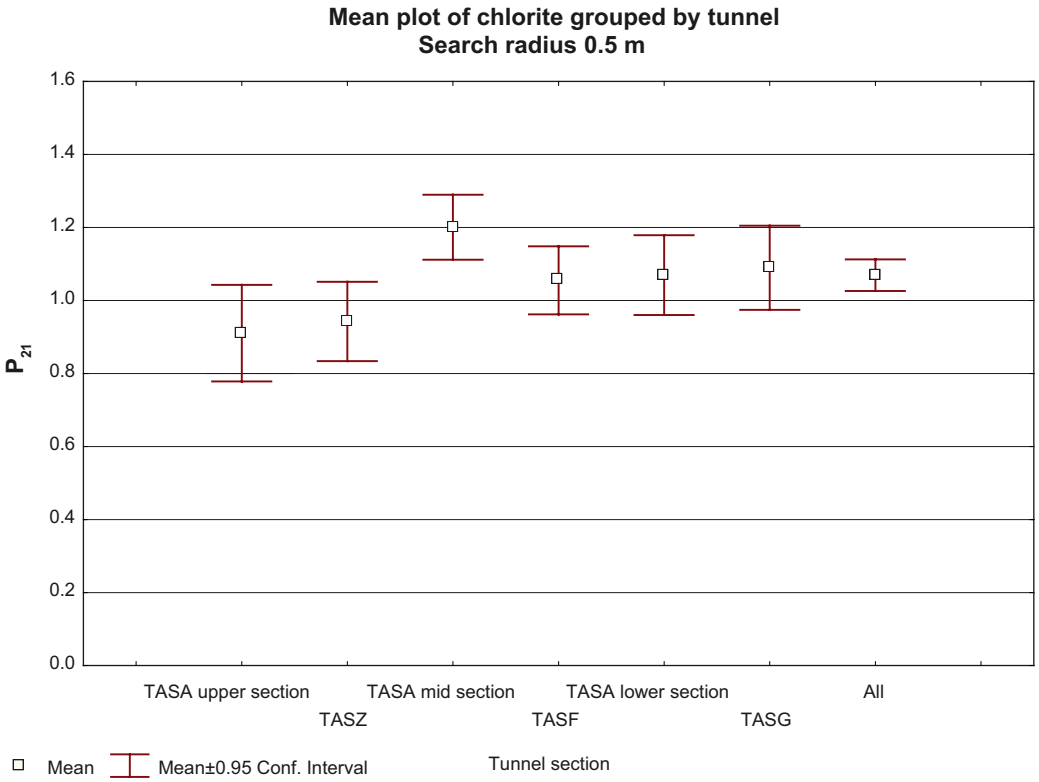

Figure E-1. *Mean plot of chlorite search radius 0.5 meters.*

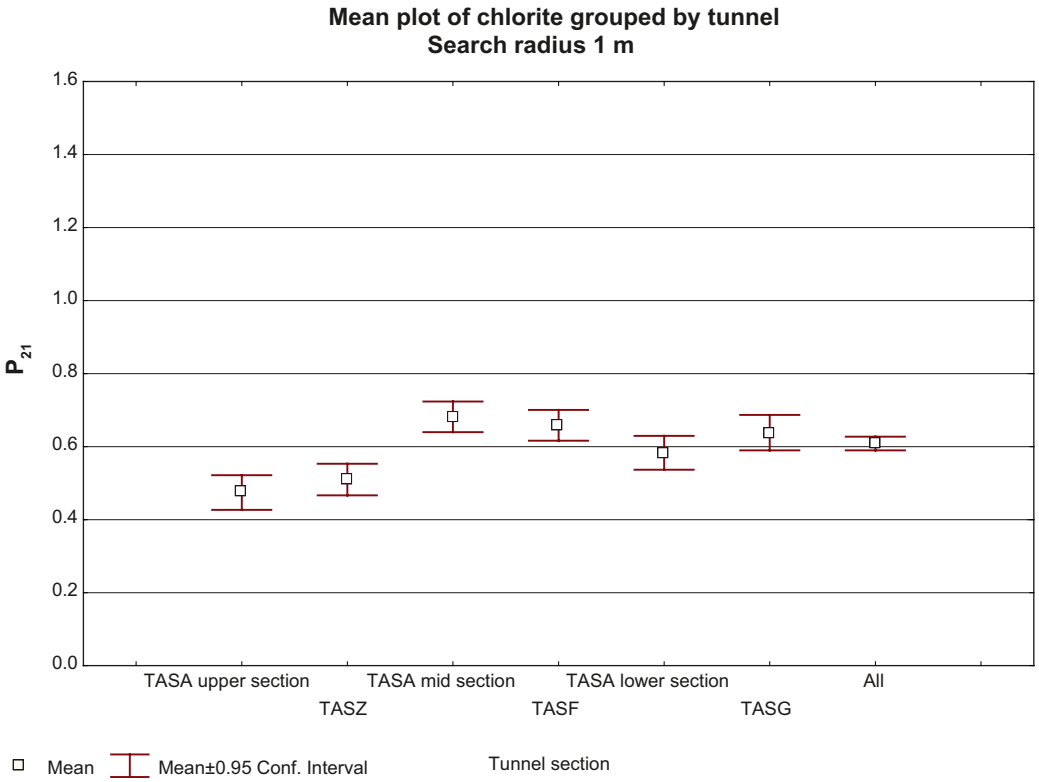

Figure E-2. *Mean plot of chlorite search radius 1 meter.*

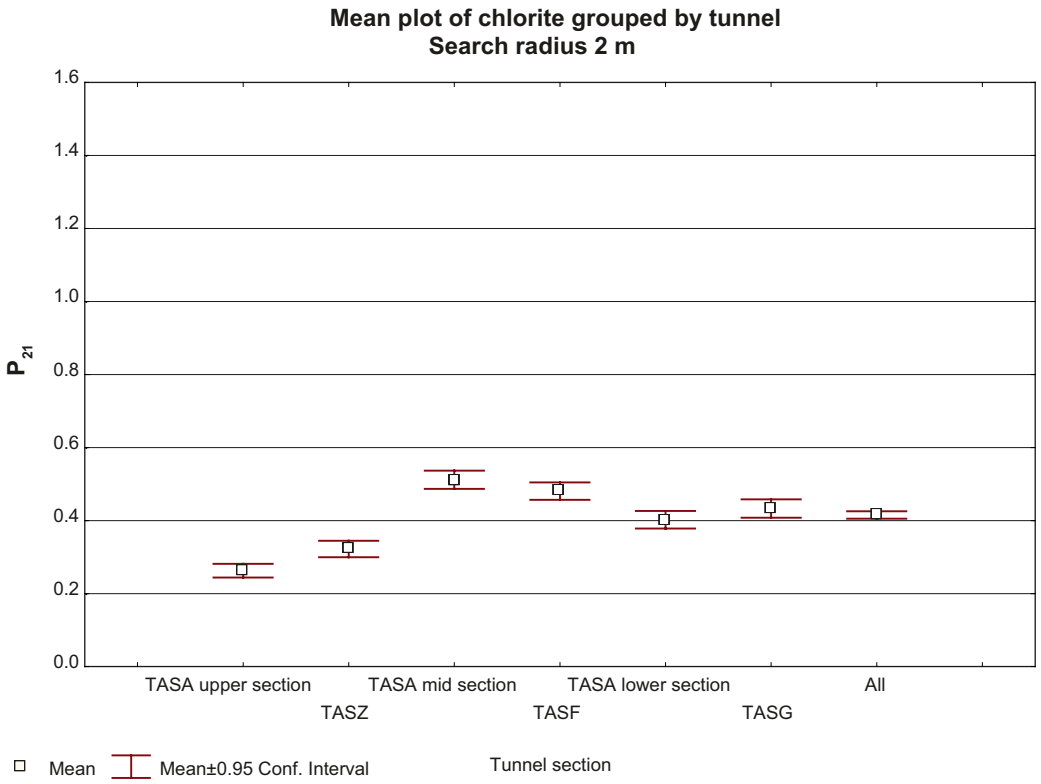

Figure E-3. *Mean plot of chlorite search radius 2 meters.*

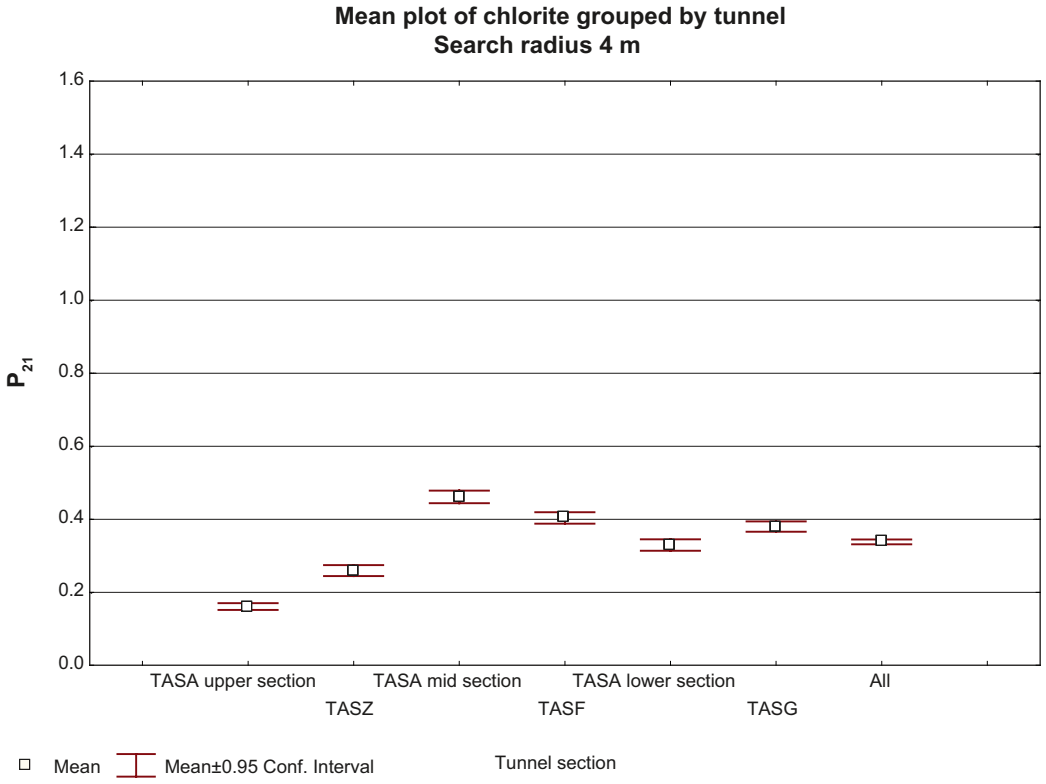

Figure E-4. *Mean plot of chlorite search radius 4 meters.*

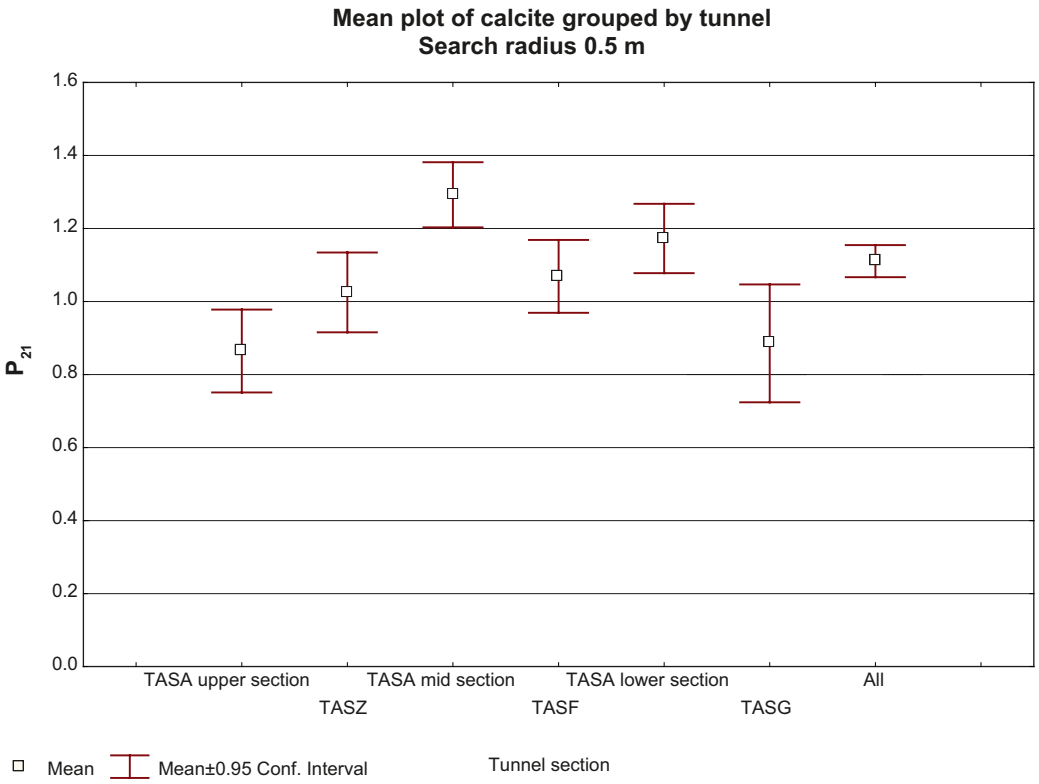

Figure E-5. *Mean plot of calcite search radius 0.5 meters.*

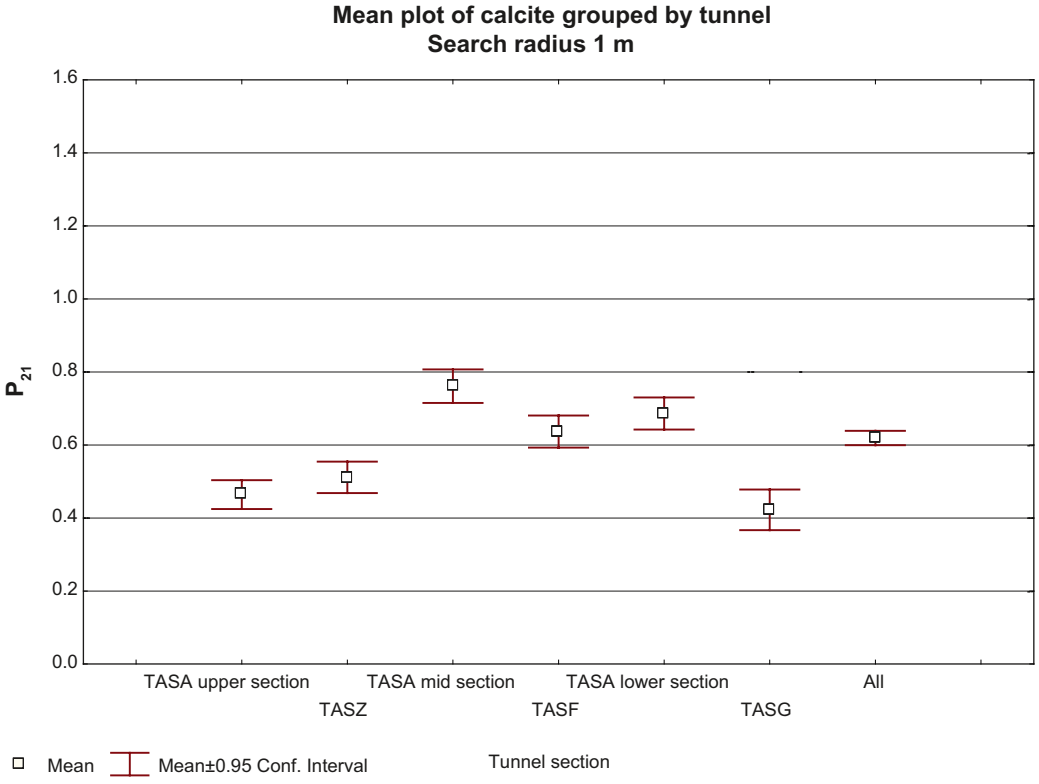

Figure E-6. *Mean plot of calcite search radius 1 meter.*

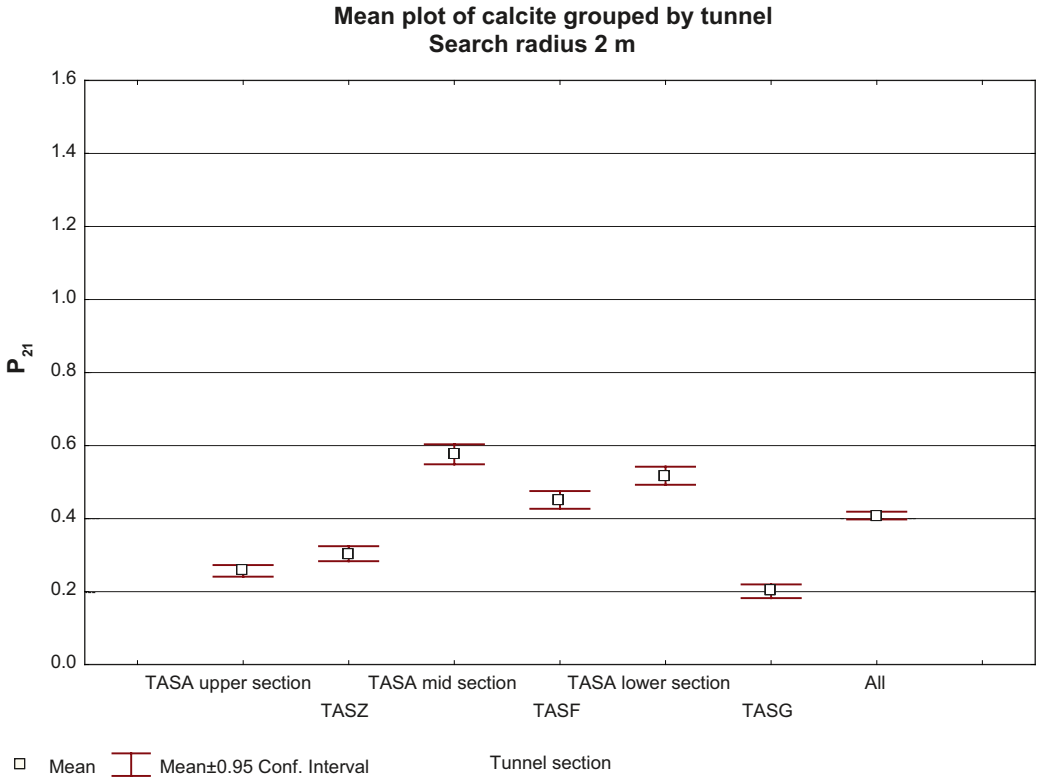

Figure E-7. *Mean plot of calcite search radius 2 meters.*

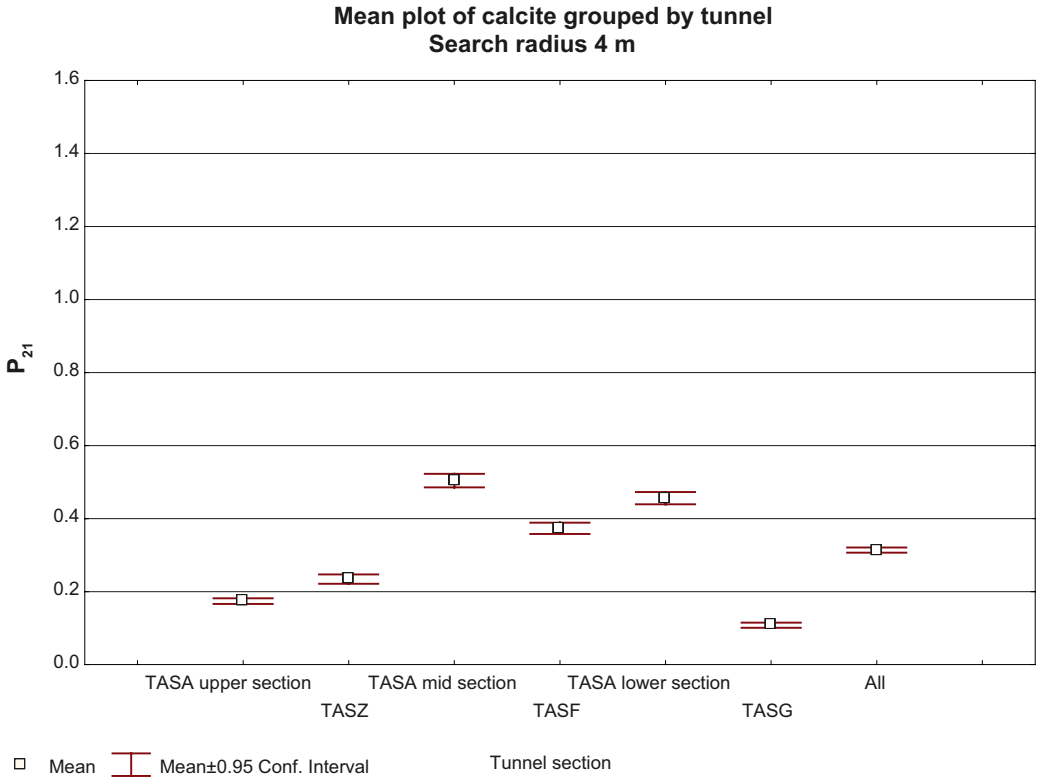

Figure E-8. *Mean plot of calcite search radius 4 meters.*

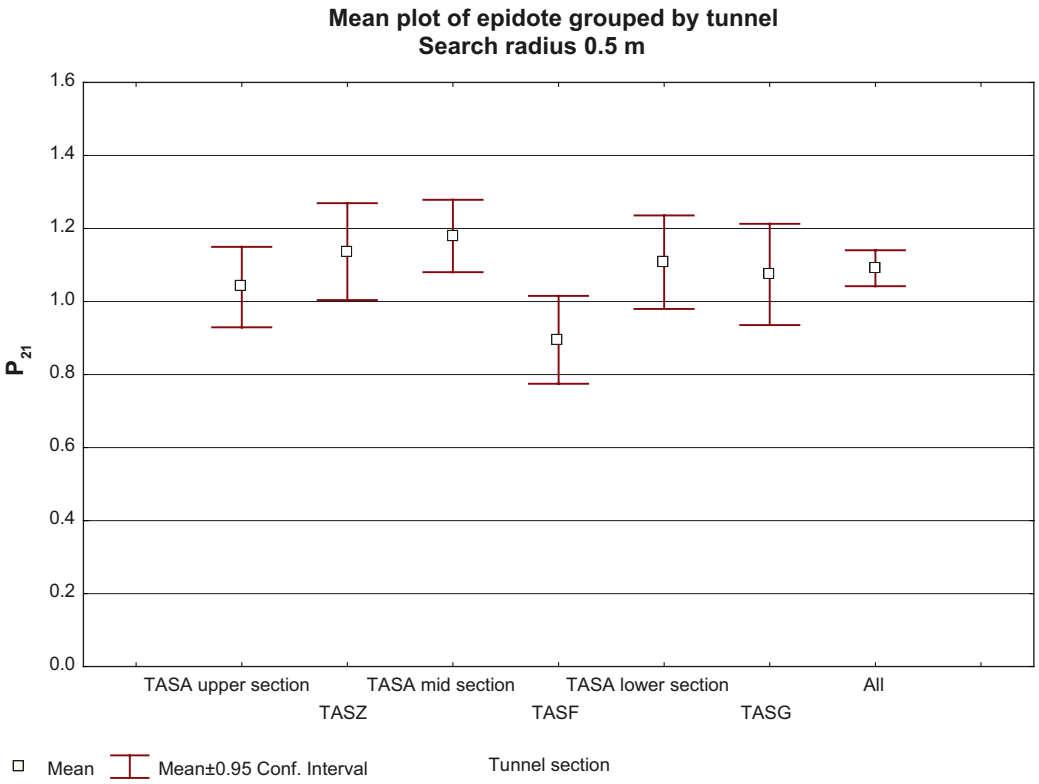

Figure E-9. *Mean plot of epidote search radius 0.5 meters.*

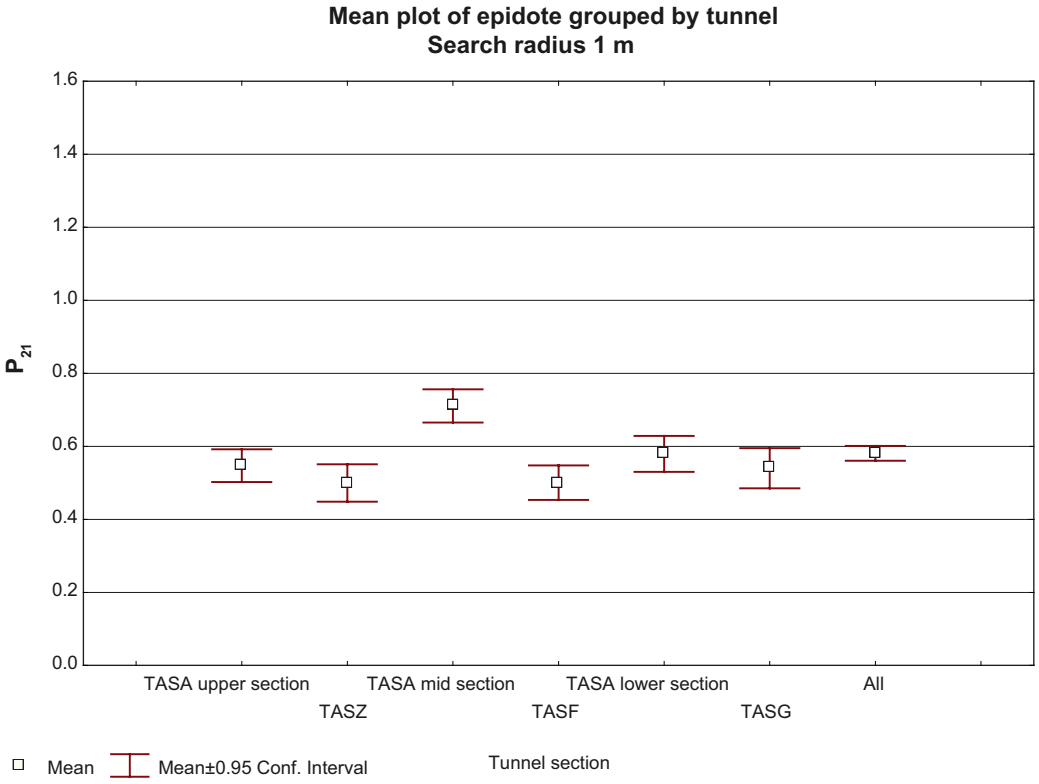

Figure E-10. *Mean plot of epidote search radius 1 metes.*

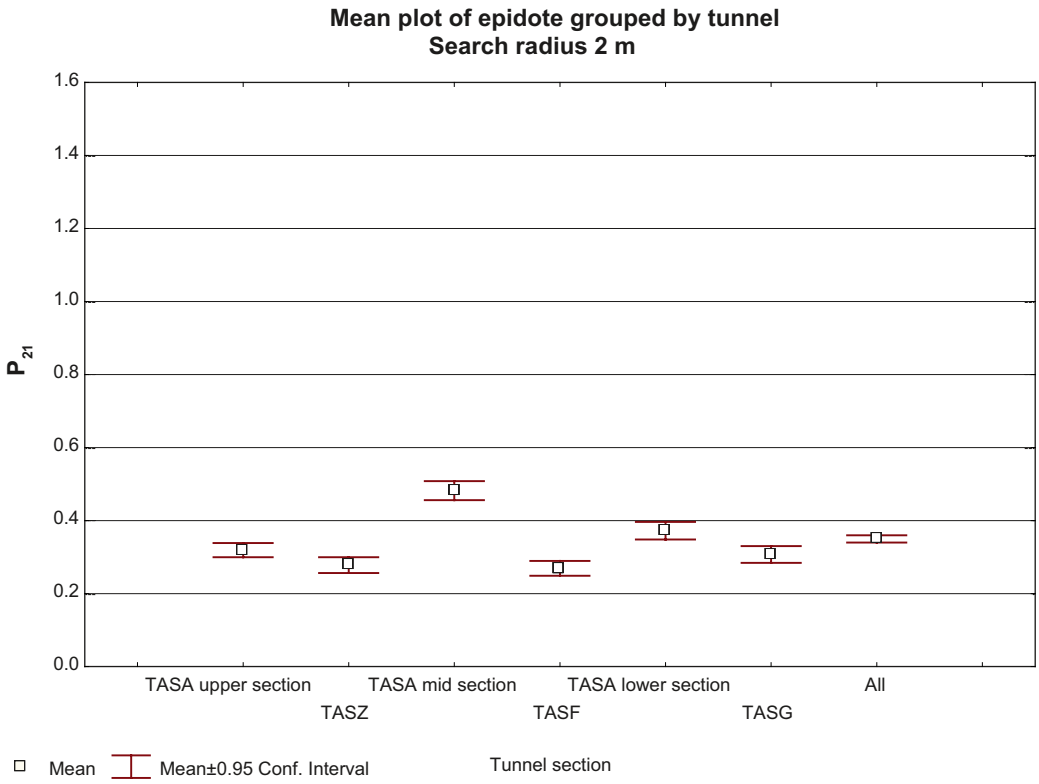

Figure E-11. *Mean plot of epidote search radius 2 meters.*

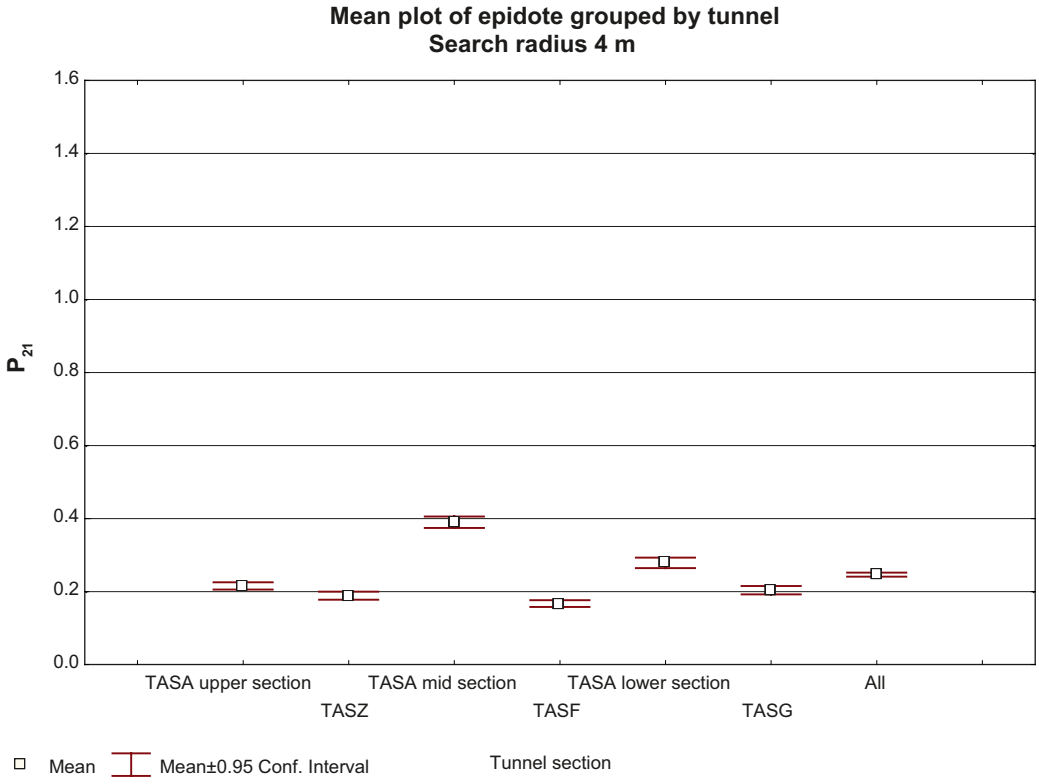

Figure E-12. *Mean plot of epidote search radius 4 meters.*

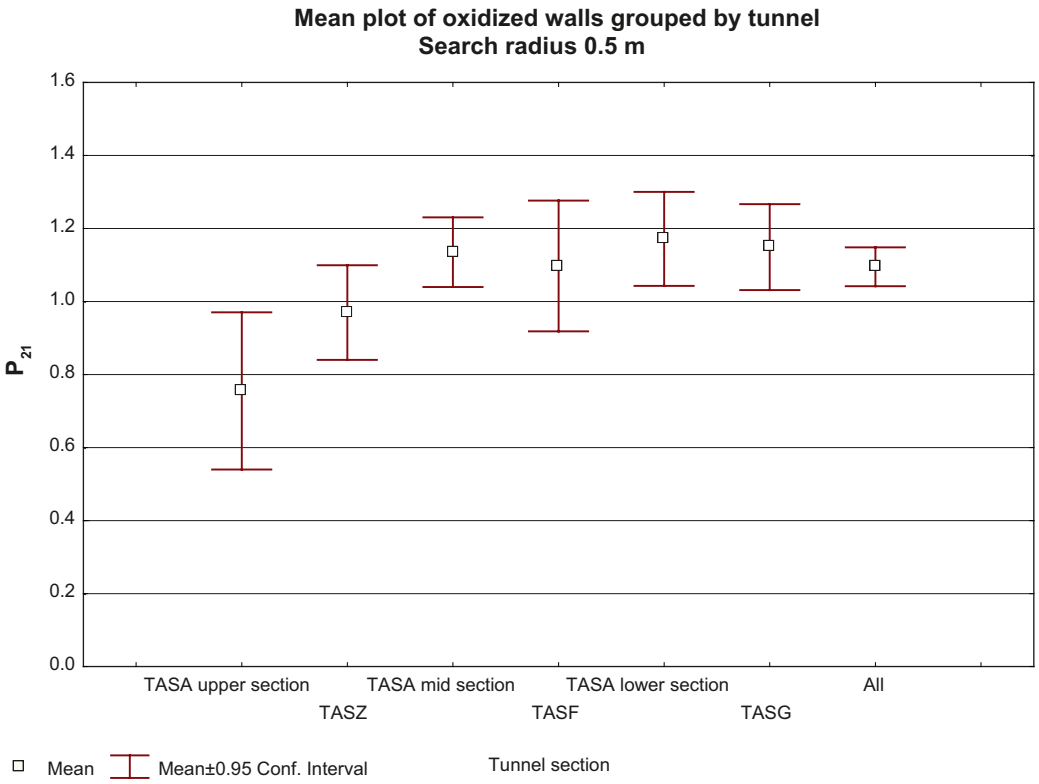

Figure E-13. *Mean plot of oxidized walls search radius 0.5 meters.*

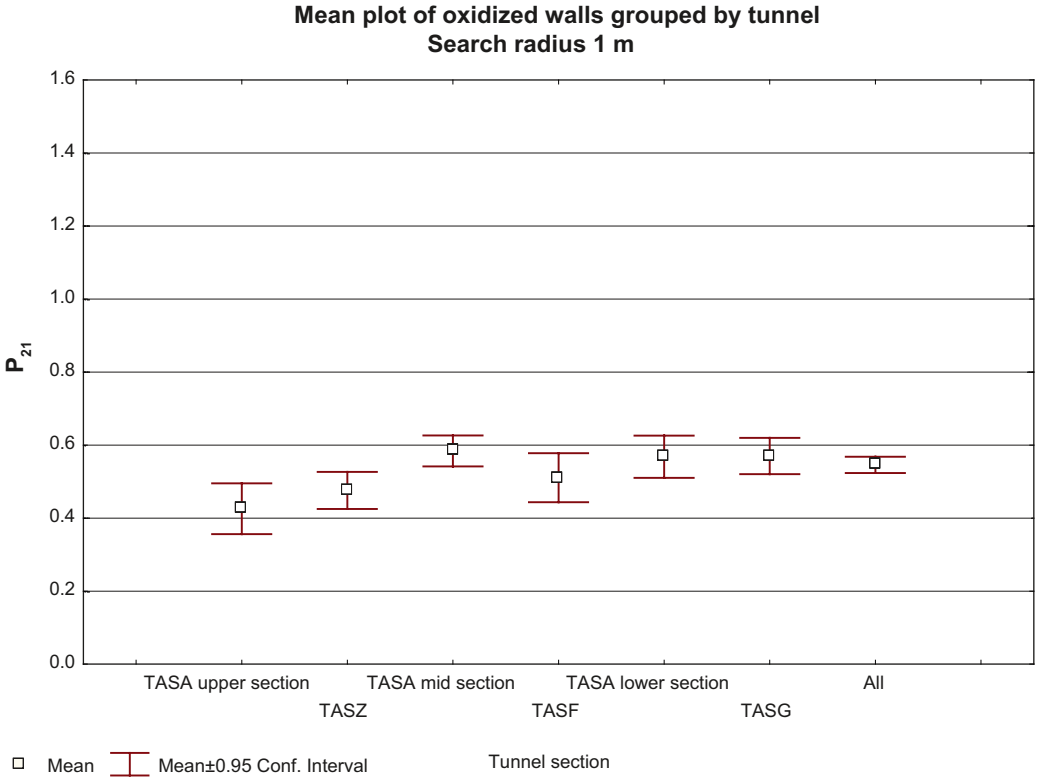

Figure E-14. *Mean plot of oxidized walls search radius 1 meter.*

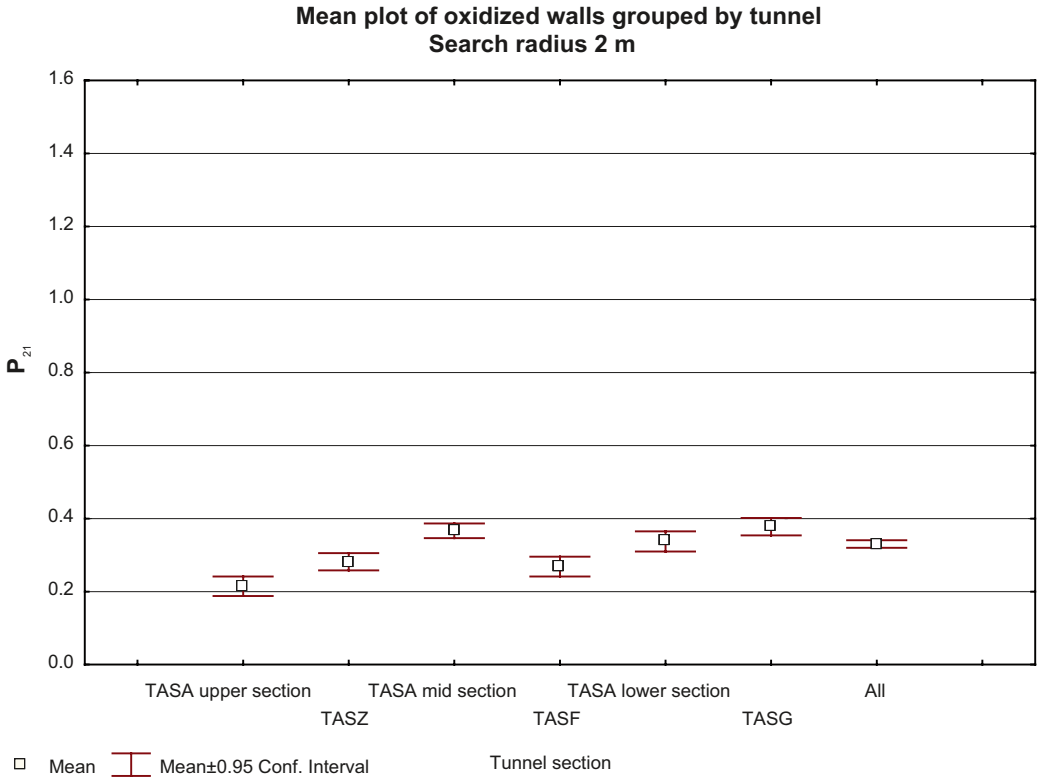

Figure E-15. *Mean plot of oxidized walls search radius 2 meters.*

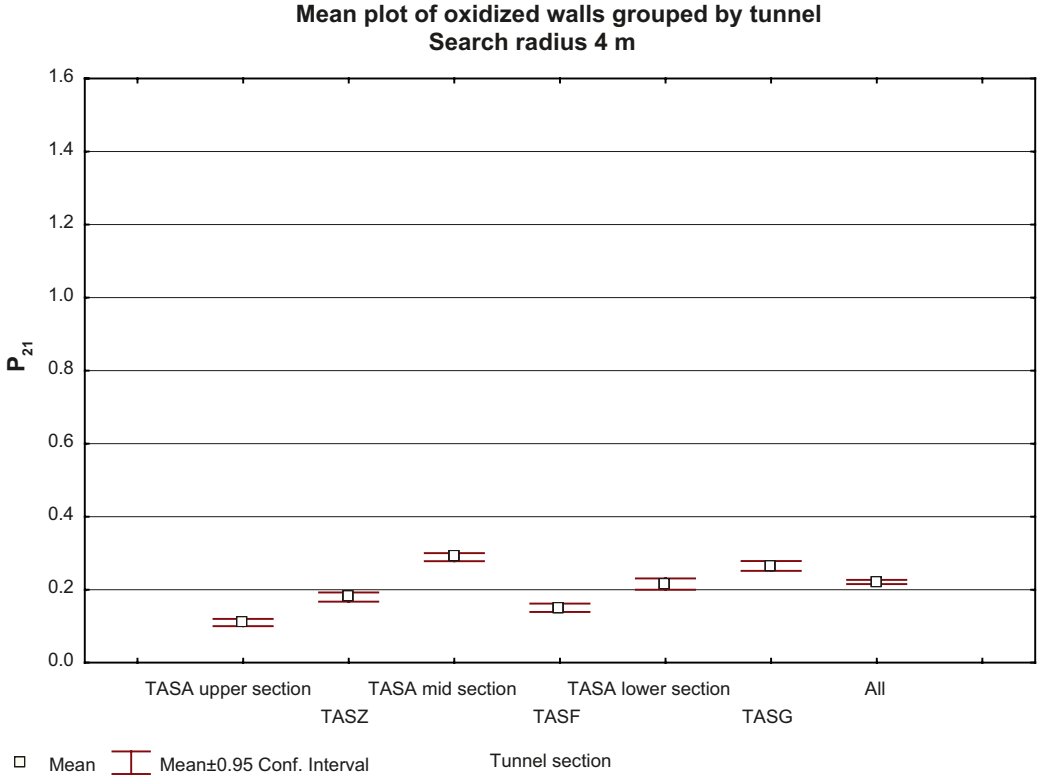

Figure E-16. *Mean plot of oxidized walls search radius 4 meters.*

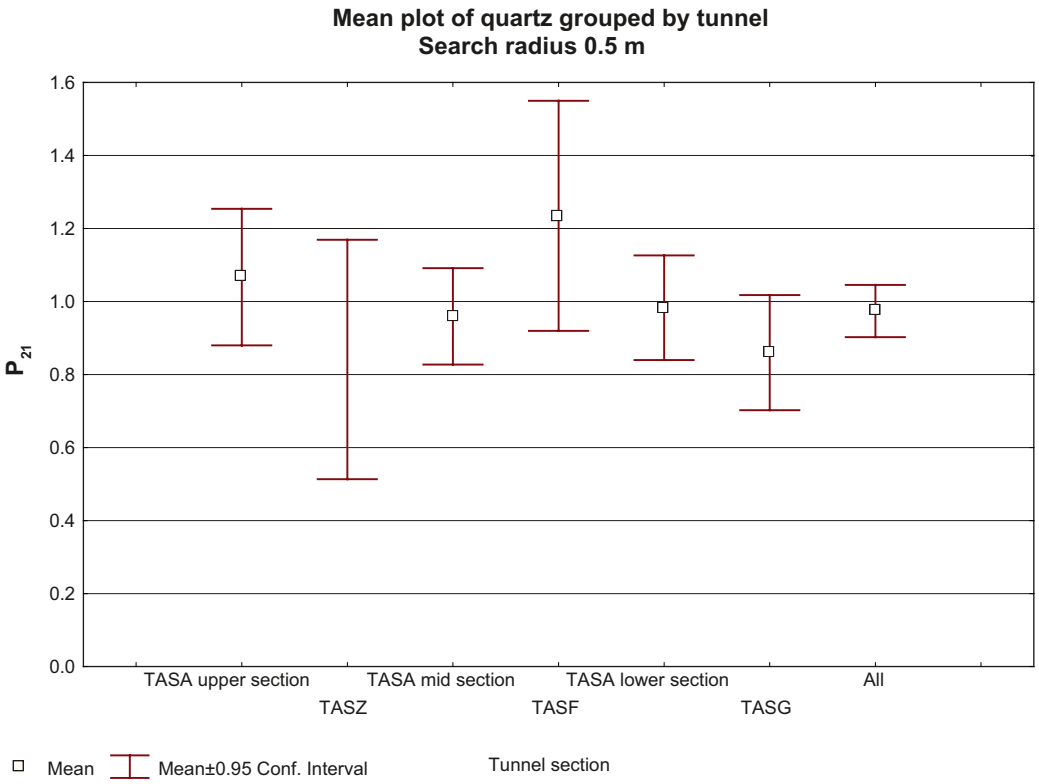

Figure E-17. *Mean plot of quartz search radius 0.5 meters.*

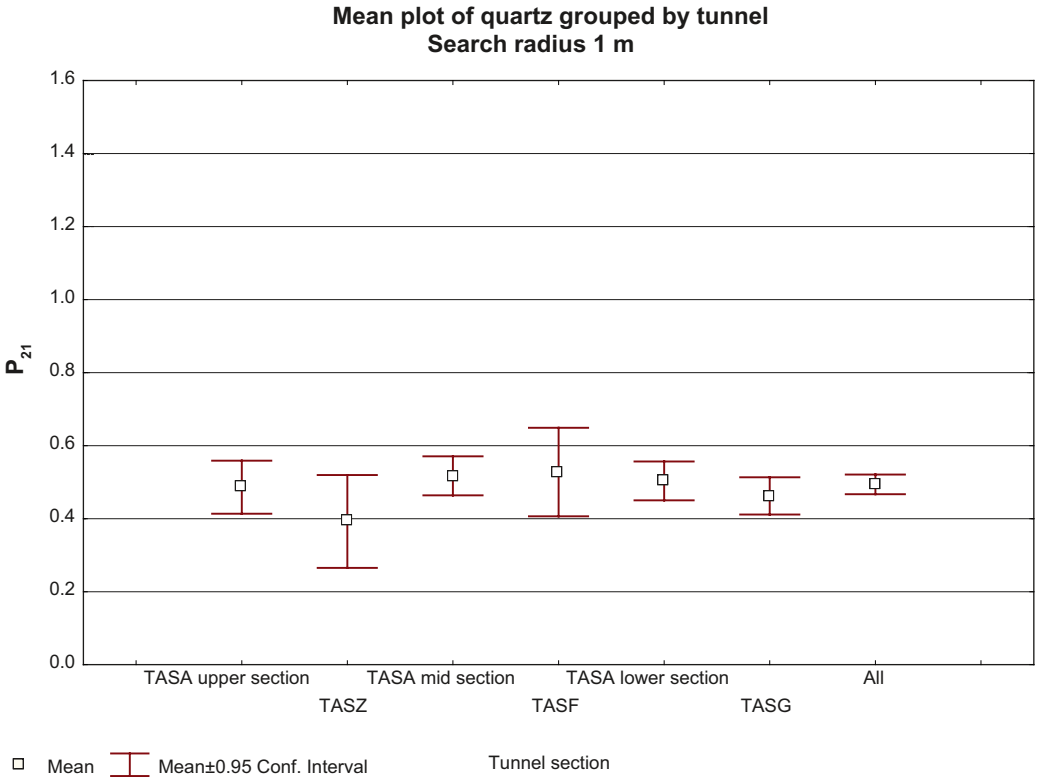

Figure E-18. *Mean plot of quartz search radius 1 meter.*

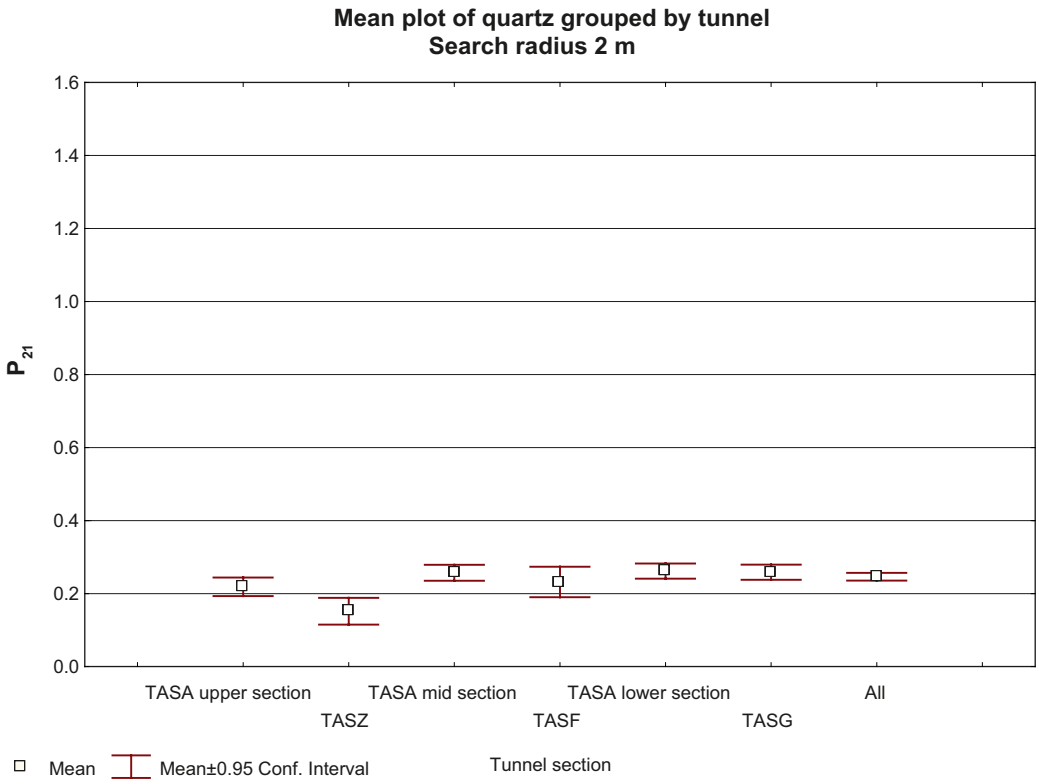

Figure E-19. *Mean plot of quartz search radius 2 meters.*

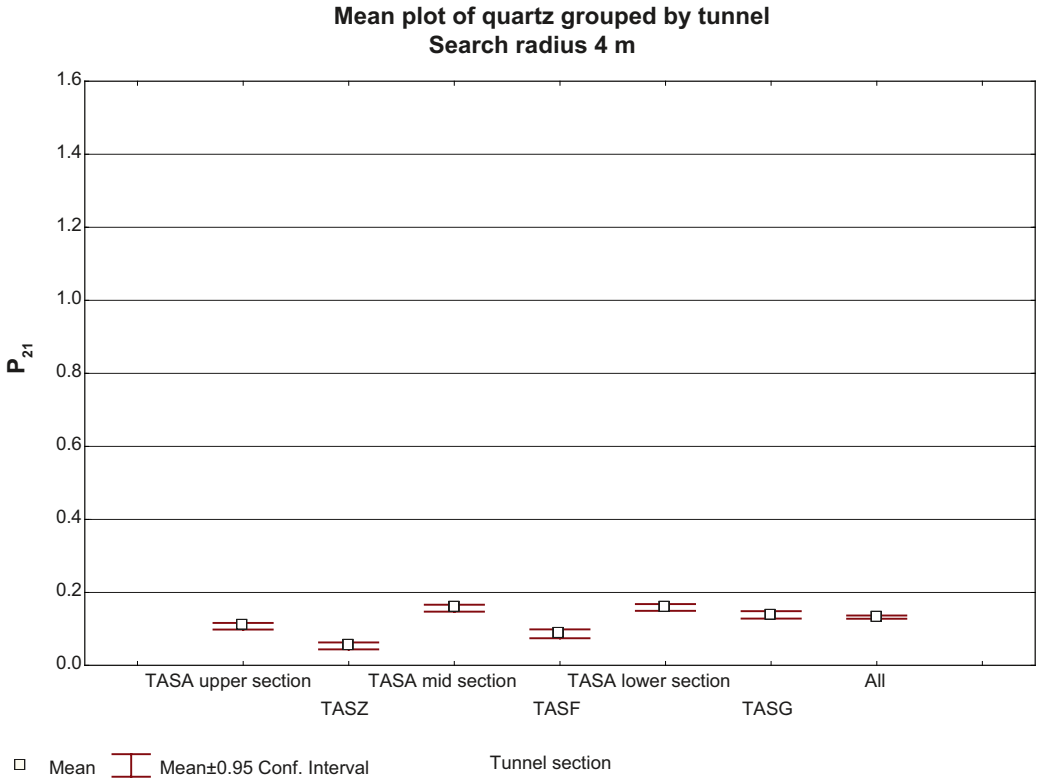

Figure E-20. *Mean plot of quartz search radius 4 meters.*